

MEDIAL MORAINES AS PART
OF A GLACIER DEBRIS SYSTEM;
THEIR FORMATION AND
SEDIMENTOLOGY

CENTRE FOR NEWFOUNDLAND STUDIES

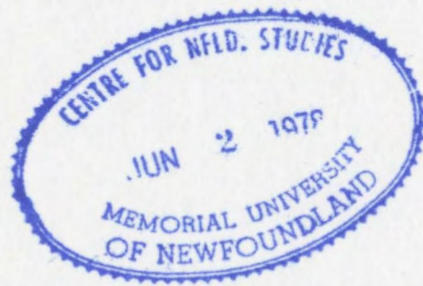
**TOTAL OF 10 PAGES ONLY
MAY BE XEROXED**

(Without Author's Permission)

NICHOLAS EYLES



100037



MEDIAL MORAINES AS PART OF A
GLACIER DEBRIS SYSTEM: THEIR
FORMATION AND SEDIMENTOLOGY

By

Nicholas Eyles

B.Sc., University of Leicester, 1974



A Thesis Submitted to the Department
of Geography in Partial Fulfill-
ment of the Requirements for the
degree of Master of Science

MEMORIAL UNIVERSITY OF NEWFOUNDLAND
1976



Frontispiece: Austerdalsbreen, Jostedal, Norway, 1974



Frontispiece: Berendon Glacier, British Columbia, 1975

TABLE OF CONTENTS

Abstract	viii
Introduction	x
Acknowledgements	xi
List of Tables	xiii
List of Figures	xiv
 CHAPTER 1.0	 1
MEDIAL MORAINES	
1.1 Previous Work	1
1.2 Derivation of Models of Medial Moraine Formation	5
1.3 Objectives of Research	7
1.31 Morphology	7
1.32 Sediments	7
1.4 Field and Laboratory Procedure	8
1.41 Ablation-dominant Model	8
1.5 Above Firn-line Formation	9
1.6 Ice-stream Interaction Model	10
 CHAPTER 2.0	 12
THE 'ABLATION-DOMINANT' MODEL: BELOW FIRN LINE SUBTYPE - AUSTERDALS-BREEN	
2.1 Recent (post 1750 A.D.) Glacier Regression	14
2.11 Glacier Flow	15
2.12 Development of Ogives	16
2.2 Englacial Dynamics: The Debris Throughput of Medial Moraines	19
2.21 The 'Ablation-Dominant' Model of Medial Moraine Formation: Below Firn Line Sub-Type	22

2.3	Supporting Field Investigations	23
2.4	Discussion	25
2.5	Conclusion	27
CHAPTER 3.0	THE ABLATION-DOMINANT MODEL: ABOVE FIRM LINE SUBTYPE - BERENDON GLACIER	28
3.1	Introductory Discussion	28
3.2	The Physical Setting, Berendon Glacier	29
3.3	Climate	32
3.4	Bedrock Geology	34
3.41	Local Structures	40
3.5	South Arm Medial Moraines	41
3.51	Medial Moraines of Upper South Arm Basin	42
3.6	Medial Moraine Derivation Sites	44
3.61	Classification of Bedrock Slopes	44
3.62	Type 1 Slopes	45
3.7	Bedrock Geology of Medial Moraine Derivation Sites	46
3.71	Debris Sample Sites	48
3.72	Western Basin	48
3.73	Eastern Basin	49
3.8	Medial moraines of Terminal South Arm Ice	50
3.81	The Terminal Zone	50
3.82	Medial Moraines	51
3.83	Outline of Field Procedure	52
3.84	Medial Moraine Morphology	53

3.9	The Nature of Englacial Debris Supply	55
3.91	Field Procedure	55
3.92	Results and Interpretation	55
3.93	Discussion: The Nature of the Debris Throughput	56
3.94	Glaciological Determinations	57
3.95	Results	59
CHAPTER 4.0	THE ABLATION-DOMINANT MODEL: ABOVE FIRM LINE SUBTYPE: NORTH ARM MEDIAL MORAINES	61
4.1	Basin Morphology	62
4.11	Medial Moraines	63
4.12	Bedrock Geology	63
4.13	Ice Structures	64
4.2	Debris Generation Sites in Upper North Arm	65
4.21	Introduction	65
4.22	Field Procedure - Debris Sample Sites	66
4.3	Medial Moraines of Terminal North Arm	68
4.31	Field Procedure	69
4.32	Moraine Morphology (Moraine N1)	69
4.33	Debris Sampling and the Nature of Englacial Debris Supply	70
4.4	Discussion	71
4.41	Nature and Distribution of the Debris Throughput and Moraine Morphology	71
4.5	Conclusions	75

CHAPTER 5.0	THE 'ICE-STREAM INTERACTION' MODEL OF MEDIAL MORaine FORMATION	78
5.1	Central Medial Moraine	78
5.12	Morphology	78
5.13	The Confluence Zone	79
5.14	Downglacier to the Terminal Ice Falls	80
5.15	Below the Terminal Ice Falls	80
5.2	Debris Bands of the Central Moraine	81
5.21	Northern Debris Band	81
5.22	Central Debris	82
5.23	Southern Debris Band	82
5.3	Longitudinal Strain-Rate, Ice Velocity and Moraine Morphology	83
5.31	Field Procedure	83
5.32	Longitudinal Strain-Rate: Results	83
5.33	Velocity Determination; Results	84
5.34	Ablation Measurements: Results	86
5.4	Confluence Zone Ice Structures and Moraine Morphology	86
5.41	The Confluence Area and the Central Medial Moraine	86
5.42	Strain-Rate Squares	89
5.43	Location of Strain-Rate Squares	90
5.44	Glacier Mapping	91
5.45	Topographical Transects	91
5.5	North Arm Ice Structures	91
5.51	The Inner Confluence Zone	92
5.51 (I)	Bedrock Marginal Hummocks	93
5.51 (II)	Structural Lineations	93
5.52	Results of Strain-Rate Measurement in the Inner Zone	94

5.6	Northern Debris Band: The Relationship with Ice-Flow	95
5.61	Field Investigations	96
5.62	Further Field Investigations	97
5.63	Discussion	98
5.64	Conclusion	98
5.7	South Arm Ice Structures	99
5.71	Discussion	102
5.8	The Nature of Englacial Debris Supply to the Central Moraine	103
5.81	Field Procedure	103
5.82	North Debris Band	103
5.83	Northern, Central and Southern Debris Bands	103
5.84	Central Debris Band	104
5.85	Results	104
5.86	Interpretation	105
5.9	Central Medial Moraine Morphology: Conclusion	106
CHAPTER 6.0	THE SEDIMENTOLOGY OF MEDIAL MORAINES	108
6.1	Introduction	108
6.2	Statement of Objectives	110
6.21	Field Procedure: Berendon Glacier	111
6.22	Preparatory Procedure	114
6.23	Data Presentation	115
6.3	Interpretation and Discussion	117
6.31	Description of Medial Moraine Debris	117
6.4	The Relationship Between Medial Moraine Debris and Parent Bedrock Texture	121

Concluding Remarks

128

Appendix I

133

Appendix II

143

Appendix III

152

Appendix IV

155

Appendix V

163

Appendix VI

176

Appendix VII

182

Bibliography

184

ABSTRACT

The morphological development of medial moraines on Austerdalsbreen, Norway and Berendon Glacier, British Columbia is dependent upon englacial debris supply. A literature review suggests that this is a general case. An 'ablation-dominant' model of moraine formation is proposed which relates englacial debris supply to the site and manner of englacial incorporation of debris relative to the firn line. On Austerdalsbreen a prominent medial moraine is formed by the confluence of two ice-cap outlet glaciers below the firn line (below firn line subtype of the model). Moraine debris is derived from extraglacial bedrock outcrops between the two ice streams and is englacially entrained via crevasses to which lower depth limits apply. Revelation of crevasse-bound debris generates a distinct ice-cored morphology which is destroyed as crevasse-bottoms are revealed downglacier. In this below firn line subtype, moraines formed by confluence of ice-cap outlet glaciers below the firn line are characterized by a discrete debris supply distinct from subglacial removal of bedrock.

On Berendon Glacier ice streams coalesce above the firn line (above firn line subtype); debris entrained between ice streams is derived both from extraglacial rock outcrops and from subnival and subglacial bedrock zones. Extraglacially derived debris undergoes seasonal sedimentation with snowfall; debris extends throughout ice depth. As a result a distinct moraine morphology is present in the terminal area in response to continuing englacial debris supply. The bulk of moraine debris is found to be transported at depth near the glacier base following subglacial and subnival derivation in the firn basin. Upper englacial debris (related to extraglacial rockslope activity in the firn basin) is of small quantity.

In addition, moraines are generated in many cases by confluence below the firn line of large ice-streams carrying a large lateral moraine load. Peculiar ice structures and patterns of ice flow commonly observed from confluence zones have been considered to determine moraine morphology rather than englacial debris supply. However this 'ice-stream interaction' model which was

tested on Berendon Glacier where two large ice-streams converge explains moraine morphology in the confluence zone only. Down-glacier, moraine morphology accords with those moraines formed above the firn-line i.e. is dependent upon the nature of englacial debris supply.

Examination of debris texture, scanning electron microscopy (s.e.m.) of quartz grains and clay mineral investigations form the basis of sedimentological analyses. Medial moraine debris cannot be rigorously distinguished from other elements of the debris system; primary comminution processes produce debris exhibiting a wide particle-size range independent of parent bedrock. A wide spectrum of particle sizes is produced. Limited comminution following initial derivation (i.e. passive glacial transport) is reflected in quartz grain surface textures and a coarser mean size of medial moraine debris compared to subglacial lodgement tills.

INTRODUCTION

Medial moraines, as distinct morphological forms, are marked and well-defined features of many glaciers and are revealed in varying states of development over and along the time-transect of the glacier surface. Debris septa upglacier, possessing an immature morphology, may evolve downglacier into medial moraines exhibiting a more mature morphology in response to increasing supraglacial debris quantities. Such debris septa and associated moraines constitute important elements in the glacier debris budget and, in contrast to subglacial debris, yield directly observable and accessible evidence of erosion in glacial valleys. In addition, debris derivation areas of medial moraines are usually well-defined and provide insight into erosional activity and rates of rock wall recession in head wall and upper valley slope areas. Sediment populations remain well-defined; little extraneous debris is contributed to moraines downglacier.

It is the purpose of this thesis to examine the morphological development of medial moraines as they are traced downglacier and to consider the changing character of included debris as it is transported through the basin. Models of medial moraine formation have been constructed; the models make possible a more precise definition of initial derivation areas for bedrock debris revealed downglacier.

ACKNOWLEDGEMENTS

Field research on Austerdalsbreen, Norway was completed in July and August 1974 while the writer was co-leader of an expedition from the University of Leicester, U.K.. Expedition members surveyed a topographic profile along the glacier centre line; this profile has been used in this thesis. Research activity by the writer and embodied in this thesis was carried out with the occasional field assistance of expedition members. The writer is indebted to Dr. T.D. Douglas, Expedition Leader, of the Department of Geography, University of Leicester for introducing him to active ice studies. Thanks are extended to Dr. N.V. Pears also of the Department of Geography for the loan of field equipment. The glacier research was funded by expedition members.

Field activities during the period June to September, 1975, on Berendon Glacier, British Columbia, were funded by an Environment Canada Water Research Incentives grant (5043-5-5-103.. 1975) extended to the writer and his supervisor, Mr. R.J. Rogerson of the Department of Geography at Memorial University. Berendon Glacier lies within 200 m. of a copper concentrating mill: while the glacier is retreating a readvance has been suggested. During the course of research in Norway, methods for increasing ice melt rates were determined and a part of Environment Canada funding was allocated for the application of such techniques, in exploratory fashion, on Berendon Glacier. Results are considered in the appendices of this thesis. The writer wishes to thank Dr. Gordon Young of the Glaciology Division, Environment Canada for field discussion.

The cheerful and willing field assistance of Charles Auger of Stewart, British Columbia under often difficult conditions is gratefully acknowledged. The writer is indebted to the Granduc Operating Company of Vancouver, British Columbia for considerable base camp support and to Mr. Paul Jurcic, Acting Chief Geologist of the company, for information and discussion.

Mr. R.J. Rogerson visited the writer, in the field during August 1975, and his field advice proved as equally rewarding as that of the continual discussion and help he has unfailingly pro-

vided both inside and outside the classroom. My grateful thanks are also extended to his family.

The writer has also been fortunate to have been associated with Dr. R.M. Slatt of the Geology Department at Memorial; continual enthusiasm and flow of ideas has generated a productive intellectual environment. The writer is grateful to Dr. Slatt for fundamental advice and instruction with regard to sedimentological research embraced within this thesis.

The writer would like to thank Dr. V.C. Barber of the Biology Department at Memorial for advice on the use of the Scanning Electron Microscope. During the writing of this thesis Dr. J.B. Macpherson of the Geography Department provided constant suggestions as to thesis format. Dr. W.H. Yoxall also of the Geography Department read and commented on a draft of Chapter 6. The writer is grateful to Dr. R.L. Shreve of the University of California for permission to reproduce Fig. 6a.

I would like to thank my family both in Montreal and London, U.K. for support and encouragement from afar. Finally, sincere thanks are extended to all those people who have helped the progress of this thesis.

LIST OF TABLES

- Table 1 Component Ice Streams of North and South Arms,
 Berendon Glacier
- Table 2 Ice Velocity Determination; Stake 26, Central
 Stake Line
- Table 3 Experimental Plots: Debris Character

LIST OF FIGURES

- Figure 1 The 'ablation-dominant' model of medial moraine formation
- Figure 2 Austerdalsbreen; Location of the Field Area, 1974
- Figure 3 Structural zones of Western Norway
- Figure 4 Austerdalsbreen medial moraine long profile; (a) photographic and (b) surveyed
- Figure 5 Austerdalsbreen medial moraine; The 'ablation-dominant' model
- Figure 6 Austerdalsbreen medial moraine; (a) 1959, (b) 1974
- Figure 7 Ablation rates over experimental plots. Austerdalsbreen, July/August 1974
- Figure 8 Berendon Glacier; Location of the Field Area
- Figure 9 Berendon Glacier; Basin Morphology
- Figure 10 Berendon Glacier; Nomenclature
- Figure 11 Berendon Glacier; The nature of its flow
- Figure 12 Berendon Glacier; Bedrock geology
- Figure 13 Berendon Glacier; Medial moraines formed above the firn line and by confluence of North and South Arms
- Figure 13a Map
- Figure 13b 1964 aerial photography by Austin Post
- Figure 14a Berendon Glacier; The nature of extra-glacial bedrock slopes
- Figure 14b Berendon Glacier; type II and III slopes
- Figure 15 Berendon Glacier; upper South Arm basin
- Figure 16 Berendon Glacier; Medial moraines in the terminal area of South Arm
- Figure 17 Berendon Glacier; 'pseudo-medial moraines' formed by longitudinal foliation
- Figure 18 Berendon Glacier; medial moraines SI and SII in the terminal area of South Arm

- Figure 19 Berendon Glacier; transverse till ridges in the terminal area of South Arm
- Figure 19a Map
- Figure 19b Photograph
- Figure 20 Berendon Glacier; medial moraine morphology in the terminal zone
- Figure 21 Berendon Glacier; medial moraine SIV in the terminal area of South Arm
- Figure 22 Berendon Glacier; debris clearance sites
- Figure 23 Berendon Glacier; newly revealed englacial debris in the terminal area of moraine SIV
- Figure 24 Berendon Glacier; medial moraine width as a function of distance downglacier from the firn line
- Figure 25 Berendon Glacier; supraglacial debris quantity along medial moraines as a function of distance downglacier from the firn line
- Figure 26 Berendon Glacier; medial moraines formed above the firn line (above firn line subtype of the 'ablation-dominant' model of moraine formation)
- Figure 27 Berendon Glacier; stake lines
- Figure 28 Berendon Glacier; longitudinal strain-rate along medial moraines SI and SII
- Figure 29 Berendon Glacier; ice velocities along moraines SI, CI
- Figure 30 Berendon Glacier; ablation rates along medial moraines SI and NI. July and August 1975
- Figure 31 Berendon Glacier
- Figure 31a Overview of the terminal area
- Figure 31b View upglacier
- Figure 31c Berendon Glacier; truncation of medial moraine morphology by shearing
- Figure 32 Berendon Glacier; terminal zone of moraine NI

- Figure 33 Berendon Glacier; newly revealed englacial debris at the head of medial moraine N1
- Figure 34 Berendon Glacier; the confluence zone of North and South Arm ice
- Figure 35 Berendon Glacier; Central moraine, formation of the northern debris band
- Figure 36 Berendon Glacier; the Central medial moraine, longitudinal strain-rate as a function of distance downglacier
- Figure 37 Berendon Glacier; the Central medial moraine, ice velocities as a function of distance downglacier
- Figure 38 Berendon Glacier; the Central medial moraine, ablation as a function of distance downglacier
- Figure 39 Berendon Glacier; ice structures in the confluence zone
- Figure 40 Berendon Glacier; debris-rich crevasse remnant, transverse debris ridge and compressed serac blocks in the confluence zone
- Figure 41 Berendon Glacier; extrusion of blocks from debris-rich crevasse remnants along South Arm ice shoulder
- Figure 42 Berendon Glacier; location and notation of strain-rate squares
- Figure 43 Berendon Glacier; topographic profiles in the confluence zone
- Figure 44 Berendon Glacier; determination of differential velocity at the contact of North and South Arms
- Figure 45 Berendon Glacier; longitudinal strain-rate over wave forms on South Arm
- Figure 46 Berendon Glacier; debris clearance site across the entire Central moraine, near the end of the melt season 1975, five weeks after initial clearance
- Figure 47 Berendon Glacier. Medial moraines; below firn line debris sample sites
- Figure 48 Salmon Glacier; medial moraine debris sample sites
- Figure 49 Berendon Glacier; measurement of sideslip

- Figure 50 Berendon Glacier; ice cavitation and an ablating debris sole (30 cm. thick) in the terminal area of South Arm
- Figure 51 Berendon Glacier; debris particle size distributions; computer print-outs
- Figure 52 Berendon Glacier; debris samples collected from medial moraine SIV
- Figure 53 Berendon Glacier; debris samples collected from medial moraines SI and SII
- Figure 54 Berendon Glacier; medial moraine debris samples derived from argillites and siltstones of the Bowser assemblage
- Figure 55 Berendon Glacier; debris samples collected from the Central, or confluence, medial moraine derived from volcanic conglomerate of the Hazleton assemblage
- Figure 56 Berendon Glacier; samples collected from frost-shattered debris
- Figure 57 Berendon Glacier; subglacial debris sole and lodgement tills
- Figure 58 Berendon Glacier; subglacial (lodgement tills and basal sole debris) and medial moraine debris samples
- Figure 59 Berendon Glacier; medial moraine debris. Mean size, standard deviation and parent bedrock. (-4.0 to 4 ϕ)
- Figure 60 Berendon Glacier; medial moraine debris. Moment measure variation as a function of distance down-glacier from firn basin backwalls
- Figure 60a Argillite
- Figure 60b Volcanic tuff
- Figure 60c Volcanic conglomerate (-4.0 to 4 ϕ)
- Figure 61 Berendon Glacier; elements of the debris system on the criteria of mean size and standard deviation (-4.0 to 4 ϕ)
- Figure 62 Berendon Glacier; elements of the debris system (-4.0 to 4 ϕ)
- Figure 63 Berendon Glacier; clay mineralogy of the finer than 9 ϕ clay fraction (after the methods of Biscaye 1964)
- Figure 64 Grain size distributions from Berendon Glacier debris system, mid-latitude tills and frost-shattered debris plotted on "Law of Crushing" Paper

- Figure 65 Berendon Glacier; morphology of the 'erratic moraine' on upper South Arm
- Figure 65a Photograph by R.J. Rogerson, 1967
- Figure 65b Morphology of the moraine, August 1975
- Figure 66 Berendon Glacier; the terminal area
- Figure 67 Berendon Glacier; minor moraine ridges of probable annual occurrence developed along the margins of South Arm ice
- Figure 68 Berendon Glacier; minor moraine ridges of probable annual occurrence, South Arm terminus
- Figure 69 Berendon Glacier; minor moraine ridge spacing and indicated annual recession, South Arm ice front
- Figure 70 Berendon Glacier; emergence of a minor moraine ridge from the ice front of South Arm, 1975
- Figure 70a July 1975
- Figure 70b August 1975
- Figure 70c September 1975
- Figure 71 Berendon Glacier; particle-size distribution of debris in the terminal area of North Arm
- Figure 72 Berendon Glacier; elements of the debris system compared with debris found in the terminal area of North Arm (-4.0 to 4 ϕ)
- Figure 73 Berendon Glacier; basal shear plane outcropping along South Arm ice front
- Figure 74 Berendon Glacier; Granduc mill stream flowing along the lower foot of a granodiorite outcrop
- Figure 75 Berendon Glacier; open, infraglacial channel flow of Granduc mill stream; the result of the collapse of the roof of a subglacial channel
- Figure 76 Berendon Glacier; aerial photographs by Austin Post of the terminus
- Figure 76a 1961
- Figure 76b 1969
- Figure 76c 1972
- Figure 76d 1974

- Figure 77 Berendon Glacier; weekly recession,
South Arm ice-front, June to September
1975
- Figure 78 The relationship between ice melt rates
and superincumbent debris depth
- Figure 79 Berendon Glacier; ablation over experi-
mental plots
- Figure 80 Berendon Glacier; experimental plots.
Two photographs are presented for
each plot; on day 1 and day 4
- Figure 81 Berendon Glacier; recessional moraines,
1750 A.D., to the present (1975)
- Figure 82 Berendon Glacier; recessional moraines,
1750 A.D., to the present. Topo-
graphic profiles
- Figure 83 S.E. Alaska; glacier recession since
1750 A.D.
- Figure 84 Comparative glacier recession rates
- Figure 85 Total cumulative recession; Berendon,
Salmon and Lemon Creek Glaciers
- Figure 86 Comparative mean temperatures; Stewart,
B.C., and Juneau, Alaska

1.0 MEDIAL MORAINES

1.1 Previous Work

Medial moraines are such marked features of glacier surfaces that their absence in some instances has invoked comment (Theakstone, 1965). A large literature discusses minor relief features on medial moraines. Dirt-cones, rock tables and supraglacial meltstream activity have been well-researched (Agassiz, 1840; Forbes, 1859; Ray, 1935; Lewis, 1940; Sharp, 1949; Lister, 1958; Wilson, 1953; Streiff-Becker, 1954; Krenek, 1958; Swithinbank, 1959; Kozarski and Szuprycznski, 1971; Drewry, 1972; Knighton, 1973); a literature on dirt-cones has, for instance, existed since 1750 (Thorarinsson, 1960). Morphological description in terms of minor relief features has preceded systematic enquiry as to the origin of moraines as a whole however. Tangential references to moraine morphology are numerous (Slingsby, 1895; Ogilvie, 1904; Wood, 1935; Nielsen and Post, 1953; King, 1959; Sharp, 1947, 1948, 1960; Allen et al., 1960; Matthews, 1973; Wojcik, 1973). On the larger scale, distinctive geology of medial moraines has been used to trace ice streams upglacier (Rutishauser, 1971). 'Perturbed' medial moraines, developed by longitudinal compression on surging glaciers have been utilised as indicators of past surges (Post, 1972).

Sedimentological analysis of medial moraines commenced with Salisbury (1894) who in a classic paper, unfortunately ignored by contemporary workers, made a full exploration of the nature of glacial debris systems, the pattern of debris through-flow and the distinctive character of medial and lateral moraines. Medial moraines formed by converging supraglacial lateral

moraines were contrasted with medial moraines formed when deep englacial debris was revealed by ablation downglacier of subglacial rock bosses. The latter 'would be, in fact, a medial moraine made up wholly of englacial-supraglacial debris and not produced by the union of lateral moraines.' By virtue of ablation and the continuing englacial debris supply 'the effect will be to widen the medial moraine ... this effect will be progressive with increasing distance.' The development of an ice-cored, ridged morphology was traced downglacier to the terminal area where the medial moraine was 'likely to lose its distinctiveness.' He rejected the possibility of elevation by flow of subglacial debris to a supraglacial position along the medial moraine.

Hess (1907a) took the analysis of medial moraine formation a stage further by field observations on some Ötztal glaciers, principally the Hintereisferner. Velocity measurements were made close to the medial moraine and the quantity of debris removed from the basin by the moraines was determined. An estimate of glacial erosion was made; this was corrected in a later paper (1907b). The contribution of subglacial debris to medial moraine sediments was discussed and supported.

Rapp (1960) estimated the quantity of debris removed by the medial moraine of Tempelfjorden, Vest-Spitsbergen. In this instance, debris derivation areas are well-defined, the moraine being formed downglacier of the firn line and perennial snow cover. In addition medial moraine debris was demonstrated to be entirely supraglacial; debris is essentially transported talus, distinct from any englacial or subglacial load carried by the glacier.

3

The emphasis in sedimentological discussion of medial moraines has been on the establishment of debris types contributing to moraines. Discussion of debris types relies on a simple positional terminology such as englacial, supra- and subglacial. Sharp (1949) has traced the different transport paths of each debris type. For example, supraglacial moraine debris below the firn-line may arrive at the glacier surface by revelation of englacial or subglacial debris or may be derived directly from extraglacial rock slopes. Englacial transport may result from incorporation of debris above the firn line. However, the glacier debris system is a continuum, characterised by a high rate of debris transfer. Debris positions within the system do not represent end-points in glacial movement paths but are transitory (Salisbury, 1894); moreover debris paths are typically erratic (Marcussen, 1973) and a simple positional terminology is unsatisfactory in attempting to describe debris history. Unfortunately sedimentological analyses of debris types contributing to medial moraines have not been reported.

Morphological discussion of medial moraines emphasizes the relationship between morphology and the nature of englacial debris supply to the moraine, the depth of supraglacial debris and the development of an ice-core. Young (1953) from examination of medial moraines on Breidamerkurjökull found a correlation between moraine height and thickness of debris cover. Loomis (1970) considered the morphology of the medial moraine on Kaskawulsh Glacier, Yukon Territory, in terms of differential ablation of debris-laden and clean ice. The medial moraine is formed by merging lateral moraines of North and Central ice arms. No analysis was made of

4
moraine sedimentology but lithological contrasts between debris bands were established. Moraine debris was considered to be predominantly supraglacial; less than ten percent of total moraine debris was estimated to be englacial. Low englacial debris quantities were also found by Lister (1958) on Britannia Gletscher, North-east Greenland. Increasing moraine width in the downglacier direction appears to be a sensitive guide to a continuing englacial debris supply (Salisbury, 1894). On Kaskawulsh Glacier, moraine width remained constant for several kilometres though lateral compression between the two ice-streams played no part in generating a distinct moraine morphology (Loomis, 1970). Loomis' observations of a low englacial debris content along the moraine accords with static moraine width downglacier.

Small and Clark (1974) related the development of medial moraine morphology to englacial debris supply on the lower Glacier de Tsidjlore Nouve. Debris is englacially entrained in crevasses at the confluence of two ice-falls below the firn-line. Since debris is entrained initially into crevasses a lower limit of englacial debris supply can be recognised; cessation of englacial debris supply results in destruction of a distinct moraine morphology.

1.2 / Derivation of Models of Medial Moraine Formation

Publication by Small and Clark coincided with field research by the writer on Austerdalsbreen, Jostedal, Norway which exhibits the same pattern of moraine development as the lower Glacier de Tsadjore-Nouve (Eyles, 1975). They suggested that medial moraines formed at the margins of ice-cap outlet glaciers, coalescing below the firn-line, are characterised by a definable lower limit of englacial debris. On the other hand on many valley outlet glaciers where ice-streams coalesce above the firn-line debris from extraglacial bedrock outcrops is not precipitated into crevasses but undergoes sedimentation with seasonal snow accumulation. In addition medial moraine debris may be derived from subnival and subglacial positions (Fig. 1). With cumulative ablation downglacier as ice moves out of upper accumulation basins progressive increase in the quantity of supraglacial sediment may occur all the way to the terminus. This may result, because of a continuing englacial debris supply, in a distinct morphology in the terminal zone. Moreover, since a continuum exists between upper englacial and supraglacial debris loads and debris transported at, or near the bed, subglacial debris elements may be contributed to moraine sediments in the terminal zone. Sedimentological analysis of debris from such moraines might substantiate the remark of Rothlisberger (1968) that 'the study of medial moraines should give some clues particularly to the erosion at depth in the high areas of a glacier.'

Thus important morphological and sedimentological contrasts may be apparent between medial moraines of above and below firn-

line formation. A continuing englacial debris supply to moraines generated above the firn-line may result in a well developed morphology in the terminal zone. Conversely moraines formed below the firn-line by coalescing ice-cap outlet glaciers are identified by a truncated and collapsed morphology downglacier.

An 'ablation-dominant' model of medial moraine formation is proposed in which moraine morphology is dependent upon the nature of englacial debris supply. Such a model includes two sub-types: (1) moraines generated above the firn-line which are characterised by continued englacial debris supply in the terminal zone (above firn line subtype);

(2) moraines formed by coalescence of ice-cap outlet glaciers below the firn-line which are characterised by a discrete englacial debris supply composed of former extraglacial debris, well-defined debris derivation areas and a collapsed moraine morphology downglacier (below firn line subtype).

By contrast, classic medial moraine morphology is generated by ice-streams coalescing some distance below the firn line, where an often substantial lateral debris load is present. Confluence areas of large valley outlet glaciers are often seen to exhibit distinct ice-structures and lateral compression between coalescing ice-streams is often evident (Sharp, 1960; Brächer, 1969; Loomis, 1970). Such ice structures, rather than englacial debris supply, may determine moraine morphology. An 'ice-stream interaction' model is proposed in which moraine morphology is dependent not on the nature of englacial debris supply but on ice structures and the pattern of ice-flow associated with large merging ice-streams below the firn-line.

1.3 Objectives of Research

1.31 Morphology

Models of medial moraine formation have been constructed on the criteria of those determinants affecting moraine morphology. In the 'ablation-dominant' model morphology is dependent upon the nature of englacial debris supply: field research considered the varying nature of englacial debris supply associated with above and below firn line formation (Berendon Glacier and Austerdalsbreen respectively). In the 'ice-stream interaction' model i.e. where moraines are generated by large merging outlet glaciers below the firn line, fundamental factors other than englacial debris supply, such as ice structures and flow character, may determine moraine morphology. The nature of structural determination of moraine morphology is investigated.

1.32 Sediments

Medial moraines are important elements in the glacier debris budget; sediment populations remain well-defined and little extraneous debris (apart from dust, organic material and debris slides that may reach the glacier centre line) is contributed to moraines. In the 'ablation-dominant' model, where moraines and associated debris septa are formed above the firn line subglacial removal of bedrock can be contrasted with the more shallow transport by moraines formed below the firn line. Analysis of subglacial moraine debris emerging in the terminal zone allows comment on the nature of glacial erosion in upper firn basins. Sedimentological analysis has concentrated on moraines revealed on Berendon Glacier, analyses have also been made of debris out-

cropping on the nearby Salmon Glacier. Moraines have been sampled at subaerial derivation sites in the firn basins, and below the firn line, downglacier to the terminal zone. As a result the effect of glacier transport in positions such as englacial, supra and subglacial on debris character can be assessed. Textural analysis of the ϕ to ϕ_4 (silt to clay; 16 to .0625 mm) size fraction has formed the bulk of such work, supplemented by consideration of clay mineralogy and surface textures of included quartz grains. A wide variety of bedrock types is evacuated by moraines on Berendon Glacier, the textural relationship between parent bedrock and daughter debris products is assessed. Finally sedimentological criteria for the discrimination of medial moraine debris from other elements of the glacier debris system are considered.

1.4^a Field and Laboratory Procedure

The following section describes field and laboratory investigations of moraines formed above and below the firn-line, and by confluence of large ice-streams.

Field observations and sedimentological investigations, primarily laboratory oriented, are briefly described.

1.41 Ablation-dominant Model

(1) Below firn-line formation - Austerdalsbreen, Jostedal, Norway
Field Procedure. Field research (1974 field season) on Austerdalsbreen, an outlet glacier of the Jostedal ice-cap, embraced the following: (1) construction of a surveyed long profile of the moraine; (2) an experimental trench in the ice surface to establish the relationship between cessation of debris supply and

9

morphology; (3) elucidation of the relationship between superincumbent debris and the underlying ice-core. Ablation rates of experimental plots of varying debris cover were compared to ablation on bare ice.

Sediments. Extensive debris sampling was not possible; sedimentological analysis relies on Scanning Electron Microscopy (s.e.m.) of the surface textures of medium sand sized quartz grains. Debris transport paths from derivation sites below the firn line are well defined and supplement s.e.m. observations.

Summary of Results. Field observation and experimentation established the pattern of development of an ice-cored moraine ridge and its subsequent truncation downglacier in response to cessation of englacial debris supply. The moraine incorporates a well-defined sediment body distinct from subglacial debris elements.

1.5 Above firn-line formation

Berendon Glacier, British Columbia

Field Procedure. The width and height of medial moraines formed above the firn line, outcropping on two ice arms were recorded. Estimates were made of supraglacial debris quantities present along the moraine. Longitudinal strain-rate, ice velocity and ablation rates were determined for well-developed moraines in the terminal zone. Areas of moraines were cleared of supraglacial debris to establish the nature of englacial debris supply.

Sediments. Medial moraine debris derivation sties were identified in the upper firn basins and samples of released debris obtained for comparison with debris emerging in the terminal zone. In addition, moraine debris was sampled at successive intervals downglacier to the terminal zone.

Summary of Results. A developing ice-cored moraine morphology is found in the terminal area in response to a continuing englacial debris supply. Englacial debris supply is not constant over the length of the moraine and the bulk of moraine debris is transported near the glacier base and is only revealed in the terminal area. Upglacier englacial debris supply is low and can be related to the activity of extraglacial bedrock slopes above the firn line. Despite deep englacial, near basal transport, moraine debris is passively transported by the glacier. The texture of moraine debris is found to be independent of parent bedrock and mode of transport. Shearing activity in the terminal zone introduces additional debris elements.

1.6 Ice-stream Interaction Model

Berendon Glacier, British Columbia

Field Procedure. A medial moraine (confluence medial moraine) 2.2 km long is generated on Berendon Glacier by confluence of two ice-streams (North and South Arms). Substantial lateral debris loads are present above the confluence. Morphological analysis considered the relationships between medial moraine morphology and (1) ice structures in the confluence zone; (2) longitudinal strain rate and velocity and (3) englacial debris supply.

A longitudinal stake line was constructed along the moraine; strain-rate squares were located in the confluence area to determine strain-rate close to the contact of the two ice-streams. Peculiar ice features of the confluence area were mapped, profiled and related to moraine morphology. Areas of the moraine were cleared to monitor release of englacial debris.

Sediments. Sedimentological analysis of debris collected from the moraine allowed comparison with that evacuated by simple medial moraines formed above the firm line and present on the adjacent ice surface of North and South Arms. Since lateral moraine debris loads are contributed to the confluence zone, sedimentological analyses embraces debris components formed on extraglacial valley-side slopes upglacier of the confluence.

Summary of Results. Peculiar ice flow and associated ice structures determine moraine morphology only in the confluence area; downglacier moraine morphology exhibits fundamental dependence upon englacial debris supply. Moraine morphology and sedimentology accord completely with moraines formed above the firm line and are best considered within the framework of the 'ablation-dominant' model of moraine formation.

2.0 THE 'ABLATION DOMINANT' MODEL: BELOW FIRN LINE SUBTYPE

Austerdalsbreen: Location and Description of Field Area

Austerdalen lies on the southern margins of the Jostedal ice-cap, Europe's largest ($1,850 \text{ km}^2$), and 50 km north of the east-west trending Sognefjord (Fig. 2). The valley of the Jostedal, draining south, lies approximately 15 km to the east. Austerdalsbreen, 1 km wide, occupies the upper 3 km of the Austerdal Valley which is oriented northwest-southeast. A marked change in orientation of the valley occurs at a rock-bar adjacent to the present glacier terminus. The lower valley below the rock-bar runs toward the south-west; as a consequence of this change in orientation, Austerdalsbreen and the upper ice falls are not visible from the lower valley.¹

Austerdalen drains southward into Veltestrønsvatn and ultimately into Sognefjord. A longitudinal valley profile levelled in 1956 from the base of the ice fall to Hafsløvatn at the southern end of Veltestrønsvatn reveals a series of rock-bars (King, 1959). Below the ice falls two rock-bars can be identified; the more northerly occupies a position transverse

¹ Slingsby (1895) comments: "Thanks to the lovely curve in the bed of the Austerdals Brae, the wondrous cirque at the head has never been seen by the Ordnance Surveyors who made many a wild guess when they mapped the Jostedal Brae and most certainly had not the remotest notion that there was to be found the finest ice-scenery in Europe." This striking valley was made known to a wider public mainly English mountaineers by Slingsby who in his classic book Norway: The Northern Playground established mountaineering as a sport. He is credited with the first exploration of Austerdals Brae in 1894 (Haugen, 1974); in 1889 he had tried to descend the ice falls but was defeated by bad snow conditions. In 1881 he had explored the adjacent Tunsbergdalsbre. He writes in 1895 "I pointed out ... the one great blank on my map which even the most casual observer must have noticed. I need hardly say that the blank was the Austerdals Brae. It was virtually a terra incognita, quite unknown to the map makers." Austerdalen lies on the margins of 1:50,000 series 1418 III (Jostedal) and 13811 (Briksdalsbreen); published 1973 by Norges Geografiske oppmåling.

to the valley trend close to the present glacier terminus. The more southerly defines the southern extent of Austerdalen which, as a result, 'hangs' above Langedalen, the adjacent glacial valley to the southwest.

The upper valley, occupied by Austerdalsbreen, is a narrow trench, approximately 1,000 m deep. Bedrock is basal Caledonian gneiss of the Jostedal complex (Holtedahl, 1960; Strand and Kulling, 1972; Carswell, 1973). The basal gneiss region, the core zone of the Norwegian Caledonides (Brueckner, 1969), lies southwest of the Trondheim Basin and northwest of the Bergen-Jotun Nappe complex (Fig. 3).

Mica-schist bands occupy an uncertain area of the upper valley. No detailed geological mapping has been carried out; Austerdalen is remote from areas of well established stratigraphy. Massive pseudo-bedding structures within the gneiss are a marked feature of both sides of the glacial valley. These structures, with an apparent 25° dip to the southeast, have clearly guided the development of upper valley side cirques; the main glacier has truncated these structures resulting in a stepped appearance of the valley sides. Unstable till slopes undergoing rapid erosion characterise the lower elevations above the glacier.

The glacier is fed by two ice falls, Odinsbre and Thorsbre, both about 800 m high and 300 m wide. A third ice fall, Lokebre, to the west, has now ablated back to the regional snow line which transverses the ice falls at an elevation of approximately 1,600 m above sea level (a.s.l.).

2.1 Recent (post 1750 A.D.) Glacier Recession

Austerdalsbreen, in common with other Jostedal ice-cap outlet glaciers, is retreating from a maximum reached during the mid-18th century (King, 1959). Measurement of the terminal activity of Jostedal glaciers commenced at the end of the last century (Faegri, 1950). Observations in the 1950's revealed that firn in the accumulation area of Austerdalsbreen was increasing in thickness. Shorter outlet glaciers such as Boyumbreen, to the southwest and Briksdalsbreen to the northwest experienced an advance during that time, but this was not seen in larger outlet glaciers such as Austerdalsbreen (King, 1959). Despite retreat, the terminus of Austerdalsbreen is active (Glen, 1960).

The marginal area of Austerdalsbreen (defined as that area exposed by glacier recession since 1750 A.D.; Andersen and Sollid, 1971) can be identified with precision. The outer, ice-distal limit is marked by a double arcuate terminal moraine dated, lichenometrically, to 1750 A.D. (unpublished 1956 work by P.J. Walker and A. Young; reported in King, 1959). Walker and Young compared the fine recessional sequence of Austerdalen with that elucidated in Nigardsdalen by Faegri (the latter published by Liestøl, 1961). Recessional moraines can be traced up to the site of the 1937 terminus, the rock bar down-valley of the present terminus (King, 1959). Glacier recession at present is too rapid for substantial recessional moraine formation; the present ice terminus is marked by annual moraines. These have been mapped by expeditions from Leicester University, U.K. (Douglas, 1970); further comparative plane table mapping was carried out in 1974 (Douglas, unpublished data).

2.1] Glacier Flow

Ice velocity along the medial line of the ice falls is of the order of $2,000 \text{ m yr}^{-1}$ at the apex, 1000 m yr^{-1} at the centre, decreasing to below 500 m yr^{-1} at the base (King, 1959). Drilling in Odinsbre ice fall during the 1956 field season indicated an ice depth of 39.3 m (Ward, 1961). In 1958 a vertical pipe was installed 1.6 km below the ice falls along the centre line. Drilling was terminated at 121 m without reaching bedrock (Ward, 1961). A gravity survey had suggested an ice depth of 90 m plus or minus fifty percent, at the same point (Bull and Hardy, 1956).

The surface of Austerdalsbreen is marked by a well-developed double ogive system on Odinsbre and Thorsbre ice. Transverse surface waves immediately below the ice falls merge downglacier into arcuate ogive banding. Bands exhibiting diffuse surficial debris alternate with clear ice bands. The lower albedo of the former results in the dominant surface character of the glacier; alternating troughs and waves. The amplitude of relief between the clean ogive crests and the debris covered troughs is not more than 1 m. The more striking development of ogive banding on the eastern half of the glacier can be related to greater quantities of surficial debris contributed by avalanche activity from Thor's Horn (Fig. 2).

The medial moraine becomes a marked morphological feature in the same zone as systematic ogive banding emerges. Here, discontinuous longitudinal debris mounds appear and merge 800 m below the ice falls to form a typical ice-cored moraine, 2,500 m

long. The moraine reaches a maximum height of 12 m relative to clean ice, about 1,200 m below the ice falls¹ (Fig. 4 a, b). The width of the moraine at this point is 40 m. Further down-glacier, width increases as height decreases and a pronounced 'beading' of the moraine commences 3,000 m from the ice falls. In the terminal zone a splaying crevasse system terminates moraine development and a distinct morphology is no longer present. Scattered superficial debris occupies a belt 200 m wide. The sediment depth on the entire moraine is less than 1 m. Rock tables, dirt-cones and melt water activity add local morphological detail.

2.12 Development of Ogives

A substantial literature is available on the development of ogives on both temperate and polar glaciers. Forbes (1859) described ogives or Forbes bands in detail, whilst Millward (reported in Forbes) had compared features developed on mudslides with ogive waves. Huxley (1857) realized from studies completed on La Brenva Glacier that the debris of dirty ogive bands was entirely superficial and could be related to the differing dust-retaining capacities of blue, coarsely crystalline ice and white ice of fine crystal size. This was re-discovered by King and Lewis (1961) who conducted experiments on the ogive suite of Austerdalsbre. Evers (1935) had earlier commented on and photographed the same ogive suite whilst Wood (1935) in reporting his rock climbs around

¹ All references made below in this thesis to moraine height or moraine relief refer to height relative to bare ice.

Austerdalsbreen stated that each ogive unit represented a year's addition to the glacier trunk from the ice falls. Leighton (1951) in a discussion of ogives proposed periodic extrusion flow whilst Streiff-Becker (1952) favoured the pressure-wave hypothesis. Nye (1959a) and King and Lewis (1961) working on Austerdalsbreen, invoked wind-blown dust, longitudinal attenuation and high melt-season ablation rates to account for qualitative and quantitative differences in ice types composing the ogive suites. Allen et al (1960) examined a weak ogive system on Lower Blue Glacier, Washington; Atherton (1963) reviewed the variety of development exhibited by ogive suites and suggested the importance of velocity changes from melt to winter seasons in explaining such differences. Hashimoro et al (1966) investigated ogives on Antler Glacier, Alaska, but added little to Atherton's conclusions. Miller (1969) reported the examination of wave ogives on Vaughan Lewis Glacier, Alaska and rejected the dominant role of ablation invoked for Austerdalsbreen by King and Lewis. Longitudinal compression and concomitant development of sub-surface recumbent isoclinal folds were considered to be important, ablation merely revealing these structures downglacier. The following discussion of the origin of Austerdalsbreen ogive suite departs little from that suggested by King and Lewis.

For most of the ablation season, an extensive snow cover is absent from the ice falls. High rates of surface velocity, resulting in extension and thinning of ice, expose a large surface area to ablation. During construction of the tunnel in the ice of Odinsbreen ice fall in 1955, 10 m of tunnel were removed by ablation during the months of July and August (Gren, 1956).

Wind-blown dust and rock debris are able to penetrate highly crevassed ice; melt water may fill some of the deeper crevasses. With freezing, blue ice-bands are formed and ice crystal enlargement may also take place (King and Lewis, 1961).

In winter while ice velocity does not change (Glen, 1956) low temperatures, extensive snow cover and snow-filled crevasses prohibit substantial incorporation of sediment or water in the icefalls.

Seracs and crevasse fillings, whether snow or ice with included dust and bedrock debris, are highly compressed in the passage through the icefalls. The decline in ice velocity from upper to lower icefalls affords some indication of the magnitude of this compression. On this basis, a maximum compression of ten times has been suggested (King and Lewis, 1961).

High summer ablation rates result in differing quantities of ice moving through the icefalls in summer and winter; these are represented by surface waves at the base of the icefalls. Wave crests represent ice passing through the icefalls in winter. The bubbly white ice of such waves contrasts with blue coarsely crystalline ice of the troughs which represent ice passing through the icefalls in summer. Downglacier, ablation removes the more chaotic surface layers and systematic ogive banding emerges. In addition, with decreasing velocity downglacier increasing compression emphasizes a distinction between light, bubbly ice and dark bubble-free bands (King and Lewis, 1961). The lower albedo of the dark ogives, consequent upon surficial concentration of diffuse englacial debris, results in enhanced ablation over these bands. A typical crenulated surface

develops with an upper value of wave height of 1 m. These wave forms are the dominant surface morphology of Austerdalsbreen.

The greater concentration of supraglacial debris on the eastern half of Austerdalsbreen can be attributed to ice avalanching below Thor's Horn. Ice moving down through this icefall encounters, at its base, little lateral containment as the valley increases in width and turns toward the southeast. As a result high rates of ice avalanching with considerable quantities of included rock debris obtain. Old dirty avalanche tracks can be distinguished from more recent avalanche tracks; the latter possess a higher albedo.

2.2 Englacial Dynamics: The Debris Throughput of Medial Moraines

Bedrock material, derived by rockfalls and slides from an extensive outcrop between Odinsbre and Thorsbre ice falls, is entrained at the margins of two ice streams by crevasse systems transgressing ogive structure. The debris is, in addition, occasionally buried by snow and ice from the ice avalanche site to the east. For such crevasse-bound material a lower depth of englacial debris penetration can be suggested (Fig. 5) which may be well-defined (Small and Clark, 1974). Penetration of the general limit may occur (Glen and Lewis, 1959), although it is

¹Slingsby (1895) utilized the rock buttress between (the then active) Lokebre and Thorsbre ice falls as a means of access to the upper ice-cap. In his account he graphically describes the mode of englacial entrainment for rock debris without realizing it. 'After crossing a weird and exceptionally deep bergschrund... the party reached the foot of the buttress; and very nasty it was too, as it consisted of steep slabs of schistose rock ready to slide down and be swallowed up by the angry jaws of the crevasse below'.

unlikely that entrained bedrock material penetrates to the base of the glacier. There is little contact between subglacial debris load and upper englacial debris for the compressive flow of the main glacier trunk at the base of the icefalls and resultant increasing ice depth (Glen, 1956) effectively sever such contact.

Debris entrained at the margins of Odinsbre and Thorsbre icefalls is progressively revealed by ablation downglacier. Discontinuous debris mounds along the medial line, with no observed systematic relationship with ogive banding, merge downglacier to form a typical medial moraine morphology. Such a zone of merging debris mounds results from continuing englacial debris supply. Isolated mounds upglacier may represent patches of englacial debris entrained in shallower crevasses at the coalescence of the ice-streams.

Differential ablation between debris-covered and clean ice results in the formation of an ice-core. Sediment depth is rarely more than 1 m and is only exceeded where morainic material is particularly coarse.

Downglacier the moraine continues to increase in height as further englacial material is revealed by ablation. The maximum height of the moraine, 12 m relative to clean ice, is reached approximately 1200 m downglacier from the base of the icefalls. The width of the moraine at this point is 40 m. The height of the moraine downglacier from this point decreases as width increases (Figs. 4, 5); lateral attenuation of sediment cover dominates over vertical development of the moraine. The maximum height of the medial moraine is 12 m, several metres greater than

an annual ablation of c. 9m (King, 1959). The ice core is thus perennial in contrast to seasonal ice cores which are generated and eradicated each melt season. Perennial ice-cores, because of greater supraglacial debris cover are not destroyed and still possess differential relief at the commencement of the following melt season (Hannell and Ashwell, 1959). It is likely on Austerdalsbreen that a perennial ice-core is associated with a continuing englacial debris supply for seasonal ice-cored forms predominate downglacier.

The moraine in its lower zone exhibits a marked beaded morphology in sympathy with ogive banding. Maximum moraine width coincides with ogives, minimum width with the light winter bands. That this is a reflection of differing seasonal quantities of rock debris entrained within the glacier (King and Lewis, 1961) can be questioned. Development of the medial moraine in sympathy with ogive banding is unlikely to represent additional accumulation derived from dirty ogives. Englacial material within these bands is negligible, being diffuse and of small particle-size. This is predominantly aeolian material blown from ice-free areas over the icefalls in summer; dust derived from rock falls may be an important constituent (Atherton, 1963). Such debris finds expression only by surface concentration. The sympathetic development of medial moraine morphology with ogive banding can best be explained by reference to the 'ablation-dominant' model (see below).

2.2.1 The 'Ablation-Dominant' Model of Medial Moraine Formation: Below Firn Line Sub-Type

On Austerdalsbreen, the highest relief attained by the moraine represents the convergence of the lower limit of englacial debris with the glacier surface. Englacial debris supply is terminated. The basic morphology of the moraine is determined by differential ablation of debris-covered and adjacent clean ice acting to produce an ice-core. This is essentially an opposite effect to that evident on the ogive suite. The height of the moraine is controlled by the relationship between sediment supply to the moraine and those forces acting to degrade the moraine by mass movement of the debris over the slopes of the ice-core. Cumulative increase downglacier of the quantity of supraglacial debris follows progressive revelation of englacial material; the moraine because of differential ablation rates between debris-covered and clean ice increases in height. In response to superincumbent debris the commencement of the ablation season of the ice-core is retarded (Østrem, 1959); a perennial ice-core develops.

Comparison of terrestrial photographs taken in 1974 from a high valley-side position with that taken by R.L. Shreve in 1959 (and published in Sharp, 1960) from almost the same position reveals greater debris quantities over the medial moraine in the later year. The 1974 photography shows the downglacier movement of rockslide debris on Thorsbre ice (Fig. 6). Boulders appear to have migrated to the margins of the arcuate sediment body. On the 1959 photography, debris on the medial moraine increases downglacier as does relief. The 1974 photography depicts moraine relief decreasing downglacier from the up-ice margin of the photograph. Clearly the point of highest relief on the moraine has migrated upglacier.

Exhaustion of englacial debris probably occurs at the present, upglacier of its point of exhaustion in 1959; a reflection of glacier thinning since that period,

2.3 Supporting Field Investigations

Field investigations were carried out on Austerdalsbreen during 1974 to consider (a) the relationship between a discrete englacial debris supply and ice-cored moraine morphology and (b) those processes operating on the ice-core after cessation of englacial debris supply.

(a) During July, 1974, in an attempt to simulate the morphological development of the moraine, an experimental trench 35 cm. deep was excavated. The trench, on a dirty summer ogive band, was filled with representative medial moraine debris. Subsequent differential ablation and development of an ice-core was monitored over a period of two weeks. With elevation of the base of the trench (i.e. the lower limit of englacial sediment) above the surrounding ogive ice surface after one week, lateral attenuation of superincumbent debris occurred. The ice-core degenerated; englacial sediment supply had ceased.

(b) Experimental plots monitored simultaneously with the trench, simulated those processes developing on the medial moraine subsequent to cessation of englacial debris supply. Medial moraine debris was placed on the same summer ogive band as the trench, in 1 m^2 plots with systematically varying sediment depth and cover values. Average ablation of the adjacent summer ogive ice during the experiment was 4.8 cm dy^{-1} (Fig. 7). The main research findings can be summarized as follows:

(1) Rock debris of varying particle size but with an intermediate axis length of greater than 10 cm, and with a depth of one grain, replicating typical distribution of such debris

on the moraine, afforded no protection of underlying ice.

- On other plots debris of particle size less than 10 mm was utilized. Similar material occupies extensive areas on the medial moraine; dirt-cones develop at those points where the depth of such sediment exceeds 1 cm. A comparable sediment depth was employed on one plot; ablation over that plot was, when an average figure was determined, only sixty percent of that over bare ice (fig. 7).¹ Dirt-cones developed.

(2) Utilizing the same particle-size (< 10 mm) at low values of cover (bare ice/sediment) and depth of sediment, ice melt was enhanced rather than retarded. With a cover of fifty percent and a sediment depth of less than 4 mm, ablation over the experimental plot was thirty percent greater than that over bare ice (Fig. 7). Observation on this plot was terminated after three days when meltwater redistributed sediment cover. Enhanced rates of ablation attendant upon thinning of surficial sediment cover have been noted elsewhere (Østrem, 1959; Mellor, 1963; Loomis, 1970; Megahan et al., 1970; Small and Clark, 1974).

(3) Lateral attenuation of surficial debris from the medial moraine occurs after the cessation of englacial sediment supply. Destruction of a distinct moraine morphology is hastened by increased water supply at the ice/sediment interface. At the same time sediment cover is reduced so differential ablation declines; enhanced ablation may instead take place. Those processes acting to produce a distinct moraine morphology are curtailed. In the terminal area a splaying crevasse system ensures complete destruction of the moraine. The nature of the relationship between ice melt and debris cover is further

examined in Appendix IV with reference to its practical applications on Berendon Glacier.

2.4 Discussion

The finer detail of moraine morphology, in particular the pronounced beading typical of the moraine, can also be accounted for by reference to the ablation-dominant model. The beading in sympathy with the dark ogive banding is developed on the glacier below the point at which all englacial debris has ablated out (x^1 on Fig. 5). The beaded form is unlikely therefore to represent seasonal differences in the quantity of entrained material. The small quantity of debris within the dirty summer ogives has already been noted. Mass movement of medial moraine debris into the faster ablating summer ogive troughs is suggested (Eyles, 1976). The beaded form is destroyed just above the terminal area by lateral meltwater streams which impose a more linear form to the moraine (Fig. 6).

Selective movement of fine supraglacial sediments into the summer ogive troughs is a feature of the glacier surface as a whole and is not limited in its effects to the environs of the medial moraine. Except in the immediate terminal area of intense crevassing, surficial debris exhibits a high, preferred concentration in the summer ogive trough. Yet much debris is, as related, derived extraglacially from the valley sides by the action of rock falls, slides and avalanches, precipitated at random onto the glacier surface (intense localization of such activity below Thor's Horn excepted).

Surficial meltwater streams were observed to have high velocities where they are entrenched through the winter ogive crests. The debris being transported by such streams is dumped where stream velocity slackens in the summer ogive troughs. Moreover, snow patches remain longer in these troughs in spring and act as filters retaining debris washed off the upstanding winter ogive crests (King and Lewis, 1961). The coarser ice crystals of the summer ogives, in addition, retain more debris along the crystal interstices. Simple washing of the ice surface with a sediment and water mixture demonstrated greater retention of debris between by the summer ogive ice crystals. Cryoconite holes are a marked feature of the troughs.

Selective movement of surficial debris serves to add local morphological detail to the gross morphology of the moraine (the latter determined by the nature of englacial debris supply). On Austerdalsbreen there is no evidence to suggest that shear planes have determined sediment supply to the moraine. Shearing activity in the manner described by Bishop, 1957 and Boulton, 1967, does not occur.

Slingsby (1895) in his early explorations of the Jostedalsglacier reports crossing two medial moraines when traversing Austerdalsbrae. A photograph in Wood (1935) shows a weak lateral moraine at the junction of Odinsbre and diminished Lokebre ice. The present glacier surface possesses only one medial moraine; the second may have represented the contribution in the past by ice from Lokebre ice fall to the main glacier trunk. Hashimoro et al. (1966) report a similar situation from the Antler Glacier, Alaska. Here a decrease in ice input from an icefall, one of two, results

in deviation of a medial moraine from the medial line to lateral margins in the upglacier direction.

2.5 Conclusion

On Austerdalsbre, the dominant processes acting to generate a distinctive moraine morphology are englacial debris supply and differential ablation of clean and debris-covered ice. Bed-rock debris is entrained from an extensive outcrop between the upper valley ice falls into the glacier body. The derivation area is below the firn line consequently debris does not undergo compaction with seasonal snow cover but is entrained englacially via crevasses to which lower depth limits apply. This upper crevasse-bound debris, in effect transported talus, is distinct from subglacial debris covered by the ice falls. With downglacier ablation, crevasse-bound debris is revealed and a prominent medial moraine is generated. The moraine increases in height downglacier and is perennially ice-cored. With revelation of the lower limit of englacial debris at the surface, debris supply ceases and the moraine morphology is truncated. Lateral attenuation of debris occurs: if critical debris thickness and cover values are reached ablation rates over the ice-core may be accelerated. Seasonal ice-cored morphology predominates downglacier where small-scale processes act to redistribute moraine sediments.

3.0 THE ABLATION-DOMINANT MODEL. ABOVE FIRN LINE SUBTYPE: BERENDON GLACIER

3.1 Introductory Discussion

In glaciers where ice-streams coalesce in the accumulation zone medial moraine debris derivation areas not only include extraglacial rock slopes but extend to subnival and subglacial bedrock outcrops. The debris derivation zone in effect extends throughout ice depth. Debris derived extraglacially is not entrained in crevasses on Austerdalsbreen but undergoes compaction and sedimentation with seasonal snowfall.

By virtue of deep debris entrainment in the accumulation zone medial moraines and septa may not attain surface expression until well downglacier. In addition an important subglacial component may be contributed to the moraine (Fig. 1). With cumulative ablation downglacier, progressive increase in the quantity of supraglacial sediment may occur all the way to the terminus, giving rise to a distinct morphology in the terminal zone. Thus it can be suggested that lateral attenuation of debris cover is offset by a continuing englacial debris supply. This is in contrast to the situation where debris is entrained below the firn line as is the case of Austerdalsbreen where moraine debris is limited in its englacial distribution to upper levels of the glacier.

Prominent medial moraines ablate out only in the immediate terminal zone of Berendon Glacier on both North and South Arm ice. Ice falls near the glacier terminus, by accelerating ablation rates, may serve to enhance supraglacial development though debris

quantity, in addition to deep burial in the accumulation zone, may also determine retardation of medial moraine development. Glaciers, in many instances reveal little debris along the medial line for there may be few extraglacial rock slopes contributing debris to the firn area. Indeed debris content may be so low that individual ice-stream components of the main glacier become difficult to distinguish (Haumann, 1960).

3.2 The Physical Setting, Berendon Glacier

Berendon Glacier, Stewart, British Columbia (Latitude $56^{\circ}50'N$, Longitude $130^{\circ}5'W$), possessing a drainage basin area of 53 km^2 , is located within one of the major metal mining areas of western Canada: the Boundary Ranges of the northern Coast Mountains (Fig. 8).

The nearest settlements, Stewart, B.C., and Hyder, Alaska, lie within 50 km of the glacier, at the head of the Portland Canal. Originating to the east and separate from the large firn basin of the Frank Mackie Glacier, Berendon Glacier consists of two branches, North and South Arms, which coalesce 2.8 km above the glacier terminus. Subsequent ice flow direction is east into the Bowser River valley (Figs. 9, 10, 11 and Table I). In the terminal zone South Arm ice approaches a prominent rock barrier between Summit Lake to the south and Tide Lake Flats to the north. Summit Lake is impounded by Salmon Glacier to the south; up to 1971 lake overspill water flowed north across the divide into the Berendon Glacier basin and subsequently into Bowser River. Lake formation and catastrophic drainage to the south under Salmon Glacier has been described by Gilbert (1969, 1972) and

TABLE I

Dimensions of Flow Units Composing Berendon Glacier and Associated Medial Moraines											
A. S. Arm Origin	(a) Flow Unit	(b) Medial Moraine	(c) Debris Lithology	(d) Greatest elevation m	(e) Terminal elevation m	(f) Firn Elevation m	(g) Length above (f) km	(h) km below (f)	(i) Total Length km	(j) Width (m)	(k) Width (m) Above confluence
Western Basin	A			2100	800	1250	4.00	3.75	7.75	196	128
Western Basin	B			1800	700	1250	4.65	4.63	9.28	180	128
Western Basin	C	S1, SII	Red silt	1900	700	1250	4.75	4.63	9.38	106	55.1
Western Basin	D			1800	700	1250	4.25	4.63	8.88	30	37
Eastern Basin	E	SIII	Green volc. Conglomerate	1900	700	1250	3.0	4.63	7.63	30	155
Eastern Basin	F	SIV		1600	700	1250	4.5	4.63	9.13	30	111
Eastern Basin	G			1650	700	1250	4.8	4.63	9.43	135	~
Eastern Basin	H			1750	1000	1250	5.25	2.5	7.75	60	~
Eastern Basin	I			1900	1050	1250	5.5	2.25	7.75	105	not present
Eastern Basin	J			1600	1100	1250	4.5	1.2	5.7	50	not present
Eastern Basin	K			1600?	1200	1250	4.0	1.0	5.0	100	not present
B. N. Arm											
	A	NI		1600	650	1250	1.75	4.7	6.45	60.1	105
	B			1900	650	1250	3.75	4.7	8.45		192
	C	NII		2300	650	1250	3.5	4.7	8.2	70	60
	D	NIII		2100	650	1250	2.5	4.7	7.2	123	90
	E	NIV		2000	700	1250	2.82	4.5	7.32	105	52
	F			1900	850	1250	3.86	3.75	7.61	165	122
	G			1900	850	1250	2.75	3.75	6.5	150	157
	H			1600	900	1250	2.45	3.57	6.2	90	35

Mathews (1965 and 1973). Annual lake levels since the late sixties have not attained those reached earlier and overspill waters no longer escape to the north. With further thinning and recession of Salmon Glacier complete drainage of Summit Lake can be expected. A similar history has been described for Tide Lake Flats, five km to the north, where varved lake clays and subaerially eroded deltas provide evidence of glacial lake ponding (Hanson, 1932). Lake water was impounded initially by ice of Frank Mackie Glacier, subsequently by a lateral moraine left as the ice receded. Haumann (1960) has described lake shorelines which are still well-preserved. The lake drained for the last time in 1930.

Berendon Glacier has attracted much interest recently by its proximity to copper concentrating facilities and a mine access tunnel portal controlled by the Granduc Operating Company of Vancouver, British Columbia. The glacier terminus lies within 200 m of the plant which commenced full-scale production in late 1970. Berendon Glacier is presently experiencing recession leaving a suite of well-defined lateral and terminal moraines. The marginal area close to South Arm ice is marked by formation of annual moraine ridges. Such ridges constitute sensitive indicators of the variability of recent retreat.

Untersteiner and Nye (1968) on the basis of 'a good deal of guesswork' estimated the change in mass balance required for terminal readvance. It was concluded that even allowing for drastic climatic deterioration, terminal readvance reaching the Granduc facilities is unlikely within the next two decades. More detailed field measurements have been made since 1967 by

the Glaciology Division of Inland Waters Directorate, Environment Canada. These enabled Fisher and Jones (1971) to comment that the possibility of terminal readvance is greater than that suggested previously. Since 1968 mass balance studies indicate a net balance that is slightly positive.

The present glacier terminus is complex; warm waste water from Granduc mill is released into the glacier system. The terminal area is marked by ice-cliffs and open ice-walled channels; these can be explained by reference to a Karst cycle of development. Shearing activity in response to subglacial obstruction of flow by bedrock adds further complexity to the terminal area.

Granodiorite bedrock outcrops in the terminal zone of Berendon Glacier. The granodiorite, part of the Summit Lake Stock (Grove 1971), intrudes siltstones and argillites of the Bowser assemblage and tuffs and volcanic conglomerates of the Hazleton assemblage. The remainder of the Berendon Glacier area lies outside the limits of detailed geological mapping (J. Smith, pers. comm. 1975).

3.3 Climate

The following summary description of the pattern of climate experienced by the Stewart area is based on a number of sources.

The essential characteristics of climate in southeastern Alaska and the Boundary Ranges result from a coastal location. Storage of heat in the Kuroshio current and easterly flow of Pacific air-streams generate humid mild conditions in this high

latitude region (Heusser, 1952); the climate of this region has been designated sub-Arctic rain forest (McKenzie, 1970). West-facing coastal slopes generate heavy orographic precipitation ranging from an annual average of 175 cm at Stewart (Grove, 1971) to 207 cm at Wrangell and 377 cm at Ketchikan (Kincer, 1941). Rainfall totals decline rapidly inland; annual precipitation at Telegraph Creek may be as low as 20.5 cm (Heusser, 1952). At Petersburg, 160 km to the southwest, precipitation averages 265 cm. Similarly, orography accounts for exceptionally high snowfalls (greater than 2,500 cm at Tide Lake) at high altitude; an annual fall of 250 cm can be expected at sea level. Winter conditions are marked by a rapid succession of intense cyclonic disturbances, generated on the Maritime Arctic front; southerly winds predominate. Settled weather and northerly winds in winter are associated with extension of Arctic high pressure. Miller (1969) examined the historical variation in the pattern of storm tracks affecting the coastal flanks of the Alaska/Canada Boundary Range.

On the Pacific Coast winter temperatures are severe only at high altitude (Miller, 1951); temperatures decline inland. The January average at Ketchikan is 0.3°C . In summer northward movement of the north Pacific High generates northeasterly moving maritime tropical air masses giving a humid, cool summer at coastal locations. July average temperatures range from 12.7°C at Sitka to 14.5°C at Wrangell (Kincer, 1941). Inland, temperatures vary with altitude, aspect and extent of surrounding ice cover. Adkins (1958) has examined the summer climate in the accumulation area of the Salmon Glacier, at an

altitude of 1,700 m. High rainfall totals may be reported in the fall in response to the reappearance of Pacific cyclones moving onto the coast.

In the vicinity of Berendon Glacier possible local climatic change may be generated by glacier recession and glacial lake drainage. This has been remarked upon by McKenzie (1970) in Adams Inlet, Alaska but remains untested in the vicinity of Stewart. Climatic data since 1906 for Stewart are presented in Appendix V. The climatic gradient between Stewart at the head of the Portland Canal and Berendon Glacier has recently been examined in part by McMechan (1975).

Apart from max./min. temperature measurements during the first week of August (for analysis of ablation rates over artificial experimental plots) temperature and rainfall records were not systematically kept during the summer of 1975.

The nature of the summer climate of Berendon Glacier is worthy of more intensive research. Upper basins of North and South Arm Ice frequently received little rain when Tide Lake in the main Bowser/Salmon valley experienced rain and low cloud. In general, upglacier winds were associated with rain. Important contrasts can also be made for Tide Lake Camp and Stewart. Simple application of altitude correction factors for Stewart climatic data is, in the opinion of the writer, not warranted.

3.4 Bedrock Geology

Snow and ice obscure 65% of the 52.8 km² basin of Berendon Glacier which occupies rocks of Mesozoic and Tertiary

age on the eastern margin of the coast crystalline belt. The Bowser Basin, into which Berendon discharges from a westerly position, occupies a tectonic depression between Coast and Cassiar Crystalline Belts (Kerr, 1948; Grove, 1971).

A detailed geology of the basin is not available; discussion of bedrock geology presented below is based on extensive, rather than intensive, field observations made during 1975, data from Granduc Operating Company concerning bedrock geology adjacent to the Granduc access tunnel, and the work of Grove (1971). The last is concerned in part with the eastern outlet of the basin near Tide Lake Flats; the terminology of Grove has been adopted, however, for the whole of the basin. A detailed discussion of the basins is beyond the scope of this thesis; with further research modification of the geologic sketch map (Fig. 12) can be expected. A geologic map of the Portland Canal area was published in 1935 by the then Bureau of Economic Geology of the Department of Mines. The basin of Berendon Glacier is depicted but only general geologic relationships are apparent. The map coincided with the publication of Memoir 175 'Portland Canal Area, British Columbia' by G. Hanson. A review of the economic development of the area, and activity of the British Columbia Department of Mines, the Geological Survey of Canada and the United States Geological Survey is presented by Grove (1971).

Bedrock adjacent to Granduc's access tunnel to the Granduc ore body is well-known; a drilling program during 1963 in upper South Arm basin of Berendon Glacier established bedrock relationships at depth. The nature of subaerial bedrock exposure over those areas of the basin north and south of the

tunnel line is not known in any detail however.

Three rock-types characterize the basin of Berendon Glacier (Fig. 12). Occupying southern and eastern sectors are volcanic tuffs and conglomerates of the Hazelton assemblage of Lower Jurassic age. These are revealed with clarity in South Arm basin. Upper Jurassic strata; argillites and siltstones of the Bowser assemblage, compose the median ridge dividing North and South Arm basins, and the northern areas of the basin. The outcrop is extensive although exposures are obscured at higher altitudes by snow and ice cover and at lower altitudes by valley-side slope debris. The most recent bedrock within the basin is a granodiorite stock of Tertiary age. The Summit Lake Stock occupies the eastern margins of the basin and floors terminal ice of Berendon Glacier.

The Hazelton assemblage of lower Jurassic age comprises lithic graywackes, volcanic conglomerates and included tuff bands. These are epiclastic strata with included pyroclastic members; 'where doubt occurs the rocks can be regarded as tuffaceous sediments' (Grove, 1971). These rocks are limited to the basin of upper South Arm. The best exposures are presented by east-facing extraglacial rock faces in the Western basin of South Arm. Fig. 12 depicts this outcrop as a westerly projection of strata revealed outside the drainage basin proper on east-facing slopes of Summit Lake basin. Hazelton assemblage strata outcropping within the drainage basin appear to represent a northwesterly extension of a large north-south outcrop of Hazelton strata extending south as far as Stewart. Lithological variations within the belt as a whole are described by Grove.

In the absence of lithological analysis in South Arm basin prominent colour differences allow crude stratigraphic divisions to be made. In the firn basin of South Arm examination of the prominent median ridge separating Western and Eastern basins allows discrimination between purplish-red and green members. The lowermost sections of the ridge are formed of a purply-red tuff overlain at height by a green member. An indistinct contact has an apparent westerly dip; the upper green member is of a coarser grain-size and will be referred to in this thesis as a volcanic conglomerate to distinguish it from the underlying purply red tuff. A maximum thickness of green volcanic strata of 150 m is apparent on the ridge. This colour and textural distinction is faithfully reflected in the medial moraines present on South Arm ice below the firn line. Medial moraines derived from ice streams draining western margins of the ridge are composed of debris derived from the green volcanic conglomerate while eastern ice streams entrain debris of purplish-red tuff. Folding with a westerly dip has been mapped by Grove (1971) in Hazelton strata on east facing slopes of Summit Lake basin; westerly dipping Hazelton strata in South Arm basin may be related.

East-facing slopes of the western firn basin of South Arm are composed of the same strata. The contact between lower red tuffs and upper green conglomerates is not revealed, but the contact is present subglacially for red tuff debris is an important component of the large central medial moraine generated by the confluence of North and South Arms. Contact between Hazelton strata and surrounding bedrock is exposed free of snow

and ice cover and in vertical section only, on east facing slopes of the Western basin. Bowser assemblage strata outcrop to the north of the contact where a black schistose/outcrop exhibits clear compression and shearing structures; minor quartzite bands are present and are represented in avalanche debris below.

" Bowser assemblage strata of Upper Jurassic age occupy the central ridge between North and South Arms; a steep (80°) southwesterly dip predominates. Prominent siltstone components can be observed on north and south-facing slopes of this ridge and are clearly continuous. The most extensive outcrop of Bowser assemblage strata lies above South Arm ice. Dark grey, black and buff coloured siltstones and argillites dominate. Steeply dipping beds may be responsible for irregularities and inflections in the ice surfaces of North and South Arms closely adjacent to the median ridge. Regionally, Bowser sediments are composed of two members; lower sandstones and conglomerates which rest unconformably upon strata of the Hazelton assemblage, and an upper siltstone and sandstone member (Grove, 1971). The Hazelton-Bowser assemblage contact while readily observable along Betty Creek, east of Berendon Glacier terminus, is not encountered within the drainage basin.

Northern slopes on rounded summit areas overlooking North Arm ice are of Bowser assemblage strata and reveal a high (80°) dip apparent to the west; outcrops are obscured by bedrock debris. The prominent backwall area of North Arm firn basin (Fig. 11) is the most westerly exposure examined during the 1975 field season; the serrate nature of the backwalls

and ridges of Mathews Cirque to the southwest suggests that the western limits of Bowser assemblage strata lie in this area. Andesite is recorded in the Granduc tunnel log lying west of argillites and siltstone of Bowser assemblage beneath South Arm; however the northern extent of andesite is unknown.

Part of the Coast Crystalline Belt, a light grey hornblende granodiorite of the Summit Lake Stock occupies 25% of basin area. Subaerial exposures are limited to eastern and southeastern sectors of the basin. Much of the terminal area of Berendon Glacier is composed of granodiorite; recently deglaciated areas provide excellent exposures. Generally, contact between the Summit Lake stock and country rock is characterized by much pyritization and silicification. In the southeast sector of the basin, contact between granodiorite and Hazelton assemblage strata is revealed subaerially 0.5 km east of Sunkist survey station. Grove (1971) describes the relationship between Summit Lake intrusion and Texas Creek and Hyder plutons to the south. The granodiorite of the Summit Lake pluton is more akin to that of the Hyder intrusion of Tertiary age and is probably a satellite body of the latter.

In the terminal area of Berendon Glacier, granodiorite has been intruded by fine-grained diorite dykes; these appear relatively more resistant to glacial erosion and differential relief is common.

In the west and northwest the granodiorite contact with Bowser assemblage siltstones and argillites is subglacial but is revealed in the Granduc tunnel. By interpolation from this con-

tact to a clear subaerial contact, adjacent to Motherball Survey Station (Figs. 10 and 12), the Bowser assemblage/granodiorite contact appears to parallel South Arm before cutting across the combined North and South Arms below the confluence zone.

3.41 Local Structures

The tectonic setting of Bowser Basin will not be considered; only local structures occurring within Berendon Glacier basin, and seen to affect bedrock or glacier topography will be discussed. On granodiorite in the terminal zone lineations are apparent from field and air photograph analysis. These range in size from less than 150 m to 1.5 km in length. A major bedrock lineation runs west from Granduc processing mill; Granduc access tunnel crosses this, a major fault, at depth. Smaller lineations to the north and south have a more northerly orientation. Grove (1971) has described characteristics of regional faulting predominantly of a north-south trend in the vicinity of Summit Lake. In that area old overflow channels from Summit Lake run north-south and are fault-guided. In the terminal area it is apparent that local faulting of a predominantly easterly trend determines variation in apparent dip directions exhibited by a pronounced pseudo-bedding structure in the Summit Lake granodiorite (Fig. 9). Pseudo-bedding dip is between 30° to 45° and bed thickness is generally of the order of 10 m. The bedrock strike has been emphasized by glacial erosion and runs west-east, parallel to the direction of ice-flow. Berendon Glacier in the immediate terminal zone swings to the north and crosses this pronounced strike, affording opportunity for subglacial

cavitation activity (Chapter 6).

Air photographs suggest that strike of the pseudo-bedding structures is not constant but runs parallel to the trend of the contact between granodiorite and country rock. Stresses generated during emplacement of the stock may be responsible for the development of pseudo-bedding structures.

A. 3.5 South Arm Medial Moraines

The following discussion of medial moraines generated above the firn line in South Arm basin falls into two parts. In Part A, medial moraines are related to debris derivation sites above the firn line. Upper South Arm basin above the confluence ice falls is described and component ice streams evacuating bed-rock debris are demarcated. The nature of ice flow exhibited by individual ice streams is discussed. Rock slopes in the glacierized basin are classified according to the nature of their contributions to the glacier debris system. Medial moraine derivation sites are well-defined and fall into a peculiar and unique category of rock slopes. Derivation areas are then related to the manner of outcrop of medial moraines below the firn line.

In Part B, medial moraines developed downglacier of the confluence icefalls are described and moraine morphology is considered in detail. The nature of englacial debris supply to moraines is established. Determinations of ice velocity and strain rate allow examination of the relationship between the nature of ice flow and medial moraine morphology. Final conclusions are stated at the end of the following chapter, which considers the morphological development of medial moraines

formed above the firn line on North Arm ice.

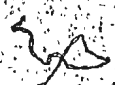
Whilst debris sample sites are described, the sedimentological character of debris released from upper South Arm basin and removed from the basin as medial moraines is considered in Chapter 6.

3.51 Medial Moraines of Upper South Arm Basin

Upper South Arm Basin. Upper South Arm is defined as that area of the basin above the confluence ice falls (Fig. 9). At the confluence ice falls South Arm is approximately 0.5 km wide; width increases upglacier. At the snow line (~ 1250 m. a.s.l.) the Arm is 1.25 km wide (Table 1). One km upglacier of the snow line a prominent ridge separates Western and Eastern basins. Each basin is 2.5 km long and 2.0 km wide.

The Salmon/Berendon Glacier divide lies at the head of Western basin at an elevation of 1620 m. a.s.l. In Eastern basin a divide at varying elevation (1800 - 2100 m. a.s.l.) defines the upper firn basins of small glacier tongues (Blue and August Mountain Glaciers) which descend westwards to the Salmon drainage system.

Nature of the Ice-Flow. The direction of ice flow above the firn line is to the north; below the firn line flow direction alters to a northeast bearing (Fig. 11). Ice streams draining Western and Eastern basins can be traced downglacier by analysis of air photographs and consideration of debris septa outcropping between ice streams (Figs. 11, 13 and Table 1). A prominent longitudinal foliation is present on South Arm ice downglacier of the confluence ice falls. This foliation is a secondary



structure and can be related to primary sedimentary layering in the firn basin. Firn layers are rendered arcuate downglacier by differential flow velocities in the same fashion as that described by Hambrey (1975) from Charles Rabotbre where arcs, convex downglacier, characterize the two main flow units of the glacier and represent original sedimentary layering tilted and deformed by flow. Folds become increasingly attenuated downglacier and a longitudinal foliation is generated. Arcuate banding on South Arm does not transgress the outcrops of debris septa and has clearly formed in contributing firn basins prior to septa formation by confluence of adjoining ice streams. An alternative situation, where folding takes place subsequent to the formation of debris septa is found on Lower Blue Glacier (Allen et al., 1960). As a result convex arcs transect septa outcrops, having formed at the base of an ice fall. Ice falls are absent from both upper North and South Arms on Berendon Glacier and longitudinal foliation on North and South Arms remains unmodified in the down ice direction; transverse ice dykes and welded-snow crevasse-fillings (along with included debris) imported to surface ice by the confluence ice falls, are eradicated by ablation. The absence of any modification of longitudinal foliation downglacier suggests there may be little deformation of ice by the topographic bed; on Lower Blue Glacier, for example, replacement of longitudinal foliation by other types is considered to be generated by the nature of the glacier bed (Allen et al., 1960). Only on the western margins of South Arm ice have bedrock structures determined the nature of glacier flow. Steeply dipping strata of the Bowser assemblage along the median

ridge possess a northwest/southeast strike. Close to the glacier margin the strike outcrop often takes on a pronounced ledge-like form, associated with which are small ice falls.

3.6 Medial Moraine Derivation Sites

Medial moraine derivation sites are identified and related to the outcrop pattern of medial moraines downglacier. The nature of debris generation and release from rock slopes in the upper basin is discussed and related to the pattern of ice cover; medial moraine derivation sites are found to be characterized by a distinctive mode of debris generation. In this section emphasis is placed on the morphology of debris derivation sites: the sedimentology of released debris is discussed together with medial moraine debris from terminal South Arm in Chapter 6.

3.61 Classification of Bedrock Slopes

A simple classification is found to be of use when considering bedrock slopes of Berendon Glacier basin (Fig. 14). Type I bedrock slopes contributing freshly released (primary) debris into the glacier debris system and found above the firn line can be contrasted with slopes of Type II and III, characterized by extensive deposition of glacial debris found over the remainder of the basin.

Type I slopes above the firn line, are found as nunatak areas surrounded by snow and ice cover. An upper ice and snow carapace is separated by rock slopes from the low gradient firn

45

basin (Fig. 15). Primary debris is generated subglacially by upper ice cover and is precipitated onto the firn surface below by avalanche activity. There is no deposition of debris on bedrock walls.

Below the firn line Type II slopes are characterized by till deposits from former more extensive ice cover and secondary removal of this debris predominates. Distinctive slope forms such as rock-chutes and extensive gully systems are common (Fig. 14). Primary debris generation rates are low.

On Type III slopes, bedrock is obscured for the most part by till, and geomorphic activity is related exclusively to secondary recycling of old glacial load. Immature soil development is common.

Medial moraine derivation areas are limited entirely to slopes of Type I character. Consequently medial moraines generated above the firn line evacuate primary debris from the firn basin; no secondary recycled debris is involved.

Slopes of Types II and III will not be discussed further here; such slopes contribute recycled debris to lateral moraines and consequently determine the nature of debris input into the medial moraine formed by confluence of North and South Arms.

3.62 Type I Slopes

Above the firn line valley side walls protrude through snow and ice cover isolating a lower firn basin surface of low gradient from an upper snow and ice carapace (generally above 1900 m. a.s.l.). Side wall height attains 500 m. in some cases. Extraglacial rock walls are found mainly on the western margins

of Western and Eastern basins (Figs. 14 and 15). In the Western basin the upper ice carapace descends to the firn basin ice either by flow as small narrow ice-streams or by avalanching. The margins of descending ice streams, which isolate sidewall segments are characterized by a very high incidence of avalanche activity. In the Eastern basin, however, east-facing side walls are continuous; descending ice-streams are absent and upper ice cover descends to the firn basin solely by avalanching.

In both basins, snow ramps against the valley side walls serve as receiving areas for bedrock, snow and ice debris released by avalanches. The debris undergoes seasonal sedimentation with the snow pack. Dirty avalanche fans are found only below unstable ice cover and the quantity of debris released from bedrock areas not capped by ice cover must be low. There is no evidence for the deposition and accumulation of bedrock debris on valley side walls and it can be suggested that extra-glacial, subaerial processes acting to release bedrock debris do not operate at a high rate. A thick basal debris layer is observed in the upper ice cover and debris inputs from Type 1 slopes into medial moraines are considered to consist primarily of debris released from such basal positions. Consequently subaerial contributions to the moraines in the firn basin consist of subglacially derived debris.

3.7. Bedrock Geology of Medial Moraine Derivation Sites

Type 1 slopes are associated in particular with brightly hued and green volcanic tuffs and conglomerates of the Hazleton assemblage whose distribution in upper South Arm basin is depicted in Fig. 12. Since the central ridge separating Western

and Eastern basins is composed of Hazleton strata, medial moraines formed above the firm luge evacuate bedrock debris from this source (Fig. 11). A major division has been made of the Hazleton assemblage strata along the ridge (pg. 37). The lower free faces and buttresses of east facing rock slopes in Eastern basin are developed on a distinctive red tuff referred to as the lower member of the Hazleton assemblage (pg. 37). The composite ice-stream d (Fig. 11 and Table 1) evacuates debris dumped on the extensive linear snow ramp at the base of free faces in Eastern basin. The ice-stream can be traced down-glacier to the terminal zone and is associated with medial moraines S1 and S11. The cap rock along the central ridge is a green volcanic conglomerate which dips westward. As a result ice stream f evacuating the western slopes of the central ridge entrains green conglomerate debris (medial moraine SIV). Sub-aerial bedrock exposures of green conglomerate are few: moraine debris revealed along the ice-stream downglacier must therefore be subglacially and subnivally derived in the upper basin. Debris released from both sides of the ridge is deeply buried in the firm basin and only attains marked supraglacial expression in the terminal zone of South Arm.

Originating from a pronounced eastward embayment in the western slopes of the median ridge a narrow 30 m wide ice stream (e, Fig. 11) can be identified in the terminal zone of South Arm ice, where a medial moraine (S111) outcrops along the contact of ice stream e with ice-stream f. Bedrock debris encountered along this septum appears to be green volcanic conglomerate and red tuff.

Ice marginal debris septa associated with flow units g, h and i above the confluence ice falls can be traced downglacier into the moraine formed by confluence of North and South Arms, and form the central and southern debris bands of this moraine (pg. 82). These marginal flow units can be related to ice inputs from hanging glaciers descending from high elevations on the western limits of Western basin; the ice-streams are narrow and of no great depth and thin out downglacier. As a result there is a large supraglacial debris input into the confluence area on western marginal ice of South Arm.

3.71 Debris Sample Sites

Sites were chosen in the upper basins with the object of sampling the debris contained in dirty avalanche fans below Type I slopes. Sample sites are described below and depicted in Fig. 14.

3.72 Western Basin

3.72 (i) Sample Site 1 (Elevation 1600 m a.s.l.; samples S6, S9, S14; volcanic conglomerate)

Sample site 1 lies 100 m below the northern margin of a small glacier tongue which descends at a high angle (50 to 60°) from the extreme southwestern margins of Western basin. The glacier tongue is about 200 m wide; although depth is unknown it is sufficient to allow confluence with the main firn basin. The margins of the glacier tongue are cliffed; sample site 1 is sited on a prominent avalanche track of high surficial debris

content. Bedrock is green volcanic conglomerate of the Hazleton assemblage. Maximum debris size observed was 0.5 m. Debris is clearly derived from the basal debris layers exhibited in upper ice cover.

3.72 (II) (Sample Site 2, Argillite)

Sample Site 2 lies at an altitude of 1450 m a.s.l., 1.9 km downglacier from Sample Site 1. The site lies near the contact zone of Bowser and Hazleton assemblages (Figs. 12 and 14a), debris is derived from the former. As at Site 1, debris is derived from basal debris layers of upper ice cover.

3.73 Eastern Basin (Sample Site 3) Samples S2, S12, S5: Volcanic tuff and Conglomerate

The site is located at the northern extremity of the central ridge separating Western and Eastern basins. A variety of bedrock debris types is found amongst chaotic ice and snow avalanche debris. Red tuff debris from subglacial load of local ice predominates (Sample S5). Other debris is derived from the upper volcanic conglomerate cap rock (Samples S12 and S2).

The cap rock cannot be seen directly due to obscuring upper ice cover and the presence of volcanic conglomerate amongst avalanche debris indicates subnival and subglacial derivation below the upper ice carapace.

B. 3.8 Medial moraines of Terminal South Arm Ice

Medial moraines on South Arm are primarily a feature of terminal ice and are not well developed upglacier; the relationship between ice-streams moving out of South Arm upper basins and medial moraines downglacier is depicted in Figs. 11, 13 and Table 1. The relationship between englacial debris supply, the pattern of ice flow and medial moraine morphology will be examined.

3.81 The Terminal Zone

The terminal area of South Arm is defined as that zone downglacier of the terminal icefalls (Fig. 9), which are characterized by large transverse crevasses extending across the centre line of the glacier onto North Arm ice. The northwest margin of the icefalls appears to demarcate a pronounced step in the granodiorite bedrock floor. The step parallels the contact of the Summit Lake stock with the surrounding Bowser assemblage. Crevasse width increases to the southeast and may indicate a greater step height in this direction. In addition the direction of ice flow of the glacier terminus swings to the north in this area generating further extensional strain.

A splaying crevasse system dominates the immediate terminal area of South Arm. Pronounced longitudinal foliation can be traced over the entire terminal area and the foliation is seen to be severely compressed close to outcropping medial moraines. Below the terminal ice falls a series of ice-hummocks characterize the glacier surface. The steep terminal ice front is greatly affected by splaying crevasses oriented subparallel to

outcropping medial moraines. In addition shearing activity, in response to basal obstruction of glacier flow by subglacial rock outcrops, has severely affected the terminal outcrop of medial moraines and englacial moraine debris has been sheared upward to the ice surface. Shearing activity on North and South Arms is briefly discussed and disruption of the ice front by Granduc waste water outfall described in Appendix II.

3.82 Medial Moraines

Four distinct medial moraines outcrop in the terminal zone of South Arm (Fig. 16). Southern and Northern moraine groups (Moraines SI, II, and SIII and SIV respectively) can be identified on the basis of debris lithology. The southern group is derived from red volcanic tuff of the Hazleton assemblage. The northern moraine group is composed of a distinct green debris derived from volcanic conglomerate of the Hazleton assemblage. Moraine SIV is characterized by a large boulder size; the largest size measured was 1.5 x 1.5 x 1.5 m.

On the basis of bedrock lithology medial moraines in the terminal zone of South Arm ice can be traced to specific derivation areas in the upper basins of South Arm ice (Figs. 11, 12). Moraines SI and SII are composed of debris evacuated by ice flow units draining east facing slopes of the Eastern basin (volcanic tuff). Moraine SIV evacuates west facing slope areas of the Western basin (volcanic conglomerate). Moraine SIII appears to be of composite lithology containing tuff and conglomerate debris.

Extensive deposition of debris from medial moraines is only a recent phenomenon of the marginal area. The role in terminal deposition played by medial moraines has increased as the glacier thins and exposes greater quantities of moraine debris. Increased exposure of supraglacial debris as a result of glacier recession has also been noted by Salisbury (1894) and Østrem (1965).

3.83 Outline of Field Procedure

The relationship between moraine morphology and the nature of englacial debris supply was examined by clearing superincumbent debris from areas of the moraines so that englacial debris could be observed. Moraines of especial interest were mapped by plane table, and long and cross profiles were constructed by altimetry and pacing.

Collection of supraglacial and newly revealed englacial debris was made for particle-size analysis. Sedimentological analyses are reported in Chapter 6 in conjunction with North Arm and central medial moraine debris and that from other elements of the glacier debris system.

Longitudinal strain-rate, velocity and ablation were determined from observations of a line of stakes parallel to moraines SI and SII. Stake movement was determined by repeated measurement to bedrock outcrop with the aim of assessing the relationship between the nature of glacier flow and medial moraine morphology.

3.84 Medial Moraine Morphology

Moraine SI developed at the contact of ice streams C and D, attains marked supraglacial expression between the confluence and terminal ice falls (Fig. 13). Moraine debris can be traced back up through the confluence ice falls and is present on serac surfaces. The quantity of supraglacial debris is very low and, as a result, the amount of debris precipitated into confluence ice fall crevasses is insignificant and there is no widening of the moraine outcrop below the ice falls. The margins of moraine SI above the terminal ice falls are well defined. The marked longitudinal foliation present on South Arm ice contributes to the definition of moraine margins; enhancement of ice melt over the debris septum adds further definition. Melt water streams below the terminal ice falls are laterally confined by upstanding white foliation ice; debris movement by supraglacial streams is limited to certain foliation bands which, as a result, resemble linear debris strips or pseudo-medial moraines (Fig. 17). A distinct moraine morphology is terminated by passage through the terminal ice falls (Fig. 18).

The moraine, in passing through the terminal ice falls, loses much supraglacial debris into crevasses; ablation down-glacier of closed crevasse remnants produces transverse debris ridges possessing a firm ice core (Fig. 19) which attain lengths of 10 m and are, in some cases, 1.5 m wide. However, the transverse ridges are destroyed by the steep slopes of the terminal zone and the activity of supraglacial meltwater streams. Marginal slopes, draining southeast away from the moraine account for

the increasing width of the moraine in the terminal area; and there is no further development of ice-cored topography.

Moraine SII attains supraglacial expression only in the immediate terminal area of South Arm. It emerges through debris derived from moraine SI as a well-defined ice-cored ridge and survives downglacier for 40 m. prior to destruction by crevasses associated with the steep slope of the ice front (Figs. 16, 17). Ridge height averaged 1.5 m toward the close of the melt season. The debris is of the same type as moraine SI and the two moraines are clearly related to the same debris septum. The development of a medial moraine ridge below the ice falls is a clear indication of continuing englacial debris supply reflected in the development of an ice core by moraine SII.

Moraine SIII. To the north and adjacent to moraine SII a longitudinal trough (10 m. wide) increases in depth downglacier to a maximum of 3 m. at the point where it is destroyed by crevasses. Along the median line of the trough a small debris-poor septum outcrops (moraine SIII). This can be traced in the up ice direction, to the foot of the terminal ice falls. Septum width does not exceed 0.3 m. and as a result the moraine is poorly developed. The quantity of supraglacial debris is insufficient for development of an ice-core; on the contrary, because of low debris depths the rate of ice melt is accelerated.

Moraine SIV. Above the terminal ice falls moraine SIV is represented by individual boulders (up to 40 cm in diameter) rather than by a distinct debris septum (Fig. 11). It achieves marked supraglacial expression on the down ice flank of an ice

hummock at the base of the terminal ice falls (Figs. 19, 20, 21). The height of the ice hummock above the surrounding ice surface is 8 m. The height of the moraine ridge increases to a maximum of 2.5 m, 50 m downglacier from the point of origin; the ridge collapses downglacier (Fig. 20) as a result of meltwater streams flowing across the moraine. The range of clast size exhibited by moraine SIV is the greatest present on medial moraines on Berendon Glacier. The largest block approached 8 m.³ in volume.

3.9 The Nature of Englacial Debris Supply

3.91 Field Procedure

Areas were selected along South Arm medial moraines to ascertain the nature of englacial debris supply and to collect samples of newly revealed debris for sedimentologic analysis (Fig. 22). Areas along the medial moraine centre lines were cleared of all supraglacial debris. These sites were inspected periodically; determination of ablation rates was made by reference to stakes.

3.92 Results and Interpretation

Moraine S1. An area of the moraine adjacent to stake 8 of the central stake line was cleared; debris depth was 3 cm. At the end of one month no further debris had ablated out. A debris sample of supraglacial debris was collected at stake 14 (Sample S16).

Moraine S11. The prominent debris ridge of moraine S11 is truncated in the immediate terminal zone by splaying crevasses. Cross

sections of englacial debris present below the moraine surface are afforded and indicate continued englacial debris supply to the moraine. This accords with observations from that area of the moraine (Fig. 22) cleared of supraglacial debris.

Moraine SIII. Whilst a cleared area adjacent to the terminal ice front (Fig. 22) demonstrated a continuing englacial debris supply, only a small quantity of debris was revealed. The moraine is an insignificant component of the total medial moraine debris load of the glacier. A debris sample of existing supraglacial debris load (Sample D15) was taken.

Moraine SIV. Two areas were cleared of all supraglacial debris on this moraine: (1) where moraine morphology is well-developed and (2) where moraine morphology has collapsed (Fig. 22). Both sites revealed continuing englacial debris supply (Fig. 23) and collapsed morphology is related to meltwater flowing across the moraine in response to transverse surface slope. A sample (S4) was taken from newly revealed englacial debris.

3.93 Discussion: The Nature of the Debris Throughput

A continuing englacial debris supply is associated with an ice cored ridged morphology in the terminal zone (moraines SII and SIV). Whilst moraine SIII is marked by a continuing englacial debris supply the quantity of englacial debris is insufficient for an ice core to develop.

In contrast moraines developed on the glacier surface above the terminal ice falls do not possess an ice core and moraine width remains constant over considerable distance

(Fig. 24). Englacial debris supply to the moraine would not appear to be constant and attains higher rates in the terminal zone where the bulk of moraine debris emerges. Under conditions of constant englacial debris distribution moraine width increases systematically downglacier (Salisbury 1894). Debris quantities along the moraine have been estimated (Fig. 25) and it can be seen that debris supply to the moraines upglacier of the terminal ice falls is minimal. The majority of moraine debris would appear to be evacuated from the upper basins as deeply entrained near basal load. Debris revealed upglacier is clearly more shallowly entrained, is of low quantity and probably related to debris inputs from Type I slopes in the firn basin. The suggested englacial distribution of debris through the glacier cross section is depicted in Fig. 26, a, b. If the distribution with depth were constant moraine width would increase downglacier (Fig. 26c) in response to increasing supraglacial debris quantities (Fig. 25, curve B).

3.94 Glaciological Determinations

Field Procedure and Rationale

Stakes were inserted along the median line of South Arm ice below the terminal ice falls adjacent to medial moraines SI/II. Three objectives were considered: (1) the measurement of variation in ice velocity close to the terminus; (2) determination of the longitudinal strain-rate in the region of prominent outcropping medial moraines; (3) measurement of ablation. The dynamic influence of the character of ice flow on South Arm medial moraines below the terminal ice falls might then be

assessed. Ice in the terminal zone may be considered as existing in one or more of three states (Lilboutry, 1965): (i) Ice composing the snout may stagnate and dam more active ice up glacier; severe compression in the terminal area may result. (ii) Ice in the terminal zone may be moved as a rigid non-deforming body. Deformation may then occur only in the zone of compression up glacier (Glen, 1960). (iii) Flow and deformation of ice may occur throughout the terminal zone.

The highest upglacier stake of the line (Fig. 27) was sited in the lower icefalls. Above this, surveying access and line of sight were limited by highly crevassed ice. The Wild T-0 theodolite was unsuitable for measuring short distances of stake movement using valley side markers and such sight lines would have been tangential to the ice surface. Tacheometric measurements were therefore made from a bedrock tie at the terminal end of the stake network to each successive stake upglacier to stake 15 in the lower ice falls. It is not possible therefore to record the true horizontal vector of ice movement; only ice movement along a vertical plane through the stakes is determined. Strain rate and velocity data are expressed as annual rates. Measurement intervals are short and measurements were made during the melt season when locally high rates of velocity may obtain (Meier, 1960); and as a result velocity and strain rate data has been used with caution. Ablation data were collected from the same stake line.

3.95 Results

High compressional strain-rates predominate in the terminal zone of South Arm (Fig. 28). Ice of the immediate terminal area is experiencing downglacier movement of 28.25 m yr^{-1} (Fig. 29) as a rigid body however and is experiencing no longitudinal strain. It is under this section that the Granduc outfall passes and the resulting accelerated basal melt makes it unlikely that this ice is in contact with the bed. Positive, extensional strains over that area between stakes 5 and 6 (Fig. 28) are reflected in splaying crevasses cutting across moraine outcrops; the pattern of serac movement adjacent to crevasses may be more erratic than surrounding ice. Thus velocity, whilst decreasing with distance from the ice fall base increases downglacier from stake 4 to the terminal ice front; a reflection of increased surface slope.

Ablation rates were measured along the stake line for three periods and reveal enhanced melt-rates in the vicinity of the terminus (Fig. 30). However increased debris depths ($> 10 \text{ cm}$) in the immediate terminal area give rise to low ablation rates.

A simple interpretation of strain rate data is impossible because of rapidly decreasing ice depth as the terminal area is approached and possible loss of contact with the glacier bed. Moreover, ice near a receding terminus cannot be in a steady or annually repeating state. Glen (1960) encountered similar problems in analysing strain rates from the snout of Austerdalsbreen and stated that the best analysis is probably an empirical search for correlations between the various parameters such as

ablation, surface slope, vertical velocity and longitudinal strain-rate. Correlation of ice structures with local strain-rate is usually unsuccessful since structures are usually formed upglacier under differing conditions of strain rate. Strong longitudinal compression of longitudinal foliation close to moraine SIV is apparent and air photographs suggest a crenulate outcrop of medial moraines on South Arm (for example 1972 aerial photography: Appendix II). It cannot be stated however that a fundamental relationship exists between the character of ice flow and moraine morphology. The evidence from South Arm appears to support Small and Clark's statement that whilst the nature of strain-rate is a factor to be taken into consideration, at best it is an indirect determinant of moraine morphology (Small and Clark, 1976). Evidence from Berendon Glacier has already indicated the fundamental importance of englacial debris supply. Strain-rates are seen to determine the character of the ice surface on which a distinct moraine morphology can develop. Thus the predominance of compressive strains in the terminal area results in a simple uncrevassed ice surface, and in response to a continuing englacial debris supply, ice-cored moraine ridges develop.

4.0 THE ABLATION-DOMINANT MODEL; ABOVE FIRN LINE SUBTYPE. 'NORTH ARM MEDIAL MORAINES

The following analysis of medial moraines developed on North Arm follows the scheme established for South Arm (Ch. 3.0). In Part A medial moraines are related to debris derivation sites above the firn-line. Upper North Arm basin is defined and component ice flow units evacuating bedrock debris identified. The bedrock geology of the basin and the nature of ice flow is discussed. Debris sample sites from derivation sites and medial moraines are described. Debris derivation sites in the upper firn basin are interpreted according to criteria used for Upper South Arm basin.

In Part B medial moraines exhibited on North Arm downglacier of the confluence zone are described; the morphology of one moraine is considered in detail. The pattern of englacial debris supply to the moraine is examined and debris sample sites described.

In Part C final discussion is presented. The sedimentology of North Arm medial moraines will not be discussed in this chapter but will be considered in conjunction with moraines from South Arm basin and other elements of the glacier debris system in Chapter 6.

Part A: Upper North Arm Basin

4.1 Basin Morphology

Upper North Arm Basin is defined as that area above the confluence zone (Figs. 9, 10). The upper basin occupies 14.5 km² or 44% of the total glacierized area of Berendon drainage basin. The component ice-streams flowing from the upper basin of North Arm are portrayed in Table 1. North Arm is 700 m wide at the confluence with South Arm ice. At 1,250 m a.s.l. (snow line position, late August 1975) width of North Arm is 1,500 m; glacier basin width at Snafu survey station increases to 7 km (Fig. 10). In this area of the basin, ice-streams converge below a prominent subaerial backwall. The ice-shed of North Arm and Frank Mackie Glacier to the west is aligned north-south, the highest point of the divide being 2,300 m.

Morphological divisions within the accumulation zone of North Arm are clear. Sub-parallel to the 1,600 m a.s.l. contour a bedrock rim (Bowser assemblage) breaks through snow and ice cover as a north-south backwall 1.5 km long, .75 km east of Snafu Survey station. Upper ice cover to the west of the backwall moves out of the basin by avalanching over the backwall. Where ice cover is more complete, to the north and south of the backwall, passage of ice over the bedrock rim generates a series of ice steps. A further series of ice steps characterizes the most southerly ice stream-components of North Arm (a,b,c,d) at 1,350 m a.s.l. (Fig. 11). Ice steps in this area appear to be determined by northwesterly extension of bedrock from the median ridge separating North and South Arm basins and may be related

to similar forms on the lateral margins of South Arm to the east, since westerly dipping bedrock structures are observed to traverse the ridge.

The prominent backwall, near its southern termination, is obscured by ice (ice-stream c) descending from Mathew's cirque as a true ice fall. To the north and south snow and ice avalanches derived from upper ice cover sweep over the backwall, depositing dirty avalanche fans in the lower firn basin. The backwall, together with scattered bedrock outcrops at the same elevation to the south, constitutes an important debris source area for medial moraines.

4.11 Medial Moraines

Below the snow line, three clearly defined medial moraines outcrop between ice streams c, d, e, f; moraines NII, III, and IV respectively (Figs. 11, 12). Debris quantities on the moraines are small; moraine width averages 4 m and no ice core has developed. Acceleration of ice melt rates has taken place along these medial moraines and their associated diffuse septa extensions. Longitudinal snowbanks which over some areas survive the entire melt season occupy areas of lower relief generated during the previous melt season.

4.12 Bedrock Geology

Bedrock exposures are less clearly revealed than in South Arm basin and accessible subaerial exposures are few. The central median ridge is known to be of argillite/siltstones of the Bowser assemblage and steeply dipping beds (70° west) observed on

the south side of the ridge are persistent to the north and typify north facing slopes of upper North Arm basin. Close inspection of North Arm backwall is not possible; bedrock of this area is identified as Bowser strata on the basis of rock samples from avalanche fans. These observations have been supplemented by consideration of debris outcropping along medial moraines in the terminal zone of North Arm ice; argillites and siltstones predominate.

The location of an andesite body intruding argillite/siltstones is not known; on the basis of Granduc's tunnel geology map, andesite may occur in the far western limits of North Arm basin (Fig. 12).

4.13 Ice Structures

Ice structures developed on North Arm ice above the confluence zone can be divided into (a) persistent and (b) non-persistent types. (a) Persistent structures, a pronounced longitudinal foliation, are generated from primary stratigraphic layers forming in the upper firn basin and are similar to that described from upper South Arm basin (p. 43). Sedimentary layering is rendered arcuate downglacier by differential transverse ice velocities and arc apices become increasingly attenuated downglacier. Ultimately longitudinal foliation is generated. Boudinage is a feature of arc limbs. (b) Non-persistent structures are imparted to southern ice stream components by major ice steps above the snow line. Snow-filled crevasse remnants are rendered arcuate downglacier, imparting a second arcuate banding to near surface ice, which conflicts with that generated

by deformation of original sedimentary layering. Non-persistent arcuate banding is eradicated by ablation downglacier.

4.2 Debris Generation Sites in Upper North Arm

4.21 Introduction

Sites of primary debris generation are few and well defined; secondary erosion of debris on extraglacial slopes below the regional snow line dominates current subaerial geomorphic activity. The character of debris removal from North Arm is less diverse than that from South Arm. In North Arm sites of subaerial primary debris generation are located on backwall bedrock areas and can be considered, within the classification evolved for analysis of South Arm extraglacial slopes, as Type I slopes (p. 44).

Slopes of Types II and III occur over the remainder of North Arm basin. These slopes do not contribute debris to medial moraines formed above the firn-line; and are consequently not discussed in detail below. Slopes of Types II and III characters contribute debris into the moraine formed by the confluence of North and South Arms.

In the upper basin an extensive snow ramp forms a toe slope to the backwall. The height of the ramp averages 80 m and the upper ramp surface parallels the 1,500 m a.s.l. contour. A prominent bergschrund may be identified from aerial photographs but field identification proved more difficult. Upper ice cover above the backwall, which may reach 200 m in height possesses a cliffed profile; only over a limited area is a

gently sloping terminal profile apparent.¹ A basal debris layer is exhibited by all upper ice cover irrespective of terminal profile. These layers are discontinuous and are found at various levels above the bedrock-ice contact. Debris is unlikely to have been incorporated by pressure-melt; englacial shearing and upward dispersal of debris from the bed is suggested. The debris is released by avalanching and contributed to the snow ramp at the foot of the backwall where the debris then undergoes compaction with seasonal snow cover. The highest rates of avalanche activity appear to obtain at the northern and southern extremities of the backwall. The distribution of areas possessing high avalanche activity is reflected in the outcrop of medial moraines which attain marked supraglacial expression as debris septa, immediately below the firn line.

4.22 Field Procedure - Debris Sample Sites

Sample Site 1 (Fig. 14). Dirty snow and ice avalanche tracks close to the northern extremity of the backwall were examined and a sample taken of newly released debris (Sample N1). The sample site lay at an elevation of 1,390 m a.s.l.. Despite subaerial release from the backwall debris was clearly released from the basal layers of upper snow and ice cover. In response to dispersed surface debris acceleration of snow melt-rates had taken place resulting in a depression of the track surface.

¹ Comparison of Boundary Survey Commission photography, exposed by White Fraser, in 1905 with present field observation indicates slight recession of the upper ice cover and areal expansion of extraglacial bedrock outcrops.

compared with surrounding clean snow. Ice blocks imbedded in the snow surface by impactation and ablation hollows added further surface variety.

Sample Site 2 (Medial Moraine NIV). Bedrock debris released from Sample Site 1 is evacuated from the basin as medial moraine NIV. Two sample points were selected along the moraine in upper North Arm basin: (a) at the head of the moraine, at that point where supraglacial outcrop is distinct (Sample N 3) and (b) 1 km downglacier (Sample N 4).

Part B: North Arm Terminus

North Arm ice enters the south western limits of Tide Lake Flats as a low gently sloping ice surface with no well-defined ice front (Fig. 31a). Increased morphological definition is apparent close to the medial moraine at the contact of North and South Arm ice since a distinct ice front in this area has been generated by the release of Granduc mill water into the glacier system; the area is marked by ice-cliffs (Appendix II). An ice-cored ramp with a flat upper surface slopes gently northeastward and seems to extend glacier ice over the northern area of the terminus. Superincumbent debris is a medium sand derived from Granduc's particulate outfall in waste mill water; active kettle hole formation is in progress (Fig. 31b).

The terminal area is marked by prominent shear plane outcrops (Fig. 31c) which in the immediate terminal area are associated with the transfer of basal debris to the glacier surface. Subglacial debris is added to medial moraine sediments

(Appendix 11).

The immediate terminal area experiences changing flow direction from that maintained upglacier and the outcrop of medial moraines undergoes a 15° change in orientation as the terminus is approached (Fig. 31a). Increasing northward flow may represent divergent flow around a subglacial westerly extension of the granodiorite rock barrier near King survey station. This divergent flow may increase in the future as terminal ice thins.

4.3 Medial Moraines of Terminal North Arm

Upglacier of Motherball Survey Station, North Arm ice is composed of few distinct flow units (a-b-c, d, e and f-g-h, Fig. 11). In the downice direction ice streams a-b-c and d broaden and can be subdivided into component ice-streams by emerging medial moraines. Debris septa upglacier are well developed compared with those on South Arm, and are a feature of the ice surface over the whole ablation area maintaining a constant width over several km. of the glacier surface. The northernmost septa formed at the margins of ice-streams d-e, e-f (moraines NIII and IV) exhibit increasing supraglacial debris load below Motherball as parent ice-streams thin out. The northwestern margin of North Arm ice consequently carries a large marginal debris load which is extensively ice-cored. Moraine NI ablates out in the immediate terminal zone, whilst moraine NII can be traced as a debris septum upglacier. The terminal area is little crevassed by comparison with South Arm and simple ice-cored ridges have developed though ridge

height nowhere exceeds 1.5 m.

4.31 Field Procedure

Moraine NI was selected for intensive field study. In contrast to other moraines on North Arm terminus it is well-defined: the moraine exhibits full development of morphological characteristics associated with medial moraines of much greater length. Changing moraine width was recorded (Fig. 20) and records of ablation were kept for two periods over the entire length of the moraine (Fig. 30) by reference to a stake line (Fig. 27) from the moraine head (Stake 1) to the terminus (Stake 9). Debris and bedrock samples were collected from the moraine and areas were cleared of all supraglacial debris to determine the nature of englacial debris supply to the moraine. Samples were collected of newly revealed englacial debris.

4.32 Moraine Morphology (Moraine NI)

The length of the moraine is 450 m and whilst a debris poor septum can be traced upglacier for a further 200 m, debris cover only becomes complete 80 m downglacier from the head of the moraine. This downglacier section possesses an ice-core and is characterized by a high concentration of dirt-cones, the highest found on the surface of Berendon Glacier (Fig. 32). Moraine width increases systematically downglacier from the head though minor crevasses strike across the moraine between stakes 4 and 7 (Fig. 20). Upglacier of that point where moraine debris cover becomes complete ice melt-rates are accelerated in response to diffuse debris cover and a negative

moraine relief relative to surrounding bare ice is generated. Downglacier, dirt-cone formation takes place and a primitive seasonal ice-core develops reaching a maximum height of 0.75 m at stake 9. Throughout the length of the moraine the lateral margins remain well-defined as a result of melt streams flowing parallel to the moraine outcrop.

4.33 Debris Sampling and the Nature of Englacial Debris Supply

Sites along the moraine were selected with the object of investigating (1) the nature of supraglacial debris; (2) the presence and nature of englacial debris delivered to a supraglacial position.

(1) The first objective was attained by sampling of debris in the vicinity of stakes 5 and 9. Samples are considered representative of debris on the moraine at these points.

(2) At stakes 1, 5 and 10 all supraglacial debris was removed from an area of 1.5 by 1.5 m (Fig. 22). Areas were inspected periodically thereafter. All sites revealed englacial debris being delivered to the surface by ablation; the entire moraine length is characterized by a continuing englacial debris supply. Freshly revealed englacial debris (Sample N7) was sampled from stake 1 (Fig. 33). The highest quantities of englacial debris are associated with the area near stake 1. Ablation measurements at stakes 1, 5, 10 taken concurrently with observation of the cleared debris areas indicate that greater delivery rates at stake 1 are not the result of higher local ablation rates but of greater concentrations of englacial debris.

4.4 Discussion

4.4.1 Nature and Distribution of the Debris Throughput and Moraine Morphology

The relationship between medial moraines and primary debris generation sites above the firn line is depicted in Figs. 11, 12 and 14. Those medial moraines attaining supraglacial expression immediately below the regional snow line can be related to prominent subaerial bedrock exposures (e.g. medial moraines at the margins of ice streams c-d, d-e, e-f; moraines NII, NIII, NIV respectively). Medial moraines emerging only in the terminal zone such as moraine NI lack subaerial bedrock origins and moraine debris is clearly derived at depth in the firn basin. The release of deeply entrained englacial debris in the terminal zone is associated with the development of an ice-core and increasing moraine width. Upglacier moraine or septa width remains constant (Fig. 24) and englacial debris is only added to the glacier surface in small quantities. Indeed small supraglacial debris quantities result in accelerated ice melt rates and a depressed surface morphology often occupied by linear snow banks until late in the melt season (e.g. 1964 aerial photography, Fig. 13b). Debris additions from an englacial position to the moraines are not significant until a terminal or near terminal position is reached. The situation depicted in Fig. 25, curve B, is not supported by evidence from medial moraines of North Arm and on Fig. 25 a revised curve is presented (Curve Y).

Medial moraine debris of North Arm is composed thus of two populations; that removed from the basin subglacially being

revealed in the terminal zone and that released subaerially from upper unstable ice cover above Type I slopes in the firn basin. The latter component is still subglacially derived however. This element need not be universally present in medial moraine sediments for if the moraine lacks subaerial derivation areas in the firn basin (such as moraine NI) moraine debris is only derived at depth and is evacuated as deeply entrained englacial load. Evidence will be discussed in Chapter 6 that indicates that the bulk of moraine debris is carried near the bed. Contrary to the opinion of Stiglbury (1894) but in agreement with Hess (1907 a,b) and Small and Clark (1976), subglacial debris is added to moraine sediments in the terminal zone. The more striking development of debris septa on North Arm compared with South Arm can be related to the more extensive outcrop of Type I slopes in the firn basin. Evidence from both Arms substantiates the remark of Haumann (1960) that the degree of development exhibited by debris septa is an index of the activity of extraglacial bedrock slopes in the firn basin. Total debris quantities from this source would appear to be small however for despite cumulative ablation downglacier from the snow line, septa width remains constant; increasing width is also prohibited by lateral containment of moraine debris by longitudinal foliation (Fig. 19). Thus it would appear that whilst englacial debris extends throughout glacier depth in the fashion depicted by Sharp (1948) (Fig. 26c) the distribution of debris with depth is not constant (Fig. 26, a, b) and the bulk of moraine debris is carried at depth. The sudden emergence of debris in the terminal zones such as moraines SIII, SIV and

NI suggests the existence of a cut-off between basal load and more diffuse upper englacial debris.

This model of moraine formation, where moraines are generated above the firn line finds some support in the literature. Loomis (1970) related the unchanging width of a medial moraine on Kaskawulsh Glacier with absence of englacial debris supply though the morphological model is not explicitly developed by Loomis. On Kaskawulsh Glacier formerly distinct debris bands merge downglacier and lose their individual identity. By comparison Young (1953) demonstrated a continuing englacial debris supply to medial moraines developed on Breidamerkurjökull by the presence downglacier over a considerable distance of distinct debris bands.

The role of longitudinal strain rates in determining moraine morphology cannot be definitely stated. Compressional strains in the terminal zone correspond with the emergence of greater quantities of englacial debris and similarly, upglacier, areas of low supraglacial debris cover are characterized by extensional strains. The increased supraglacial expression of medial moraines below icefalls (such as on South Arm) may reflect compressive strains in addition to the acceleration of ablation rates. Ablation rates may be high in icefalls (Glen, 1956, Wojcik, 1970) and may generate higher debris delivery rates to the surface. However on Berendon Glacier increasing moraine width below icefalls is a reflection of crevasse-entrained debris recycled to a supraglacial position. Extensional strains and associated crevassing hasten the collapse of moraine morphology on the Lower Glacier de Tsidiore Nouve following ces-

sation of englacial debris supply (Small and Clark, 1976). This may not be the case on Austerdalsbreen, since in the area of collapsing moraine morphology the glacier surface is crevasse free.

Ice-cores on Berendon Glacier can be demonstrated to be of seasonal occurrence. The glacier surface was first inspected by the writer during mid-June when the snow-line lay at 750 m a.s.l.. At this time no differential relief between debris covered and bare ice profiles was apparent. An ice-cored morphology which, at the close of the melt season, nowhere possessed a differential relief greater than 1.5 m is destroyed following the termination of melt season conditions. During the second week in September, from general observation, and not measurement, it was apparent that some reduction in the relative relief of debris-covered and bare ice profiles was taking place. The mechanism may be one of increased radiation absorption by debris compared with bare ice over which ablation had almost ceased. It is not known however whether eradication of differential relief is complete by the time of permanent snow cover.

With particular reference to dirt-cone formation, the seasonality of ice-core formation has been discussed by Hannell and Ashwell (1959) and Wojcik (1970).

On glacier surfaces where destruction of relative relief can be demonstrated it appears that degradation of ice-cores is a function of insufficient supraglacial debris. Maximum supraglacial debris depths rarely approach 5 cm on Berendon Glacier; ice-cores developed during summer melt periods are

ephemeral.

4.5 Conclusions

Above firn line subtype, Berendon Glacier

(1) Medial moraine morphology is primarily dependent upon the nature of englacial debris supply. The relationship between longitudinal strain rate and morphology is at best an indirect one; whilst some compression and concentration of englacial debris-rich foliation is indicated in the terminal areas, strain rate affects moraine morphology by determining the nature and extent of surface crevassing. Minor, ephemeral relief forms may be added to the moraine by recycled supraglacial debris. Crevassing determines the clarity with which moraine morphology, fundamentally related to englacial debris supply, is exhibited on the glacier surface. Seasonal and perennial ice-cored moraine morphologies can be distinguished.

(2) Where moraines possess derivation areas above the firn line englacial debris is not limited to upper crevasses but extends throughout ice depth. Debris added to the firn surface and derived from subaerial bedrock exposures and associated ice cover, undergoes sedimentation with seasonal snowfall and is ultimately evacuated at depth which with subglacial and subnival bedrock derivation results in an englacial debris column that extends from the glacier surface to the base.

(3) Moraines formed above the firn line are characterized by both a continuing englacial debris supply and a developing ice-cored morphology in the terminal zone (moraines SI, II, III, IV).

(4) The distribution of englacial debris within the glacier body is not uniform and as a result delivery rates to the surface are not constant. The distribution of englacial debris is not that depicted by Sharp (1948) in Fig. 26c. Up-glacier of the terminus, there is little release of englacial debris to the moraines and supraglacial debris quantities remain low. Moraine width does not change over considerable distances and because of low supraglacial debris quantities an ice cored morphology is not generated. Indeed, as a result of small debris quantities acceleration of ice melt rates and the production of a depressed morphology can occur. Delivery of englacial debris in sufficient quantity for generation of ice cores is a feature only of the terminal and near terminal zones. An upper cut-off in englacial debris supply is indicated. On Berendon Glacier the bulk of moraine debris is removed from the upper basins, at depth, near the bed.

(5) Subglacial debris is added to the moraines in the terminal areas. Upper englacial debris of small quantity, revealed upglacier, is derived from subaerial rock slopes and associated ice cover in the firn basins. This debris element is present throughout ice depth and is revealed as a result close to the firn line; the more marked development of medial moraines immediately below the firn line on North Arm is a reflection of the greater debris contribution by subaerial bedrock walls in the firn basin compared with South Arm. On the latter medial moraines exhibited immediately below the firn line are few in number. However, the more marked outcrop of medial moraines on the terminal ice of South Arm suggests greater subglacial

erosive activity in the upper firn basin compared to North Arm where moraines do not exhibit comparable debris quantities in the terminal zone. The remark of Rothlisberger (1968) that the study of medial moraines should give some clues particularly to the erosion at depth in the high areas of a glacier is substantiated.

5.0 THE ICE-STREAM INTERACTION MODEL OF MEDIAL MORaine FORMATION

Distinct ice structures are known to develop where large valley outlet glaciers converge (Brecher, 1969; Anderton 1970; Loomis 1970). In these zones, medial moraines are often formed by the merging of lateral moraines. In the 'ice-stream interaction' model it is suggested that ice flow such as lateral compression between the merging ice streams, longitudinal strain-rate and ice velocity determine the morphology of the moraine rather than the nature of englacial debris supply. This model can be tested on Berendon Glacier where North and South Arms combine.

5.1 Central Medial Moraine

5.12 Morphology

The central medial moraine on Berendon Glacier is generated by the confluence of North and South Arms about 2.2 km above the terminus (Figs. 10, 11). The moraine can be divided into three zones: (1) the immediate confluence area; (2) down-glacier to the terminal icefalls; (3) below the terminal icefalls and in the terminal area. A distinct moraine morphology is found in zone (1) as a response to the peculiar pattern of ice flow and associated ice structures found in that zone. In zone (2) these ice structures and a distinct moraine morphology are eradicated and are replaced by a more simple pattern of ice flow and a simple, immature moraine morphology. Below the terminal ice falls i.e. in zone (3) the quantity of supraglacial debris along the moraine rapidly increases and, despite severe cre-

or confluence medial moraine; the terms will be used interchangeably.

vassing there is some development of an ice-cored form.

5.13 (1) The Confluence Zone

The central medial moraine consists of three lithologically distinct debris bands; northern, central and southern (Fig. 34). The southern and central bands are carried into the confluence area by South Arm ice and originate in the Western basin of Upper South Arm which is developed on Hazleton assemblage volcanics. These two bands form the bulk of medial moraine debris; total supraglacial debris quantities remain small in contrast to the substantial lateral moraine debris loads carried by both Arms above the confluence. This lateral debris is englacially ingested into marginal crevasses and little supraglacial debris is introduced to the confluence zone. A large debris pool is present submarginally in the confluence zone (Fig. 35). Debris from North Arm is elevated, possibly by shearing, along the contact with South Arm ice; in this fashion a third distinct debris band, the northern, is generated. This band which is composed of three longitudinal debris ridges serves to demarcate the contact between the two Arms; a quartz-rich tuff and an argillite predominate among debris of this band.

The nature of ice flow through the confluence area imparts a characteristic form to the moraine. South Arm ice enters the confluence area as an ice fall at a high angle to that of North Arm; the ice fall base is undergoing severe compression. Wave forms and a series of ice bulges in adjacent North Arm ice testify to lateral compression between the two Arms.

5.14 (2) Downglacier to the Terminal Icefalls

The distinct morphology imparted to the moraine in the confluence area is lost downglacier as the pattern of ice flow becomes more simple. Whilst individual debris bands can still be identified the morphology of the moraine above the terminal icefalls is indistinct and the constituent debris bands are not ice-cored. Distinct debris ridges of the northern band are eradicated above the terminal ice falls. Differential relief over the moraine developed as the melt season progressed; rock tables and scattered dirt-cone groups added diversity to a moraine morphology of little relief. Differential relief over the moraine is of seasonal development only. Moraine width (about 40 m) does not change downglacier; surface slope is low and the glacier surface declines only 80 m in elevation over a distance of 900 m. The contact between North and South Arms can be traced downglacier to the terminal ice falls but below these it cannot be identified.

5.15 (3) Below the Terminal Icefalls

Below the terminal icefalls a splaying crevasse system and calving from terminal ice cliffs associated with the passage of Granduc Mill outfall water (Appendix II) disrupt moraine development. Despite much greater quantities of supraglacial debris an ice-cored form is poorly developed and individual debris bands described from the medial moraine above the terminal ice falls cannot be distinguished. However an additional debris component is added to the moraine for red tuff of the Hazleton assemblage is revealed below the terminal

ice falls. Moraine width reaches 100 m. in the terminal zone; whilst the northern margin of the moraine is well-defined, to the south the margin is not clearly demarcated and moraine debris is lost by ice calving from terminal ice cliffs.

5.2 Debris Bands of the Central Moraine

The three dominant longitudinal debris bands composing the central moraine will now be discussed.

5.2.1 (a) Northern Debris Band

The northern band serves to demarcate the contact of North and South Arm ice and represents collapsed and merged till ridges formed in the immediate confluence area. A distinctive debris colour allows discrimination between debris of this northern band and that of the central band. The former is composed of a quartz-rich tuff weathering to a distinctive red colour, no subaerial outcrop of which was observed in North Arm basin. As till ridges collapse, the band width increases although debris delivery to the surface is still limited to the well-defined longitudinal contact between North and South Arm ice.

Three debris ridges present in the confluence area die out in the down ice direction, but one distinct ridge demarcating the North/South Arm ice contact can be traced down-glacier to the terminal ice falls. Despite a debris depth of 5 cm., in some areas, an ice-core is not generated and acceleration of the rate of ice melt occurs. Following collapse of formerly distinct till ridges the width of the debris band is

approximately 6 metres. The northern debris band is only disrupted by crevassing in proximity to the terminal icefalls.

5.22 Central Debris Band

The central debris band is composed primarily of green volcanic conglomerate of the Hazleton assemblage which can be related to derivation sites in the Upper basin of South Arm (pg. 48). Supraglacial debris is ingested by the transverse crevasse system associated with the confluence ice falls. Transverse till ridges result from the ablation of crevasse-bound debris of the ice fall base; these rapidly degenerate downglacier as englacial debris is exhausted and a diffuse supraglacial debris cover results. Dirt-cone development and supraglacial stream activity add morphological diversity. The line of contact with the northern debris band is determined by lithological contrasts.

5.23 Southern Debris Band

The southern debris band can be traced as a distinct debris septum upglacier and related to debris derivation sites in the firn basin. Debris is transported through the basin between flow units g and h (Fig. 11). The diffuse debris surface of the southern dirt band is a response to disruption of the debris septum during transit through the confluence ice falls; band width may approach 10 m. A longitudinal zone of clean ice divides central and southern debris bands.

5.3 Longitudinal Strain-Rate, Ice Velocity and Moraine Morphology

It was considered desirable to investigate the nature of downglacier longitudinal strain-rate and velocity close to the central medial moraine. Longitudinal strain-rate and flow velocities have been measured close to moraines S1 and S11 outcropping on terminal ice of South Arm. While discussion of the results (pg. 59) indicates only a minor role played by longitudinal strain-rate in determining moraine morphology, conditions of ice flow found in the terminal area are relatively more simple than those occurring in the confluence zone.

5.31 Field Procedure

A line of 26 stakes was set up along the medial moraine on the northern margin of South Arm ice from the terminus (stake 1) to the confluence zone (stake 26), a distance of 2,101 m. The stake network was tied to a prominent bedrock marker (Fig. 27) at the confluence. Stake velocity and strain-rate were determined by repeated measurement of position by tacheometry from the bedrock marker, in the same fashion as that described for South Arm stakes (pg. 58).

5.32 Longitudinal Strain-Rate; Results (Fig. 36)

No simple pattern of strain-rate fluctuation is apparent. Extensional strains occur immediately downglacier of the confluence (stakes 26 and 25) whilst compressional strains prevail downglacier to stake 22 and severe compression is evident in the region of stake 20. Extensional strains predominate

downglacier as ice moves through the terminal ice falls and whilst compressional strains are low in this zone severe compression occurs at the ice fall base. Downglacier of stake 8 South Arm ice is increasingly disturbed by terminal ice cliffs and splaying crevasses, reflected in widely fluctuating strain-rates. There appears to be no simple relationship between strain-rate and moraine morphology; the simple subdued moraine morphology revealed upglacier of the terminal ice falls can be contrasted with the complex pattern of strain occurring over this area.

5.33 Velocity Determination - Results

Velocity data presented in Fig. 37 were obtained by successive measurement over a period of two weeks. The central stake line was not redrilled following determination of stake position in late July. Stake 26 was redrilled and velocity determinations made there until September (Table 2).

Relatively high stake velocities associated with stakes 26 and 25 ($52, 81 \text{ m yr}^{-1}$ respectively) decline to a steady value at stakes 24, 23 and 22 (30 m yr^{-1}). A low velocity at Stake 20 disturbs a trend of increasing velocity which attains a maximum value of 87 m yr^{-1} at stake 18. Downglacier, velocity rates decline though a simple decreasing trend is disturbed by stakes 12 and 13. The velocity data strengthen the suggestion made above that any relationship between moraine morphology and the character of ice flow is at best an obscure one. It is not possible to link the pattern of ice flow with moraine morphology in any systematic fashion.

TABLE 2Velocity measurements at Stake 26

<u>Time interval</u>	<u>Velocity yr.⁻¹ (m)</u>
17 - 30/7	50.82
30/7 - 17/8	59.41
17/8 - 1/9	36.48
17/7 - 1/9	52.68 (Mean for period of measurement)

5.34 Ablation Measurements: Results (Fig. 38)

Ablation rates are found to increase downglacier whilst below the terminal ice falls increased depths of supraglacial debris account for the great variation in ablation data. The absence of a well-developed ice-cored moraine morphology indicated that further analysis of ablation was not required.

5.4 Confluence Zone Ice Structures and Moraine Morphology

The relationship between ice structures developed in the confluence zone and the morphology of the central medial moraine will be considered. The morphology of prominent ice structures is described for both Arms and related to the pattern of ice flow. A further series of field measurements was made for this purpose.

5.41 The Confluence Area and the Central Medial Moraine

A well-defined contact zone between North and South Arm ice is observed in the confluence area and individual character of the two ice-streams is still retained. The medial moraine formed in this area extends 2.2 km downglacier from an elevation of 950 m at the confluence to 650 m at the terminus. The morphology of the medial moraine in the confluence area can be related to the contrasting character of confluent ice streams from North and South Arm basins. North-Arm ice moves through the confluence area carrying little supraglacial debris, is little crevassed and deviates little in flow direction as the confluence area is passed (Fig. 34). In

addition, surface slope, except for local steepening above the confluence, is low. On South Arm however, flow direction alters by 45° . Above the confluence South Arm ice is heavily crevassed following transit through a 100 m high ice fall. North Arm ice contributes only submarginal debris to the confluence zone (Fig. 35). No supraglacial lateral moraine is added by the Arm to the central moraine which in the immediate confluence area is composed entirely of South Arm debris.

The differing mode of debris transport by North and South Arm ice can be related to the character of crevassing immediately up ice of the confluence zone. North Arm ice exhibits large marginal crevasses and steep surface slope above the confluence area and a large supraglacial debris load, derived by mass movement from Type II and III slopes, is englacially ingested. Debris is introduced into the confluence area submarginally and is transported out of the confluence along the contact of North and South Arm ice. Shearing between the two arms may play some role in elevating debris to the surface; three distinct debris ridges demarcate the contact between the arms over a downglacier distance of 200 m (Fig. 39). These ridges are not ice-cored and lose a distinct morphology downglacier by coalescence.

On the other hand, South Arm ice also carries a large supraglacial load above the confluence ice falls. In the ice falls debris is ingested into large transverse crevasses and with ablation and revelation of crevasse-bound debris, transverse till ridges are found at the ice fall base, where they compose South Arm debris contribution to the medial

moraine (Figs. 39, 40). Ridges are destroyed downglacier as crevasse remnants are eradicated and a moraine morphology of low relief is generated. Supraglacial debris is derived from two debris septa which originate above the firm line in the Western basin of Upper South Arm.

South Arm ice is characterized over a distance of 300 m below the ice fall base by a series of 6 wave forms which are best developed on ice to the north of medial moraine S1 (Fig. 34). The wavelength is about 60 m throughout but wave height declines from a maximum value of 10 m to 1.5 m downglacier where wave crests are difficult to identify.

For a distance of 250 m downglacier of the confluence, the elevation of South Arm ice is greater than that of the adjacent North Arm surface. A distinct shoulder between the upper and lower ice surfaces was occupied until late in the melt season by a linear longitudinal snow bank. The maximum height of the shoulder approaches 10 m declining downglacier. Initial observation suggested that the shoulder base defined the contact between North and South Arms. However, till ridges demarcating the contact, occur along the shoulder face (Fig. 35) not at the base. Since the lower shoulder is composed of North Arm ice trimming and accentuation of the shoulder by melt water is evident. Debris-rich crevasse remnants are also revealed along the shoulder face (Fig. 41).

The surface of North Arm adjacent to the base of the shoulder increases in absolute elevation downglacier for a distance of 100 m and differential relief between the two arms is eradicated. Meltwater on North Arm in the proximity

of the confluence flows upglacier marginal to the ice shoulder, terminating in a large moulin in the inner confluence zone. The central median ridge at the confluence of North and South Arm ice is characterized by free-faces developed on buff coloured siltstone of Bowser assemblage; minor black argillite bands outcrop close to the ice level of North Arm ice. The free-faces are punctuated by wide debris covered ledges. An ice-cored talus slope obscures the contact between bedrock and ice where North and South Arms combine and it is evident that debris is added to the glacier margins from upper ledges.

5.42 Strain-Rate Squares

In addition to a longitudinal stake line from the confluence area to the glacier terminus strain-rate squares were constructed. It was felt that determination of other components of the strain-rate in addition to the longitudinal was desirable. The presence of lateral compression between the two ice arms and its influence on medial moraine morphology might then be assessed.

The method of construction for all squares follows that of Nye (1959). Repeated measurement by tachymetry of the sides (approx. 15 m long) and diagonals of these squares enables strain-rates to be derived; notation for each square is presented in Fig. 42. The c axis is subparallel to the estimated line of ice flow for rotation of strain-rate squares was necessary to avoid crevasses; deviation from flow line direction is not of a great magnitude (generally less than 15°). Eight measurements

90

of strain-rate are made from each square ($a_1, a_2, b_1, b_2, c_1, c_2, d_1, d_2$) (Fig. 42). These are reduced by averaging to four determinations: $\frac{a_1+a_2}{2}, \frac{b_1+b_2}{2}$, etc., etc.) corresponding to components of the strain-rate at $0^\circ (\epsilon'0)$, $45^\circ (\epsilon'45)$, $90^\circ (\epsilon'90)$, and $135^\circ (\epsilon'135)$ respectively, measured clockwise from oz. Yearly strain-rates are then calculated. The measurement interval varied from square to square.

Theoretically $\epsilon'0 + \epsilon'90 = \epsilon'45 + \epsilon'135$ (Nye 1959). This internal check on consistency demonstrates for the confluence strain-rate squares that further analysis of strain-rate data (such as derivation of the strain-rate tensor) is not warranted; generally high gradients of strain-rate are found over the areas covered by squares. In addition, strain-rate data were necessarily collected over short time periods; consequently, in the following discussions, results will not be referred to in detail. Fortunately ice structures found in the confluence zone support strain-rate data.

5.43. Location of Strain-Rate Squares

Three areas of the confluence zone and the central medial moraine were considered of interest. Two strain-rate squares were erected in the immediate confluence zone on North and South Arm ice and 'tied' by a stake at the square centre to the bedrock marker at the head of the longitudinal stake network. One further strain-rate square was constructed along the medial moraine on South Arm ice. The objective here was to determine the nature of surface strain-rate close to the contact of the two arms downglacier of the confluence. The

square was tied into the longitudinal stake line in the proximity of stake 20.

5.44 Glacier Mapping

A plane table map was constructed of the confluence area at a scale of 1:200. A rectangular area (120 m wide) was mapped, extending downglacier from the confluence bedrock cliffs for approximately 250 m. Ice properties such as the character of foliation, crevassing and metamorphic features generated at the bottom of South Arm confluence ice falls were noted in addition to the distribution of debris, its character and relationship to ice structures. Supraglacial drainage, and moulin distribution were also noted. Corner stakes of strain rate squares erected on North and South Arm ice served as control points as did stakes of the longitudinal line. No elevations were determined on the map; distances between control points and minor survey stations were calculated by tacheometry using a Wild self-reducing alidade and staff. The map is reproduced as Fig. 39.

5.45 Topographical Transects

Topographical transects were constructed along and across the central medial moraine by steel tape and altimeter. Relative elevation was noted; no attempt was made to determine absolute elevation. The location of topographical transects is shown in Fig. 43.

5.5 North Arm Ice Structures

Structures developed on North Arm in the confluence zone appertain to two distinct areas. An inner wedge-shaped zone

can be identified, associated with the immediate confluence area, and an outer zone unaffected by stresses imparted on ice flow by confluence with South Arm (Fig. 39). The inner zone is the more complex; transverse crevasses are developed immediately below the rock wall of the median ridge but die out rapidly in the down-ice direction and are not seen to affect moraine morphology. Lineations of two distinct types can be identified and are thought to represent crevasse remnants. These are not persistent structures and limited englacial depth is suggested by their absence downglacier. The inner zone is also marked by a supraglacial mud layer and high melt stream activity; moulins are present along the contact of North and South Arm ice. By contrast the outer zone possesses no supraglacial debris and is marked by well-developed longitudinal foliation.

5.51 The Inner Confluence Zone

The southern boundary of the inner zone is the distinct ice-shoulder of South Arm. The contact between North and South Arms demarcated by longitudinal till ridges occurs along the shoulder face and was obscured in some areas for the entire melt season by a linear north-facing snowbank. To the west, whilst free-faces of the median ridge define the limits of the inner zone, remnant snowbanks and ice-cored talus obscure the contact between ice and bedrock.

5.51 (I) Bedrock Marginal Hummocks

North Arm ice entering the inner confluence area is of low surface slope following passage through a steep ice ramp approximately 175 m long. Two well-defined ice-hummocks are present at the base of the ramp close to the bedrock wall (Fig. 39) and remnant snowbanks occupy trough areas throughout the melt season. The nature of strain rates associated with the hummocks was not investigated but it is possible that buckling of thin marginal ice under longitudinal compression occurs at the ramp base. Whilst there is no direct relationship between hummocks and the morphology of the medial moraine any longitudinal compression at the ramp base acts at a high angle to the moraine.

5.51 (II) Structural Lineations

Lineations developed on inner zone ice are distinct from longitudinal ice structures associated with the contact of North and South Arms for the latter are demarcated by till ridges of the northern debris band. Lineations however are not aligned parallel to glacier flow but, diverging from that direction downglacier, can be traced under debris of the northern debris band. On the basis of orientation, lineations can be divided into two groups, neither of which is associated with englacial debris. One group (no. 3, Fig. 39) converges within the contact between the two arms, as they are traced downglacier, the other (no. 4, Fig. 39) diverges.

Transverse crevasses are well-developed on inner zone ice and can be distinguished from crevasse remnants in various stages of closure at the base of the steep ice ramp. Lineations converging with the northern debris band are probably remnants of crevasses formed upglacier, their orientation indicating a greater degree of rotation compared with those lineations diverging from the contact. The latter group may represent remnants of transverse crevasses developed more locally on inner zone ice.

Significantly, remnants of crevasses generated above the ice ramp are not associated with the release of englacial debris to the inner zone, despite complete ingestion of substantial quantities of lateral moraine debris. This may confirm the observation that this ingested debris is delivered to the confluence as submarginal load, transported out of the area as till ridges. As a result of thin marginal ice crevasses probably penetrate to the bed, allowing debris to be transported submarginally, and not englacially in crevasses. As a result structural lineations are not observed to determine the morphology of, or debris supply to the medial moraine.

5.52 Results of Strain-Rate Measurement in the Inner Zone

The method of construction of a strain-rate square placed on inner zone ice (Fig. 42) has already been described. Strain rates were determined for a short time period only, and must therefore be used with some degree of caution. A stake in the square's centre was employed to determine ice

velocity by repeated measurement to the confluence bedrock marker. A velocity of 33 m yr^{-1} was determined but since the line of sight from the central stake to the marker does not lie parallel to ice flow a definite error of unknown magnitude is introduced. Extensional (positive) strains occur in the direction parallel with the central medial moraine agreeing with strain-rate data from the central stake line and accounting for the development of transverse crevasses on North Arm in the confluence zone. Ice emerging from the steep ice ramp above the confluence (Fig. 34) is undergoing severe compression which may be associated with the ice hummocks at the ramp base (pg. 93). This compressive strain acts perpendicular to the contact with South Arm ice. Further evidence of lateral compression between the two ice Arms is presented later.

5.6 Northern Debris Band: The Relationship with Ice-Flow

Three debris ridges of the northern debris band which serve approximately to locate the contact between North and South Arm ice may be formed by upward shearing of englacial debris between the two Arms. This debris is that formerly carried supraglacially by North Arm above the confluence zone (pg. 87 and Fig. 35). Careful observation of these debris bands where revealed in a large moulin in the confluence area indicates that the supraglacial longitudinal till ridges are generated from vertical englacial debris dykes.

5.61 Field Investigations

The nature of ice movement close to the debris ridges was investigated. Eight pegs (a-h; Fig. 44) were placed in a line transverse to the till ridges, extending from South to North Arm ice. The site lay adjacent to stake 24 of the central stake line. Nine days later up- or downglacier deviation in peg position from an arbitrary line at right angles to a selected stake was measured by pocket steel tape. Peg deviations are presented in Fig. 44. If it can be assumed that the relative difference in displacement between two adjacent pegs is an index of strain-rate developed over intervening ice, then the highest strain-rate is developed over ice between pegs d and e. Areas of greater strain-rate can be correlated with debris ridges; strain-rate varies little over ice to the north of debris ridge A. The velocity (i.e. absolute peg deviation) in this area is lower than that of ice to the south. If correlation of debris ridge A with the North/South Arm ice contact is correct, then it would appear, on the basis of a single set of measurements, that North Arm ice along the contact has a lower ice velocity than that of South Arm. Unfortunately the character of differential movement between North and South Arms and its relationship with surface till ridges cannot be resolved. Ice between pegs d and e may be actively deforming under high strain-rates or may be moving along a shear surface associated with the debris ridge. Measurement of ice crystal size along the transect parallel to the peg network or a peg network with a greater number of

more closely set stakes is required.

Stenberg (1966), whilst primarily interested in the nature of differential movement in the vicinity of crevasses, has recorded data from what the writer infers to be a medial moraine. Variation in horizontal ice velocity was monitored by a system of stakes, 5 to 17 m apart, placed transverse to the moraine. Local increases in ice velocity were associated with 'ice in immediate connection with the surface moraine'. No mention is made of shear zones. Anderton (1970) measured independent velocity profiles across North and Central Arms of Kaskawulsh Glacier at the confluence zone: a medial moraine was associated with velocity minima. No evidence was found of discrete shear between the two arms. Unified flow was established within 1.0 km downglacier of the confluence.

5.62 Further Field Investigations

The nature of differential velocity between North and South Arms was examined downglacier. A strain-rate square was erected with stake 20 as the centre (Fig. 42). There would appear to be only slight lateral compression between North and South Arm ice; the northern stake was placed in ice of North Arm. It is significant that Glen's (1959) test of consistency (pg. 90) when applied to surface components of the strain rate indicates that low gradients occur within the square. No differential velocity between North and South Arms, such as that recorded by a series of transverse pegs proximal to stake 24, can be determined.

5.63 Discussion

On the basis of one strain-rate square it would appear that unified flow of North and South Arms is established between stakes 24 and 20. The three longitudinal ridges of the northern debris band which demarcate the contact between North and South Arms in the confluence zone, are not present downglacier of stake 21; one simple well-marked contact zone is evident.

Further evidence that unified flow is established in this area comes from the outcrop of crevasses. Crevasses, gently arcuate downglacier, developed on North Arm ice, extend into and truncate the central medial moraine downglacier of stake 20. Upglacier of this point North Arm crevasses do not penetrate the central medial moraine. It is suggested that unified flow across the contact of North and South Arm ice is established within 800 m of the confluence.

5.64 Conclusion

Ice structures revealed in the inner confluence zone of North Arm ice are not seen to impart distinctive morphological characteristics to the central medial moraine. However, lateral compression between North and South Arms may determine the outcrop of the northern debris band of the moraine. The three longitudinal debris ridges of the band may reflect shearing activity and the delivery of englacial debris to the surface of the combined ice arms. The existence of a sub-

marginal debris pool consisting of englacially ingested lateral moraine debris in the inner confluence zone is clear (Fig. 35), shearing between North and South Arms transports and elevates debris to the surface. Distinct debris ridges are not found immediately above the terminal ice falls; all englacial debris has been expended by the time ice moves through this zone. A limited depth of the sub-marginal debris pool is indicated.

5.7 South Arm Ice Structures

Ice structures developed on South Arm in the confluence zone provide further evidence of lateral compression between North and South Arms. These structures are only briefly described for they are not seen to impart persistent morphological characteristics to the central medial moraine (central and southern debris bands: Fig. 34).

The most striking feature of South Arm ice surface is a series of wave forms (Figs. 34, 43, 45). Wave height is 10 m upglacier, declining in the down ice direction to 1.5 m. Wavelength is about 60 m which may approximate to annual velocity of ice in this area. Waves become increasingly well-defined as they are traced towards the contact of North and South Arms, i.e. in the direction of increasing compression at the base of South Arm icefalls. Decreased serac width and transverse till ridge spacing is also observed in this area (Fig. 39). The outcrop of transverse till ridges is subparallel to the wave crests; debris from debris-rich crevasses that are traced into wave fronts increase local ablation rates. This and supraglacial meltstream activity eradicates distinct wave

forms downglacier. Wave forms are most clearly defined immediately downglacier of the ice falls (waves 4, 5 and 6, Fig. 45). A longitudinal stake line was constructed and longitudinal strain-rates were determined by repeated measurement of stake intervals; stakes were set in wave crests (curves A, B, Fig. 45). This basic stake line was supplemented by additional stakes set in wave troughs; these supplementary stakes allowed separate determination of strain-rates over wave crests and troughs (curve C, Fig. 45). Strain-rates would appear to support a compressional origin for the wave system though the relationship between slight extensional strains and wave morphology is not clear. Certainly a strong compressive strain is seen to act against North Arm ice. Further evidence suggests that this is indeed so. On North Arm ice 300 m down ice of the confluence area and 60 m north of the central medial moraine a longitudinal depression characterizes the ice surface.

The depression whilst of extensive longitudinal extent is difficult to identify from the surface of the glacier but is clearly depicted by aerial photography (Fig. 13) where the hollow is occupied by a remnant snowbank. A slush-zone occurred in this area during the early melt season of 1975. The site of linear bulging and generation of relative relief lies adjacent to that part of South Arm where surface waves are developed at the base of the confluence ice falls. Lateral compression generated by the angle of entry of South Arm ice and possibly locally high ice velocities by attendant steep surface slope,

may generate surface bulging in adjacent ice of North Arm.

Anderton (1970) describes a number of small anticlinal folds with axes perpendicular to the principal compressive strain-rate, from the confluence area of North and Central Arms of Kaskawulsh Glacier, Yukon Territory. These are related to transverse lateral compression at the confluence and ice of both arms undergoes retardation of velocity as the confluence zone is entered.

South Arm ice exhibits a well-developed longitudinal foliation related to deformation of primary sedimentary stratification in the upper firm basin (pg. 43). Severe longitudinal compression at the base of South Arm ice falls, acting at a high angle to the Central medial moraine is indicated by severely compressed foliation on serac block surfaces close to the contact with North Arm (Fig. 39). The distinct ice shoulder which characterizes the contact between the two arms in this area (pg. 43) may be formed by lateral compression of South Arm against North Arm. Measurements of a strain-rate square sited on top of the ice shoulder support this interpretation. Furthermore, observations in transverse crevasses indicate that the contact between the two Arms deviates from the vertical. Over longitudinal distances of 3-6 m a contact dipping into North Arm was observed. This is not unusual at the contacts of ice arms undergoing lateral compression (Tarr and Martin, 1914).

5.71 Discussion

Morphological criteria, wave forms, the angle of entry of South Arm into the confluence zone, a distinct shoulder in South Arm along the contact and a longitudinal ice bulge in adjacent North Arm ice, indicate lateral compression between North and South Arms in the confluence area. Strain-rates determined from (1) an area of wave forms and (2) South Arm ice along the contact, whilst affording only a single picture of ice flow also indicate lateral compression between the two ice Arms. However, whilst lateral compression between the two Arms can be demonstrated, persistent morphological characteristics are not imparted to central and southern debris band components of the Central moraine.

Loomis (1970) in his description of the morphology of the medial moraine developed at the margin of North and Central arms of Kaskawulsh Glacier, Yukon Terr., suggests that lateral compression between the two arms plays no role in determining moraine morphology. The writer has argued elsewhere (Eyles, 1976) that certain features of moraine morphology exhibited on Kaskawulsh Glacier can be reinterpreted as being generated by lateral compression but the evidence is far from conclusive. As on Berendon Glacier a marked lateral compression between the merging arms has been measured on Kaskawulsh Glacier (Anderton, 1970) but there would appear to be no fundamental relationship between such compression and moraine morphology except in the immediate confluence area.

The 'ice-stream interaction' model of medial moraine development was evolved for moraines formed by confluence of

outlet valley glaciers such as North and South Arm Ice. In this model the nature of ice flow exerts fundamental control on moraine morphology. On Berendon Glacier however whilst lateral compression between the two Arms has been demonstrated, and its importance in determining the morphology of the northern debris band suggested, factors other than the nature of ice flow determine moraine morphology downglacier.

5.8 The Nature of Englacial Debris Supply to the Central Moraine.

5.81 Field Procedure

Four areas were selected along the medial moraine at successive downglacier intervals to determine the nature of englacial debris supply and to collect samples of newly revealed debris where present. Site locations are depicted on Fig. 22 and are ordered according to position downglacier. Ablation stakes were erected at each location. Cleared areas were large, to facilitate identification of ice structures.

5.82 North Debris Band

Site 1 lay 200 m downglacier of the confluence area adjacent to a series of transverse pegs drilled across the contact of North and South Arm Ice. All supraglacial debris was cleared from an area 3 x 6 m. A sample was taken of ridge debris ablating out subsequently (Sample N10).

5.83 Northern, Central and Southern Debris Bands.

Site 2. 700 m downglacier of the confluence a strip 3.5 m wide was cleared across the entire central moraine. Length of the cleared strip was 60 m (Fig. 46). Ice is of a simple

structure and a simple longitudinal lineation marks the boundary of North and South Arm ice.

5.84 Central Debris Band

Sites 3 and 4 lie downglacier of the terminal ice falls; site 3 lies close to the centre line of the medial moraine, on an area free from longitudinal crevassing. All supraglacial debris was cleared from a strip 3 by 7 m lying transverse to the moraine. Debris depth over this area was about 5 cm.

Site 4. An area of 4 x 5 m was cleared on the uncrevassed surface of the fringing remnant ice berm below King Survey station. The generation of this remnant ice body is described in Appendix II. Subglacial observations indicate englacial debris is present throughout ice depth. The area lay on the southern margins of the central moraine prior to isolation by cavern collapse.

5.85 Results

All plots cleared of supraglacial debris were inspected periodically. Above the terminal ice falls site 1 is associated with englacial debris supply to the surface; debris characteristics are discussed below (Chapter 6). Site 2, after 6 weeks of inspection did not reveal any debris being delivered to the ice surface from areas of the central and southern debris bands. Neither is the northern debris band associated with debris delivery to the surface. In this area the band is characterized by merged and collapsed debris ridges demarcating the contact between North and South Arm ice.

Below the terminal ice falls, site 3 is characterized by englacial debris delivery to the surface (debris sample 016); site 4 also exhibits an englacial debris supply (debris sample 016).

5.86 Interpretation

The central and southern debris bands of the Central medial moraine consist entirely of supraglacial debris above the terminal ice falls and are only associated with the delivery of englacial debris to the glacier surface in the terminal area. The immature morphology exhibited by the moraine, viz. absence of a substantial ice core; low supraglacial debris quantities and unchanging width upglacier of the ice falls can be related to the absence of englacial debris supply. The central and southern debris bands of the moraine can be traced upglacier to parent debris derivation sites in the Western firn basin of upper South Arm and as a result, exhibit the same morphological development downglacier as moraines formed above the firn line on North and South Arms and discussed in Chapters 3 and 4. These moraines evacuate two debris populations through the basin (pg. 76); (a) debris derived entirely subglacially, emerging only in the terminal zone and associated with a developing ice-cored moraine morphology and (b) debris, contributed subaerially from Type 1 slopes, which undergoes sedimentation with seasonal snow loads and is revealed close to the firn line where it is associated with debris septa and an immature moraine morphology. The bulk of moraine debris is transported sub-

glacially at depth. In contrast the northern debris band is derived from local debris inputs into the confluence zone by lateral moraine load; englacial debris from this source is exhausted downglacier and band morphology collapses.

Thus the morphology of the central medial moraine can be more explicitly explained in terms of the varying pattern of englacial debris supply (i.e. the 'ablation-dominant' model of medial moraine formation); other factors such as lateral compression between merging ice-streams and the nature of ice structures ('ice-stream interaction' model) play only a minor role.

5.9 Central Medial Moraine Morphology. Conclusion.

Peculiar and unique patterns of ice flow and associated ice-structures are known to develop where large valley outlet glaciers converge (Brecher, 1969; Anderton, 1970; Loomis, 1970) and large medial moraines are often generated by merging of lateral moraines in these zones. In the 'ablation-dominant' model of medial moraine formation, moraine morphology is determined by the nature of englacial debris supply. Other factors such as longitudinal strain-rate and associated crevassing determine the clarity with which this relationship is revealed at the glacier surface. The 'ice-stream interaction' model was formulated to allow for the influence of peculiar ice structures in the confluence zones of large valley outlet glaciers where, for example, lateral compression between merging ice arms may determine moraine morphology.

Along the medial moraine formed by the confluence of North and South Arm ice complex patterns of ice flow, lateral compression and prominent ice structures are not seen to impart fundamental and persistent morphological features to the moraine. Whilst a diverse moraine morphology is established in the confluence zone, moraine development downglacier reveals the fundamental relationship between englacial debris supply and medial moraine morphology. Small scale forms such as transverse ridges are eradicated below the confluence and longitudinal debris ridges associated with the contact zone of North and South Arm ice degenerate downglacier. In the down ice direction moraine width remains constant, no englacial debris is added to the moraine and there is no development, because of insufficient debris, of an ice-cored form. A similar static morphology is exhibited by moraines on adjacent North and South Arm ice. Englacial debris supply to the moraine occurs only below the terminal ice falls where despite crevassing some development of moraine morphology takes place. Thus the morphological development exhibited by this moraine can be accommodated within the 'ablation-dominant' model; complexity introduced by confluence of North and South Arms is not a persistent determinant of moraine morphology. The emergence of englacial debris only in the terminal areas is explained in terms of its distribution with depth (Chapter 4). The medial moraine formed in the confluence zone contains debris bands generated above the firn line and moraine morphology can be accounted for by reference to the above firn line subtype of the 'ablation-dominant' model (Chapters 3 and 4).

6.0 THE SEDIMENTOLOGY OF MEDIAL MORAINES

6.1 Introduction

Nearly all natural ice contains small amounts of insoluble fragments of other minerals and rocks which range in size from clay particles derived from weathering and atmospheric dust fall-out to substantial boulders (Schumskii, 1964). Mineral additions represent sources of salination and, possessing a larger coefficient of absorption for incoming radiant energy many act as centres of localized ice melt. Partial melting may subsequently give rise to local enrichment though the timing and periodicity of accumulation may also yield similar results. More usually, localization and concentration of debris is characteristic of sedimentary ice such as glaciers. In the sedimentary and subsequent metamorphic environments of valley glaciers extraglacial debris additions above the firn line undergo seasonal compaction with snow loads and as a result englacial debris extends throughout ice depth. Additional debris is derived subglacially and subnivally. Below the firn line however, debris can only be entrained englacially via crevasses to which lower depth limits apply (Sharp, 1949). The 'ablation-dominant' model of medial moraine formation has related above and below firn line debris incorporation to the varying morphological and debris-transport characteristics of medial moraines. To reiterate, moraines possessing debris derivation sites above the firn line such as those on Berendon Glacier, evacuate two sediment populations from the glacier basin; that from subaerial Type 1 slopes in the firn basin (debris contributions being from the basal

debris layer of upper ice carapaces and that derived entirely subglacially and subnivally (Fig. 26). The latter element accounts for the bulk of moraine debris, is deeply entrained and emerges only in the terminal area where it is associated with the development of a mature ice-cored moraine morphology. In contrast, debris derived from Type 1 slopes extends throughout ice depth, is revealed close to the firn line and by its small quantity is associated only with an immature moraine morphology. Sedimentological analysis considered in this chapter will concentrate on medial moraines developed on Berendon Glacier; moraines formed at the margins of ice cap outlet glaciers below the firn line will not be discussed in detail.

Medial moraines provide an excellent natural laboratory for the study of bedrock comminution and the generation of daughter sediments in the glacial environment. Moraines remain well-defined; no other sediment bodies, apart from rockfall debris and windblown dust are added to moraines which evacuate primary derived debris through the basin. In particular, on Berendon Glacier, whilst four contrasting bedrock lithologies are evacuated by moraines in the basin as a whole (Fig. 12) individual moraines evacuate debris of one lithology only and sediments are lithologically well-defined. Thus, it is possible to compare the bedrock comminution process for varying bedrock types under identical derivation and transport conditions. Such comparisons are of great value since discussion in the literature focusses on the textural relationship exhibited by tills between parent bedrock and daughter products.

Dreimanis and Vagners (1971) have described a bimodal grain size distribution of glacial tills in mid-latitude North America; a coarse mode in the gravel fraction dependent upon the character of parent bedrock and a fine mode in the sand/silt fractions reflecting the crushing properties of individual minerals. Till texture can therefore be related to that of parent bedrock. Bimodal grain-size distributions have been reported for tills from mid-latitudes affected by continental ice sheets. In contrast, tills derived from certain temperate valley glaciers do not reveal a bimodal particle size distribution, irrespective of parent bedrock type (Slatt, 1971, 1972).

Consideration of the sedimentology of medial moraines since they are lithologically well-defined adds to such discussion. So far, no attempt has been made in the literature to consider medial moraine sedimentology although tangential reference has been made in discussion of supraglacial debris in general and the sedimentology of minor morphological features such as dirt cones (see Knighton, 1973). Whilst Garwood and Gregory (1898), Ogilvie (1904), Tarr and Martin (1914), Ray (1935), Sharp (1949) and Derbyshire (1975) have remarked upon the coarse angular character of supraglacial debris no sedimentological analyses have been conducted. Finally consideration of the sedimentology of medial moraines formed above the firn line may substantiate Røthlisberger's (1968) comment that 'the study of medial moraines should give some clues particularly to the erosion at depth in the high areas of a glacier.'

6.2 Statement of Objectives

Two objectives can be enumerated:

- (1) Sedimentological description of medial moraine debris in

terms of particle-size analysis, scanning electron microscopy of quartz grains and clay mineralogy. Moraine debris might then be distinguished from other elements of the glacier debris system such as subglacial lodgement tills or extraglacial valley side slope debris.

(2) Consideration of the textural relationship between medial moraine debris and parent bedrock in order to establish whether a dependent or an independent relationship exists.

6.21 Field Procedure: Berendon Glacier

Sample sites for debris released from upper firn basin backwalls and moraine debris below the firn line have been described for moraines of North and South Arms in Chapters 3.0, 4.0 and depicted in Figs. 1, 22, 47. All samples collected during 1975 are numbered and collection sites briefly described in Appendix VI. Newly revealed englacial debris was sampled in the terminal zone and along the central and southern debris bands of the Confluence moraine formed by the combined Arms (Chapter 5.0 and Figs. 22, 47). In this fashion medial moraine debris was sampled from above firn line derivation sites (Type 1 slopes; Fig. 14a) to the terminal area where subglacial debris elements emerge after deep englacial transport. Further samples of medial moraine debris were collected from Salmon Glacier (Fig. 48). Additional debris types were sampled from above the confluence area (Fig. 14b). Observations of subglacial activity and sampling of basal debris sole sediments were made at two locations; in terminal South Arm ice below Berendon survey station, where the character of the rock bed

allows extensive subglacial cavitation, and along the margin of a small ice body ('Saddle glacierette'; Figs. 9, 14a) at an altitude of c. 1,250 m. a.s.l. overlooking South Arm ice. In terminal South Arm ice flow direction is transverse to the strike of emplacement structures in the granodiorite stock (Fig. 9 and page 41). Extensive cavitation is generated as thin but active (Fig. 49) marginal ice flows over whaleback strike outcrops. In basal ice, a thin (<10 cm) basal regelation layer could be distinguished from much thicker (up to 1.5 m) debris layers (Fig. 50). Regelation layer thickness accords with that described by Kamb and LaChappelle (1964) and Boulton (1975). Regelation layer ice was detached, melted and debris retained (samples SS68 + D3). It is not likely that thicker debris layers are formed by successive accretion of regelation layer ice, the latter seldom survive more than local transport and are destroyed by further pressure-melt downglacier. McCall (1952) records a basal debris layer 30 cm thick, at the base of a small cirque glacier in Norway, related to percolating meltwater refreezing and incorporating basal debris. A similar process is likely on the margins of South Arm ice; much debris is contributed to the margins by the erosion of recessional lateral moraines.

South of Beckert survey station and occupying a saddle in the ridge demarcating the divide between the Salmon and Berendon drainage basins is the truncated accumulation zone of a small ice tongue (Blue Glacier) which descends to the east but does not quite reach Summit Lake water. The length of the truncated firn is 150 m and the progressive alteration of firn to glacier

Ice can be traced on the front; while ice thickness is generally less than 5 m and a pronounced debris sole is present (debris samples 2NE, 4NE, 8NE). Meltwater from the glacierette is not turbid and, in conjunction with low surface slope and thickness, indicates that subglacial erosive activity cannot be great. It may well be that the debris layer was formed by freeze-thaw prior to the resurgence of ice cover in the area. A similar situation is discussed by Boyé (1952). Granodiorite bedrock surfaces within 40 m of the ice front exhibited a thin precipitate which later analysis demonstrated to be calcium carbonate. Precipitate thickness reached 0.5 cm and a laminar structure was commonly observed. Dissolution by rain and snow melt water may account for the declining extent of calcite precipitate away from the ice front. A bedrock leeside distribution was noted and a subglacial origin is likely.¹

¹ The literature on subglacial calcium carbonate primarily describes Scandinavian occurrences, the distribution of which would appear to be more extensive than those described elsewhere. Kers (1965) has summarized the literature on Quaternary subglacial limestones (subglacialt kalkstenar). Up to 1945, distribution in Scandinavia was considered to be limited to Atlantic coast areas and consequently was up to that time grouped with stromatolitic limestones. Following the theory of Ljunger (1936), Kers (1965) demonstrated a subglacial origin. Since that time new glacier proximal occurrences have been reported (Samuelsson, 1964); Nigardsbreen, 15 km northeast of Austerdallsbreen is one occurrence. Ford et al, (1970) report calcite precipitates at the soles of glaciers in Banff National Park. Ford et al implicitly considered that such deposits were formed from free subglacial melt waters despite low solute carbonate concentrations. This hypothesis was rejected by Page (1971) in favour of Kers' and Ljunger's hypotheses of formation by pressure melt water. Corrosion by pressure melt water enriched with CO₂ derived from englacial CO₂ enriched gas bubbles takes place on stoss faces. Importantly, carbon dioxide required for solution is derived from fossil carbon dioxide incorporated in the ice. As a result any radio-carbon determinations on such precipitates will yield old dates for the initiation of calcite precipitation at that site. In the Rockies Ford et al report calcite precipitates restricted to limestone benches. Occurrences in Nigardsbreen reported by Samuelsson are developed on basal Caledonian gneiss.

6.22 Preparatory Procedure

The following textural analysis refers to the -4.0 to 4.0 (16 mm to .0625 mm) size fraction. The mud fraction (< 4.0; .0625 mm) of medial moraine debris is generally less than the minimum needed for particle-size analysis of silt and clay components (Folk, 1968). Since particle-size distributions are compared statistically this dictated that the same size class be used for other elements of the debris system. In a few instances mud fractions were retained for analysis of clay mineralogy (< 9.0; .002 mm) but these results will not be discussed in detail.

The size of field samples varied but was generally of the order of 2 kg. In the laboratory all samples were wet-sieved using a 4.0 (.0625 mm) sieve following standard preparation to remove organic material. Dried samples (about 300 g) were sieved according to standard methods (Folk, 1968). Sample fractions were weighed; the 1-2.0 (.5 - .25 mm) size fraction was retained for scanning electron microscopy of included quartz grains. Cumulative particle-size and frequency curves, and descriptive statistical parameters (all four moment measures; mean size, standard deviation, skewness and kurtosis) were derived from raw weight data by computer. The computer programme used was that of Slatt and Press (1976) for a Hewlett-Packard desk-top calculator (Model 9820A) - plotter (model 9862A) in which textural statistical parameters are derived by the graphic method rather than by the method of moments. Initial computer plotting of size data was completed using the -4 to 4.0 size fraction and statistical parameters used throughout this

thesis refer to this fraction. Computer print-outs presented below describe however the distribution of particles in the -3 to 4 ϕ size range.

6.23 Data Presentation

Cumulative particle-size and frequency curves and a histogram showing the distribution of particles in the -3 to 4 ϕ (8 mm - .0625 mm) size fraction are presented for all debris samples in Fig. 51. On the same figure textural statistical parameters describing the cumulative particle-size curve are depicted. Grouped particle-size curves have been constructed for different debris elements and these will be considered below under separate headings.

1. Medial Moraines.

South Arm, Moraine S.IV, Hazelton assemblage, volcanic conglomerate.

Fig. 52 depicts grouped particle-size curves for sample collected from the terminal zone (S3, 5, 11, 15, D5, 15) to upper firm basin derivation sites (Type I slopes: sample nos. S2, 12, Fig. 14a). The same scheme is employed for moraines S1 and 11 derived from volcanic tuff in Fig. 53 (Samples S5, S1, 16, 17, D6 respectively).

North Arm, Moraines N1, 11, IV, Bowser Assemblage, argillite/siltstone.

Cumulative particle-size curves of all samples collected from this bedrock source are grouped in Fig. 54 (Samples N1, N2, 3, 4, 6, 9, 10, 11, 12, 13, 14, 15, 16). Medial moraine samples from Salmon Glacier are derived from the same bedrock and

are included in Fig. 54 (Samples D10, 12, 13, 14).

Confluence-Medial-Moraine, Hazleton assemblage: volcanic conglomerate and tuff.

The moraine is composed of three debris bands (Fig. 34). The central and Southern bands are derived from upper South Arm basin; debris samples collected from the upper firn basin (Fig. 14a) are considered in Fig. 55 (S6, 8, 19 and 14, S13, C1, 2, 4, 5, 6, 7, 16, D16, E1). A further debris band, a tuff outcrops only in the terminal area and is included in Fig. 53 (Sample C3). The Northern debris band is composed of debris from valley side slopes of North Arm above the confluence (Figs. 14b, 35) and being derived from argillite have been included in Fig. 54.

2. Other Debris Groupings

Samples of frost-shattered debris (S4, N9, Ho, C11) are considered in Fig. 56. Subglacial debris sole and lodgement tills (C12, D2, 3, 8, 11, E6, 7, SSS8, 8NE) are depicted in Fig. 57 and are plotted for comparison with representative medial moraine samples in Fig. 58.

Textural Statistical Parameters (-4 to 40); 16 to .0625 mm)

All medial moraine samples are depicted in Fig. 59 on the criteria of first and second moment measures (mean size and standard deviation): discrimination is made between bedrock types. In addition, samples are depicted on the basis of all four moment measures as a function of distance downglacier from upper firn basin derivation sites (60a,b,c) for respective parent lithologies.

All debris samples

In Fig. 61 all samples are plotted on the criteria of first and second moment measures. On the same criteria Fig. 62 discriminates more closely between elements of Berendon and Salmon Glacier debris systems.

6.3 Interpretation and Discussion

6.31 Description of Medial Moraine Debris

According to the classification of Folk (1968) medial moraine debris can be generally classified as a sandy pebble gravel, moderately to poorly sorted strongly fine-skewed with a mean size varying from granule to coarse sand size (4 mm to 0.5 mm). Particle size distributions do not exhibit modal or deficient size fractions. Basal lodgement tills exhibit greater textural variety (varying from muddy sandy pebble gravels, poorly sorted, strongly fine-skewed, to granular or pebbly silty medium sand very poorly sorted and strongly fine-skewed with a mean size in the coarse to medium sand fraction (1.0 to 0.25 mm). Distinct modes or deficiencies of particle-size fractions are again absent. The glacier debris system as a whole does not contain highly variable debris types¹ and the same particle-size distribution is exhibited by frost-shattered debris.

Whilst a distinct medial moraine debris type cannot be recognized, Fig. 61 suggests that such debris is generally

¹ Analysis of clay mineralogy reveals the expected dominance of chlorite/illite in the glacial environment (McKenzie, 1970) and invariant chlorite/illite abundances (Fig. 63).

characterized by a greater mean size and reduced value of standard deviation compared with subglacial lodgement tills. In cases of primary comminution mean particle-size is inversely related to standard deviation, as comminution continues mean particle-size diminishes and standard deviation increases. Extreme values of mean size exhibited by medial moraine debris (Fig. 59) are not determined by bedrock texture but reflect the more limited comminution experienced by medial moraine debris. Neither are reduced values of mean size, indicative of glacial comminution, exhibited by moraine debris emerging in the terminal area following subglacial and subnival derivation in the upper firn basin (Fig. 62). Indeed increasing distance of englacial transport from upper firn basin derivation sites is not associated with any evolution of moraine debris texture (Figs. 60 a,b,c). In Fig. 60c textural statistical parameters derived from subglacial lodgement tills are plotted for comparison with newly emergent medial moraine debris in the terminal area; the generally lower values of mean size exhibited by lodgement tills is clearly indicated. The greatest distance of transport (9 km) is experienced by debris near the glacier bed (Fig. 1), emerging in the terminal zone. Such debris does not appear to make extensive contact with the subglacial bed since textural characteristics indicating limited comminution are preserved. Johnson (1974) found on Kaskawulsh Glacier, preservation of angular debris characteristics despite basal debris transport over great distances, and suggested only a minor role for basal load in scour of the glacier bed as distinct bed load zones in the basal layers of the glacier, but not in contact with the bed.

Passive englacial transport from derivation sites in the upper firn basins is substantiated by scanning electron microscopy of the 1-2 ϕ (0.5 - 0.25 mm) quartz sand fraction. Textural discrimination cannot be made between medial moraine grains from Berendon Glacier and Austerdalsbreen which exhibit textures typical of primary release from bedrock and which, despite 'glacial' appearance (Whalley and Krinsley, 1974) can be contrasted generally with grains found in subglacial debris soles exhibiting textures indicative of greater comminution. Röthlisberger (1968) has commented that basal englacial zones in proximity to medial moraines are sites of enhanced bed scour as a result of high englacial debris content. Evidence from Berendon Glacier does not support this contention.

Debris of extended supraglacial transport is also present in the terminal area. No coarsening of debris texture down-glacier is exhibited in Figs. 60 a, b, c and clearly fines (fine sand fractions) are not removed during supraglacial transport by meltwater. Thus the coarser texture of medial moraine debris relative to subglacial debris may not be determined by meltwater winnowing of fines as suggested generally for the coarser texture of supraglacial debris, by many workers (Garwood and Gregory, 1898; Ogilvie, 1904; Tarr and Martin, 1914; Ray, 1935; Sharp, 1949; Price, 1973). Surprisingly, textural analyses were not made by any worker. Elson (1961) presumed that supraglacial tills lose fines following surface ice ablation and distinguished supraglacial and lodgement tills on the basis of grain-size distribution plotted on Rosin and Rammler's "Law of Crushing" paper. Poorly sorted sediments, such as tills, plot as a straight line,

described as a 'crushing type of grain-size distribution' (Elson 1961). As a result of loss of fines during transport supraglacial tills however 'may not have the crushing type of grain-size distribution' (Elson 1961) and he depicts typical curves of ablation and lodgement tills (Fig. 64). In Fig. 64 a number of grain-size distributions from Berendon Glacier (derived from medial moraines, subglacial debris soles, freeze-thaw and scree debris) have been plotted. In addition grain-size data of freeze-thaw daughter products derived by laboratory experimentation were abstracted from Wiman (1963), Martini (1967) and Potts (1970). Grain-size data relating to talus, tills with rockfall debris and solifluction tills were derived from Rapp (1961). All samples plot in the coarser, upper right area of "Law of Crushing" paper, typical of immature comminution tills; supraglacial medial moraine and subglacial lodgement tills cannot be distinguished. By contrast, tills derived by ice sheets from the mid-latitudes of North America and presumably of far-travelled character yield curves of lower slope (Fig. 64) in addition to which textural differences between ablation and lodgement tills are more striking. There appears to be little variation in the character of debris transported from the glacierized basin by Berendon Glacier. Transport distances are insufficient to allow the development of mature comminution tills and as a result supraglacial debris cannot be rigorously distinguished from other elements of the glacier debris system. Under conditions of more extensive transport contrasts between medial moraine and subglacial tills may be more striking; this could easily be tested on glaciers of greater length.

In summary, Berendon Glacier transports debris products typical of initial bedrock comminution; a wide variety of sedimentary particles are produced and modal and deficient size-fractions are not found, a reflection of limited comminution and short transport distances. As a result particle-size distribution is not found to be a rigorous discriminant between medial moraine debris and other elements of the debris system. A slightly coarser texture exhibited by medial moraine debris is not determined by bedrock source or meltwater winnowing of fines but reflects limited comminution; passive englacial, sub- and supraglacial transport from sites of initial release is suggested.

6.4 The Relationship Between Medial Moraine Debris and Parent Bedrock Texture

Within the glacierized basin of Berendon Glacier, debris particle-size distribution appears to be independent of parent bedrock (Fig. 59, 60 a,b,c) and a wide range of particle size is produced irrespective of bedrock type. This again is a feature of immature comminution tills. For example tills from mid-latitude areas previously affected by continental ice sheets frequently reveal a bimodal grain-size distribution of lithologic components (Dreimanis and Vagners, 1971). Clasts (rock fragments) are contrasted with matrix (mineral fragments) with the 'natural' boundary between the two modes varying within the -1 to 3.25ϕ (0.50-0.105 mm) size interval depending upon the particular lithology (Dreimanis and Vagners, 1971). Near the source, where the ice incorporates rock fragments, the clast-size mode is always greater than the matrix mode; the latter, with increasing transport dis-

tance from the source grows larger, recording increasing comminution of clast-size particles. Thus, following considerable transport distance and extended comminution, the texture of tills reflect 'the crushing characteristics of the dominant lithological and mineralogical components' (Derbyshire, 1975).

That these textural characteristics are not exhibited by glacially comminuted bedrock products of Berendon Glacier may be due to several factors. For example, till samples may often be texturally similar because of varied lithologic components and mixing of bimodal grain-size distributions (Dreimanis and Vagners, 1971; Slatt, 1972; Karrow, 1976). However, apart from subglacial debris sole samples which, whilst derived from granodiorite, may contain volcanics from the upper firn basins, (Figs. 11, 12) all other debris samples from Berendon Glacier are lithologically well-defined and are derived from one lithology only, though four contrasting lithologies are represented in the basin as a whole (Fig. 12) varying in texture from fine-grained tuffs to coarse-grained conglomerates.

The absence of a bimodal grain-size distribution exhibited by debris from Berendon Glacier may reflect differences in derivation processes compared to those associated with ice-sheet glaciation; the debris system however displays little variation in debris texture (Figs. 52, 53, 54, 55, 56, 57, 58, 61) despite processes of derivation ranging from subglacial processes to subaerial freeze-thaw.

Above all, the absence of bimodal grain-size distributions such as those reported in mid latitudes, reflects the short transportation distances associated with temperate valley glaciers.

where textural evolution of the type discussed by Dreimanis and Vagners (1971) is precluded (Slatt, 1972). Initial comminution of bedrock produces a wide range of particle-sizes irrespective of bedrock lithology. For example Ichikawa (1958) examined the texture of debris in the size range ϕ -8 to ϕ 30 (256 to 0.125 mm) released by valley side slopes and landslides. Over this large grain-size range, continuous disintegration was recognized; a wide range of particle sizes were produced. Slatt (1971) considered the texture of 26 sediment samples from ice-cored deposits at the termini of ten Alaskan valley glaciers eroding metamorphic, intrusive, extrusive and sedimentary bedrock terrains. The sediments are the products of primary derivation processes. Slatt indicates that 'primary sediment forming processes associated with valley glaciers produce detrital particles of all sizes irrespective of bedrock type.' In a further paper (Slatt, 1972) he found that tills from parent rocks of contrasting texture, were of similar texture. Till samples from the Avalon Peninsula, Newfoundland, were of local derivation and limited transport; 'The results suggest initial or limited comminution of rock which results in till consisting of an eventually continuous spectrum of particle-sizes regardless of rock type.' Interestingly, laboratory experimentation by Martini (1967), Potts (1970), and Brockie (1973) reveals an independent relationship between grain-size of parent rock and resultant daughter products under the action of freeze-thaw. Hoskin and Sundeen (1975) documented grain-size analyses of parent bedrock (a coarse grained tonalite) and derived local sediment produced by coastal erosion: an independent relation-

ship was established.

No textural influence of parent bedrock on produced sediment was detected by Stromquist (1973) from particle-size analysis of sediments, associated with blockfields in Northern Scandinavia, generated by secondary weathering (mainly freeze-thaw) of primary derived blocks. However, initial block size varied according to rock type a reflection of rock mechanical characteristics. The same situation is found with Berendon Glacier basin. For example, volcanic conglomerates produce a large block size, typified by medial moraine SIV in the terminal zone of South Arm ice, where boulder size is the largest found on Berendon Glacier. In contrast, on North Arm, argillites and siltstones break down readily and large blocks are not produced. The surface of South Arm below the firn line is marked by a multi-ridged longitudinal moraine ('terratic moraine', Figs. 14a, 15, 65a,b) unrelated to nearby medial moraines. Debris clast size is large (1 m^+ in diameter) and is derived from volcanic conglomerate. In situ, secondary weathering of clasts (probably by freeze-thaw) produces a wide range of sedimentary particles (samples S3, S11, Figs. 14a, 59). Further in situ comminution of supraglacial debris blocks was observed on moraine SIV and probably occurs over the whole glacier surface. By its position close to the firn line such debris has been only shallowly entrained and is most likely derived by rockfall activity from the ridge dividing Western and Eastern firn basins.¹ In the

¹ An 'extremely unusual medial moraine' on the surface of Castner Glacier, Alaska was described by Nielsen and Post (1953). The moraine abruptly ended in the downglacier direction and was considered to have been generated by the sudden collapse of a rock spire.

marginal area of Berendon Glacier, the recessional moraine dated at '1884' A.D. (Appendix IV) is composed of the same debris type and is considered to be a 'dump' moraine formed by sliding of supraglacial load from the ice front.

On Austerdalsbreen, there is much evidence of rock mechanical characteristics as a determinant of the nature of primary debris input into the glacier system. Austerdalen transects apparently southeasterly dipping, massive pseudo-bedding structures which serve to divide the valley side walls into a series of steps, which accord with the description by Battey (1960) of thrust features in gneiss from the Jotunheimen, Norway. In addition, Austerdalen exhibits major evidence of pressure-release and the development of 'valley-jointing' (Bjerrum and Jørstad, 1968) which by intersecting features of possible thrust origin result in frequent rockslides from the valley walls.¹ A large sediment body on the glacier surface (Figs. 2, 6) derived in this fashion consists of large slabs (up to 10 x 4 x 3 m); a similar sediment body composes the recessional moraine dated at 1909 (King, 1959), formed in the same fashion as the moraine dated at '1884' A.D., around the margin of Berendon Glacier.

6.5 Conclusions

(1) A well-defined medial moraine debris type cannot be recognized on Berendon Glacier on the basis of particle-size

¹ Bjerrum and Jørstad (1968) stress the importance of distinguishing rockfalls (Norw. Steinsprang) and rockslides (Norw. Fjellscred). Rockfalls are derived mainly from rock surfaces; slides such as that on the glacier surface and marginal area of Austerdalsbreen are more deep seated.

distribution in the range -4 to 4ϕ , (16 mm to 0.625 mm); the textural character of debris transported from the basin by Berendon Glacier does not vary and as a result, elements within the debris system cannot be rigorously distinguished. Clay mineralogy also, cannot be used as a discriminant.

(2) In general, however, on Berendon Glacier, medial moraine debris in general possesses a slightly coarser mean size and a reduced value of standard deviation compared with subglacial tills, related rather to the limited comminution experienced by moraine debris, than to bedrock or progressive loss of fines by meltwater. The retention of this textural characteristic by debris emerging in the terminal zone following subglacial and subnival derivation in the firn basin indicates passive englacial transport at depth. Thus care must be used in describing such debris as 'subglacial' for active contact and scour of the glacier is not supported.

(3) In that deep, englacial load is passively transported from the basin similarity can be found with moraines formed below the firn line (i.e. Austerdalsbreen) where englacial moraine debris is limited to crevasses and is separate from subglacial debris in contact with the bed. Scanning electron microscopy of moraine quartz sand grains from both Berendon Glacier and Austerdalsbreen indicates limited comminution following initial derivation from bedrock. Thus whilst striking differences in morphological and debris transport characteristics are found between moraines formed above and below the firn line passive glacial transport is indicated in both cases. Neither is the addition of former lateral moraine load to the central medial moraine formed at the confluence of North and South Arms

associated with a distinct medial moraine sediment type. Thus it is suggested that no discrimination can be made between the character of debris caused by medial moraines formed in different fashion though this statement must be qualified in that particle-size analysis has not been carried out on debris from Austerdalsbreen. However, as discussion of the relevant literature makes clear, products of primary comminution transported by temperate valley glaciers, generally are very poorly sorted and characterized by a wide range of particle-size irrespective of bedrock type. Thus the arguments stated here are likely to be widely applicable on other temperate valley glaciers.

(4) Throughout the glacier debris system particle-size distribution is found to be independent of parent bedrock. A bimodal grain-size distribution reported from the analysis of tills from mid-latitudes, reflecting parent bedrock texture and the physical properties of included lithological and mineral components, is not encountered, emphasizing the short distances of transport and limited comminution associated with temperate valley glaciers. Immature primary comminution tills predominate.

(5) The gross mechanical character and structure of parent bedrock may determine the character of primary debris input, such as block size, into the glacier debris system; secondary weathering of such blocks produces typical immature till debris.

Concluding Remarks

Two models of medial moraine formation, the 'ablation-dominant' and the 'ice-stream interaction' model were constructed to explain the development of medial moraine morphology exhibited on temperate valley outlet glaciers.

(A) The 'ablation-dominant' model related moraine morphology to the nature of englacial debris supply and on this basis two subtypes were formulated. (1) above firn line formation and (2) below firn line formation.

(1) Where moraines are formed above the firn line debris released from rockwalls is precipitated onto the firn surface where it undergoes sedimentation with seasonal snowfall. As a result debris extends throughout ice depth, from the glacier surface to the bed, where additional debris derivation takes place. With the merging of flow units a distinct vertical column of debris, a medial moraine or debris septum, is generated. With cumulative ablation downglacier the quantity of supraglacial moraine debris increases and is associated with an ice-cored ridged morphology. The moraine is characterized by a continuing englacial debris supply downglacier and an important subglacial debris element may be added to moraine sediments in the terminal zone.

(2) Where moraines are formed below the firn line at the margins of ice cap outlet glaciers moraine debris is derived subaerially from nunatak areas in the confluence zone. Such debris is precipitated into crevasses and comes to occupy only a shallow englacial position. The quantity of englacial debris below the base of the deepest crevasses is small and

is attenuated further by the thickening of ice in response to compressive strains at the ice fall base. Crevasse-bound debris is revealed downglacier and an ice-cored moraine ridge is generated. With the cessation of englacial debris supply as crevasses ablate out moraine morphology collapses. This is in contrast to the situation where moraines are formed above the firn line.

(B) Medial moraines are generated in many instances below the firn line by the confluence of large valley outlet glaciers transporting lateral moraine debris. Medial moraine width is seen to remain constant downglacier until the terminal zone is reached. An 'ice-stream interaction' model of moraine formation related unchanging moraine width to lateral compression between outlet glaciers and the complex patterns of ice flow found in these zones.

The two models were tested on Austerdalsbreen, Norway (below firn line subtype of the 'ablation-dominant' model) and on Berendon Glacier, British Columbia (above firn line subtype). The 'ice-stream interaction' model could also be tested on Berendon Glacier for the glacier trunk is formed by the confluence of two large outlet arms below the firn line, transporting lateral moraines. The following results were obtained.

Austerdalsbreen, below firn line subtype of the 'ablation-dominant' model.

A lower limit of englacial debris is present as the result of moraine debris being derived subaerially from nunataks

in the confluence zone and being precipitated into crevasses. As a result of the termination of englacial debris supply downglacier moraine morphology collapses. 'Annual' and 'perennial' ice-cores can be recognized.

Berendon Glacier, above firn line subtype of the 'ablation-dominant' model

On Berendon Glacier englacial moraine debris is found to extend throughout ice depth and medial moraines are found to be associated with a continuing englacial debris supply in the terminal zone. Subglacial debris is also contributed to moraines in the terminal zone. The distribution of englacial debris with depth is not constant and the bulk of moraine debris is transported near the bed and is only revealed in the terminal zone where it is associated with a developing ice-cored morphology. An ice-core is not present upglacier, supraglacial debris quantities remain low and moraine width remains constant. This is related to the decline in the quantity of englacial debris above the bed. This upper debris is derived entirely from extraglacial rock slopes and upper ice carapaces; the clarity with which medial moraines and debris septa are revealed immediately below the firn line reflects the rate of erosion in these areas.

Berendon Glacier 'Ice-stream Interaction' Model

On Berendon Glacier the 'ice stream interaction' model is only substantiated in the immediate confluence area of two large valley outlet arms. Unchanging moraine width and the

absence of an ice-core can be related to the absence of englacial debris supply which commences only in the terminal zone. Moraine morphology is more clearly explained by reference to the above firm line sub-type of the 'ablation-dominant' model since debris septa contributing to the lateral moraine load of the arms are formed above the firm line.

Moraine Sedimentology

A distinct moraine debris type cannot be distinguished on Berendon Glacier on the basis of particle-size distribution in the range ϕ to ϕ (16 mm to .0625 mm). The elements of the glacier debris system as a whole are characterized by non-modal grain-size distribution, a wide range of particle-size is produced independent of parent bedrock. A bimodal grain-size distribution reported from the analysis of tills from mid-latitudes is not encountered and emphasizes the short distances of transport and limited comminution associated with temperate valley glaciers. Discussion of the literature makes clear that this may be a general case on many temperate valley glaciers. As a result no discrimination can be made between the character of debris carried by medial moraines formed in different fashion.

The Origins of the Models and Future Potential

In 1974, Small and Clark had related the morphology of the medial moraine on the Lower Glacier de Tsildjore Nouve to englacial debris supply; the moraine in this case is formed by the confluence of two ice falls below the firm line. Publication by Small and Clark coincided with research by the

writer on Austerdalsbreen where a similar glacial situation exists. This basic model had had to be developed further in the case of Austerdalsbreen where a well-defined ogive suite adds complexity. In addition 'annual' and 'perennial' ice cores were distinguished. The 'ablation-dominant' model was developed and tested further on Berendon Glacier in 1975. The 'ice-stream interaction' model was formulated at the same time. A moraine formed by the confluence of lateral moraines on Kaskawulsh Glacier, Yukon Territory, had earlier been described by Loomis (1970) but had not been examined in terms of englacial debris supply.

The 'ablation-dominant' model in relating medial moraine morphology to englacial debris distribution may be applicable in interpreting moraine morphology on many other glacier surfaces and further research is warranted.

Appendices I to V

Berendon Glacier - Recession Characteristics and Granduc Mill

Berendon Glacier terminus lies within 200 m of the Granduc access tunnel portal and processing facilities. The ice front is receding at present. Untersteiner and Nye (1968) on the basis of a 'good deal of guesswork' estimated the change in mass-balance required for terminal readvance. It was concluded that even allowing for drastic climatic deterioration, terminal readvance reaching Granduc facilities is unlikely within the next two decades. More detailed field measurements have been made since 1967 by the Glaciology Division of Inland Waters Directorate, Environment Canada. These enabled Fisher and Jones (1971) to comment that the possibility of terminal readvance is greater than that suggested previously. Since 1968 mass-balance studies indicate a net balance that is slightly positive (R.J. Rogerson, pers. comm. 1974). McMechan (1975) calculated the net specific balance for the years 1968-72; more positive balances were recorded.

The marginal area adjacent to South Arm ice terminus is characterized by a fine series of minor moraine ridges. Analysis of air photographs and field mapping suggest an annual origin. Construction of moraine ridges began in 1956 and annual recession rates computed from moraine spacing allow determination of terminal activity since that date. The changing state of mass-balance may be inferred and supporting data obtained for mass-balance determinations made by Environment Canada. This

analysis is made in Appendix I.

As a result of the release of warm waste mill water into the glacier system recession characteristics of Berendon Glacier have been fundamentally altered. The nature of recession following the release of mill outfall in 1970 is examined (Appendix II) and the nature of present (1975) recession determined (Appendix III).

Artificial enhancement of ice melt rates by reducing albedo values was investigated on the surface of Austerdalsbreen in 1974. In Appendix IV critical debris depth and cover values for enhancement of melt rates on the surface of Berendon Glacier are determined and the practical value of accelerating ice melt rates in the event of a re-advance by Berendon Glacier threatening Granduc mill is commented on.

The recessional activity of Berendon Glacier from 1750 A.D. to 1956 A.D. is examined in Appendix V and the modern recession characteristics placed in a much broader perspective.

Appendix I

1.0 Post 1956 A.D. Minor Moraine Ridges Around the Margin of Berendon Glacier

The outer marginal area of Berendon Glacier, deglaciated between 1750 A.D., and the mid 1950's is described in Appendix V. The following is an analysis of a fine series of minor moraine ridges oriented transverse to the direction of ice flow, that occur in an ice proximal position (Figs. 66, 67, 68). Interpretation suggests these washboard moraines have formed with an annual periodicity since 1956. The zone of minor moraine ridges (known as "mora"; Elson, 1968) is limited to a linear strip fringing the ice front south of King survey station. The southerly limit is the westward flowing waste water stream from Granduc's processing mill. Isolated moraine ridges occur to the south of this limit though their temporal relationship with the northern "mora" is obscured by a large tailings dump associated with Granduc's access tunnel portal (Fig. 66).

Minor moraine ridges when rigorously dated are sensitive indicators of terminal ice recession; an expression of the state of mass balance since the mid 1950's. Moraines are considered to be of annual occurrence though this cannot be demonstrated conclusively. Recession rates determined from ridge to ridge distance allow the post 1956 recession characteristics of Berendon Glacier to be determined for the eastern margin of South Arm ice front. Following Worsley (1974), usage of annual to describe this moraine sequence will be qualified by quotation marks.

While minor moraine ridges or washboard moraines have been well described from areas influenced by formerly extensive glaciation, descriptions of the generation of such forms at the margins of temperate valley glaciers are not numerous. Elson (1968) has reviewed the literature concerning the origin of minor moraine ridges associated with formerly more extensive ice cover and presents a forum for discussion of presently developing washboard moraine sequences. Cross-valley ridges at the margins of Athabasca and Saskatchewan Glaciers considered to be of an annual origin are described by McPherson and Gardner (1969). Douglas (1970) has described similar moraine ridges of true annual occurrence near the snout of Austerdalsbreen. Andersen and Solliid (1971) considered that a well-defined suite of washboard moraines in the marginal zone of Midtdalsbreen, Hardangerjokulen, was of an annual periodicity. Minor moraine ridges near the snout of Skeidarajökull have been described by Thorarinsson (1967) and an annual origin suggested on the basis of their regularity whilst a strict chronological analysis on the basis of terrestrial and aerial photography allowed Worsley (1974) to reach a similar conclusion regarding a series of minor moraine ridges in front of Austre Okstindbreen. In all the cases reported above glaciers are experiencing recession, the particular pattern of which is marked by annual winter still-stand or slight re-advance conditions. Worsley (1974) has discussed the relationship between varying seasonal ablation conditions over the ice front and mass balance and the consequent nature of glacier activity.

Minor or washboard moraine ridges in the ice proximal marginal area of Berendon Glacier are well-defined, being limited

to a lodgement till surface (Fig. 66). The latter is demarcated on the eastern or ice distal margin, by a linear north-south granodiorite bedrock/till contact. Eastern embayments in the bedrock outcrop are infilled by fluvio-glacial gravels and till; minor moraine ridges are absent from these areas. The elevation of the lodgement till surface is approximately constant over the length of moraine ridges; a transverse slope is apparent from 720 m. a.s.l. at the ice distal bedrock margin to 710 m. a.s.l. at the 1975 ice front. Minor moraine ridges can be identified as far north as a bedrock ridge descending westwards from King Survey station (767.88 m. a.s.l.); a distance of 350 m from the southern limit. A distinct isolated "mora" is identified to the north-east of King survey station. Close to the westerly trending bedrock ridge, bedrock protrudes through, and isolates, pockets of the lodgement till surface. Till is being actively eroded in this northern sector; two westerly trending streams draining down to active glacier ice demarcate northern sectors of the lodgement till surface on which minor moraine ridges are poorly developed (Fig. 67).

The southern limit of the moraine ridges is a turbid, waste-water stream from Granduc processing mill, flowing westward to the ice front. Mill water has truncated moraine ridges and eroded lodgement till; the stream now flows on bedrock. To the south of the mill stream, minor moraine ridges contiguous with the northern group, are known to have existed from analysis of aerial photographs. The area is now covered by

a large mine tailings dump whose ice proximal edge is now ice-cored, an indication of encroachment by the dump onto active glacier ice.

Present ice recession rates were determined by painting bedrock and stable debris surfaces; results are presented in Appendix III.

1.1 Ridge Morphology

Ridge height averages 0.5 m; width approaches 1.5 m in some instances. Well-formed ridges, irrespective of site, are composed of lodgement till derived predominantly from granodiorite. Close to medial moraines that outcrop along the medial line of South Arm ice, moraine ridges possess a diffuse cover of medial moraine debris of volcanic Hazleton assemblage type. Such debris does not play a constructional role. It is useful to distinguish between constructional debris i.e. that of which the moraine is composed, and covering, surficial debris. Former supraglacial debris can safely be distinguished from lodgement till on the basis of colour and angularity. Inter-ridge corridors and ice distal ridge slopes are observed to carry higher loads of former supraglacial debris. Ice proximal slopes are covered to a smaller extent.

Over certain limited areas, inter-ridge corridors are characterized by transverse ridges oriented parallel to the direction of glacier flow (Fig. 67). These pass without break into normal minor moraine ridges and in one area traverse several inter-moraine ridge corridors. Debris type is that of ridges parallel to the ice front.

In addition crevasse-fillings of supraglacial debris extend out from parent crevasses as minor ridges normal to

the ice front, bearing no clear relationship with lodgement till ridges of the same orientation occupying inter-moraine ridge corridors. All minor moraine ridges are for the most part free of vegetation; colonization by Salix arctica (Arctic willow) is apparent only in the furthest ice distal areas.

1.2 Age of Minor Moraines

The easternmost minor moraine ridge, defined on its eastern limb by a north-south stream, displays small morphological characteristics not typical of more recent minor moraine ridges further west. Moraine height is greater as is width. The volume of debris incorporated in the moraine is estimated to be up to three times greater than till volumes incorporated in ridges to the west. In the south, near Granduc's waste water stream the moraine has been destroyed by stream and construction activity. The moraine can be readily identified on aerial photographs. Air photographs of August 1956 (B.C. 2185: 9 and 10) depict this moraine ridge lying transverse to direction of ice flow, emerging from the ice front. On this basis this easternmost minor moraine ridge is dated at 1956 and will be referred to hence as the 1956 moraine.

Minor moraine ridges were mapped during the 1975 field season by Brunton compass and pacing. Baselines and control points were erected by steel tape measurements. The area from Granduc tailings dump in the south to the bedrock ridge descending to the ice front from King survey station, 350 m to the north, was mapped to the scale 1:400. No record of relative height was made. Slope was recorded however.

A primary baseline 80 m. long was constructed at right angles to the present ice front to pass through the 1956 moraine at that point where the moraine is especially distinct (transect A-B, Fig. 67). Ridge to ridge distances along this transect are recorded in Fig. 69. Five transects, normal to the ice front, covering varying surface slope and ridge conditions are recorded. Statistical comparison of ridge to ridge distance along these transects allows the nature of glacier recession extending over the 350 m north-south ice margin, and a maximum time period 1956-1975, to be identified. Identification of a minor moraine ridge that is laterally extensive enabled the correlation of transects where doubt surrounds the exact location of the 1956 moraine due to constructional activity in recent years.

Recession data (ridge to ridge distances) of the five transects has been ranked and analyzed by Spearman's Rank Correlation Coefficient and a t-test.

Ridge to ridge transects cover a variety of surface slope and moraine conditions. Significant cross correlations are obtained in all cases except with transect G-H. Minor moraine ridges identified on transects E-F, X-Y, A-B and C-D appear to be time equivalents.

Minor moraine ridges are clearly, in view of melt season recession rates, of winter formation (Fig. 70, a,b,c). As a working theory such moraine ridges can be assumed to be of annual winter occurrence. Whilst no absolute dates are available a highly significant relationship exists between the number of minor moraine ridges over the transect A-B (18)

and the number of years that transect represents (19; 1956 to 1974). It is not likely that more than one ridge is formed seasonally and confidence is felt in ascribing an annual origin to these minor moraine ridges. Nonetheless, as Price (1973) has pointed out it is impossible to prove annual formation simply on the basis of the correlation between number of ridges and number of years.

The inter-moraine distances are assumed to be sensitive indicators of terminal ice recession since 1956 and therefore an expression of the state of mass-balance since that date. Ridge to ridge distances (Fig. 69) yield 'annual' recession rates. No data are available before 1956. The greater size of the moraine dated to 1956 may indicate still-stand conditions at that time. From a low value in 1958 increased rates of recession are apparent until 1962 when a maximum rate of 9 m is recorded from transect E-F. Recession rates appear to decrease until 1968; a low recession rate continues until 1971 when dramatic increases occur.

Low recession rates, apparent from "annual" moraine spacing from 1968 to 1971, may reflect the changing nature of the net balance on Berendon Glacier. An average annual recession of about 3.1 m yr^{-1} is exhibited by transect A-B from 1956 to 1971. This can be compared to an average annual recession rate of 5.5 m yr^{-1} for the period 1750 to 1800 A.D., 3.15 m yr^{-1} for the period 1800-1905 and 4.19 m yr^{-1} for the period 1905 to 1956 (Appendix IV).

At present, (1975) Berendon Glacier is still in active recession. Mass-balance studies conducted on Berendon Glacier

since 1967 by Glaciology Division of Inland Waters Directorate, Environment Canada, indicate a slightly positive net balance in contrast to negative balances before that date. This may be reflected in the decreased recession rate apparent from minor moraine ridge spacing.

Moraines constructed after 1972 are small and ill-defined; one factor is certainly the decreasing quantity of lodgement till available for moraine construction. It is also probable that consequent upon year-round release of Granduc processing mill water (pg. 144), winter still-stand and generation of moraine ridges has been replaced by continuous year-round recession. This is examined in the following section.

Simple statistical correlation with the mean temperature trend exhibited by the Stewart and Juneau climatic record is possible. Still-stand conditions associated with the 1956 moraine ridge may correlate with declining temperature means to the early 1950's (Fig. 86).

Appendix II

2.0 The Effect of Granduc Mill on the Present (1971-1975)

Recession Characteristics of Berendon Glacier

The discovery of the Granduc ore body and the development of mining and processing facilities have been described by Walsh (1963), Mamen (1966), Benson (1971), and Grove (1971). Discussion below will focus on the effects of the release of warm waste mill water from the processing site at Tide Lake Camp into the terminal sub-marginal water system of Berendon Glacier. To the writer's knowledge this is the first description of the effects of pumping warm water onto a glacier terminus. Full-time production and associated processing commenced in the Fall of 1970. Diversion of Summit Lake overflow water was effected by Granduc Operating Company in 1966 to facilitate construction of the main mill site. With falling lake levels in the 1960's (Gilbert, 1969) this outlet is no longer occupied by Summit Lake water but is still used by local drainage of the Berendon/Salmon basin divide area (Fig. 66).

The effect of the Granduc mill outfall has been to generate a new mode of recession: increased basal melt, extensive ice-calving from frontal ice cliffs and possible cessation of winter freeze-up and stillstand. Terminal ice of South Arm is greatly affected by the penetration of warm mill water; North Arm ice is less severely affected. Berendon Glacier terminus exhibits features such as concentric and crescentic crevasse patterns associated with ice-walled

channels formed by extensive roof collapse and massive ice fall activity from terminal ice cliffs. Such activity can be conveniently discussed by reference to a model of ice recession similar to karst development in limestone terrain.

In addition, the release of particulate matter in mill water outfall has radically altered the character of terminal sedimentation. The immediate terminal area of Berendon Glacier is characterized by extensive shearing activity. Arcuate shear plane outcrops can be traced on the glacier surface and are particularly marked on North Arm where they truncate medial moraine N1 (Fig. 32). Shearing is activated by the obstruction of glacier flow by the granodiorite rock barrier of the Salmon/Bowser watershed; more northerly flow in the immediate terminal area in recent years has already been noted (pg. 68) and is also related to subglacial obstruction of flow and thinning terminal ice. Shearing activity has been a feature of the ice front since at least 1964. On aerial photographs of that year (Fig. 13b) the central medial moraine experiences a rapid increase in width as the rock barrier is approached and areas of moraine debris appear to be defined by shear plane outcrops. At the present (1975) extensive marginal sedimentation of Granduc particulate outfall is taking place; waste mill water (from the copper flotation process) is discharged year round, at 30°C, at the rate of 3,000 gallons per minute; 3,350 tons of particulate matter predominantly finer than medium sand is released daily. (P. Jurcic, Acting Chief Geologist, Granduc Operating

Company, pers. comm. 1976). Suspended sediment load is deposited as the mill stream encounters the low gradient of the subglacial bed.

Shear planes on North Arm elevate subglacial Granduc sediment to the glacier surface where it is mixed with medial moraine debris. Medial moraine debris in proximity to shear plane outcrops exhibits a distinct particle-size distribution consisting of a distinct mode, generally within the 1-5 to 30, (0.354 to 0.125 mm) (medium to fine-sand fraction) in harmony with shear plane and Granduc sediment (Fig. 71). Mill sediment and shear plane debris occupy a distinct area on a plot of mean size and standard deviation (Fig. 72) separate from subglacial lodgement tills found in the terminal zone. South Arm ice front exhibits stacked and imbricated englacial medial moraine debris but subglacial debris is not elevated from the bed (Fig. 73). The upward transfer of shear plane debris on North Arm has resulted in the generation of extensive ice-cored topography (Fig. 31b).

2.1 Morphological Effects on Accelerated Ice Melt Rates

The terminal ice west of Granduc's tailings dump (Fig. 66) is characterized by a gently sloping margin. Melt water drainage in this sector is lateral to the ice front with a channel often cut in ice, prior to subglacial penetration (at x, Fig. 66). Drainage from lateral moraines and the divide area between the Salmon and Bowser drainage basins also utilizes this subglacial inlet.

The main subglacial melt water outlet of Berendon Glacier lies on the western margin of North Arm terminus and remains unaffected by the entry of warm waste mill water.

Warm mill water enters the glacier system to the north of the tailings dump and enters to the glacier bed. Thick ice layers from the side walls of the large inlet tunnel are actively exfoliating.

75 m to the north a subaerial channel between ice cliffs, commences a northward run of 300 m to where it empties onto the silt-floored, marginal area recently evacuated by North Arm ice. Channel sides to the west are of active ice whose depth declines from 30 m in the south to 3 m at the far northern end of the channel. The limits of the channel to the east are determined by the sharp break in slope between the granodiorite outcrop of the Berendon/Salmon divide and the glacier bed; the channel is oriented along and against the 'toe' of granodiorite (Figs. 74, 75). The lower bedrock slope is marked by a fringing berm of ice 15 m wide and of similar depth isolated from active glacier ice. When inspected toward the end of the melt season (1975) the channel was unobstructed except for a roof of thinning debris-covered ice, adjacent to the terminal outcrop of the large medial moraine present along the centre line of the glacier. The channel has clearly formed through the action of roof collapse over a subglacial tunnel.

The channel intake is a large amphitheatre bounded by ice cliffs undergoing basal sapping by warm water. Ice falls

are common. On the surrounding ice surface a concentric crescentic crevasse pattern (Paige, 1956) has developed; transected by a splaying crevasse system; failure of rectangular ice blocks results. The inner margins of this unroofed cavern are marked by a chaos of fallen ice.

The fringing ice berm is connected with active glacier ice only in the south where it adjoins terminal ice of South Arm on which prominent medial moraines outcrop (Fig. 66). The marginal area of this latter ice is marked by a fine series of "annual" moraines (Appendix I). Annual recession rates are presented in Fig. 69. Recession rates were derived by measurement of ridge spacing along a transect normal to the ice-front (p. 140). Dramatic increases in annual rates occur after 1971.

Moraine ridges constructed after 1971 are small and ill-defined. The present recession rate of this area is 11.2 m yr.^{-1} (pg. 153). This is the highest annual recession rate since 1956. It may be that basal melt and recession continues year round as a result of Granduc water outfall. Generation of ridges before 1971 is considered to have taken place during winter freeze-up and stillstand.

Analysis of aerial photographs (1961-1974) and observations made in the field in 1975 permit interpretation of karst features found in the terminal area of Berendon Glacier. The analysis is of importance since contrary to analysis of glacial

¹This figure is on the basis of a 16 week recession period - from June to October (R.J. Rogerson; pers. comm. 1976).

karst made elsewhere (Clayton, 1964), Berendon karst features have developed on active glacier ice.

1961 aerial photography (Fig. 76a) depicted a lobate ice front during the height of the melt season. Summit Lake overflow water in its passage northward into the Bowser River maintained an ice marginal course. Subglacial penetration only occurred near the large central medial moraine. The ~~ice~~ marginal channel has produced local steepening of the ice front. Ponding ice marginal water was a feature of the ice front at this time. No ice surface depressions can be discerned.

1964, 1968 and 1969 (Fig. 76b) aerial photographs depict ice thinning and terminal recession away from the granodiorite divide area. Subglacial penetration of Summit Lake water is suggested at the time of 1964 photography by the absence of thermal erosion of the ice front by marginal melt streams. By 1968 Summit Lake water has been diverted by Granduc construction; mill production commenced in Fall 1970.

By 1972 (Fig. 76c) marked depressions 75 m in diameter and attendant concentric crevassing are apparent. 200 m above the terminus and to the north of medial moraines of South Arm ice, intersection of concentric and radial crevassing has taken place. A linear depression 50 m wide extends to the north. This terminates in an area of intense crevassing near the central medial moraine, taking the form of an oval depression in the ice surface. The subglacial inlet of mill water (Fig. 66) is marked by localized recession

and cavern formation. This is not apparent on 1969 aerial photography.

By 1974 collapse and enlargement of the central circular depression has occurred (Fig. 76d). Roof collapse has occurred along the linear depression demarcating a subglacial tunnel; sections of the roof were still in place in 1975. Terminal ice has retreated away from the granodiorite barrier leaving on its lower slopes kamiform sand deposits. Isolation of a fringing ice berm at the foot of the granodiorite rock barrier has taken place. Granduc outfall flows along the contact of the glacier bed and the rock barrier. The situation may be foreseen when Berendon Glacier has retreated out of this area of high basal melt; slope reduction in cliffed areas may take place with a return to a normal gently sloping ice front.

2.2 Discussion

Whilst karst features developing on Berendon Glacier are the result of pumping mill water onto the glacier terminus, they can be compared with descriptions of glacial karst reported in the literature. Glacial karst is usually developed in stagnant ice with high supraglacial debris cover (Healy, 1975). In contrast Berendon Glacier terminus is active and debris cover is low.

DeBoer (1949) described surface depressions and associated concentric crevasse patterns from Leirbreen, Norway. Here overflow channels from ice marginal lakes had effected subglacial erosion of impounding ice; a collapsed surface topo-

graphy and concentric crevasses marked roof collapse of subglacial tunnels. Haefeli (1951) described 'entonnoirs' or funnel-shaped holes at Gornergletscher. Nielsen and Post (1953) reported sink-holes in the terminal areas of Castner, Eel and Canwell Glaciers, Alaska.

Stokes (1957) describes channel formation by ice cavern collapse from Flatisen, Norway. Clayton (1964) considered the topography of stagnant glaciers in terms of a karst cycle. 'Ice-sinks' formed by roof collapse of subglacial caverns, natural bridges and blind valleys are described on stagnant ice of the Malaspina and Martin River Glaciers, Alaska. He suggested that for such features to form, glacier ice must be stagnant and debris-covered; the absence of glacier movement and a protective debris layer allows karstic development. Lliboutry (1965) describes circular concentric crevasses from the Glacier Juncal sud, generated on the margins of subglacial caverns. Hashimoro et al., (1966) describe similar crevasse patterns from the Antler Glacier, Alaska.

On a large scale, surface troughs and vertical displacement of the ice surface have been associated with the Grimsvötn glacial outburst in Vatnajökull where thermal activity and accelerated basal melt have produced the Grimsvötn depression, which was $35 - 40 \text{ km}^2$ in extent when reported by

Thorarínsson (1953). He suggests that Grimsvötn can be considered 'as an area characterized by a very specific glacial regime where ablation primarily takes place from below'.

Mougin (1934) reported glacier surface depression associated

with the 1892 Glacier de Tete-Rousse outburst near Mont Blanc.

Where surface depressions and concentric crevasse patterns are found in terminal areas thinning of ice roofs may lead to collapse. Paige (1956) described canyons in terminal ice of Black Rapids Glacier, Alaska. These canyons marked the subaerial exits of a large meandering subglacial stream. Thermal erosion by melt water was strongly localized within crescentic meander patterns. Roof collapse generated a meandering canyon form with sidewalls 24 - 30 m high. Upglacier where ice composing the roof was thicker, surface expression was less marked. Concentric crescentic crevasse patterns reflected subglacial thermal erosion along the stream course. McCall, reported in Paige, referred to the manner of recession as being 'unique' and proposed the terms 'subglacial stoping' or 'block-caving' for such forms. Photographs published in Paige (1956) are similar to Fig. 76 c, d, depicting the same activity at the terminus of Berendon Glacier.

Appendix III

3.0 The Nature of Glacier Recession, 1975

Recession of South Arm ice front over a twelve-week period (June-September 1975), was monitored. The ice front is marked by outcropping medial moraines and consequently by a wide variety of supraglacial debris depth and cover values. Vertical ablation at the recession site averaged 4.6 cm a day. An estimated average thickness of supraglacial debris was about 5 cm; pockets up to 20 cm thick could be located. The recession site was established where ice is least crevassed.

Horizontal ablation was determined by reference to a bedrock marker nearby. Recession data is presented in Fig. 77. Ice with a frontal slope of 30° receded 8.4 m during the period of observation; an annual rate of 11.2 m yr.^{-1} .

This value must be considered as a best estimate of annual recession. Complete winter stillstand is unlikely in this area following year-round discharge of waste outfall from Granduc mill. A series of small lunate debris ridges about 15 cm high can be identified near the present ice front and may represent temporary recessional stillstands during the winter of 1974/75.

The ice front is receding from an extensive body of lodgement till whose upper surface slopes gently towards the ice front. The ice distal edge of the till surface is demarcated by a moraine ridge dated at 1956 (Fig. 66). Bedrock

slope steepens near the recession site; granodiorite outcrops protrude through the ice proximal edge of the till surface. The ice front is therefore well-defined.

Medial moraine debris, derived from volcanic tuffs and conglomerates of the Hazleton assemblage, is added to the lodgement till surface by sliding from the ice front. The recession site is bounded to the north and south by prominent crevasse fillings extending from crevasses in active glacier ice as ridges about 25 cm high and 1 m wide, normal to the ice front.

Measurements of recession were made with a steel tape at the end of weeks 1, 2, 6, 7 and 9 and during week 12.

The mean recession rate was 0.6 m wk^{-1} (Fig. 77). The horizontal velocity of the ice is 28.25 m yr^{-1} (pg. 59). Recession data is also considered representative of those areas of the ice front devoid of supraglacial debris. For example Leigh (1972) measured short term (less than 1 day) horizontal and vertical fluctuations at the terminus of Storbreen, Norway. Whilst the influence of supraglacial morainic debris in decreasing ablation rates was discerned over a 25 day period, differential horizontal ablation totals between moraine-covered and clear ice amounted to less than 2.5 m (from graphs presented in Leigh, 1972). In addition, yearly recessional data derived from annual moraines fringing Berendon ice front indicate uniform recession of debris-covered and clean ice (pg. 140). Analysis of air photos from 1956 to 1971 demonstrates that a steep ice front has been in existence during this time; low ice slopes in terminal areas may promote greater debris

depths and decreased recession rates.

The annual recession rate of 11.2 m a year is high compared to the average rate determined from 1956 to 1971 (3.1 m^{y-1} a year; pg. 141). A suggestion that high rates of recession since 1971 are due to enhanced basal melt by waste Granduc millwater has been made above.

Appendix IV

4.0 Artificial Acceleration of Ice Melt Rates: Determination of Critical Sediment Depth and Cover Values

Artificial enhancement of ice melt rates was considered as a means of controlling the activity of Berendon Glacier terminus in the event of readvance. Plots on the glacier surface were constructed to examine the relationship between superincumbent debris depths, and resultant ice melt rates. Such work replicated and extended experiments conducted on the surface of Austerdalsbreen in 1974 (pg. 24). Albedo modification of ice and snow surfaces has long been a method of accelerating ablation rates. The decay of sea ice along inshore navigation channels has been hastened by artificial dusting (Antrushin, 1956; Mellor, 1963). Coal dust, added to snow, has released agricultural land earlier in the spring and has improved soil moisture conditions (Bensin, 1952), freed snow-and-ice-bound air fields and broken ice jams on rivers (Williams, 1970). Avsiuk (1953) reports investigations into methods of increasing the output of hydro-electric facilities by dusting contributing glacierized basins. Colbeck (1974) considered artificial dusting of glacier ice in a projected infraglacial open pit mine, as a method for the removal of ice. Ice dusting has also been considered for controlling glacier ice in a potential nickel mining project beneath the Brady Glacier, Glacier Bay National

Monument (H. Worley, pers. comm. 1975).

Debris additions to glacier surfaces may either retard or enhance ablation rates (Østrem, 1959); a critical debris depth is apparent above which retardation of ice melt occurs and below which enhancement may take place. The relationship between surface ice ablation and superincumbent debris depth is depicted in Fig. 78.

The debris can be of a wide particle-size, from volcanic dust and loess, to major rockfalls and slides affecting large areas of glacier basins. The albedo of bare glacier ice determines absorption of short wave solar radiation.

Typical albedo values for bare glacier ice range from 0.2 to 0.4 (Paterson, 1969). Since the visible part of solar radiation is nearly 50% of the energy derived from the sun over a snow or ice surface (Bloch, 1964), ablation can be substantially increased by discoloration. Darkening or colouring materials need only be added to ice or snow surfaces in small quantities to increase radiation absorption (Megahan, 1970).

An experiment on Austerdalsbre during July and August 1974, attempting to model the relationship between ice ablation rates and varying thickness and size characteristics of superincumbent debris has been described above (Sect. 2.3). Results indicated that at sediment depths less than 4 mm with low values of debris cover ice melt is enhanced (Fig. 7). For example, with a sediment depth of less than 4 mm and a debris cover of 50% the ablation rate over an experimental area was 30% greater than that over bare ice.

Field experiments were carried out on Berendon Glacier during the first week of August 1975 to determine critical sediment depth and grain size required for modification of albedo values of ice and concomitant enhancement of ablation rates.

Weather conditions vary greatly over Berendon Glacier; any scheme proposing to utilize artificial enhancement of ablation rates must consider this factor. In the present analysis, emphasis has been placed on the recording of total albedo over a duration of one week. Such determinations are integrals of varied weather conditions. Further, the importance of the availability of glacial debris of sufficient quantity for possible large scale application in the future was realized. The largest sediment bodies in the vicinity are tills and outwash in the marginal zone of the glacier and medial moraine debris occupying a supraglacial position. Granduc Operating Company has already exploited till and outwash bodies of the Tide Lake Flats for gravel extraction.

4.1 Field Procedure

The experimental area was located on South Arm ice on a gently sloping ice surface, 100 m below the terminal ice falls. No distinct foliation or crevasse remnants cross the area (though one plot later revealed a longitudinal lineation).

Eleven 1 m^2 square plots were laid out in four rows. A boundary of bare ice approximately 20 cm wide was left around each plot; in this way any interaction between ablation forms developing on adjacent plots was avoided.

Two debris types were selected for experimentation; dirt-cone debris from medial moraine S1 and recently dumped subglacial tills from the ice front. In this way, effort expended in haulage by hand was reduced. Till was utilized on plots A to G inclusive. Three size fractions were obtained by hand sieving of dried sediment (finer than 1 mm, 1 to 4 mm, 4 to 35 mm). Two debris cover values were employed (50% and 100%) at three debris depths 1, 0.5 cm, and 1 grain). Depth, cover and grain-size data for respective plots are presented in Table 3.

Dirt-cone debris was not sieved; superincumbent debris depth and cover were varied over four plots (H, I, J, K). Debris was applied by hand. Plot J consisted of dirt-cone debris applied without any cover or depth change and was considered a sufficient control on experimentation. With subsequent ablation dirt-cones developed.

Ablation stakes were drilled into each plot in addition to a stake recording ablation over bare ice. The debris plots were laid out on August 1, 1975 and the experiment was terminated on August 7, 1975.

Intensive recording of meteorological variables during this period was not attempted, the object of the experiment being primarily to determine sediment depth and cover values generating the greatest enhancement of ablation rates under varying weather conditions. During the week of observation maximum temperatures ranged from 21°C (5-8-75) to 7°C (7-8-75) at 10 cm above the ice surface. Minimum temperatures ranged at the same height from 0°C (overnight 3/4-8-75) to 2°C (over-

TABLE 3

Experimental Plots: Debris Character

Plot	Debris Size	Lithology	Depth	Cover	Origin
A	1-4 mm; 0-2 ϕ	Granodiorite	1 cm	100	Subglacial debris
B	" "	"	1 grain	100	"
C	" "	"	"	50	"
D	< 4mm; < -2 ϕ + odd pebbles	"	"	100	"
E	" "	"	"	100	"
F	4mm-35mm; > -2 ϕ	"	"	100	"
G	" "	"	"	50	"
H	Dirt & one debris	Tuff Bowser Assemblage	2 cm	100	Medial Moraine SI
I	" "	"	1 cm	75	"
J	" "	"	$\frac{1}{2}$ cm	50	"
K	" "	"	$\frac{1}{2}$ cm	25	"

night 5/6-8-75). All days during the experiment were with rain except for the 7th. Highest rainfall was recorded during the 4th. The significance of rainfall in terms of sediment movement is described below.

Total ablation recorded at the end of the week was an integral of many weather conditions. Ablation rates were determined on all plots except J, on seven occasions at time intervals of 11-35 hours. The error in ablation readings is considered to be within 2 mm.

4.2 Results

Ablation rates are presented in Fig. 79; total ablation for bare ice over the seven day period was 33 cm, a daily average of 4.7 cm. Highest cumulative ablation was reported at plot H (43.3 cm; an increase over bare ice of 30%). A similar figure was obtained using comparable debris depth and cover values on Austerdalsbre in July/August 1974 (Fig. 7). Total ablation rates for all plots, except J, are shown on Fig. 79. Percentage increase in ablation over the bare ice value is also recorded.

On plots F, G, and I, ice melt rates approximated that over bare ice for the seven day period. The lowest ablation total was recorded at plot D; total ablation at this plot however is only 1.8 cm below the value for bare ice (Fig. 79). Coarse debris (4 mm to 3.5 cm) on plots F, G, afforded no protection to underlying ice; a similar result was obtained on Austerdalsbre in 1974. Dirt-cone debris from medial moraine S1 is derived from dark-red volcanic tuffs of the Hazleton assemblage and consequently has a lower albedo than till derived from granodiorite.

Vertical polaroid photographs were taken of each plot at the commencement and fourth day of experimentation (Fig. 80). On those plots with debris cover values of 50 and 25% (E, F, H, K) debris dispersion over the ice surface of the plot can be assessed.

Rainfall is an important dispersive force. At the end of seven days different debris cover values on dirt cone plots cannot be discerned; 100% cover has been achieved by debris dispersion (plots H and K). Debris depth was reduced over these plots; initial cover values may therefore only be important in that they determine how much debris is available for subsequent dispersion.

4.3 Interpretation and Recommendations

Experimental plots of varying sediment depth, particle size and cover value on the surface of Austerdalsbre, Norway and Berendon Glacier, B.C. support the suggestion that thin debris thicknesses (less than 1 cm) increase ice ablation rates.

Maximum enhancement (30%) was achieved in both glacial environments by unsieved dirt-cone debris applied at an initial cover value of 50% at an average debris thickness of about .5 cm. It is not known whether the same debris depth, and cover value is applicable to ablation enhancement of snow cover; experiments on Austerdalsbre and Berendon Glacier were not made above the seasonal snow line. Slaughter (1969) has reviewed literature on snow albedo modification. It would appear however that experimentation utilizing the same debris depth, type and cover values as recommended here might be

profitable over large areas of the glacier surface below the snow line.

Highly crevassed areas would not be amenable to such application. If such work is planned, it is recommended that sediment depth type and cover value, suggested here on the basis of field experimentation, be utilized. Using readily available medial moraine debris, widespread application to the glacier would be relatively inexpensive. Dispersion of debris noted during experimentation with 1 m² plots in 1974 and 1975 may suggest that the re-application of debris to the glacier surface is needed.

4.4 Final Comment

The effectiveness of increasing ablation rates by application of debris to the ice surface has been shown. However it is likely that the effect of warm water mill outfall in accelerating glacier recession by increased basal melt (Appendix II) is more effective than acceleration of supra-glacial ablation rates.

Appendix V

5.0 The Recession History of Berendon Glacier, 1750 to 1956 A.D.

The following discussion is an attempt to relate the recession history of Berendon Glacier to the greater north-western North American chronology. The following analysis is tentative; a more detailed attempt at dating the recession of Berendon Glacier is outside the scope of this thesis. However, as is discussed below, the magnitude of debris removal by medial moraines and other debris elements of South Arm ice has not been constant in time. The analysis of debris deposition exhibited in the marginal zone of Berendon Glacier complements and extends studies of debris movement in the present glacier debris system. The marginal area of Berendon Glacier can be defined as that area between the outer terminal moraines and the present ice front. The marginal area has been mapped from air photographs (1956-1974) terrestrial photographs of sporadic age and altimeter traverses conducted in the field (Figs. 81, 82). The marginal area under consideration is lunette shaped (1.1 km^2 in area). A prominent bedrock ridge upon which King and Glay survey stations are sited constitutes the northern border of the area under consideration (Fig. 81). Recessional moraines are well-developed and will be considered along a transect from the present (1975) ice front to the outermost moraines. This transect (AB on Fig. 81) is considered as being representative of moraine development.

The complex nature of recessional sedimentation in the marginal zone of Berendon Glacier can be attributed in part,

to bedrock surface slope which, being toward ice, is typical of conditions more frequently encountered on glacier lateral margins. Much sedimentation is morphologically kamiform (Embleton and King, 1968). A long history of pro-glacial melt water ponding (Haumann, 1960) and ice marginal drainage by Summit Lake overflow water is clear.

The marginal area can be conveniently divided into two areas. On the basis of air photograph analysis a moraine dated at 1956 divides an outer marginal zone extending to the outer terminal moraines and characterized by sporadic moraine building, from an inner zone characterized by a distinct moraine type of apparently regular formation. Moraines of the inner zone are considered to be of annual occurrence; the nature of sedimentation over this inner most recent marginal area of Berendon Glacier has already been examined in Appendix I. As far as could be determined by surface observations, moraine ridges of both inner and outer zones are not ice-cored.

5.1 Past Research

The pattern of recession exhibited by Berendon Glacier as revealed by the character of recessional moraines in the marginal zone, has not attracted detailed research. Haumann (1960) discussed the significance of Berendon Glacier activity in terms of Summit Lake overflow and considered that the outermost moraine system had been occupied in 1850 A.D.. This suggestion was made on the basis of his experience of recessional moraines dating from the mid-nineteenth century glacial maximum in the European Alps. McMechan (1975) mapped the marginal zone from air photographs and suggested a date of 1750 A.D..

for the outermost moraines in accordance with recessional patterns in North America and Europe. Moraines of 1905 and 1956 age were identified from Boundary Survey Commission photography and recent aerial photography.

5.2 Northwest North American Glacial Chronology

The following discussion is limited to northwest North America; similar trends are evident in the European record following the retreat of late Wisconsin ice (Porter and Denton, 1967). The present distribution of ice bodies in northwestern North America is determined primarily by climatic events of Neoglacial age. Following Wisconsin deglaciation (c. 8000 years B.P., Mathews, 1951; Capps, 1931; Kulp et al., 1951), amelioration of climate to a post-glacial maximum mean temperature warrants usage of the term Hypsithermal for this period (Deevey and Flint, 1957; Porter, 1966; Porter and Denton, 1967). Between 7000 and 4000 B.P., mean annual temperatures in Alaska were about equal to those of the present (Goldthwait, 1966). Rising freezing levels resulted in thinning and retreat of low-neve glaciers (with some thickening of glacier ice at high altitude; Miller and Anderson, 1974). Widespread retreat of valley glaciers ensued; the culmination of late Wisconsin deglaciation (Borns and Goldthwait, 1966; Denton, 1974). Alpine glaciers predominated during this period (Kerr, 1948). Encroachment of forest into glacial valleys ensued (Heusser, 1952). Buried forest horizons inundated by subsequent glacierization are described by Russell (1893) from Yakutat; Cooper (1931 c.) observed forest remains at Glacier Bay.

Glacial outwash of the Tasekwe Glacier in the Taku River District contains forest remains (Kerr, 1948b) attributed to early post-glacial time. Further evidence of interstadial conditions is provided by sedimentation rates during periods of delta building in deglaciated areas (Kerr, 1936a; Hansen 1934), by pollen analytical studies by Hansen (1947b), and reports by Borns and Goldthwait (1966) of loess activity. Evidence of glacier retreat until around 3,500 years B.P., is clear.

Peat regrowth and extension of muskeg (Heusser, 1952, 1954), appearance of Alpine fir (Miller and Anderson, 1974) and glacial lake formation (Hanson, 1932) indicate decreasing temperatures and a return of freezing levels to low altitudes. Resurgence of glacier valley systems commenced about 3,500 years B.P.. McKenzie (1970) has documented the pattern of early Neoglacial glacier activity in Adams Inlet, southeast Alaska; forests were overwhelmed by shifting outwash deposition accompanied by glacial lake formation and till deposition. Grove (1971) reports the finding of yellow cedar (about 1,500 years old) in glacier ice from the northern valley side of the Bowser Valley near Berendon Glacier. At present yellow cedar grows locally only on the coast, and this discovery suggests that yellow cedar previously grew well inland at 1,500 years B.P.. Resurgence of ice cover culminated in a post-Wisconsin maximum of late Neoglacial time (c. 1750 A.D.), although there is evidence in Adams Inlet of local retreat of ice between 1150 - 1300 A.D., the so-called Little Optimum (McKenzie, 1970). Local glacier advances of short duration also complicate this simple picture (Barendsen et al, 1957); a

glacial advance about 1550 A.D. is described by Goldthwait (1966).

The nature of the post 1750 A.D. glacial activity of Berendon Glacier is discussed in detail below. Literature describing glacial activity subsequent to 1750 A.D. in southeast Alaska is summarized in Fig. 83.

5.3 Recessional Moraines of Berendon Glacier 1750-1956 A.D.

Tree ring counts were made during 1975 on Alpine firs recently cut by Granduc 200 m inside the outer moraine ridges on a minor moraine ridge southwest of Clay survey station. Five tree ring counts yielded a maximum of 169 years. Allowing for an ecesis period of 10 years (for the establishment of vegetation) subsequent to deglaciation, a date of 1800 A.D. is suggested for this ridge which will be referred to as the 1800 A.D. moraine ridge. Haumann's ascribed date of 1850 A.D. for the outer moraine ridges cannot be supported but McMechan's 1750 date can be.

From the Juneau Ice Field, Lawrence (1953) reports recession from a maximum late Neoglacial extent commencing in 1769 (Mendenhall Glacier) and 1783 (Eagle Glacier). Heusser and Marcus (1964) dated initiation of recession at 1750 A.D., (Lemon Creek Glacier, S.E. Alaska). Dates such as these are widespread not only in North America, but Scandinavia and Iceland (Faegri, 1950, Thorarinsson, 1943). The error in ascribing a 1750 A.D. date to the outer moraine ridges of Berendon Glacier is not likely to be great therefore. No

attempt is made to resolve the double arcuate character of these moraines though double arcuate moraines dating from this period are described by King (1959) from Austerdalen and by Albrecht (1972) from Storbreen. Okko (1955) and Andersen and Sollid (1971) report from Iceland and Norway departures from a simple terminal moraine at this date.

Up to seven subdued moraine ridges occupy the intervening marginal area between the outer 1750 A.D. moraines and that ridge dated at 1800 A.D. These can be identified from air photographs but field identification is made difficult by absence of vegetation differences between inter-moraine corridors and moraine ridges. Northeast of the 1800 A.D. moraine, two melt-water channels, leave Berendon Glacier basin and continue over to Betty Creek. These were probably occupied by Berendon Glacier and Summit Lake melt waters following withdrawal of the ice-front from the outermost 1750 A.D. moraines. The subdued moraine ridges do not possess an obvious relationship with these channels yet are clearly of similar age.

Boundary Survey Commission photography and air photographs allow positive identification of recessional moraines formed in 1905 and in 1956 (Fig. 81). Determination of the width of inter-moraine corridors along the transect AB (Fig. 81) allows recession rates to be calculated. Recession rates away from 1750 moraine(s) to a position dated at 1800 A.D. by tree ring counts are high; 5.5 m yr^{-1} . This is the highest interpolated rate of recession evident from 1750 to 1971 (Fig. 84); since 1971 the rate of recession has been artificially

accelerated. Between 1800 A.D. and 1905 A.D., the margin of Berendon Glacier receded at a mean rate of 3.15 m yr^{-1} . During this period Berendon Glacier constructed four prominent moraine ridges. The recession rate between 1905 and 1956 is high, 4.89 m yr^{-1} , less than that obtaining from 1750 to 1800 A.D., but greater than that of the preceding century. Following 1956 the mean recession rate has declined to a figure lower than that obtaining since 1750 A.D. For the period 1956 to 1971 a suite of well-defined terminal moraine ridges, whose formation is demonstrated to be of annual occurrence, allows more precise measurement of annual recession rates (Appendix I).

Total recession along the transect AB, 1950 to 1971 A.D., is 903 m (Fig. 85), over a range of elevation from 850 to 720 m a.s.l. The glacier has been receding down-slope; this may in fact explain the peculiar nature of terminal sedimentation exhibited in the marginal area since 1750 A.D. General observations of the margins of other glaciers in the vicinity of Tide Lake indicate that, in this area, existing glacier bodies carry little debris load; supraglacial or basal. Marginal areas are dominated by polished bedrock exposures containing shallow drift pockets. Large deltas exposed by drainage of Tide Lake indicate that much debris load has been evacuated by glacial melt water. On the northern slopes of Bowser Valley, the steep downglacier gradient of the rock floor and low debris quantity has prevented terminal moraine construction. Marginal barrens undifferentiated by moraines characterize these glaciers. Yet it is safe to

assume that the glacial recession since late Neoglacial times (1750 A.D.) has been characterized by periods of still-stand; comparisons made below with respect to glacier recessional patterns in coastal Alaska make this clear. Indeed, continuous recession unpunctuated by still-stand conditions since 1750 A.D., is rarely met with in glacier studies. Debris quantity in the marginal area of Berendon Glacier is small; the possibility that terminal moraine building is determined by debris provision rather than by glacier mass-balance must be entertained. That Berendon Glacier exhibits in its marginal zone the clearest pattern of recessional moraines in the Tide Lake region, may be due to upglacier bedrock slope. Evidence is presented below that supports a non-climatic origin of certain terminal moraines in the marginal area of Berendon Glacier.

Terminal moraines occupying the area between the 1800 and 1905 moraine ridges are tentatively dated by reference to annual recession rate determined for the period (3.15 m yr^{-1}). 100 m downslope of the position occupied by ice in 1800 A.D. is a pronounced trim-line associated with a moraine ridge, devoid of vegetation, separating a well-vegetated outer area from an inner vegetation free area that extends to present glacier ice. On the basis of interpolated recession rates described above the moraine ridge is tentatively dated at 1835 A.D. The trim-line can be traced into the northern marginal zone where it conforms to the trim-line at 785 m a.s.l. associated with the glacially impounded Tide Lake surface. Tide Lake, occupying the upper Bowser River Valley,

was impounded by Frank Mackie Glacier in the northwest (Haumann, 1960). Well-preserved shore lines, varved lake clays and sub-areally eroded deltas provide evidence of lake history. The lake drained for the last time in 1930.

The 1835 A.D. moraine can be traced over a considerable distance. Ice marginal ponding of water is indicated by lithological contrasts inside the 1835 A.D. moraine ridge; sporadic boulder distribution may reflect berg-drifted debris. Terraces identified by Haumann (1960) and McMechan (1975), considered to reflect changing lake levels, may in fact be sub-aqueous moraines. Continued ponding at the 1835 A.D. moraine level would explain striking vegetation differences over ice proximal and ice distal zones. Moss, alpine fir and willow colonization is extensive on distal surfaces.

Downslope from the 1835 A.D. moraine a further moraine ridge can be identified, tentatively dated at 1852 A.D.. This moraine is locally complex; three closely spaced moraine ridges are present in some areas. Moraine debris is composed predominantly of rounded granodiorite boulders, testifying to subglacial transport, now experiencing granular disintegration. An 1867 A.D. moraine can also be identified, granodiorite again predominates.

A dominant moraine ridge dated at 1884 A.D. is characterized by strong lithological, clast size and shape contrasts with surrounding moraines. Boulder diameter exceeds 4.5 m in some instances. The rock type is green volcanic conglomerate of the Hazleton assemblage; referred to on pg. 37 as the upper member of the stratigraphy revealed in upper

South Arm Basin. The moraine does not contain granodiorite clasts. On South Arm ice, medial moraines SI-III and SI-V, in addition to an anomalous erratic moraine on upper South Arm ice (Fig. 65) are composed of similar debris and are also distinguished by relatively large boulder size. Debris of the 1884 moraine is clearly not subglacial load. In toto, evidence suggests that this moraine has no climatic significance and is a dump moraine (Embleton and King 1968). The 1884 moraine is formerly supraglacial debris load, dumped upon attainment of an ice frontal position.

DeGeer (1940) in an examination of annual or washboard moraines identified ridges characterized by very large debris size and considered that such moraines resulted from earthquake activity releasing uncharacteristic debris into the glacier system. Such 'seismic' moraines were in fact, transported scree debris. Such moraines have been called pseudo-morainic ridges (von Engel, 1933) and false moraines (Bentham, 1941).

The 1884 moraine can be correlated by aerial photography with a series of small, arcuate moraines developed 350 m north of Tum I survey station where Granduc processing mill is now sited. The mill is sited on a granodiorite bedrock outcrop protruding through an extensive kamiform till deposit, which is traceable northwards to King survey station and westwards to present glacier ice. The sediment platform may be related to former sub-marginal melt water ponding by Berendon Glacier and the nature of the bedrock surface slope. It is evident that the moraine dated at 1905 (by analysis of Boundary

Commission photography by White Fraser in 1905) is superimposed on the till surface. In the field the 1905 moraine is not well-defined; a subdued ridge-like form is identified and mapped from air photographs. Granduc's access road to Tide Lake Flats utilizes the upper surface of the moraine.

Small discontinuous arcuate moraines are associated with recession of the ice front to the south of the Granduc mill rock outcrop. A deep channel extends from these moraines and is cut into the kamiform till surface. The gully bottom is bedrock, indicating a maximum sediment depth of 10 m.

1959 aerial photography shows Summit Lake overflow water utilizing this channel. The pre-1966 (i.e. prior to diversion by Granduc Operating Co.) outlet effected great erosion of the western margin of the kamiform deposit; isolated mounds bear evidence of a formerly more extensive sediment body in this area.

The character of recession exhibited by Berendon Glacier after 1905 is not known in detail until 1956 when air photographs reveal an extensive moraine ridge emerging from the ice front. A terrestrial photograph of 1920¹ shows the position of the ice front at that time. Since 1956 a series of well-developed recessional moraines has been formed. Annual occurrence of moraine ridges has been indicated (pg. 141).

¹ B.C. Minister of Mines and Petroleum Resources. Annual Report 1921, facing p. 64.

5.4 Discussion: Glacier Behaviour during the 19th Century in Northwest North America

Glacier recession rates during the 19th century in northwest North America declined from rates of recession during the period 1750-1800 A.D.. The period is associated with stationary ice fronts and in some instances with terminal advance (Fig. 83). At Herbert and Mendenhall glaciers, prominent terminal moraines were constructed in the 1830's and the 1860's (Lawrence, 1950b, 1953). At Lemon Creek Glacier, recession rates declined between 1819 and 1891; a similar pattern emerges from East and West Twin Glaciers (Heusser and Marcus, 1964) and Black Rapids, Castner, Canwell, Gulkana and College Glaciers (Reger and Pewe, 1969). In Wachusett Inlet, McKenzie and Goldthwait (1971) on the basis of extrapolation of recession rates observed by Reid in the late nineteenth century, suggest that ice remained at or near its maximum late Neoglacial position until 1835. The recession rate of Berendon Glacier during the period 1800-1905 is lower than that of the preceding fifty years. The possibility of still-stand accompanied by subsequent higher recession rates must be entertained. Moraine dating must remain tentative therefore. In addition the recessional moraine dated to 1884 is of slight climatic significance being related instead to debris provision. Haumann (1960) describes resurgence of Salmon Glacier during the mid-19th century. The 1880's in Northwestern North America were characterized by temperatures lower than any subsequent record (from the graphs of Mathews, 1951 and Longley, 1954).

The last decade of the 19th century was characterized by rapid recession of glaciers in response to a general amelioration of temperature (Heusser and Marcus, 1964). This period of rapid glacier recession was observed in coastal Alaska by Klotz (1899, 1907). The 1905 A.D. Berendon moraine may be associated with declining temperatures until 1920 A.D.. At Lemon Creek and Herbert Glaciers, recession during the period 1902 to 1909 A.D. was also small.

5.5 Twentieth Century Recessional History

The collection of climatic data at Stewart, close to sea level, began in the second decade of the present century (Fig. 86). Mean annual temperature at Stewart declined to 1917 (-2.7°C) rising subsequently to a peak (8.3°C) in 1926. The general trend of temperature can be correlated with the record from Juneau presented by Heusser and Marcus (1964). In Juneau, temperature means declined to a minimum in 1918 to 1920, rising thereafter until 1926. Temperatures at both stations after 1926 reveal a decline to the mid 1930's, more elevated temperatures occurred at Stewart until 1947, a more distinct peak at Juneau occurring in 1942. Subsequent declining mean annual temperatures are evident at both stations until the early 1950's, while an increase is evident thereafter.

BERENDON GLACIER DEBRIS SYSTEM

APPENDIX VI

Debris Samples (Upper grain-size limit -4 φ)

SOUTH ARM

Sample No.	Position	Lithology
S1	Moraine S1 in confluence icefall	volcanic tuff
S2	Dirty Avalanche fan. (Fig. 14a) Eastern Basin, Upper S. Arm Basin	volcanic conglomerate
S3	'erratic' (Fig. 14a) moraine on S. Arm ice.	volcanic conglomerate
S4	Newly emergent englacial debris Moraine SIV	volcanic conglomerate
S5	Dirty avalanche fan: Eastern basin. Upper S. Arm (Fig. 14a)	volcanic tuff
S6	Western basin - Upper S. Arm dirty avalanche fan. (Fig. 14a)	volcanic conglomerate
S7	Granodiorite grus Upper S. Arm	Summit Lake stock
S8	Dirty avalanche fan. Western basin. Upper S. Arm (Fig. 14a)	Argillite
S9	Dirty avalanche track. Western basin. Upper S. Arm (Fig. 14a)	volcanic conglomerate
S11	'erratic' moraine-Upper S. Arm basin. (Fig. 14a)	" "
S12	Dirty avalanche fan. Eastern basin. Upper S. Arm. (Fig. 14a)	" "
S13	Crevasse-fill abating out in confluence zone	volcanic conglomerate
S14	Dirty avalanche fan. Western basin. Upper S. Arm. Site no. 1	" "
S15	Moraine S11. Terminal ice	" "
S16	Stake 14. Moraine S1	volcanic tuff
S17	Sheared basal debris S. Arm ice terminus	" "

BERENDON GLACIER DEBRIS SYSTEMDebris Samples (Upper grain-size limit - $-4 \phi = 16 \text{ mm}$)NORTH ARM

Sample No.	Position	Lithology
N1	North Arm Backwall	(Bowser assemblage)
N2	Terminus: Medial Moraine N1, Stake 10	" "
N3	Lateral Moraine: North Arm	" "
N4	Medial moraine N11 above confluence	" "
N6	Newly revealed englacial medial moraine debris close to shear planes; Moraine N1	" "
N7	Fresh englacial debris: Stake 1, Medial moraine NL	" "
N9	Lateral moraine: frost-shattered debris	" "
N10	Northern debris band - Central medial moraine	" "
N11	0.5 kilometre upglacier of sample N4 - Moraine N11	" "
N12	Stake 5, Moraine N1 - Terminus	" "
N13	Lateral moraine of North Arm above confluence derived from valley side slopes	" "
N14	Lateral moraine on North Arm	" "
N15	Lateral moraine on North Arm	" "
N16	Lateral moraine on North Arm	" "

SALMON GLACIER (Fig. 48)

Debris samples (Upper grain size limit -4-φ)

Northern, Summit Lake Terminus

<u>Sample No.</u>	<u>Description</u>	<u>Lithology</u>
D10	Medial Moraine	Argillite/siltstone
D11	Ice berg - rafted debris. Summit Lake	?
D12	Medial Moraine	Argillite/siltstone
D13	" "	" "
D14	" "	" "

BERENDON GLACIER DEBRIS SYSTEMDebris Samples (Upper grain size limit -4 ϕ)Central Medial Moraine and others

<u>Sample No.</u>	<u>Position</u>	<u>Lithology</u>
C1	Below terminal ice falls	volcanic conglomerate
C2	Bulk supraglacial stake 8	" "
C3	Below terminal ice falls	volcanic tuff
C4	Terminus	tuff and conglomerate
C5	Terminus, Stake 3	" "
C6	Terminus, Stake 6	" "
C7	Terminus, Stake 5	" "
C10	Shear plane debris; terminus N. Arm. Granduc waste particulate matter	? ?
C11	Frost-shattered granodiorite	granodiorite
C12	Subglacial debris sole	"
C13	Medial moraine debris (moraine H1) close to shear planes	" "
C14	Granduc mill particulate outfall. N. Arm terminus	? ?
C16	Fresh englacial debris; remnant berm. Terminus	Green volcanic conglomerate (Hazleton assemblage)

BERENDON GLACIER DEBRIS SYSTEM

Debris sample (Upper grain size limit - 4.0 ϕ)

Sample No.	Position	Lithology
D2	1956 Recessional Moraine	Granodiorite + volcanics
D3	Subglacial debris sole (Fig. 50)	Granodiorite + volcanics
D4	North Arm terminus; shear plane debris over ice core (Fig. 31b)	? ?
D6	Englacial debris - Moraine S11	Hazleton assem- blage tuff
D8	Subglacial debris sole	Granodiorite + volcanics
D15	Berendon Glacier, Moraine S1V; newly emergent en- glacial debris (Fig. 24)	volcanic conglomerate
D16	Central moraine newly emer- gent englacial debris	" "

BERENDON GLACIER DEBRIS SYSTEM

Sample No.	Position	Lithology
1NE	Muds in stream	Granodiorite
2NE	Muds in meltstream from Summit Glacierette	Granodiorite
3NE	Surface mud at confluence of North and South Arms	Argillite Siltstone
4NE	Summit glacierette debris sole	Granodiorite
5NE	Extraglacial scree debris	Pyritized granodiorite
6NE	Newly revealed muds along the contact of North and South Arms	Argillite
7NE	Subglacial debris sole	Granodiorite
8NE	Summit glacierette debris sole	Granodiorite
9NE	Soil near Beckert survey station	"
10NE	Scree on margins of Salmon Glacier	? ?
B3	Soil near AL-South survey station	Argillite/siltstone
SSS8	Debris sole (Fig. 50)	Granodiorite + volcanics
E1	Dirt-cone debris in confluence area	Argillite/siltstone
E6	Basal debris sole; margins of South Arm	Granodiorite + volcanics
E7	Basal debris sole; terminal South Arm	Granodiorite + volcanics
Ho	Frost-shattered granite - Holyrood, Avalon Peninsula, Nfld.	Granite

APPENDIX VII

Berendon Glacier: Air Photographs

BC-2180:58

BC 2185:9 and 10 Aug. 14, 1956 B.C. Gov't

67R2-13 8-29-67 10,000 Ber. Term. A. Post

67R2-13 8-29-67 10,000 N. Arm Basin A. Post

F-3-61-124 8-8-61 Berendon A. Post

Ex 137 Roll V642 8-22-64 12,000 Berendon A. Post

Ex 138 Roll V642 8-22-64 12,000 Berendon A. Post

A-20706 (16-17) Aug. 68

A-20857 (19-21,23, 25,27) Aug. 22/68 Can. Gov't

69 R1-127 6,800' 16:22 8-24-69 Berendon A. Post

68 L1-72 6,800' 16:22' 8-24-69 Berendon A. Post

72 V3 005 8,900 9-2-72 Terminus A. Post

74 V1-121 10,000 8-29-74 Terminus A. Post

74 V1-122 10,000 8-29-74 Terminus A. Post

74 V1-123 10,000 8-29-74 Terminus A. Post

74 V1-124 10,000 8-29-74 Terminus A. Post

138-05670 Track 120 FC 5821 9-1-74 False Colour, satellite

388-45070 Track 120 NTS 1030 8-1-73 False Colour, satellite
NB 103p

Berendon Glacier: Terrestrial Photographs

Berendon 1905 - White Fraser (Boundary Survey)

1920 - B.C. Dept. of Mines. B.C. Minister of Mines and
Petroleum Resources. Annual Report 1921, facing
p. 64

Maps

Lockwood Map. Surveys and Mapping Branch, Dept. Energy, Mines, Res.
compl. March 1969.

Ground control by Granduc 1:10,000

IWB 1009 Berendon Glacier 1:10,000

Ground control by Granduc and Surveys and Mapping Br.
Dept. Lands and Forests, B.C.

Compilation by Surveys and Mapping Branch, Dept. Energy, Mines,
Resources, Ottawa

Produced by Inland Waters Br. 1971

Geology: Berendon Glacier

Canada. Department of Mines. Bureau of Economic Geology,
Geological survey. Map 307A (1935)

Portland Canal Area
Cassiar District. British Columbia.

BIBLIOGRAPHY

- Adkins, C.J. (1958). "The Summer Climate in the Accumulation Area of the Salmon Glacier." J. Glac., 3, 195-206
- Agassiz, L. (1840). Etudes sur les glaciers. Translated by A.V. Carozzi, Hafner, London 1967
- Albrecht, J. (1972). "A Study of Till Fabric in the 1750 moraine, Storbreen." Horizon, The Journal of the King's College, London, Geog. Ass., 21, 68-70
- Allen, C.R., Kamb, W.B., Meier, M.F. and Sharp R.P. (1960). "Structure of the Lower Blue Glacier, Washington." J. Geol., 68, 601-25
- Andersen, J.L. and Sollid, J.L. (1971). "Glacial chronology and Glacial geomorphology in the marginal zones of the Glaciers, Midtdalsbreen and Nigardsbreen, South Norway." Norsk. Geogr. Tidsskr., 25, 1-38
- Anderton, P.W. (1970). "Deformation of surface ice at a glacier confluence, Kaskawulsh Glacier." Icefield Ranges Research Project, Scientific Results 2, 59-76
- Antrushin, N. (1956). "Aircraft are destroying ice." Grazdanskaya Aviatsiya, 4, 33
- Atherton, D. (1963). "Comparisons of ogive systems under various regimes." J. Glac., 4, 547-57
- Avsiuk, G.A. (1953). "The problem of artificially increasing the melt of Tien Shan glaciers." Institut Geografii Nauk SSSR. Moscow
- Barendsen, G.W., Deevey, E.S. Jr. and Galenski, L.J. (1957). "Yale natural radio-carbon measurements." Science, 126, 908-919
- Bathey, M.H. (1960). "Geological factors in the development of Veslgjuv-Both and Vesl-Skautboth, in Lewis, W.F. (ed.) (1960). Investigations on Norwegian Cirque Glaciers. The Roy. Geog. Soc. London. Res. Series No. 4
- Bensin, B.M. (1952). "Coal dust absorbs solar heat." Building Systems Design, 49, 86
- Benson, N. (1971). "The Granduc Project." Western Miner, 1971, v. 44, 49-54
- Bentham, R. (1941). "Structure and glaciers of Southern Ellesmere Island." Geogr. J., 97, 36-45
- Biscaye, P.E. (1965). "Mineralogy and sedimentation of recent-deep sea clay in the Atlantic Ocean and adjacent seas and oceans." Bull. Geol. Soc. Am., 76, 803-832

- Biscaye, P.E. (1964). "Distinction between Kaolinite and Chlorite in recent sediments by X-ray Diffraction." Amer. Mineral., 49, 49-50.
- Bishop, B.C. (1957). "Shear moraines in the Thule area, Northwest Greenland." SIPRE Research Report, 17, 1957, 46 pp.
- Bjerrum, L. and Jørstad, F. (1968). "Stability of rock slopes in Norway." Norwegian Geotechnical Institute Publication, 79, 1-11.
- Bloch, M.R. (1964). "Dust-induced albedo changes of polar ice sheets and glacierization." J. Glac., 5, 241-4.
- Boer, G. De (1949). "Ice-margin features, Leirbreen, Norway." J. Glac., 1, 332-7.
- Borns, H.W., Jr. and Goldthwait, R.P. (1966). "Late-Pleistocene fluctuations of Kaskawulsh Glacier" Am. J. Sci., 269, 600-619.
- Boulton, G.S. (1967). "The development of a complex supra-glacial moraine at the margin of Sørbreen, Ny Friesland, Vestspitsbergen." J. Glac., 6, 717-35.
- Boulton, G.S. (1975). "Processes and patterns of subglacial sedimentation: a theoretical approach" in Ice Ages: Ancient and Modern, Geological Journal Special Issue 6. Eds. Wright, A.E. and Moseley, F., 7-42.
- Boye, M. (1952). "Neves et érosion glaciaires." Rev. Geomorph. dyn., 1, 20-36.
- Brecher, H.H. (1969). "Surface velocity measurements on the Kaskawulsh Glacier." Icefield Ranges Research Project, Scientific Results, 1, 127-43.
- Brockie, W.J. (1973). "Experimental frost-shattering." Proc. 7th Geog. Soc. Con. Series, 7, 177-186.
- Brueckner, H.K. (1969). "Timing of ultramafic intrusion in the core zone of the Caledonides of Southern Norway" Am. J. Sci., 267, 1195-1212.
- Bull, C. and Hardy, J.R. (1956). "The determination of the thickness of a glacier from measurements of the value of gravity." J. Glac., 2, 755-762.
- Capps, S.R. (1931). "Glaciation in Alaska." U.S. Geol. Survey Prof. Paper, 170A, 8 pp.
- Carswell, D.A. (1973). "The age and status of the basal gneiss complex of N-W Southern Norway." Norsk Geol. Tidsskrift, 53, 65-78.

- Clayton, L. (1964). "Karst topography on stagnant glaciers." J. Glac., 5, 107-112.
- Colbeck, S.G. (1974). "A study of glacier flow for an open-pit mine: an exercise in applied glaciology." J. Glac., 13, 401-15.
- Cooper, W.S. (1931). "Third Expedition to Glacier Bay, Alaska." Ecology, 12, 61-95.
- Deevey, E.S., and Flint, R.F. (1957). "Postglacial hypsithermal interval", Science, 125, 182-84.
- De Geer, G. (1940). Geochronologica Svecica Principes, Vetenskaps Akad., Handl. Ser. 3, 18, 96-130.
- Denton, G.H. (1974). "Quaternary Glaciations of the White River Valley, Alaska, with a regional synthesis for the northern St. Elias Mountains, Alaska and Yukon Territory." Bull. Geol. Soc. Am., 85, 871-892.
- Derbyshire, E. (1975). "The Distribution of Glacial Soils in Great Britain." The Midland Soil Mechanics and Foundation Engineering Society. Symposium on the Engineering Behaviour of Glacial Materials. Apr. 1975, Birmingham, U.K. Unpublished conference paper.
- Douglas, T. (1970). "Methods of assessing the retreat of valley glaciers," Confluence, Leicester University Geog. Jour. 9-13.
- Dreimanis, A., and Vagners, U.J. (1971). "Bimodal distribution of rock and mineral fragments in basal tills," in Goldthwait, R.P. (ed). Till: A Symposium. Columbus, Ohio State Univ. Press., 237-250.
- Drewry, D.J. (1972). "Quantitative assessment of dirt-cone dynamics." J. Glac., 11, 431-46.
- Elson, J.A. (1961). "The geology of tills." Canadian Soil Mechanics Conference. 1960 Proc. 5-17.
- Elson, J.A. (1968). "Washboard moraines and other minor moraine types" in Fairbridge, R.W., ed. The Encyclopedia of geomorphology, New York, Reinhold Book Corporation, 1213-19.
- Embleton, C. and King, C.A.M. (1968). Glacial and Periglacial Geomorphology. Edward Arnold. London.
- Evers, W. (1935). "Gletscherkundliche Beobachtungen auf dem Austerdalsbræ (Südnorwegen)." Zeitschrift für Gletscherkunde, 23, 98-102.

- Eyles, N. (1975). "Models of Medial Moraine Development" in Abstracts, Can. Ass. Geog. Annual Conf., Vancouver, May 1975
- Eyles, N. (1976). "Morphology and development of medial moraines: comments on the paper by R.J. Small and M.J. Clark." J. Glac., 17, 161-2 [Letter]
- Faegri, K. (1950). "On the variations of western Norwegian glaciers during the last 200 years." Union Geodesique et Geophysique Internationale. Ass. Int. d'Hyd. Sci. Ass. Gen. d'Oslo, 19-28, aout, 1948, Proc. T. 2., 293-303
- Fisher, D.A. and Jones, S.J. (1971). "The possible future behaviour of Berendon Glacier, Canada; a further study," J. Glac., 10, 85-92
- Folk, L. (1968). Petrology of Sedimentary Rocks. Hemphill's, Austin, Texas, 170 pp
- Forbes, J.D. Theory of Glaciers, Adam and Charles Black, Edinburgh, 1859
- Ford, D.C., Fuller, P.G. and Drake J.J. (1970). "Calcite precipitates at the soles of temperate glaciers" Nature, 226, 441-2
- Garwood, E.J. and Gregory, J.W. (1898). "Contributions to the glacial geology of Spitzbergen." Q.J. Geol. Soc. Lond., 54, 197-227
- Gilbert, R. (1969). "Some aspects of the hydrology of ice-dammed lakes: observations on Summit Lake." Unpublished M.A. thesis, University of British Columbia
- Gilbert, R. (1972). "Drainage of Ice-Dammed Summit Lake, British Columbia." Scientific Series no. 20. Inland Waters Directorate Water Resources Branch, Environment Canada
- Glen, J.W. (1956). "Measurement of the deformation of ice in a tunnel at the foot of an ice-fall." J. Glac., 2, 735-45
- Glen, J.W. (1960). "Measurement of the strain of a glacier snout." Int. Un. Geod. Geophys. Int. Ass. Sci. Hyd. Ass. Gen., 1960, 562-7
- Glen, J.W., and Lewis, W.V. (1961). "Measurement of side-slip at Austerdalsbreen, 1959," J. Glac., 3, 1109-22
- Goldthwait, R.P. 1966. "Evidence from Alaskan Glaciers of Major Climatic Changes" in Roy. Met. Soc. World Climate from 8000 to 0 B.C. 229 pp. Proc. Met. Int. Symp. Lond.

- Grove, E.W. (1971). "Geology and mineral deposits of the Stewart area, B.C." B.C. Dept. Mines and Petroleum Resources, Bull. 58, 219 p.
- Haefeli, R. (1951). "Some observations on glacier flow." J. Glac., 1, 496-8
- Hambrey, M.J. (1975). "The origin of foliation in glaciers, evidence from some Norwegian examples." J. Glac., 14, 181-185
- Hannell, F.C. and Ashwell, I.Y. (1959). "The recession of an Icelandic glacier", Geog. Jour., 125, Pt. 1, 84-88
- Hansen, H.P. (1947b). "Postglacial forest succession, climate and chronology in the Pacific Northwest." Am. Phil. Soc. Trans., 37, 1-130
- Hanson, G. (1932). "Varved clays of Tide Lake, British Columbia," Roy. Soc. Can. Trans., 26, 335-343
- Hanson, G. (1934). "The Bear River delta, British Columbia and its significance regarding Pleistocene and Recent Glaciation." Roy. Soc. Can. Trans., 28, 179-185
- Hanson, G. (1935). "Portland Canal Area, British Columbia." Memoir 175, Canada, Department of Mines. Bureau of Economic Geology, Geological Survey
- Hashimoro, S. et al (1966). "Glaciological studies of the Antler Glacier, Alaska." Hokkaido University, Sapporo, Faculty of Science, Ser. IV. Journal of Geology and Mineralogy, 13, 237-56
- Haugen, H.E. (1974). "A paradise for climbers." The Norseman, 5, 1974, 128-132
- Haumann, D. (1960). "Photogrammetric and glaciological studies of Salmon Glacier." Arctic, 13, 75-111
- Healy, T.R. (1975). "Thermokarst - a mechanism of de-icing ice-cored moraines." Boreas, 4, (1), 19-24
- Hess, H. (1907a). "Ueber der Schutthalt der Innenmoränen einiger Oetztaler Gletscher." Zeitschrift für Gletscherkunde, I (1906/7), 287-292
- Hess, H. (1970b). "Die grösse des Jährlichen Abtrages durch Erosion in Firnbecken des Hintereisferners." Zeit. für Gletscherkunde, I (1906/7), 355-6
- Heusser, C.J. (1952). "Pollen profiles from Southeastern Alaska," Ecological Monographs, 22, 331-352
- Heusser, C.J. (1954). "Additional pollen profiles from Southeastern Alaska." Am. J. Sci., 252, 106-119
- Heusser, C.J. and Marcus, M.G. (1964). "Historical variations of Lemon Creek Glacier, Alaska, and their relationship to the climatic record," J. Glac., 5, 77-86

Holthedahl, O. (Ed.) (1960). "Geology of Norway," Norges. geol. undersøkelse, 208, 540 pp.

Hoskin, C.M. and Sundeen D.A., (1975). "Relationship between grain size of source rock and derived sediment, Biorka Island Tonalite, Southeastern Alaska." J. Geol., 83, 567-78

Huxley, T.H. (1857). "Observations on the structure of glacier ice." London. Edin. and Dubl. Phil. Mag. and Jour. of Sci., 4th ser. 14, 241-60

Ichikawa, M. (1958). "On the debris supply from Mountain slopes and its relation to river bed deposition." Tokyo Kyoiku Daigaku. Sci. Rep. Sect. C (Geog), 6, 1-29

Johnson, P.G. (1974). "Glacier load variations, West Lobe, Kaskawulsh Glacier," Geoscope 5, 63-76

Kamb, W.B. and Chapelle, E. (1964). "Direct observation of the mechanism of glacier sliding over bedrock." J. Glac., 5, 159-172

Karlstrom, T.N.V., (1961). "The Glacial history of Alaska: its bearing on paleoclimatic theory." Ann. New York Acad. Sci.

Karrow, P.F. (1976). "The texture, mineralogy and petrography of North American Tills" in Glacial Till: an inter-disciplinary Study, Royal Soc. Canada Spec. Pub. no. 12, Ed. R.F. Leggett. 83-98

Kerr, F.A. (1936a) "Quaternary glaciation in the Coast Range, Northern British Columbia and Alaska." J. Geol., 44, 681-700

Kerr, F.A. (1948). "The character of the Coast Range Composite Batholith in Northern British Columbia and Southeastern Alaska." Trans. Roy. Soc. Canada, Sect. 14, XXVI, 305-316

Kerr, F.A. (1948b) "Taku River map-area, British Columbia," Canada Geol. Survey, Mem. 248, 84 pp.

Kers, L.E. (1964). "Förekomst av subglacialt utfäld Kalksten i Solna samt i Gardvik Västerbottens Län." Geol. För Stockh. Förh., 86, 282-310

Kincer, J.B. (1941). "Climate in Alaska" in Climate and Man, 1211-1215, U.S. Dept. Agr. Yearbook, Washington, D.C.

King, C.A.M. (1959). "Geomorphology in Austerdalen, Norway." Geog. Jour., 125, 357-69

King, C.A.M. and Lewis W.V. (1961). "A tentative theory of ogive formation." Jour. Glac., 3, 913-39

- Klotz, O.J. (1899). "Notes on glaciers of Southeastern Alaska and adjoining territories," Geog. Journal, 14, 523-534.
- Klotz, O.J. (1907). "Recession of Alaska glaciers," Geog. J., 30, 419-421.
- Knighton, A.D. (1973). "Grain-size characteristics of super-glacial drift," J. Glac., 12, 522-4.
- Kozarski, S. and Szuprycznski, J. (1971). "Ablation cones on Sidujökull, Iceland", Norsk. geogr. Tidsskr., 25, 109-119.
- Krenek, L.O. (1958). "The formation of dirt cones on Mount Ruapehu, New Zealand", J. Glac., 3, 312-314.
- Krinsley, D.B. (1964). "Pleistocene geology of South-west Yukon Territory." J. Glac., 5, 385-97.
- Kulp, J.E., Feely, H.W., Tryon, L.E. (1951). "Lamont natural radiocarbon measurements." Science, 114, 565-568.
- Lawrence, D.B. (1950b). "Glacier fluctuation for six centuries in Southeastern Alaska and its relation to solar activity." Geog. Rev., 40, 191-223.
- Lawrence, D.B. (1953). "Recession of the past two centuries" First part of Lawrence, D.B. and Elson, J.A. (1953). "Periodicity of deglaciation in North America since the late Wisconsin maximum." Geog. Ann., 35, 83-104.
- Leigh, C. (1972). "Short-term studies of the Storbreen Glacier snout subsystem." Horizon. Journal of the King's College and the London School of Economics, Geog. Ass., 21, 74-7.
- Leighton, F.B. (1951). "Ogives of the East Twin Glacier, Alaska - their nature and origin" J. Geol., 59, 578-89.
- Lewis, W.V. (1940). "Dirt cones on the northern margins of Vatnajökull, Iceland." J. Geom., 3, 16-26.
- Liestøl, O. (1961). "Bremålinger og brevariasjoner." Den Norske Turistforenings Arbok, 1961, 24-34.
- Lister, H. (1958). Glaciology (3): "Glacial Prehistory or the Evidence of Debris" in Venture to the Arctic, (ed.) R.A. Hamilton, Penguin Books Ltd. 1958
- Lister, H. (1959). "Micro-meteorology over dirt coned ice." Jökull, Ar. 9, 1-5.
- Ljunger, E. (1936). "Hällskulpturen och den Kvartära skågerack-skalkens tillkomst." Autoreferat av föredrag hållet för Naturv. Studentsälsk. i Upsala. Göteborgs Handels-och Sjöfart stidning, Nr. 121.
- Lliboutry (1965). Traité de Glaciologie I and II. Masson and Co. Paris. 1039 pp.

Longley, R.W. (1954). "Temperature trends in Canada." Proceedings, Toronto Meteorological Conference 1953, 207-11

Loomis, S.R. (1970). "Morphology and Ablation processes on Glacier ice," (in Bushnell, V.C., and Ragle, R.H. (eds.) Icefield Ranges Research Project. Scientific Results v 2. New York, American Geographical Society: Montreal, Arctic Inst. of N. America, 27-31

Mamen, C. (1966). "Granduc drives tunnel under Glacier" Canadian Mining Journal, 87, 45-9

Marcussen, I. (1973). "Stones in Danish tills as a stratigraphic tool. A review." Bull. Geol. Inst. Univ. Uppsala., 5, 177-82

Martini, A. (1967). "Preliminary experimental studies on frost weathering of certain rock types from the West Sudetes" Biuletyn Peryglacjalny, 16, 147-194

Mathews, W.H. (1951). "Historic and prehistoric fluctuations of Alpine Glaciers in the Mount Garibaldi Map-area, south western British Columbia," Jour. Geol., 59, 357-380

Mathews, W.H. (1965). "Two self-dumping ice-dammed lakes in British Columbia," Geog. Review, 55, 46-52

Mathews, W.H. (1973). "Record of two jökullhlaups" Union Geodésique et Geophysique Internationale. Symposium on the Hydrology of Glaciers. September, 1969. Publication no. 95 de l'Association Internationale d'Hydrologie Scientifique, pp. 99-110

Matthews, J.A. (1973). "Lichen growth on an active medial moraine, Jotunheimen, Norway," J. Glac., 12, 1973, 305-315

McCall, J.G. (1952). "The internal structure of a cirque glacier: report on studies of the englacial movements and temperatures." J. Glac., 2, 122-31

McKenzie, G.D., (1970). "Glacial geology of Adams' Inlet, southeastern Alaska." Ohio State Univ. Inst. Polar Studies Rept. 25, 121 p.

McKenzie, G.D. and Goldthwait, R.P. (1971). "Glacial history of the last 11,000 years in Adams' Inlet, Southeastern Alaska." Bull. Geol. Soc. Am., 82, 1767-82

McMechan, R.D. (1975). A study of Berendon Glacier, near Stewart, British Columbia; Recent history, variations and flow rates. Unpublished B.Sc. thesis - Univ. British Columbia

McPherson, H.J. and Gardner, J. (1969). "Glacial landforms at Saskatchewan Glacier." Can. Alp. Journal., 52, 90-96

- Megahan, W.F. (1970). "The effect of albedo-reducing materials on net radiation at a snow surface." Int. Union. Geol. Geophy. Int. Ass. Sci. Hyd. Bull. XVE, 69-80
- Meier, M.F. (1960). "Mode of flow of Saskatchewan Glacier, Alberta, Canada." U.S. Geol. Surv. Prof. Paper 351, 70 pp.
- Mellor, M. (1963). "Promoting the decay of sea-ice." Arctic, 16, 142
- Miller, M.M. (1951). "Midwinter expedition to Juneau Ice Field, New York: Amer. Geogr. Soc., Mimeo. 3 pp.
- Miller, M.M. (1964). "Morphogenetic classification of Pleistocene Glaciations in the Alaska-Canada Boundary Range." Proc. Am. Phil. Soc., 108, 247-273
- Miller, M.M. (1969). "The Alaska Glacier Commemorative Project Phase I." Nat. Geogr. Soc. Res. Repts., 1964 Projects, 135-152
- Miller, M.M. and Anderson, J.H. (1974). "Pleistocene - Holocene Sequences in the Alaska-Canada Boundary Range." Alaskan Glacier Commemorative Project. Phase IV. National Geog. Soc. Res. Rep., 1967 Projects, 197-223
- Mougin, P. (1934). "Cinematique glaciare," Etudes glaciore, I, 239-268
- Nielsen, L.E. and Post, A.S. (1953). "The Castner Glacier Region, Alaska." J. Glac., 2, 277-80
- Nye, J.F. (1959). "A method of determining the strain-rate tensor at the surface of a glacier." J. Glac. 3, 409-419
- Nye, J.F. (1959a). "The deformation of a glacier below an ice-fall." J. Glac., 3, 387-408
- Ogilvie, I.H. (1904). "The effect of superglacial debris on the advance and retreat of some Canadian glaciers." J. Geol., 12, 722-43
- Okko, V. (1955). "Glacial drift in Iceland, its origin and morphology." Bull. Comm. Geol. Finl., 170, 1-133
- Østrem, G. (1959). "Ice melting under a thin layer of moraine, and the existence of ice-cores in moraine ridges" Geog. Ann., 41, 228-30.
- Østrem, G. (1965). "Problems of dating ice-cored moraines." Geog. Ann., 47A, 1-38

- Page, N.R. (1971). "Subglacial limestone deposits in the Canadian Rocky Mountains." Nature, 229, 42-3
- Paige, R.A. (1956). "Subglacial stoping or block caving; a type of Glacier ablation" J. Glac. 2, 727-9
- Paterson, W.S.B. (1969). The physics of glaciers. Pergamon. 250 pp.
- Porter, S.C. and Denton, G.H. (1967). "Chronology of Neoglaciation in the North American Cordillera" Am. J. Sci., 265, 177-210
- Post, A. (1972). "Periodic surge origin of folded medial moraines on Bering piedmont Glacier, Alaska." J. Glac., 11, 219-226
- Potts, A.S. (1970). "Frost action in rocks: some experimental Data." Trans. Inst. Brit. Geog., 49, 109-124
- Price, R.J. (1973). Glacial and Fluvio-glacial Landforms. Oliver and Boyd, Edinburgh
- Rapp, A. (1960). "Talus slopes and mountain walls; Tempelfjorden, Spitsbergen." Skr. norsk. Polarinst., 119, 96 pp.
- Rapp, A. (1961). "Recent development of mountain slopes in Karkevagge and surroundings, Northern Scandinavia." Geog. Ann., 42, 65-200
- Ray, L.L. (1935). "Some Minor Features of Valley Glaciers and Valley Glaciation." J. Geol., 43, 297-322
- Reger, R.D. and Péwé, T.L. (1969). "Lichenometric dating in the Central Alaska Range." pp. 223-248, in Péwé, T.L. (ed.) The Periglacial Environment Past and Present. Arctic Institute of North America, Montreal, McGill-Queen's University Press, 1969
- Röthlisberger, H. (1968). "Erosive processes which are likely to accentuate or reduce the bottom relief of valley glaciers." Int. Ass. Sci. Hyd., pub. 79, 87-97
- Russell, I.C. (1893). "Malaspina Glacier" J. Geol., 1, 219-45
- Rutishauser, H. (1971). "Observations on a surging glacier in east Greenland." J. Glac., 10, 227-36
- Salisbury, R.D. (1894). "Superglacial drift," J. Geol., 2, 613-632
- Samuelsson, L. (1964). "Nya fynd av subglacialt bildade Kalkstenar" Geol. Förel. Förh., 85, 414-427

- Schumskii, P.A. (1964). Principles of structural glaciology. Dover Publications Inc. N.Y.
- Sharp, R.P. (1947). "The Wolf Creek Glacier, St. Elias Range, Yukon Territory." Geog. Rev., 37, 26-52
- Sharp, R.P. (1948). "Constitution of valley glaciers" J. Glac., 1, 182-189
- Sharp, R.P. (1949). "Studies of superglacial debris on valley glaciers" Am. J. Sci. 247, 289-315
- Sharp, R.P. (1960). Glaciers. Condon Lecture, Ohio State System of Higher Education. University of Oregon Press
- Slatt, R.M. (1971). "Texture of ice-cored deposits from ten Alaskan valley glaciers." J. Sed. Pet., 41, 828-834
- Slatt, R.M. (1972). "Texture and composition of till from parent rocks of contrasting textures: southeastern Newfoundland." Sediment Geol., 7, 283-90
- Slatt, R.M. and Press, D.E. (1976). "Computer program for presentation of grain-size data by the graphic method." Sedimentology, 23, 121-132
- Slaughter, C.W. (1969). "Snow albedo modification: a review of literature." U.S. CRREL. Tech. Rep. 217
- Slingsby, W.C. (1895). "Unknown corners of the Justedalsbrae." Den Norske Turistf. Arb. Chr., 16-39
- Small, R.J. and Clark, M.J. (1974). "The medial moraine of the Lower Glacier de Tsidjiore Nouve, Valais, Switzerland." J. Glac., 13, 255-63
- Small, R.J. and Clark, M.J. (1976). "Morphology and development of medial moraines: reply to comments by N. Eyles." J. Glac., 17, 162-4
- Stenborg, T. (1966). "Some observations of differential ice-movements on Mikkaglaciären." Geog. Ann., 48A, 32-42
- Stokes, J.C. (1957). "An esker-like ridge in process of formation, Flatisen, Norway." J. Glac., 3, 286-288
- Strand, T., and Kulling, O. (1972). Scandinavian Caledonides, Wiley Interscience
- Streiff-Becker, R. (1954). "The initiation of dirt cones on snow; comments on J.W. Wilson's paper." J. Glac., 2, 365-66

Stromquist, L. (1973). "Geomorfologiska Studier av Blockhav och Blockfält i Norra Skandinavien." Uppsala Universitet Naturgeografiska Institutione, Rep. 22, 159 pp

Swithinbank, C.W.M. (1950). "The origin of dirt cones on glaciers." J. Glac., 1, 461-5

Tarr, R.S. and Martin, L. (1914). Alaskan Glacier studies, Nat. Geogr. Soc. Washington. 498 p

Theakstone, W.H. (1965). "Recent changes in the glaciers of Svartisen," J. Glac., 5, 411-31

Thorarinsson, S. (1943). "Oscillations of the iceland glaciers in the last 250 years," Geog. Ann., 25, 1-54

Thorarinsson, S. (1953). "Some new aspects of the Grimsvotn problem." J. Glac., 2, 267-77

Thorarinsson, S. (1960). "Glaciological knowledge in Iceland before 1800." Jökull, 2, p. 1-17

Thorarinsson, S. (1967). "Washboard moraines in front of Skeidarajökull." Jökull, 17, 311-312

Untersteiner, N. and Nye, J.F. (1968). "Computation of the possible future behaviour of Berendon Glacier, Canada." J. Glac., 7, 205-13

Von Engel, O.D. (1933). "Palisade Glacier," Bull. Geol. Soc. Am., 44, 575-99

Walsh, D.C. (1963). "Reclaiming the shaft of Granduc Mines." Western Miner, 36, 86-93

Ward, W.H. (1961). "Experiences with electro-thermal ice-drills on Austerdalsbre 1956-9." Int. Comm. Snow. Ice. Int. Ass. Sci. Hyd. Pub. 54, 1961

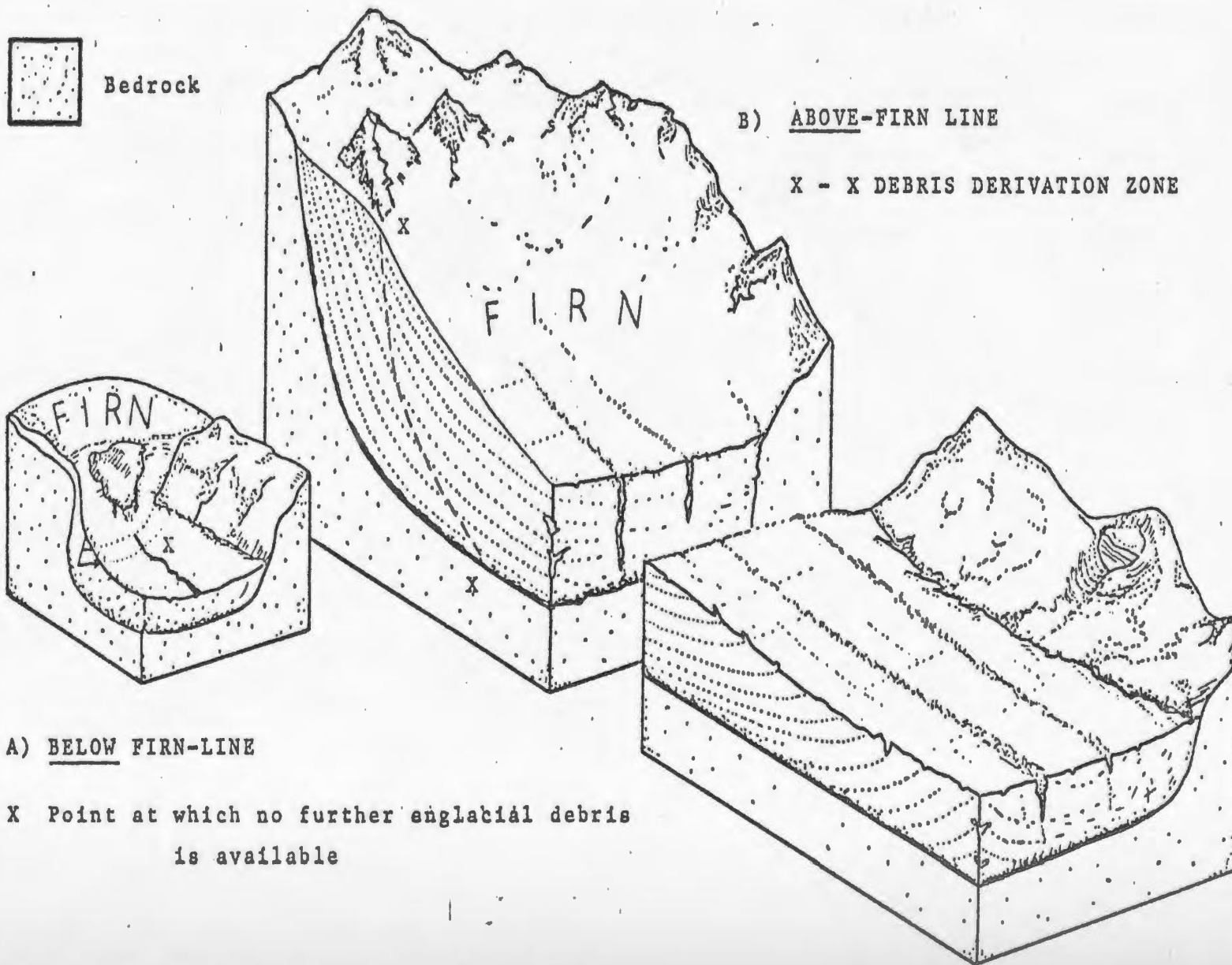
Whalley, W.B. (1974). "Rock glaciers and their formation as part of a glacier debris-transport system." Geographical paper no. 24, Dept. of Geography, Univ. of Reading, U.K.

Whalley, W.B. and Krinsley, D.H. (1974). "A scanning electron microscope study of surface textures of quartz grains from glacial environments." Sedimentology, 21, 87-105

Williams, G.P. (1970). "Break-up and control of river ice." Int. Ass. Hyd. Res. Symposium Proc. 1970. Reykjavik, Iceland, Sect. 3.12

Wilson, J.W. (1953). "The initiation of dirt cones on snow." J. Glac., 2, 281-7

- Wiman, S. (1963). "A preliminary study of experimental frost weathering." Geog. Ann., XLV. 113-120
- Wojcik, G. (1970). "Ablation processes on the Skeidararjökull (Iceland)." Bull. de l'Acad. Polon. des. Sci. (Geol. and Geog). XVIII, 251-258
- Wojcik, G. (1973). "Glaciological studies on the Skeidarajökull." Geog. Polon., 26. 185-208
- Wood, A.L. (1935). "Mountaineering in the Jostedalshrae." Alpine J., 47, 272-282
- Worsley, P. (1974). "Recent "Annual" moraine ridges at Austre Okstindbreen, Okstindan, North Norway," J. Glac., 13, 1974 265-77
- Young, R.A. (1953). "Some notes on the formation of medial moraines," Jökull, 3, 32-3



THE 'ABLATION-DOMINANT' MODEL

Figure 1. The 'ablation-dominant' model of medial moraine formation.

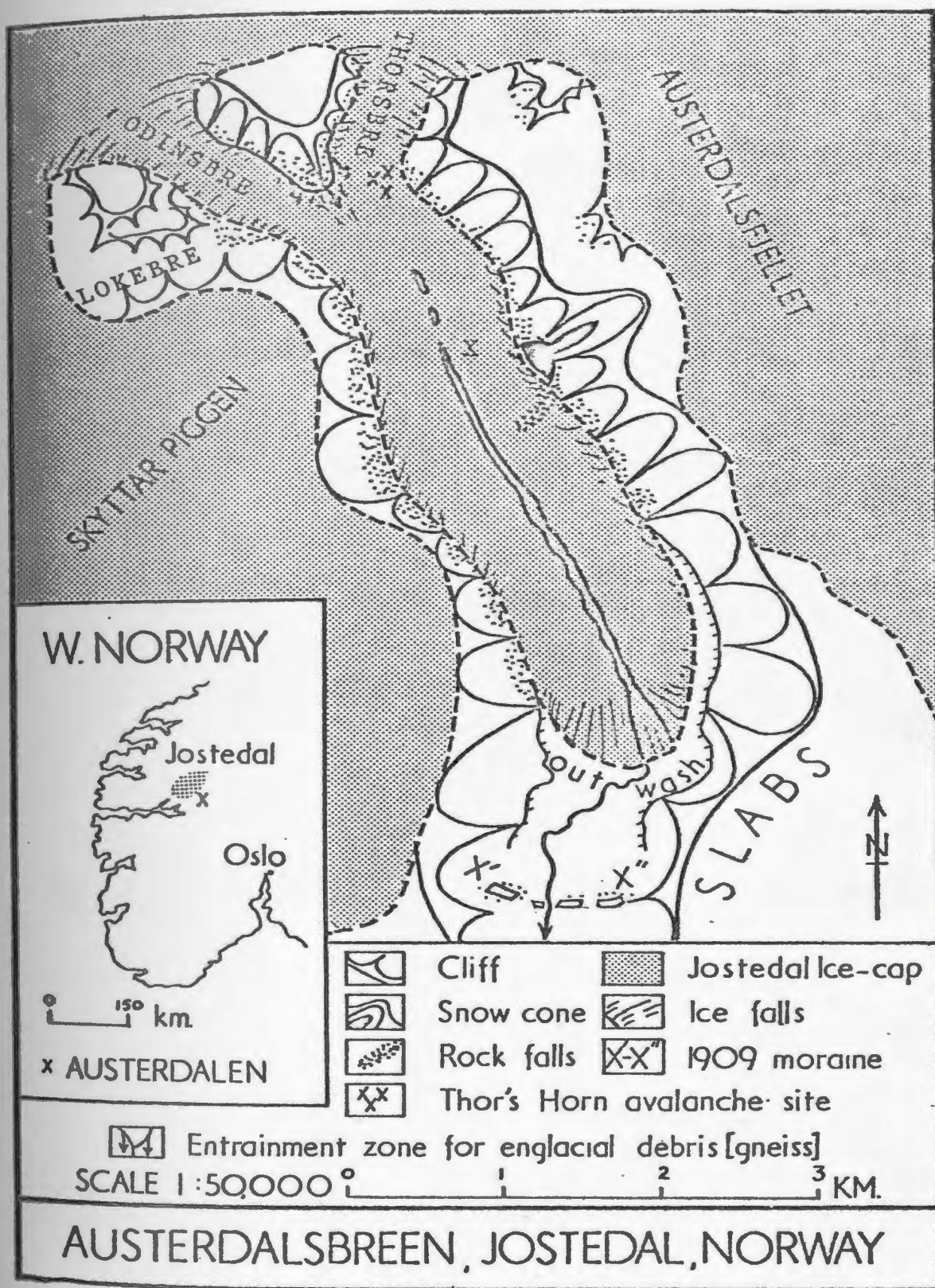


Figure 2. Austerdalsbreen ; location of the field area.
(1974)

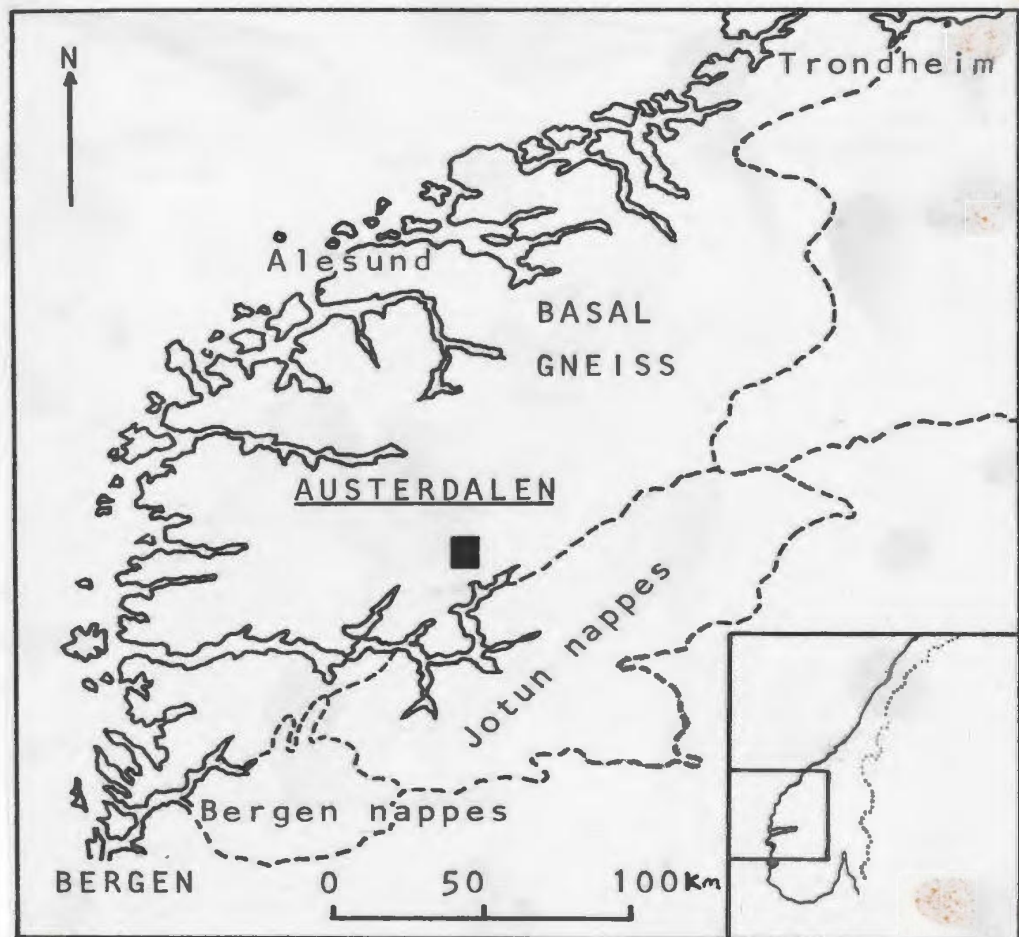


Figure 3. Structural zones of Western Norway.



Figure 4a.

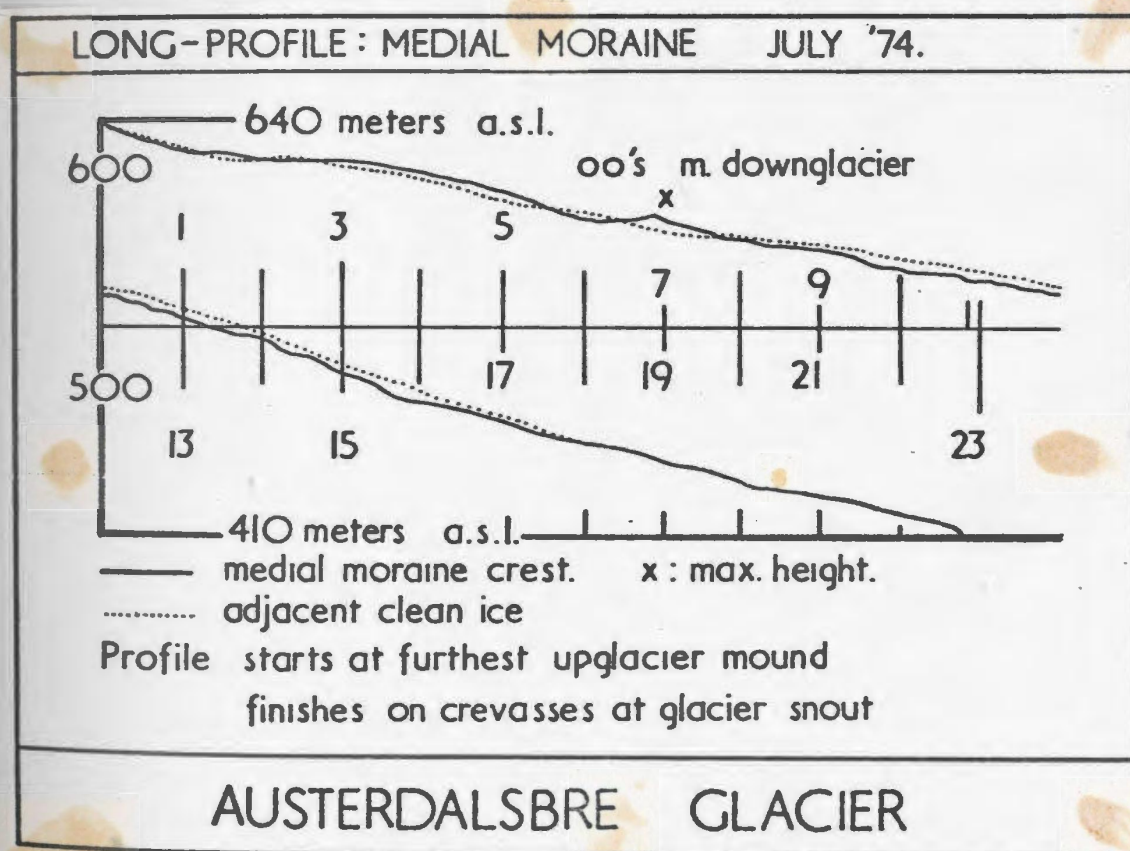


Figure 4b.

Figure 4. Austerdalsbreen medial moraine long profile;
 (a) photographic (from the snow cone, fig 2) 1974.
 (b) surveyed (T. Douglas and undergraduates,
 University of Leicester Jostedal Expedition) 1974.

Figure 5. Austerdalsbreen medial moraine: the 'ablation-dominant' model; below firn line subtype

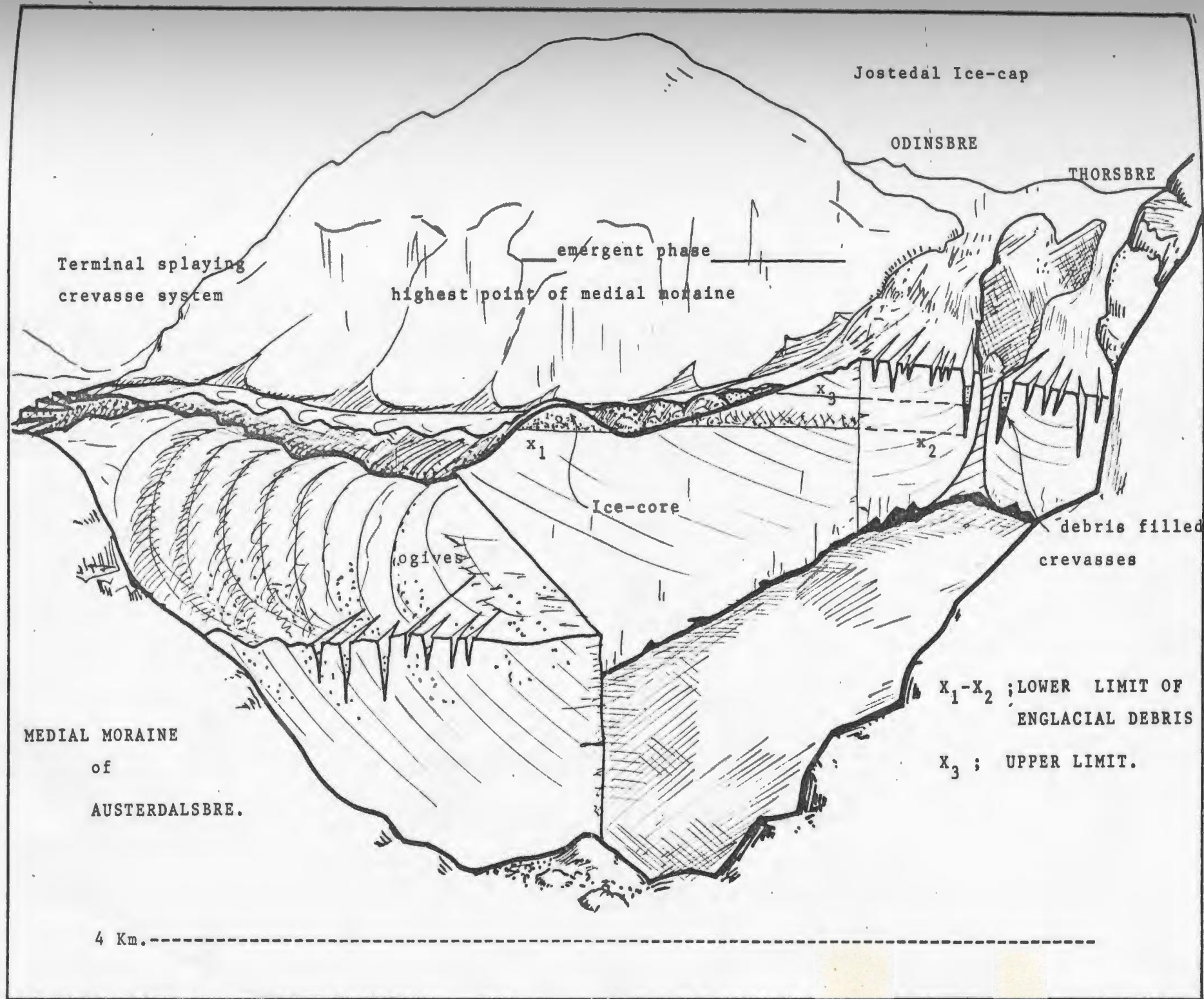




Figure 6a. Austerdalsbreen medial moraine; 1959 ¹



Figure 6b. Austerdalsbreen medial moraine; 1974. ²

²Reproduced by permission of R.L.Shreve.

1

"

"

"

" T.Douglas.

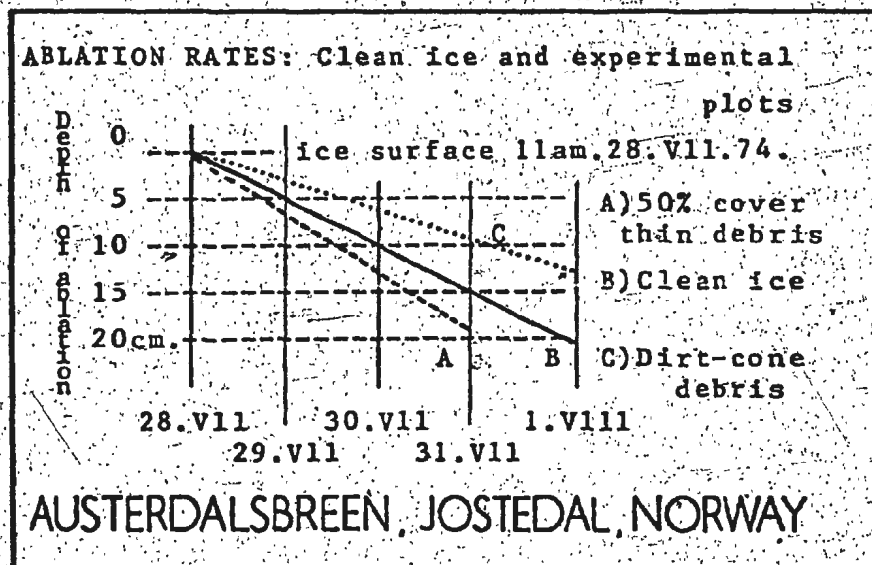


Figure 7.

Ablation rates over experimental plots.

Austerdalsbreen, July/August 1974

Mean daily ablation rate over clean ice ; 4.8 cm.

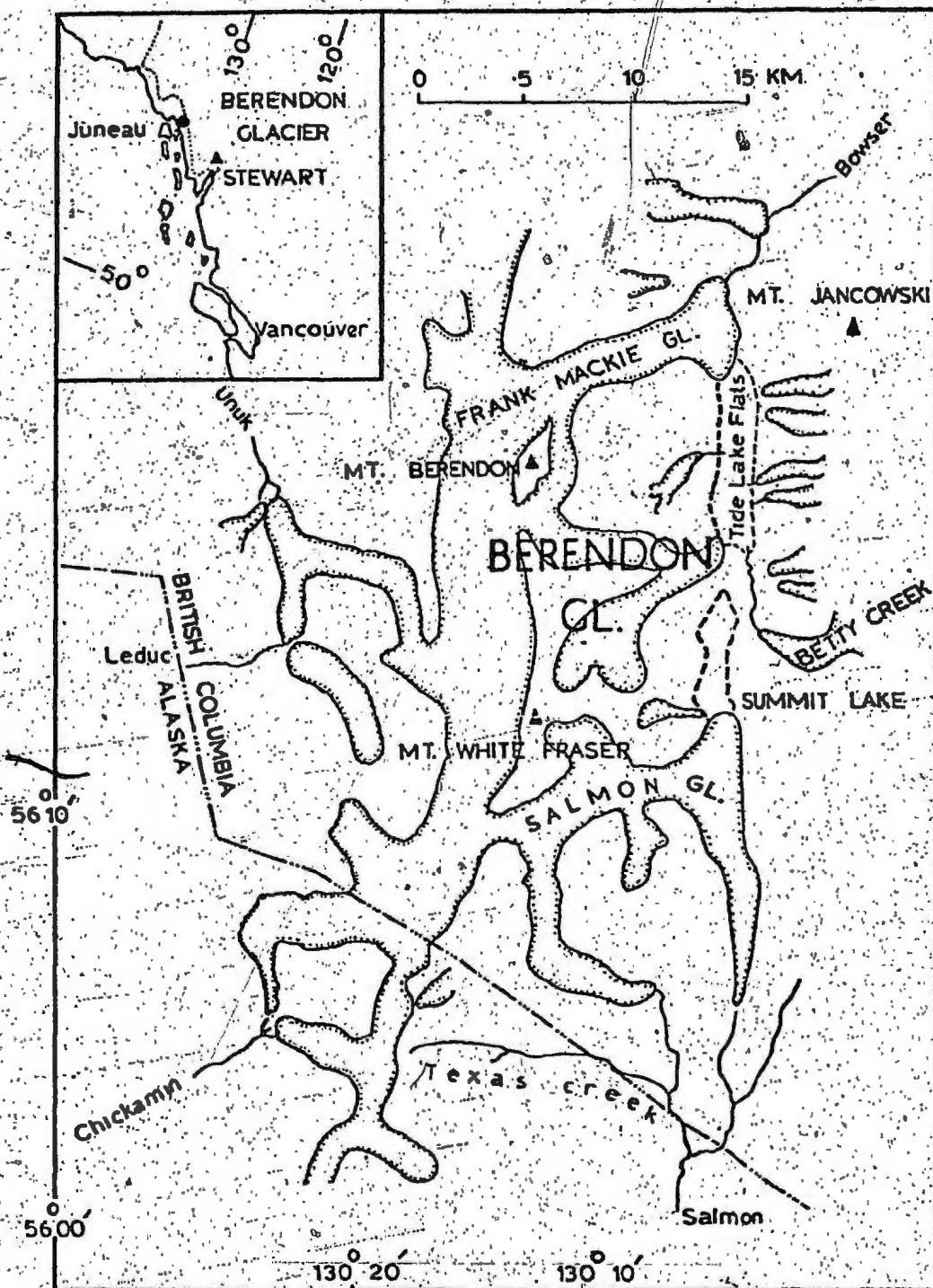
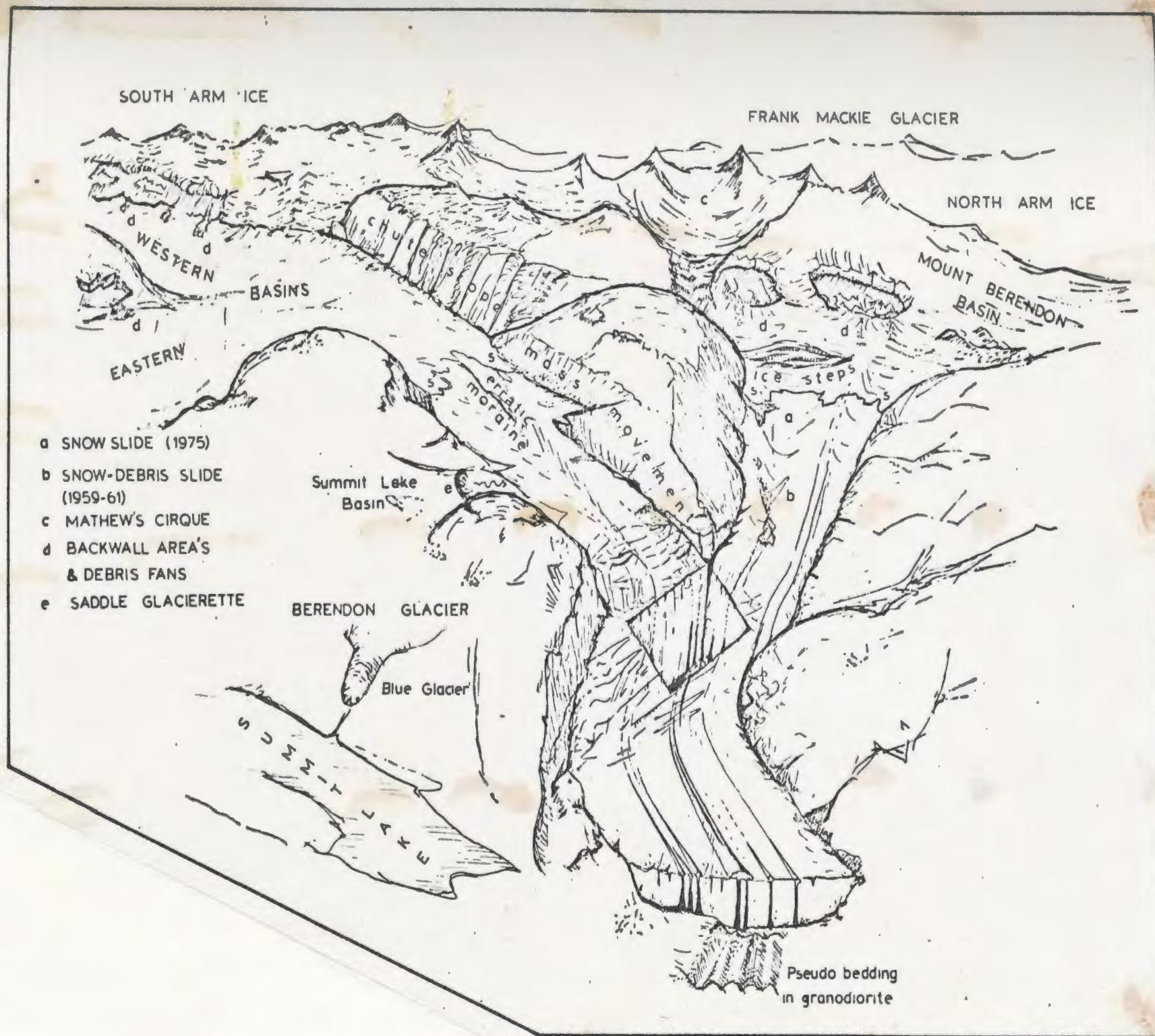


Figure 8. Berendon Glacier: location of the field area.

Figure 9. Berendon Glacier; basin morphology.



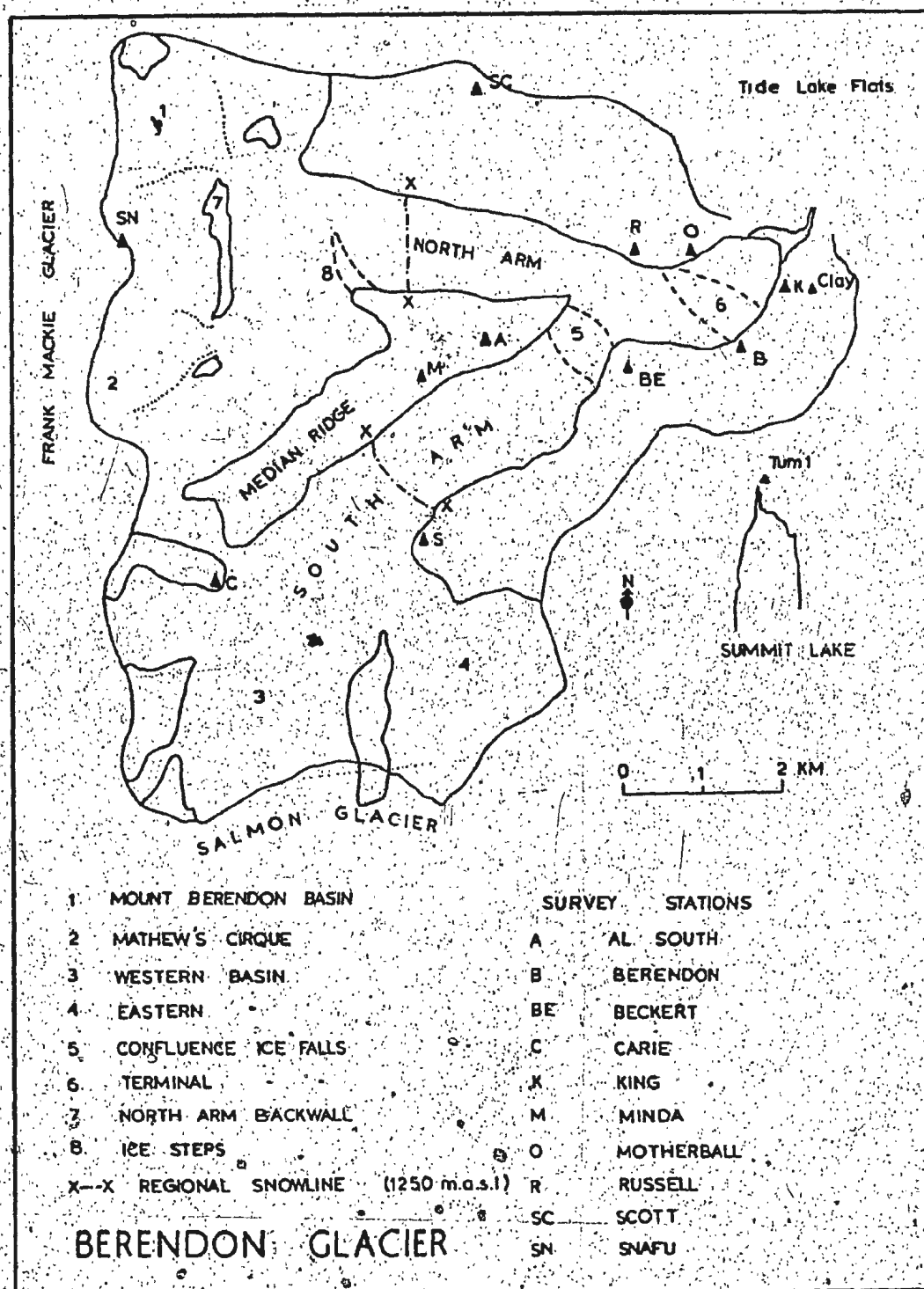


Figure 10. Berendon Glacier; nomenclature.

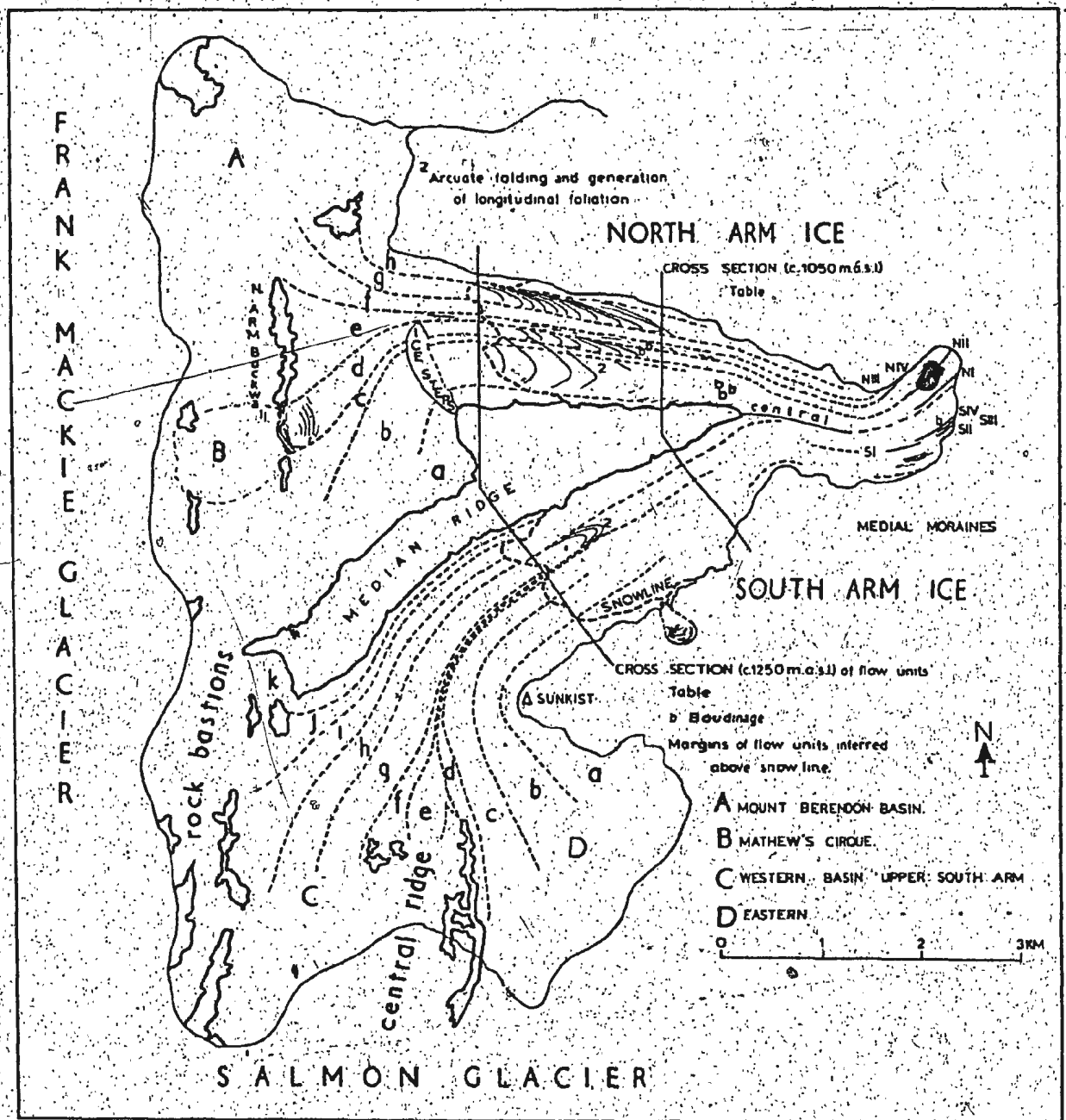


Figure 11. Berendon Glacier; the nature of ice flow.

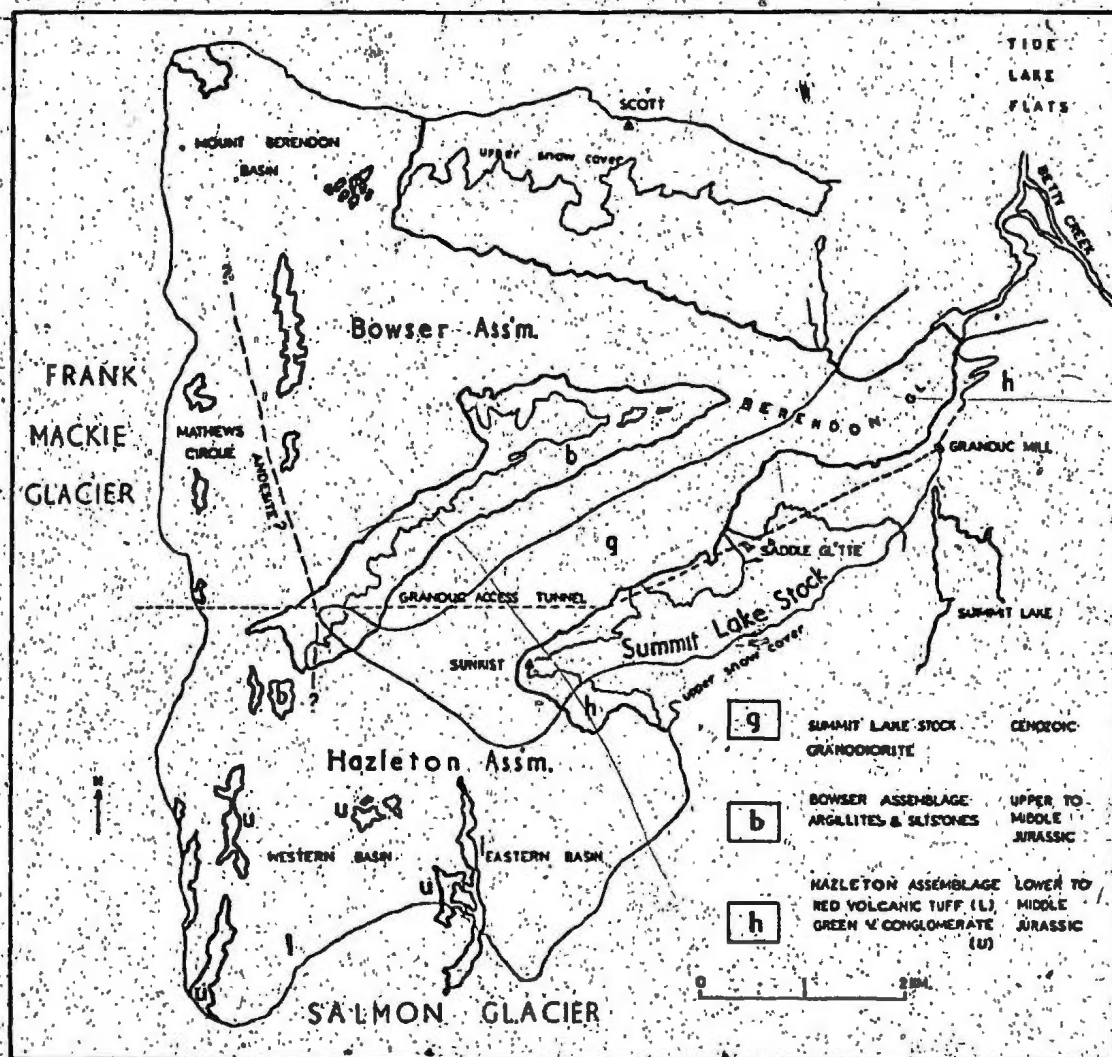


Figure 12. Berendon Glacier; bedrock geology.

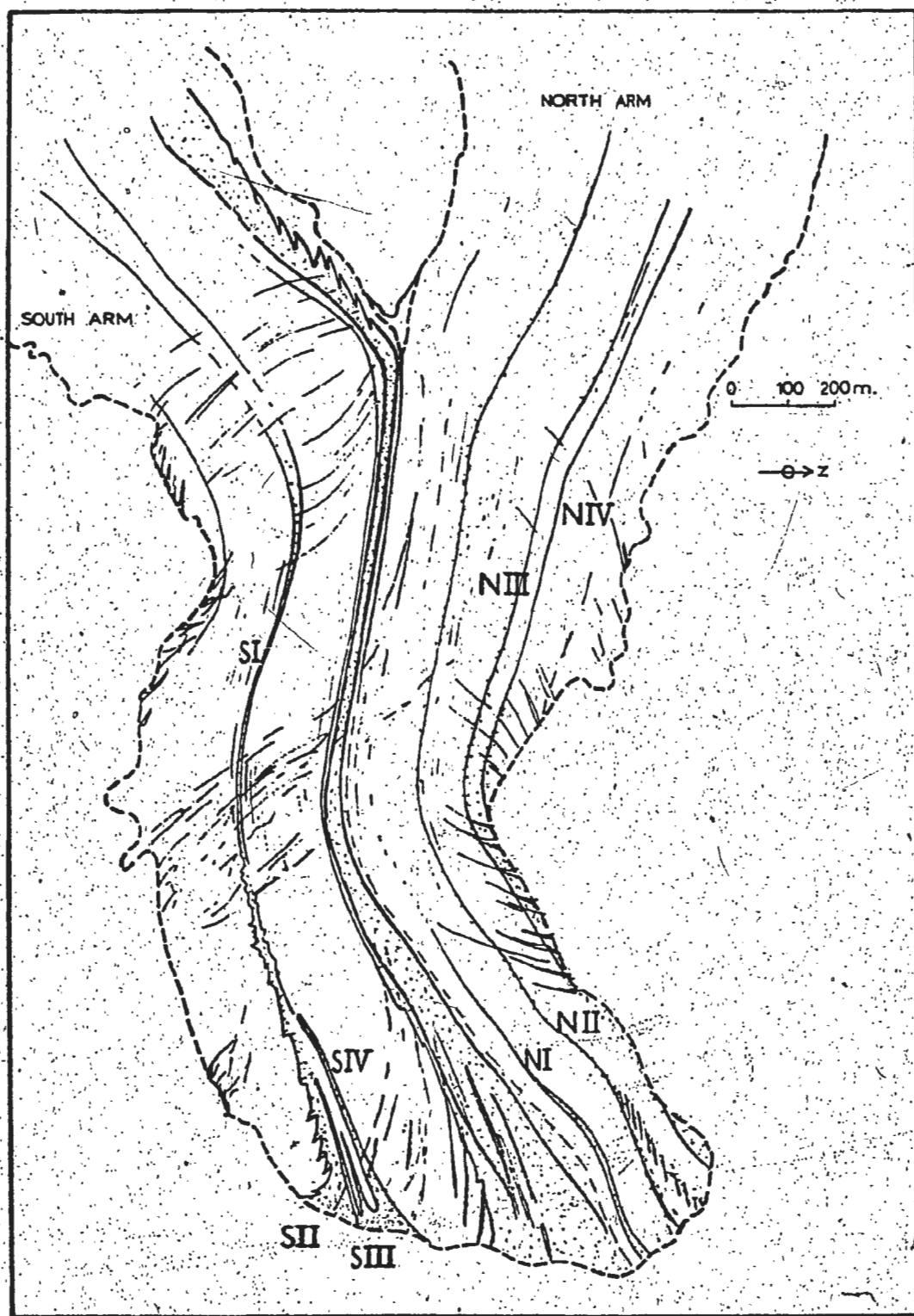


Figure 13a.

Figure 13. Berendon Glacier; medial moraines formed above the firn line and by confluence of North and South Arms (a) map (b) photograph.



Figure 13b. 1964 aerial photography by Austin Post.
Berendon Glacier.

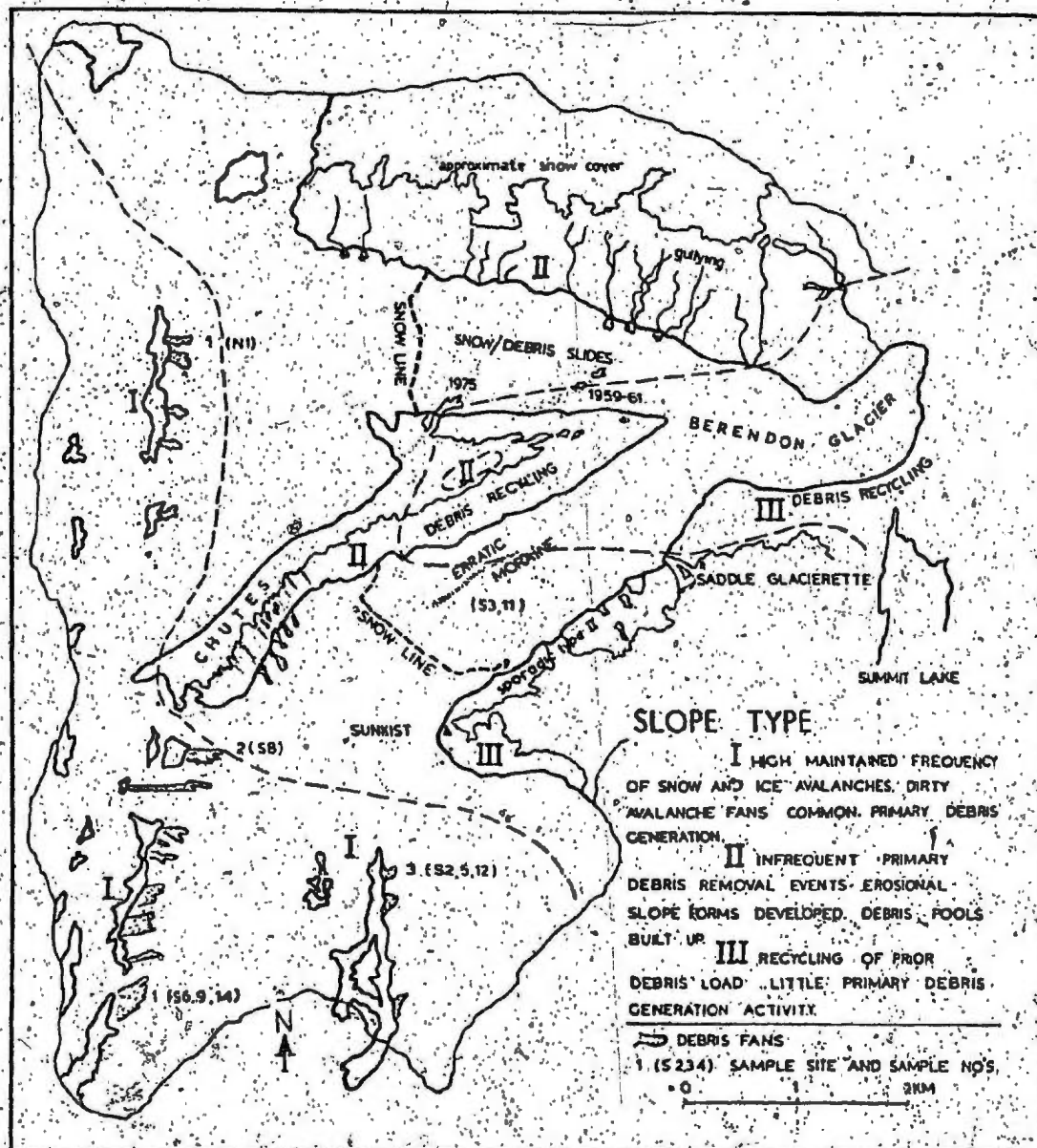


Figure 14a. Berendon Glacier; the nature of extraglacial bedrock slopes.

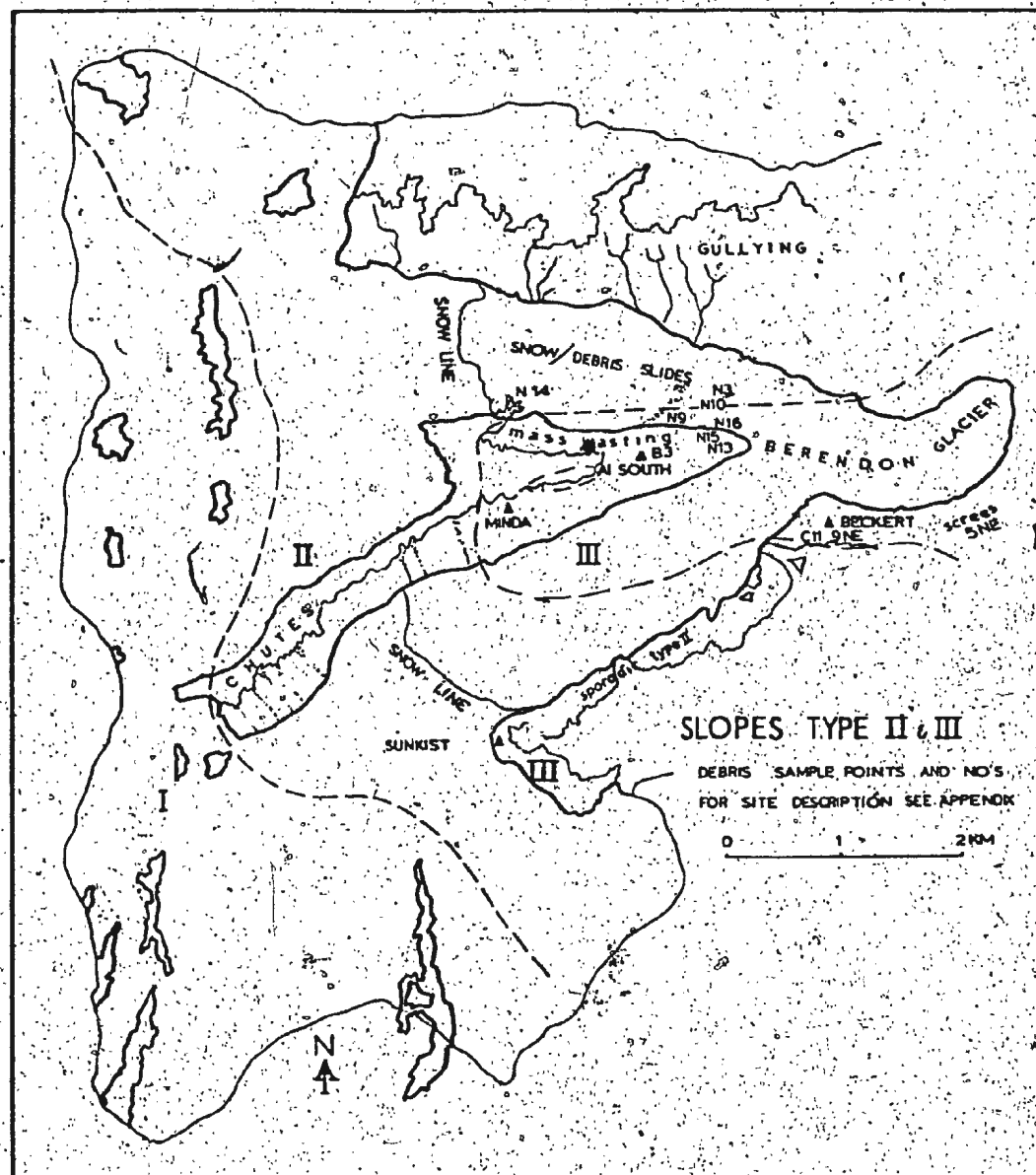


Figure 14b. Berendon Glacier; type II and III slopes.



1,2,3; debris sample sites (see fig 14a) for Type I slopes.



Type II slopes.

A----B defines a series of 'chute slope' forms (see Rapp, 1960) which increase in height and maturity upglacier. Analysis of aerial photographs (1964 to 1974) suggests that these are not very active at present.

Figure 15. Berendon Glacier; upper South Arm basin.



A¹

A ¹ --A ² :	medial moraine	SIV.
B ¹ --B ² :	"	" SIII.
C ¹ --C ² :	"	" SII.
D ¹ --D ² :	"	" SI

Figure 16. Berendon Glacier; medial moraines in the terminal area of South Arm.



Figure 17. Berendon Glacier; 'pseudo-medial moraines'
formed by longitudinal foliation.

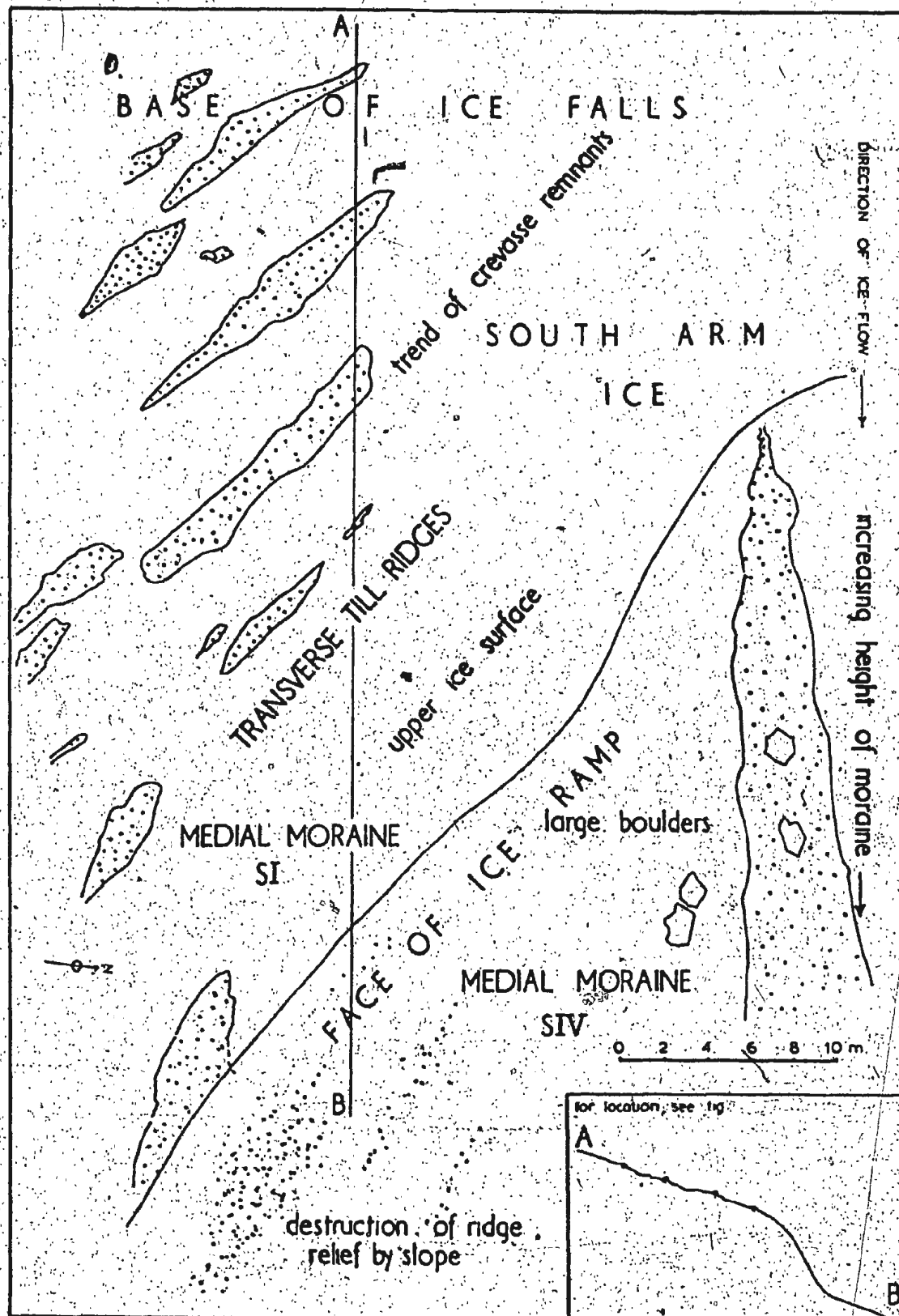


Figure 19a.

Figure 19. Berendon Glacier; transverse till ridges in the terminal area of South Arm.

(a) map

(b) photograph



Base of ice falls

Direction of ice flow. →

Figure 19b.

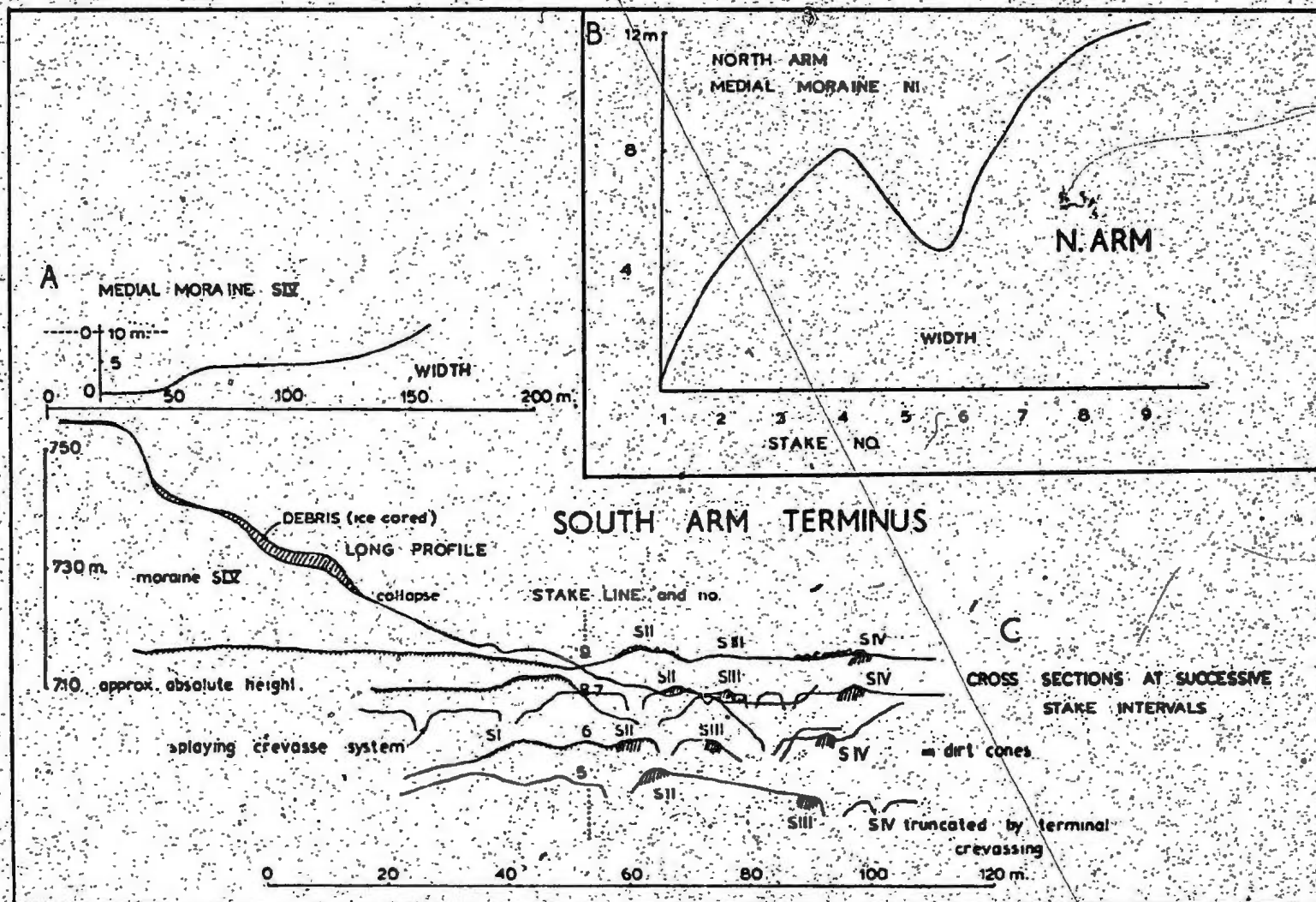


Figure 20: Berendson Glacier; medial moraine morphology in the terminal zone.



July 1975 (view downglacier)



September 1975 (view upglacier)

Figure 21. Berendon Glacier; medial moraine SIV in the terminal area of South Arm. Note outward dispersal

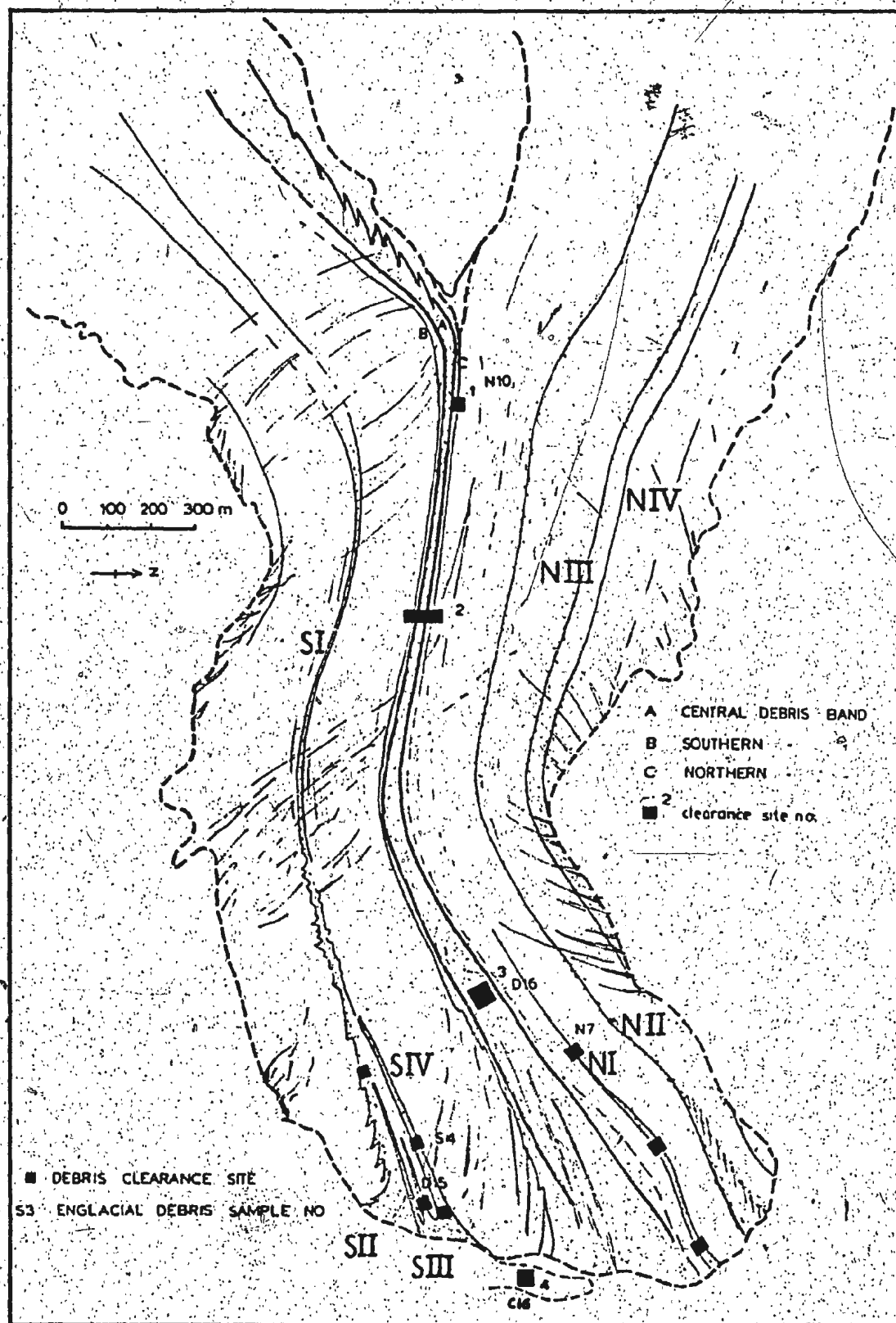


Figure 22. Berendon Glacier; debris clearance sites.



Figure 23. Berendon Glacier; newly revealed englacial debris in the terminal area of moraine SIV.

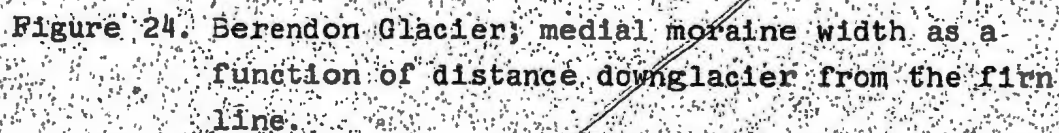


Figure 24. Berendon Glacier; medial moraine width as a function of distance downglacier from the firn line.

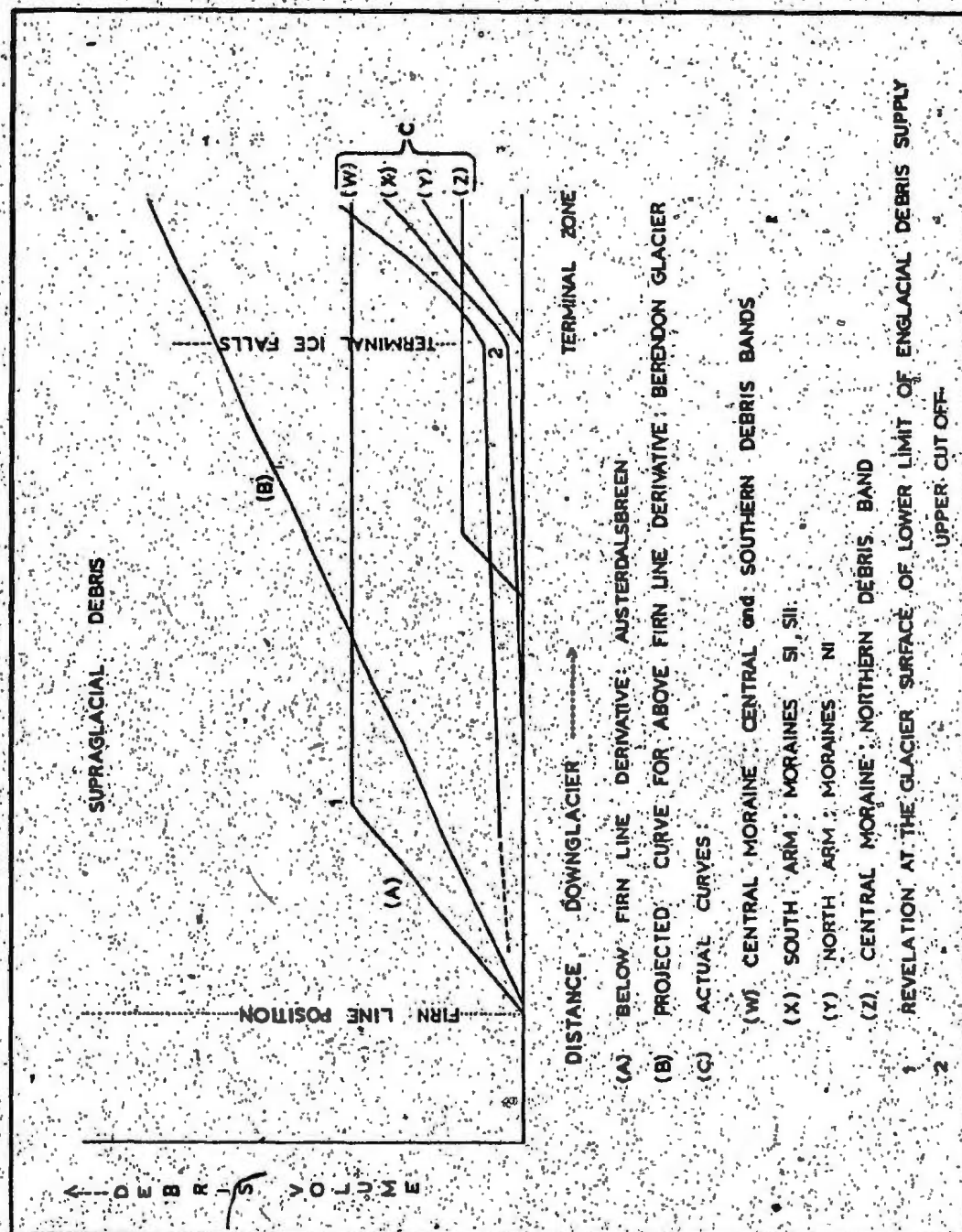


Figure 25. Berendon Glacier; supraglacial debris quantity along medial moraines as a function of distance downglacier from the firn line.

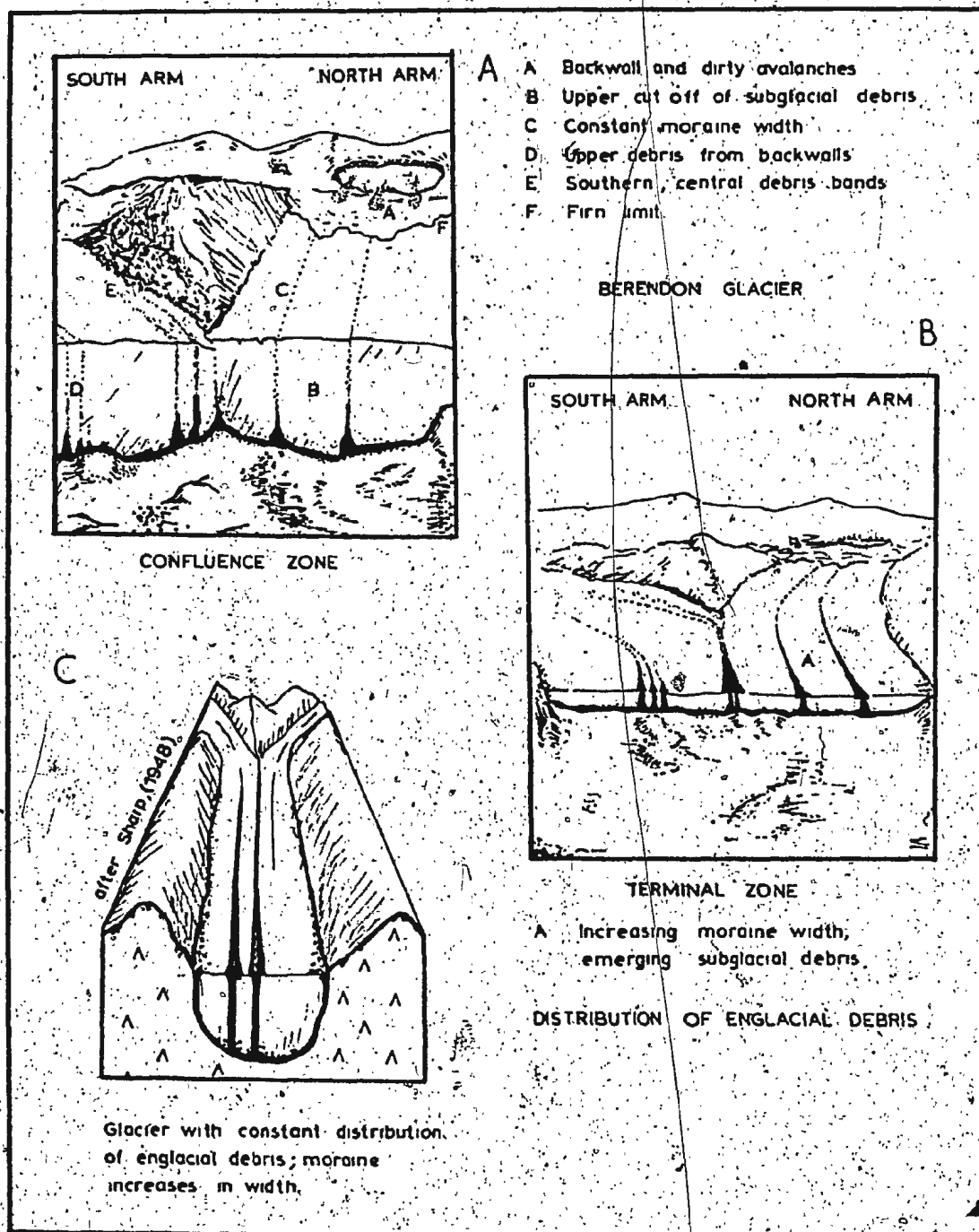


Figure 26. Berendon Glacier; medial moraines formed above the firn line (above firn line sub-type of the 'ablation-dominant' model of moraine formation).

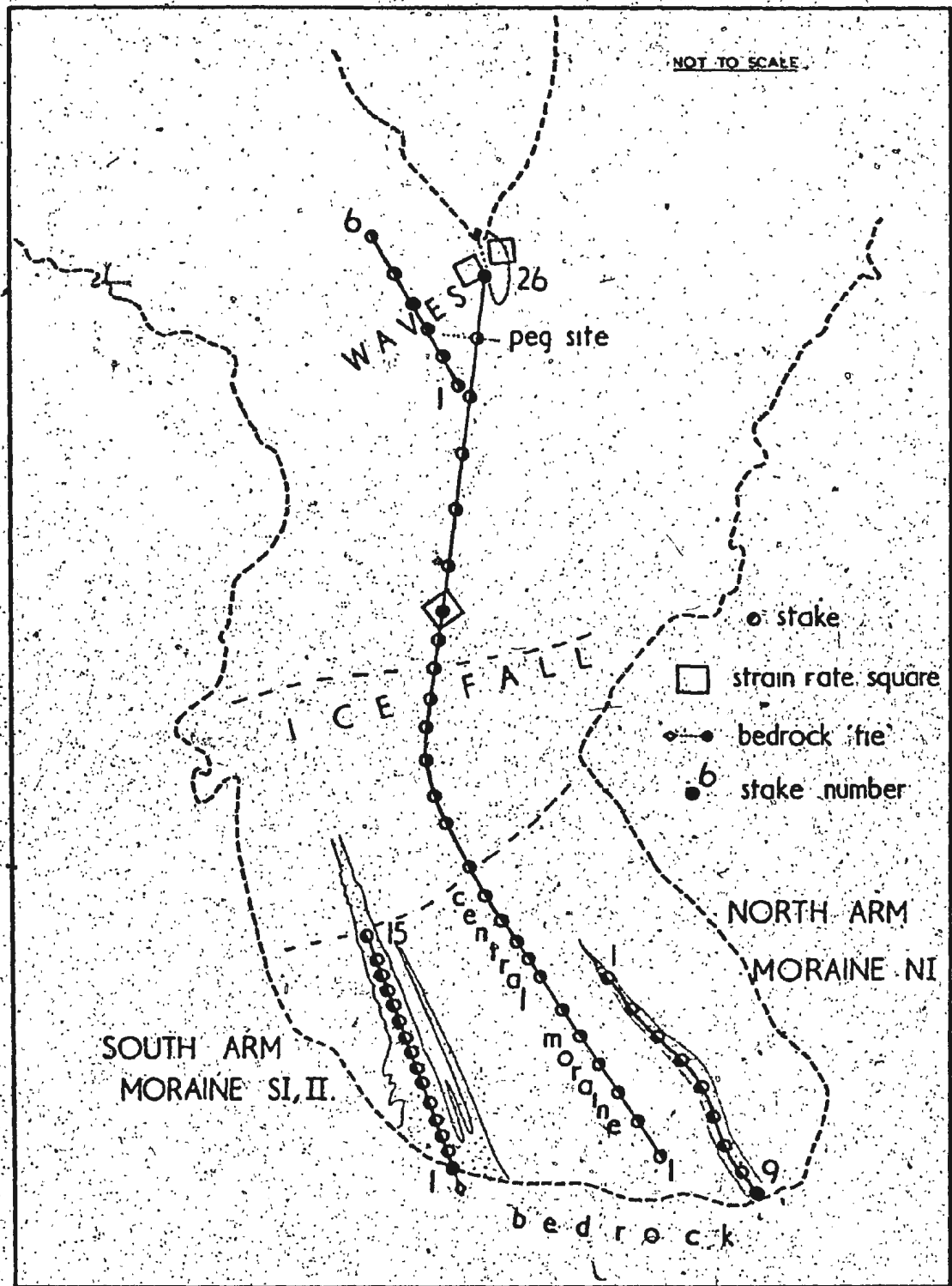


Figure 27. Berendon Glacier; stake lines.

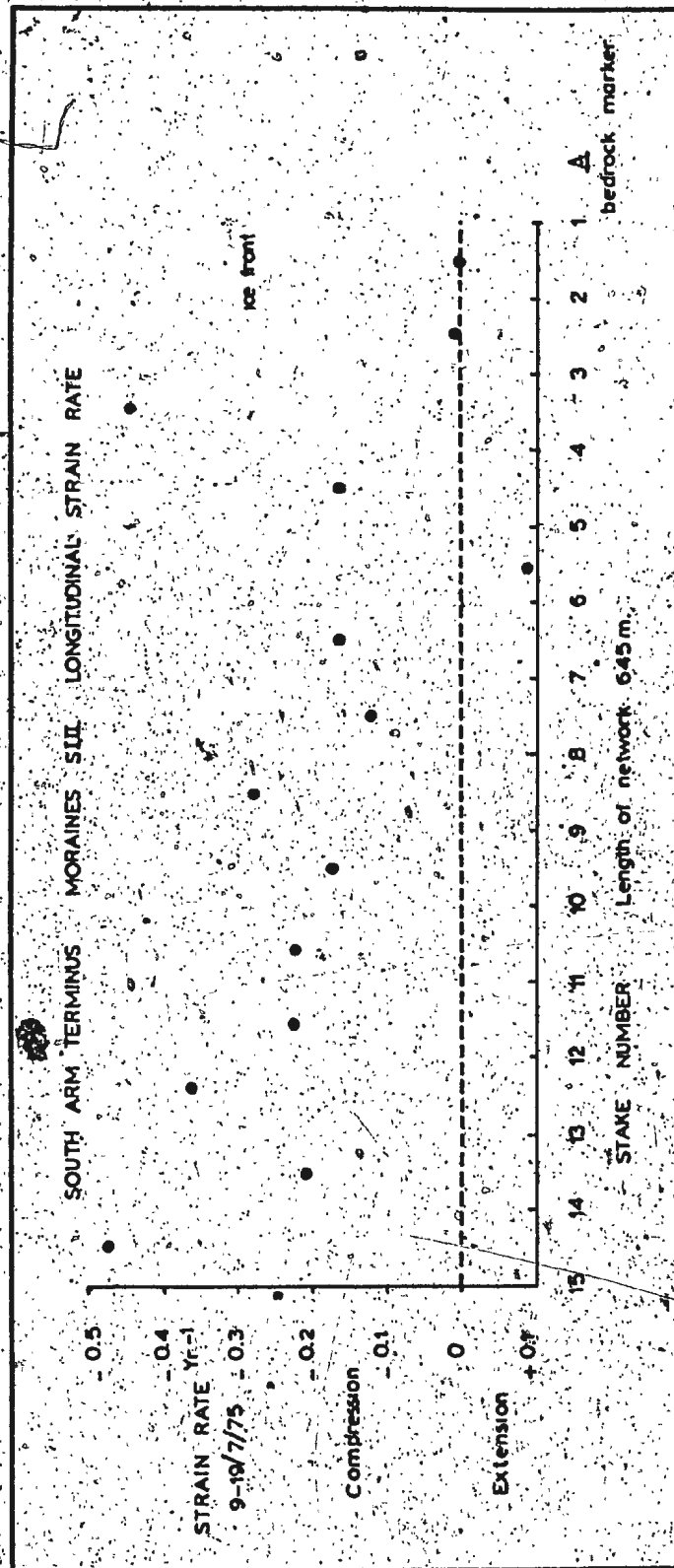
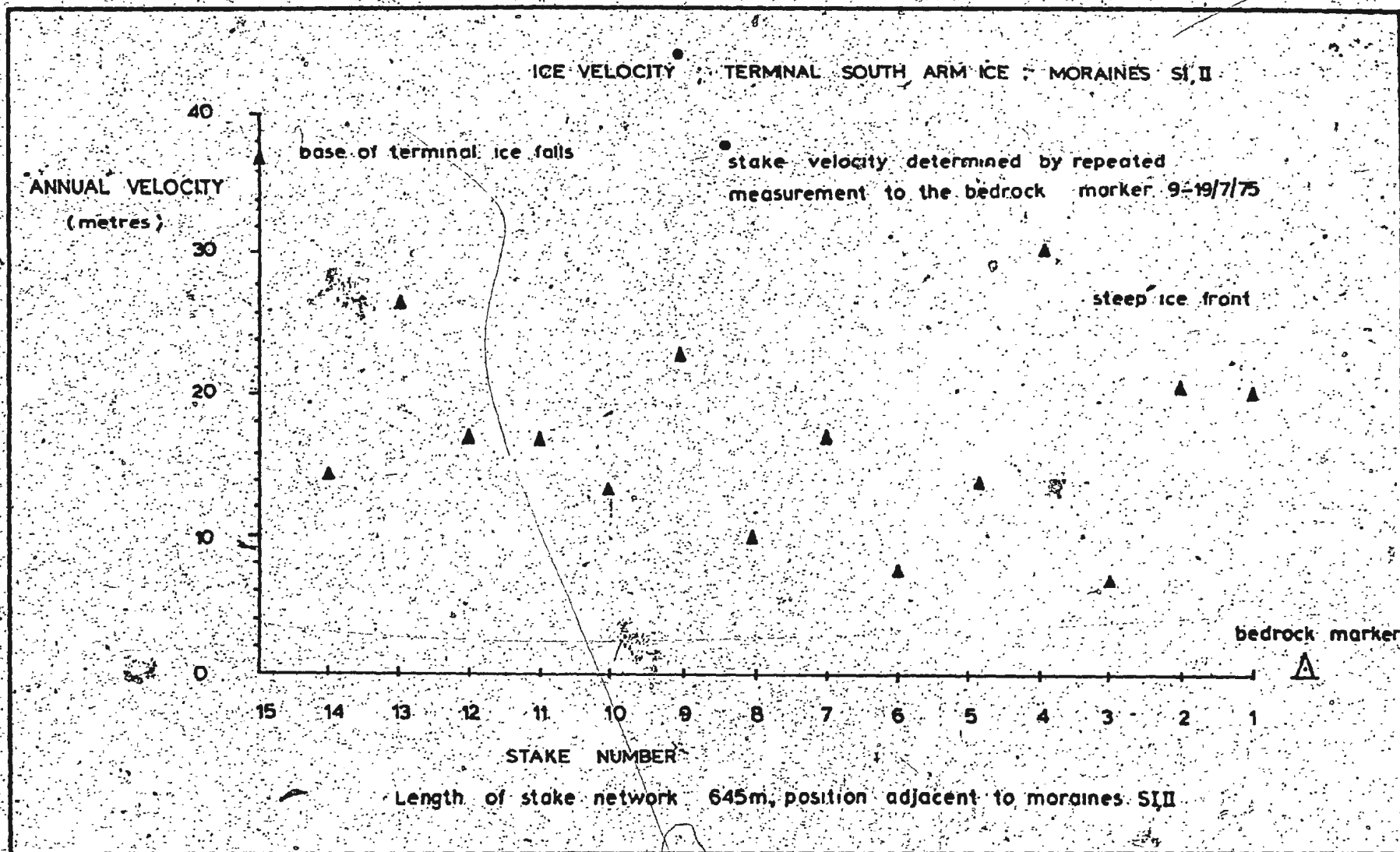
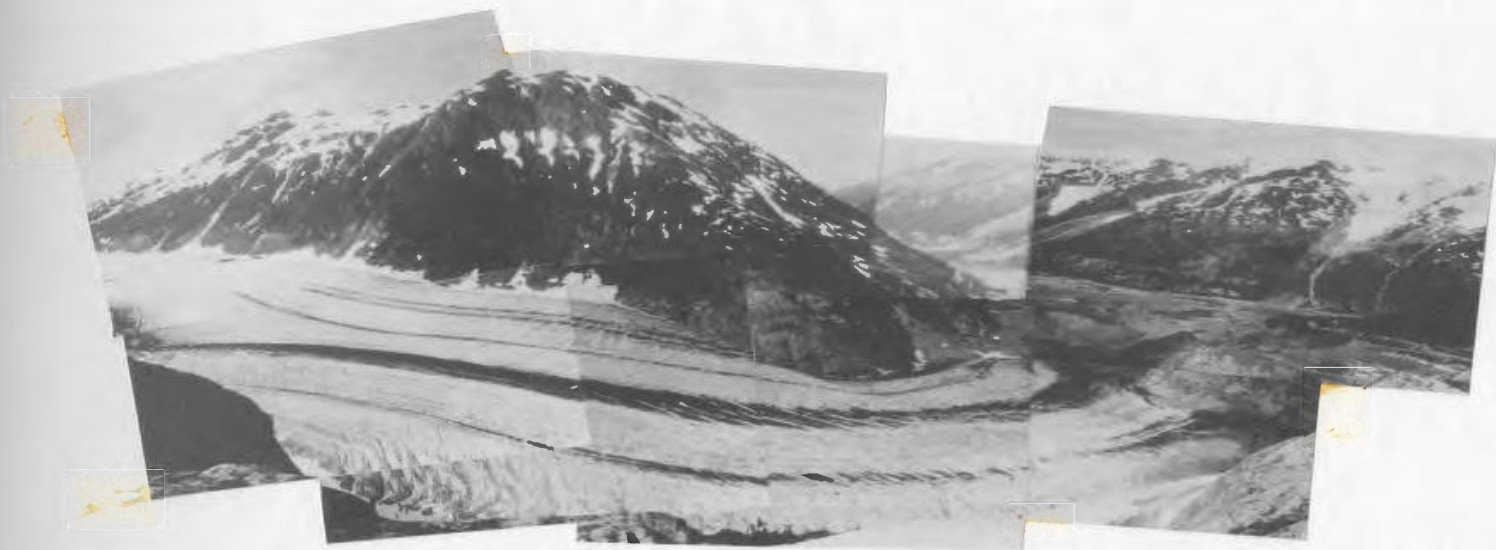


Figure 28.
Berendon Glacier;
longitudinal strain-
rate along medial
moraines SI and SII.

Figure 29. Berendon Glacier; ice velocities along moraines SI, II.





(a)



(b)

Figure 31. Berendon Glacier;

- (a) overview of the terminal area.
- (b) view upglacier ; in foreground active kettle hole formation in ice-cored sediment from Granduc mill. In the background note the truncation of terminal ice by a shear plane. Sheared-up

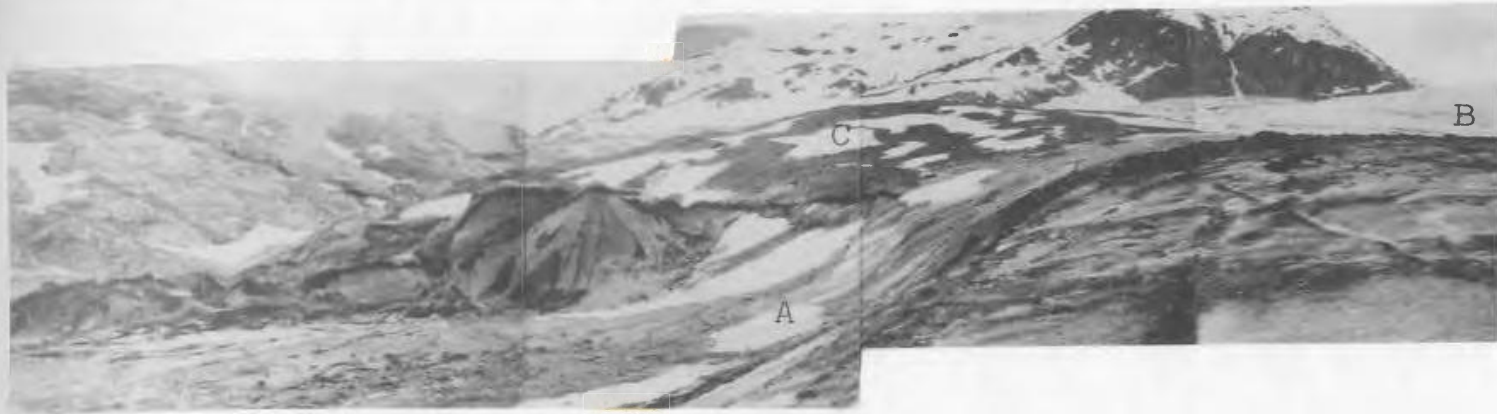


Figure 31c. Berendon Glacier; truncation of medial moraine morphology by shearing. A---B; moraine NI.
C; Central moraine.



Figure 32. Berendon Glacier; terminal zone of moraine NI.
Note the complex character of the ice core, the low relief of the moraine and outcropping shear planes.

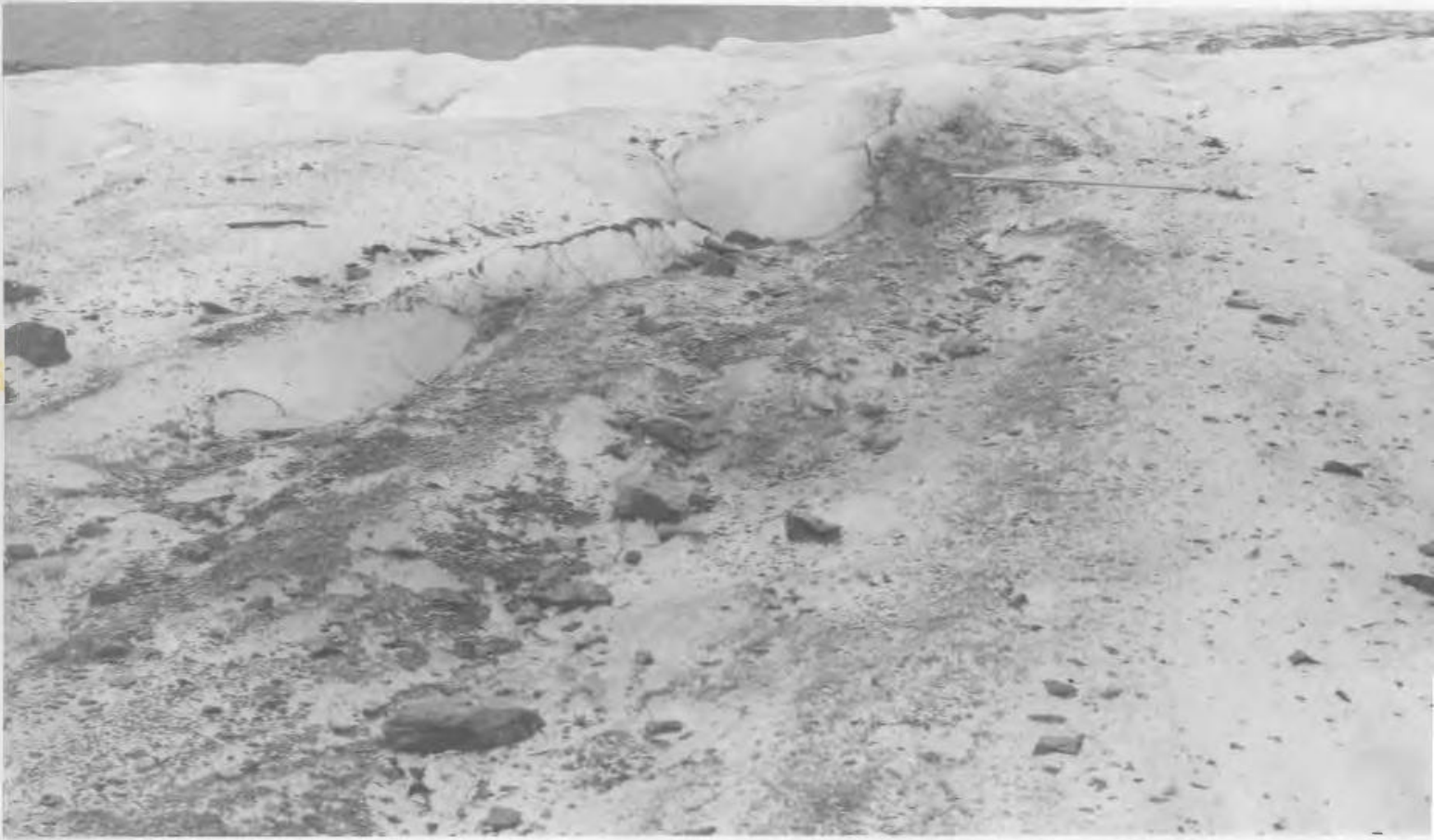


Figure 33. Berendon Glacier; newly revealed englacial debris at the head of medial moraine NI.

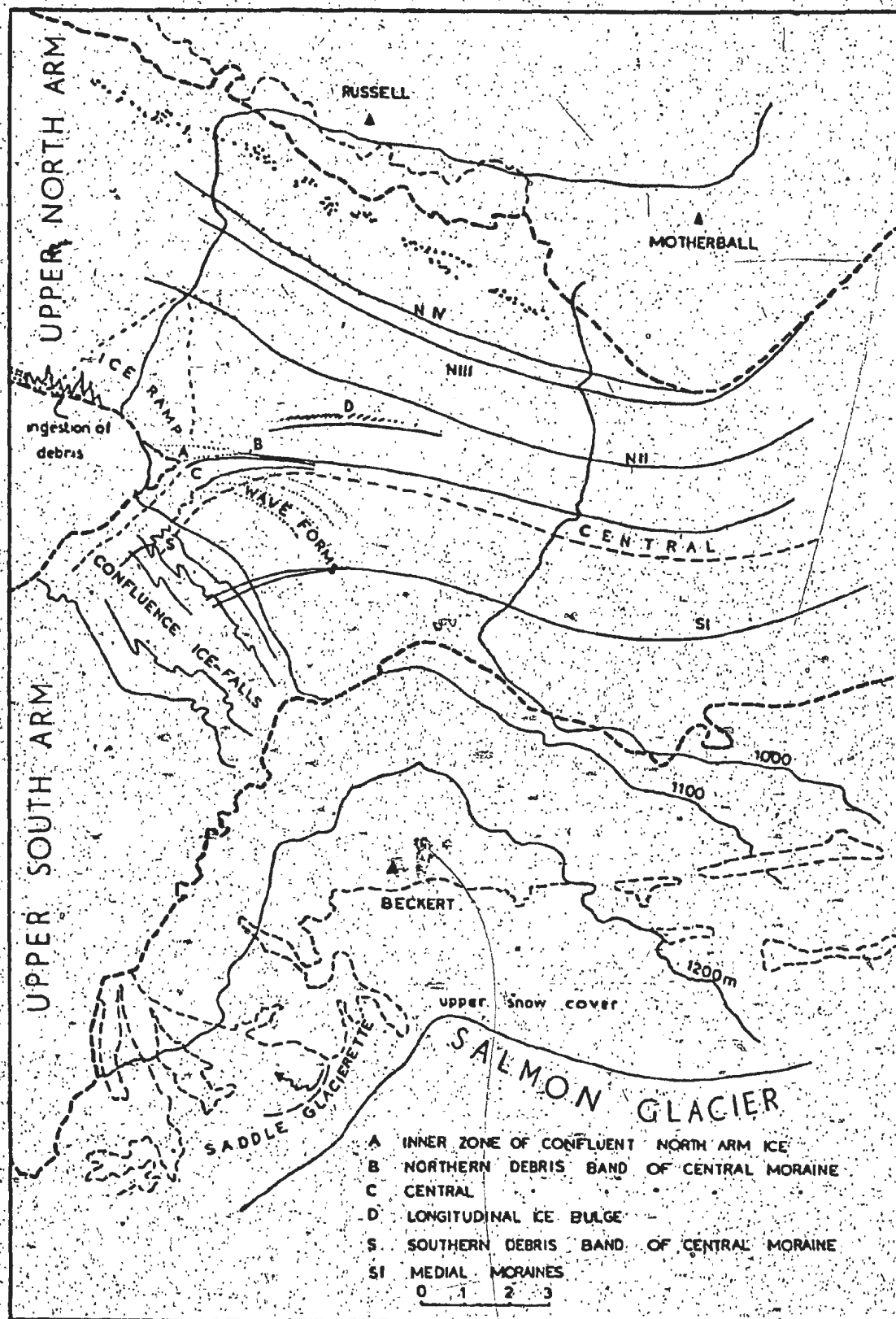


Figure 34. Berendon Glacier; the confluence zone of North and South Arm ice.

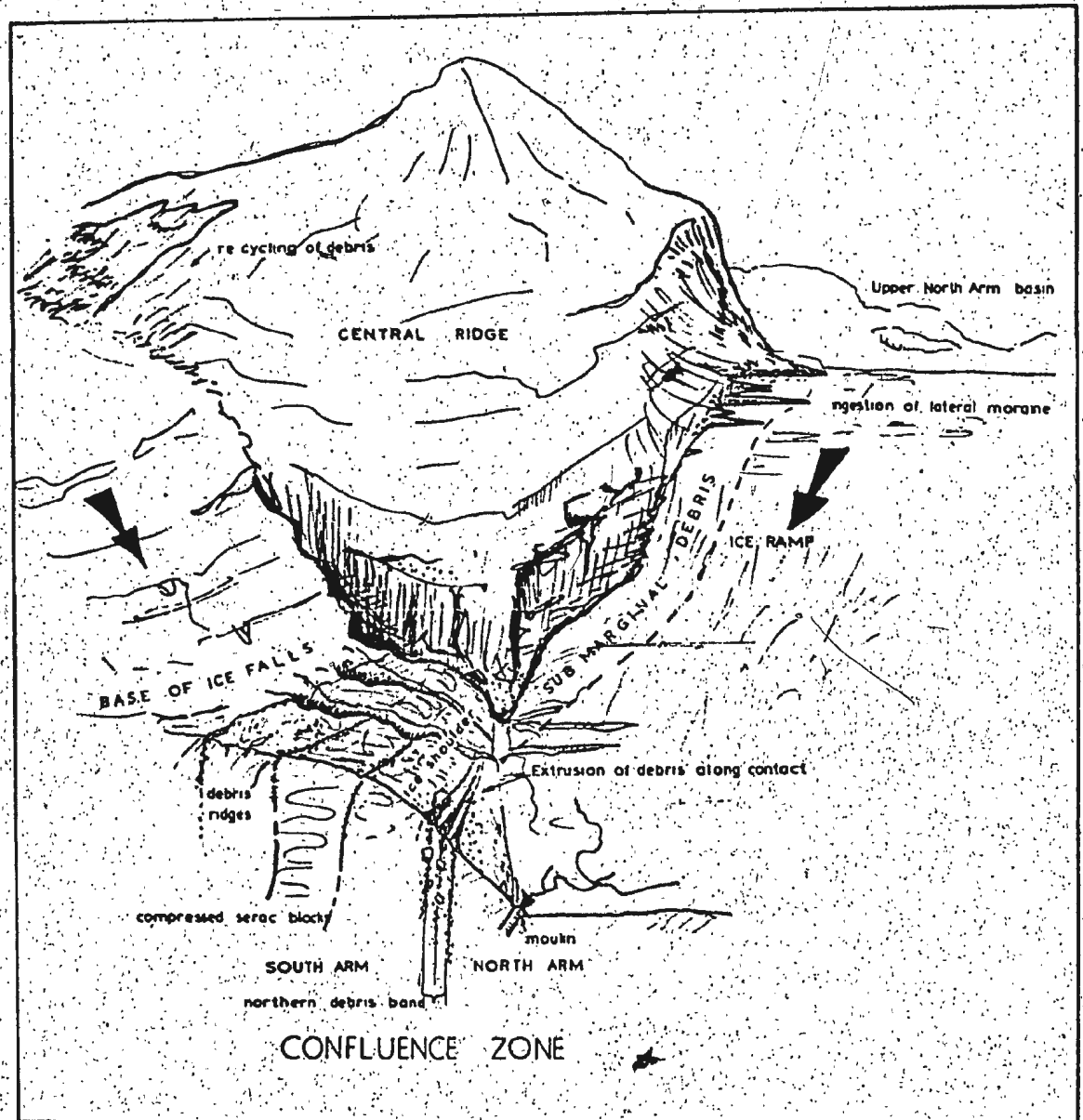


Figure 35. Berendon Glacier; Central moraine, formation of the northern debris band.

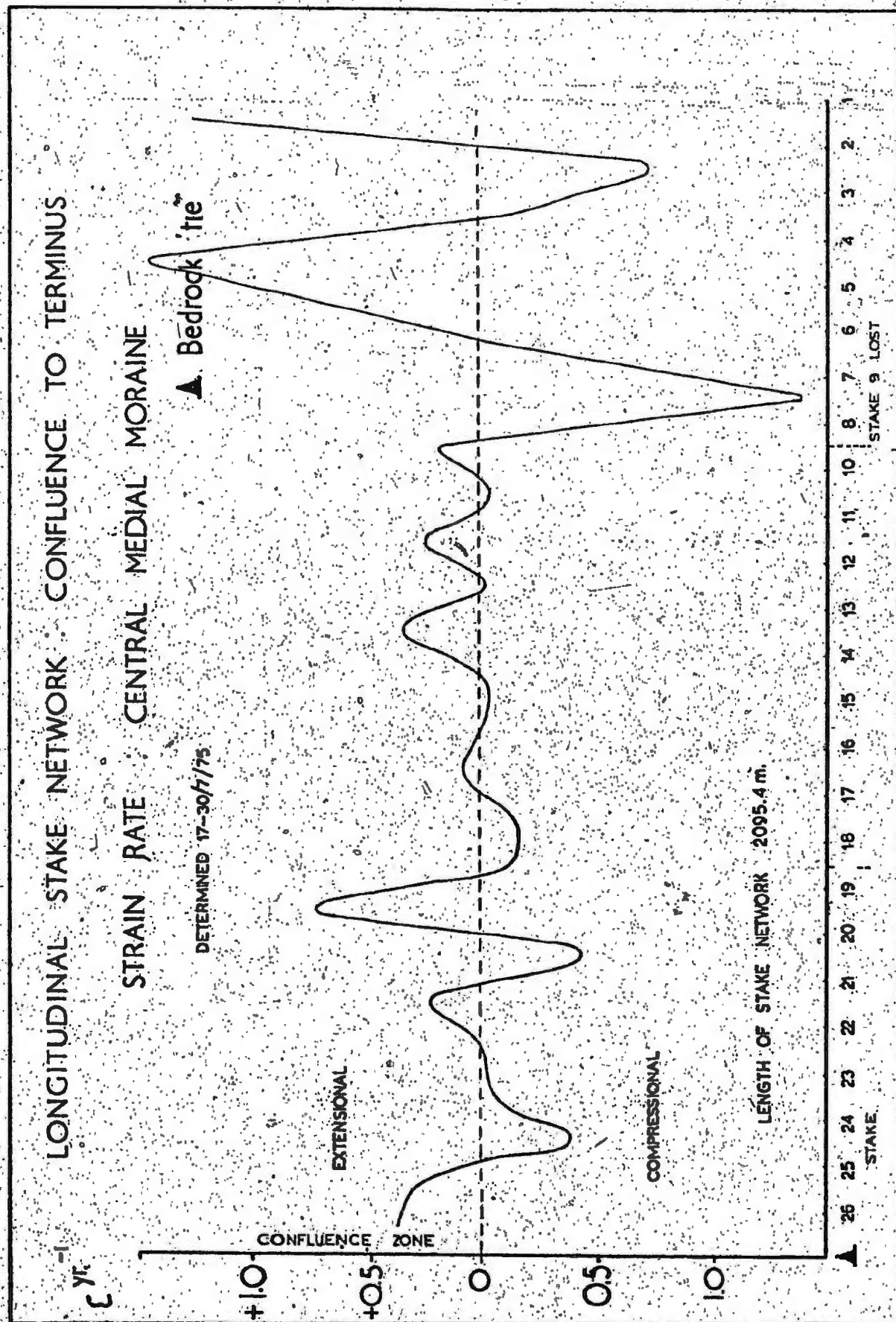


Figure 36. Berendon Glacier; the Central medial moraine, longitudinal strain-rate as a function of distance downglacier.

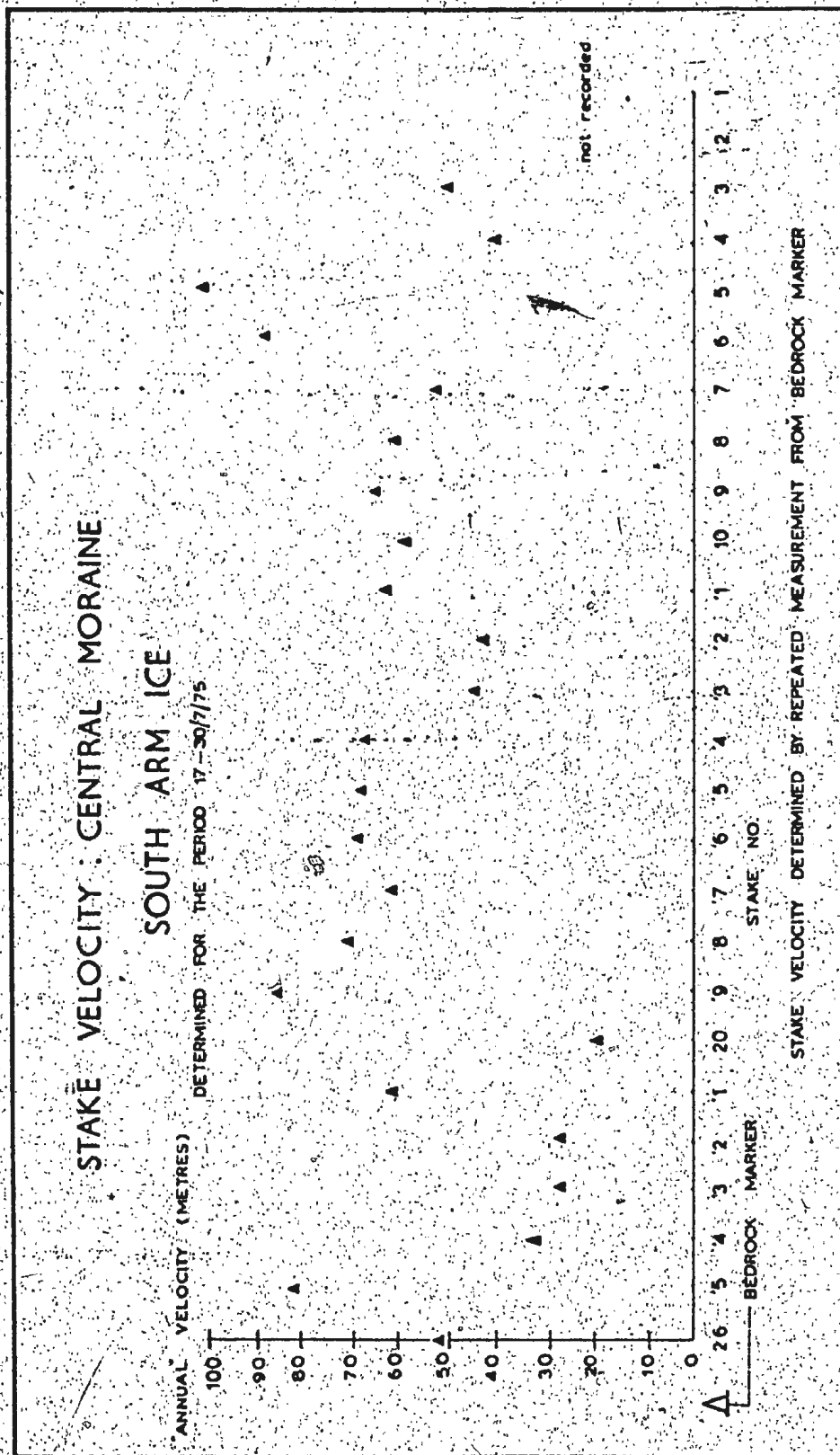


Figure 37. Berendon Glacier; the Central medial moraine, ice velocities as a function of distance downglacier.

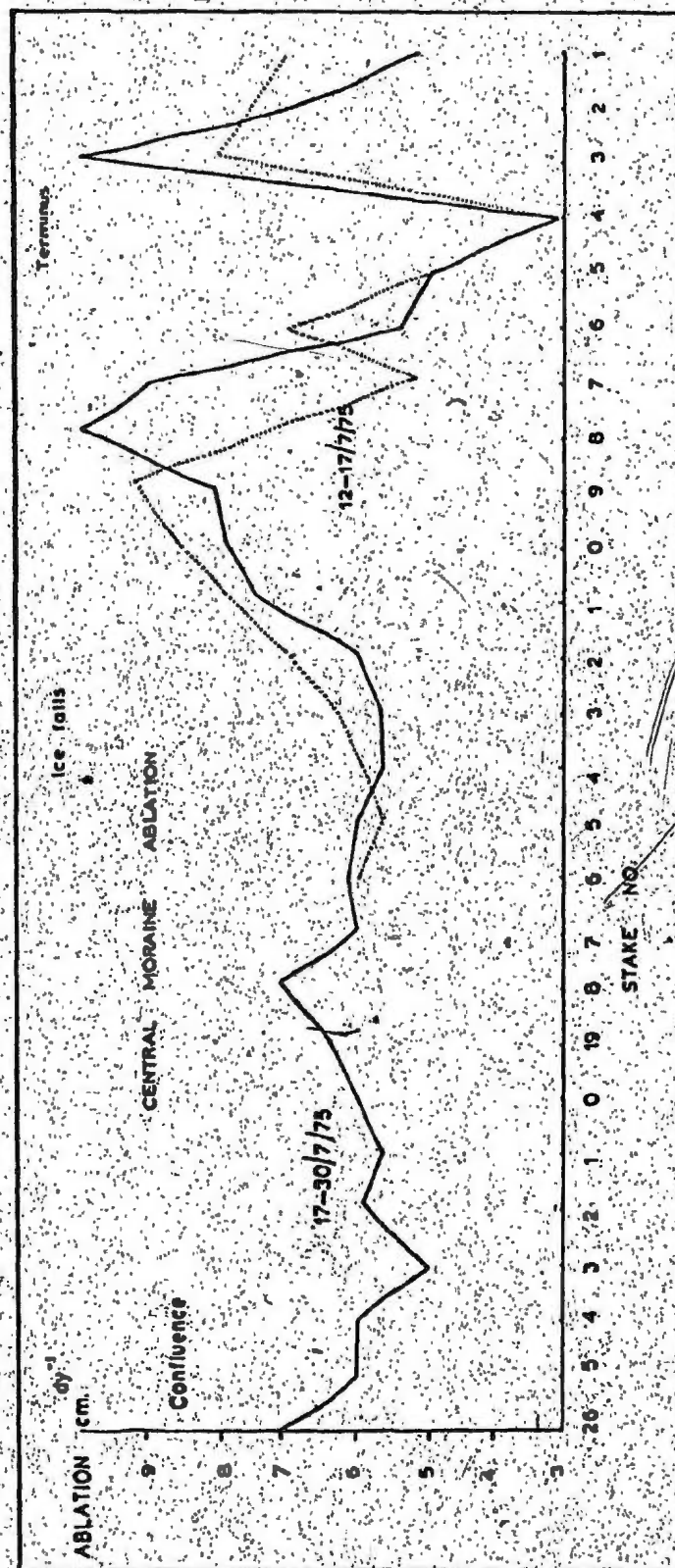


Figure 38.
Berendon Glacier;
the Central medial
moraine, ablation as
a function of
distance downglacier.

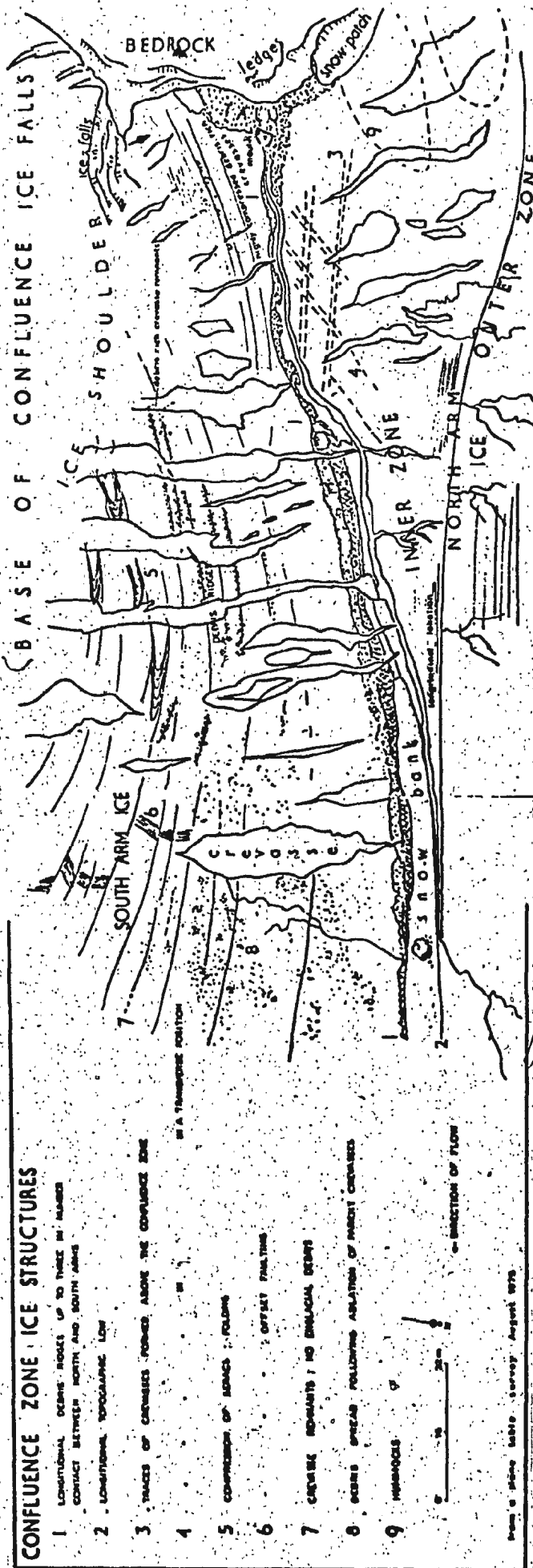


Figure 39. Berendon Glacier; ice structures in the confluence zone.



Figure 40. Berendon Glacier; debris-rich crevasse remnant, transverse debris ridge and compressed serac blocks in the confluence zone.



Figure 41. Berendon Glacier; extrusion of blocks from debris-rich crevasse remnants along South Arm ice shoulder.

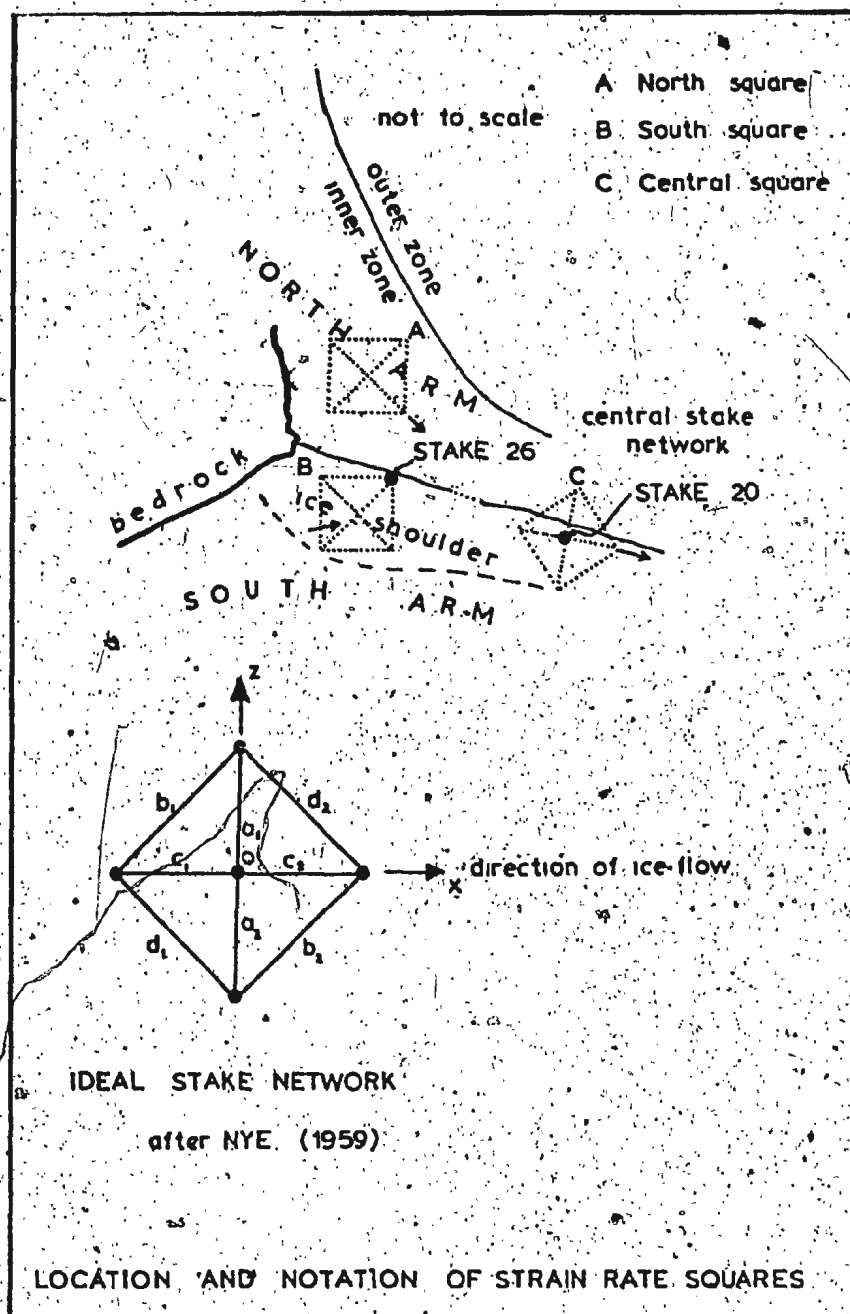


Figure 42. Berendon Glacier; location and notation of strain-rate squares.

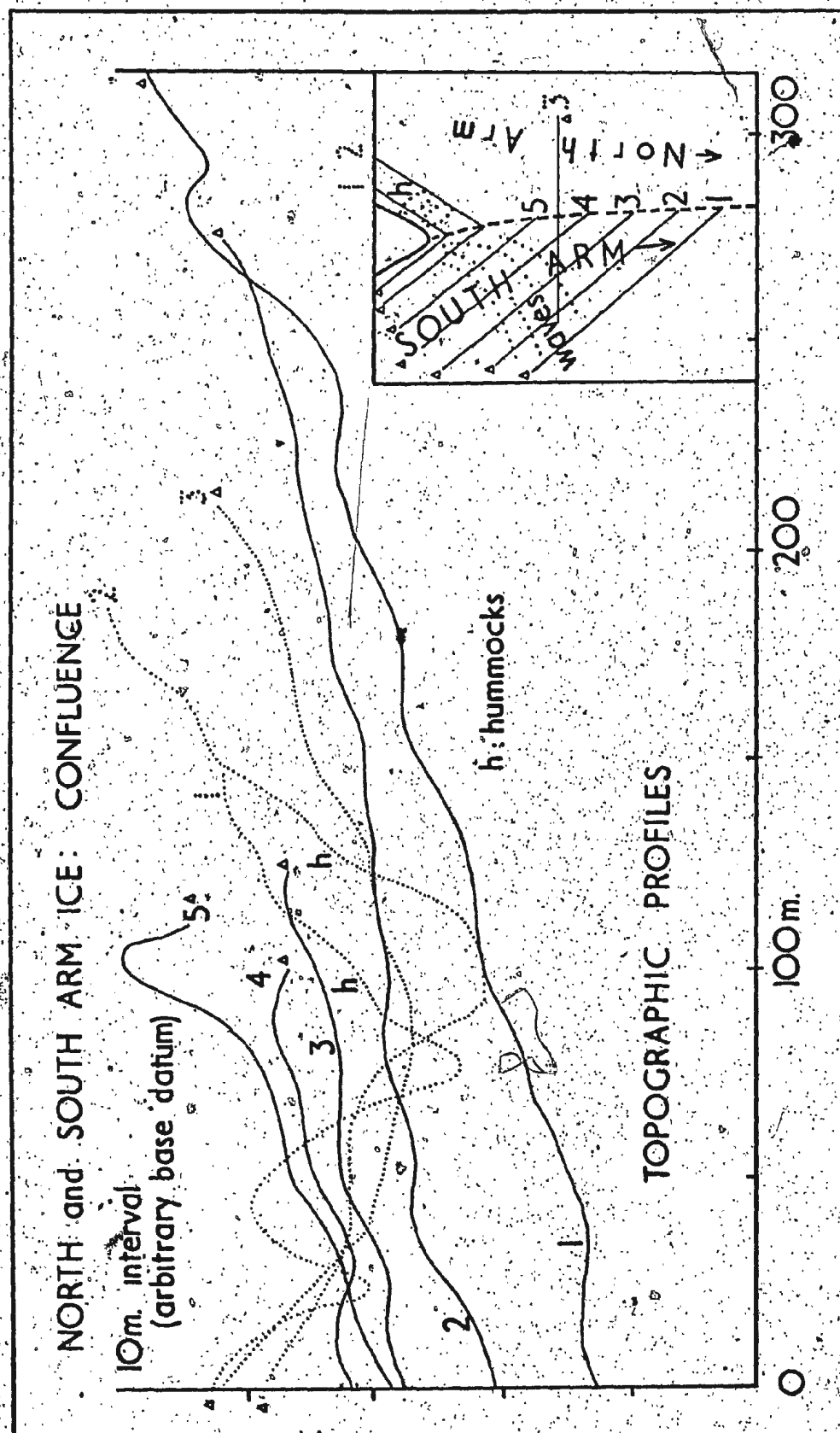


Figure 43. Berendon Glacier; topographic profiles in the confluence zone.

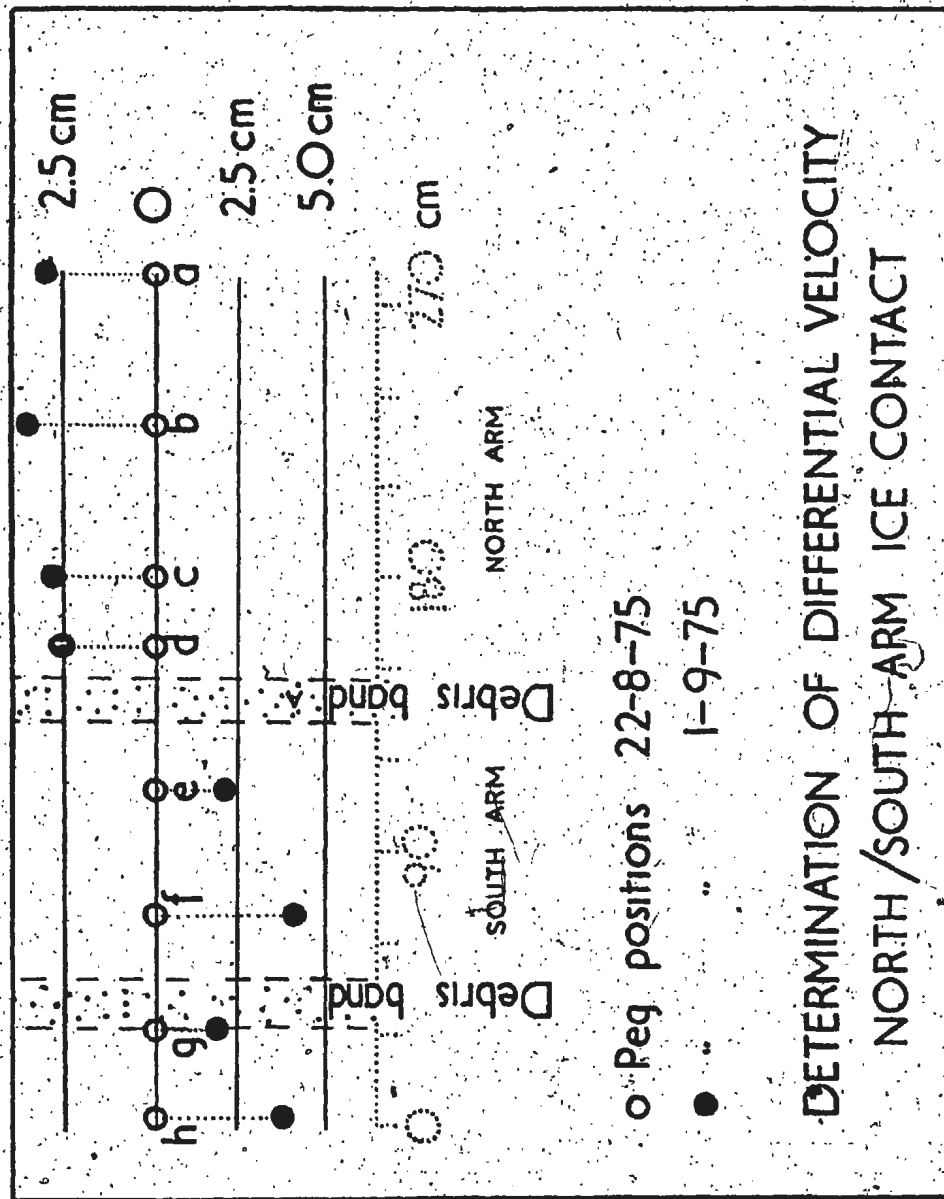


Figure 44. Berendon Glacier; determination of differential velocity at the contact of North and South Arms.

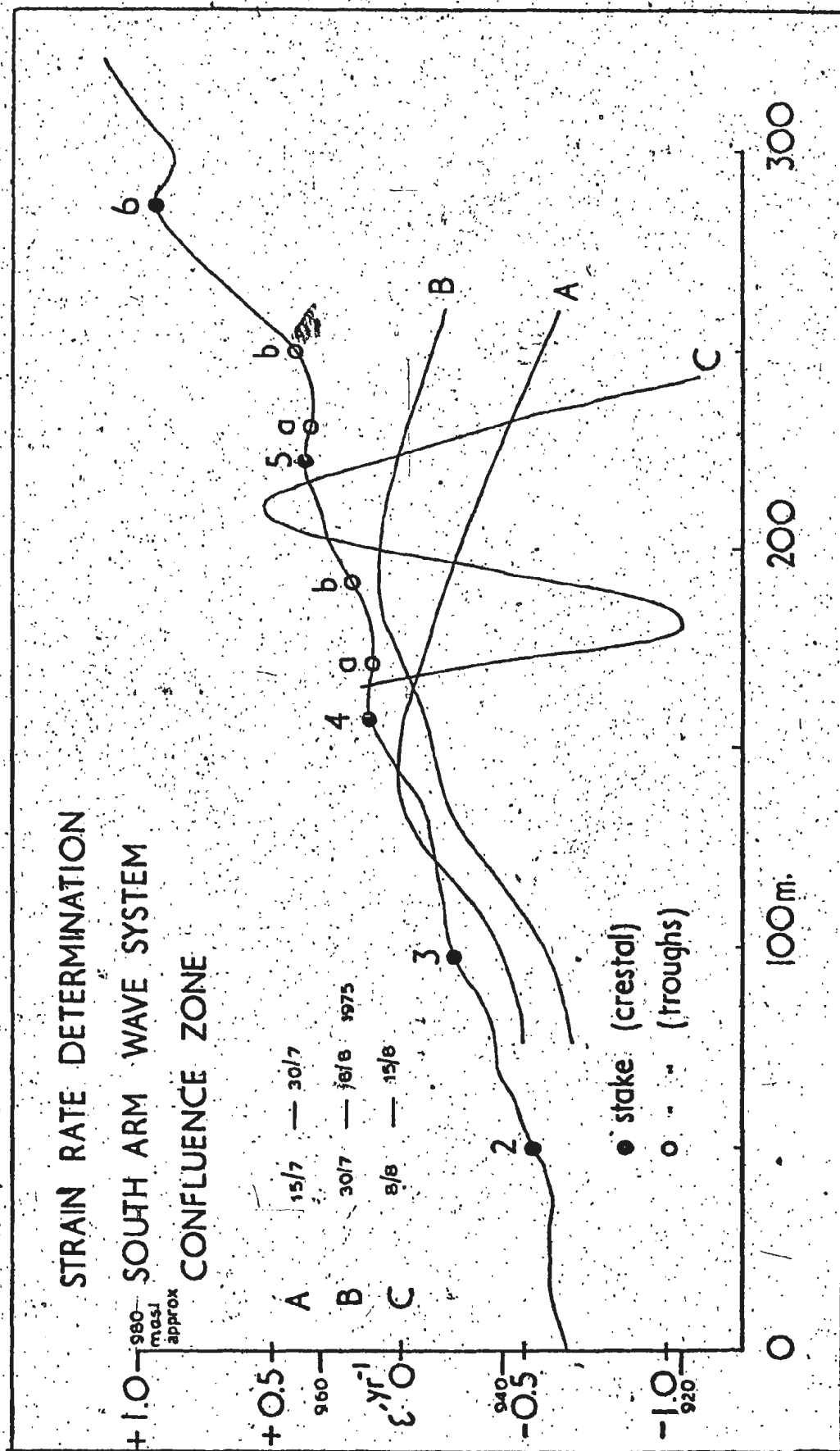


Figure 45. Berendon Glacier; longitudinal strain-rate over wave forms on South Arm.



Figure 46. Berendon Glacier; debris clearance site across
the entire Central moraine, near the end of the
melt season 1975, five weeks after initial
clearance. Boulders have migrated from the
surrounding moraine; no englacial debris is present.
Note the absence of an ice core in surrounding
moraine and the development of an ice core where
debris has been concentrated by clearance.

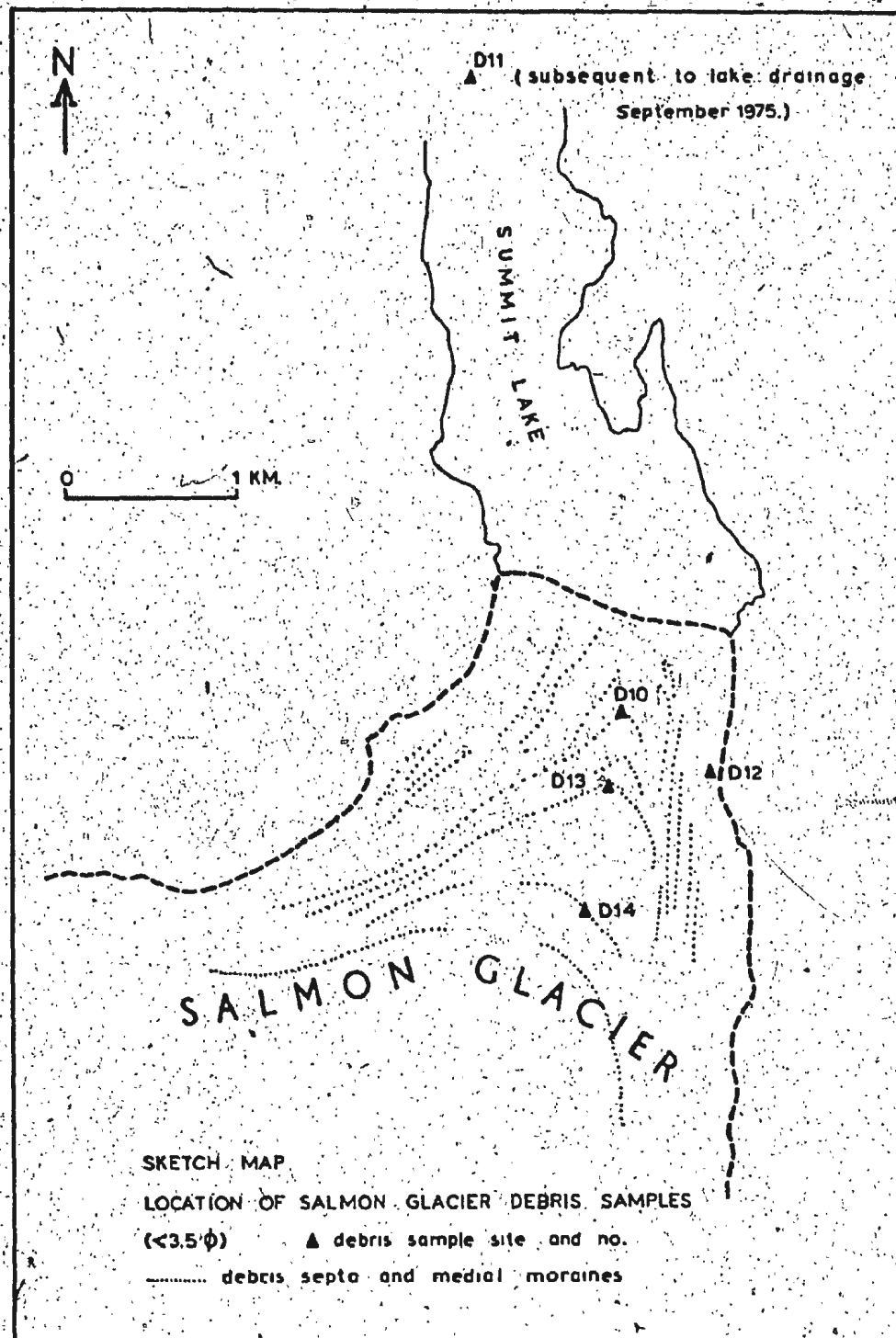


Figure 48. Salmon Glacier;
 medial moraine debris sample sites.



Figure 49. Berendon Glacier; measurement of sideslip.

From the ice surface a stake was drilled in allowing the stake end to rest on the bedrock surface. Two methods were employed for recording ice movement. Carbon paper inside a waterproof plastic envelope and fastened to a rigid cardboard base was firmly attached to bedrock by a rock piton. A spring, containing a scribe, attached to the stake end moved over the carbon paper as the ice slipped over the bedrock surface. This method provided a record of sideslip for up to three days. After three days ablation of the stake hole resulted in erratic stake movement. Bedrock markers and an ice-screw were also utilised. Whilst systematic daily observation proved impossible an average daily sideslip velocity of 4cm. ($14.6\text{m}^{\text{yr}^{-1}}$) was derived from several observational periods.



Figure 50. Berendon Glacier; ice cavitation and an ablating debris sole (30cm. thick) in the terminal area of South Arm. Debris samples D3 and SSS8 were taken from the sole at this site. The debris sole is widely exposed in the terminal area of Berendon Glacier as a result of extensive ice cavitation.

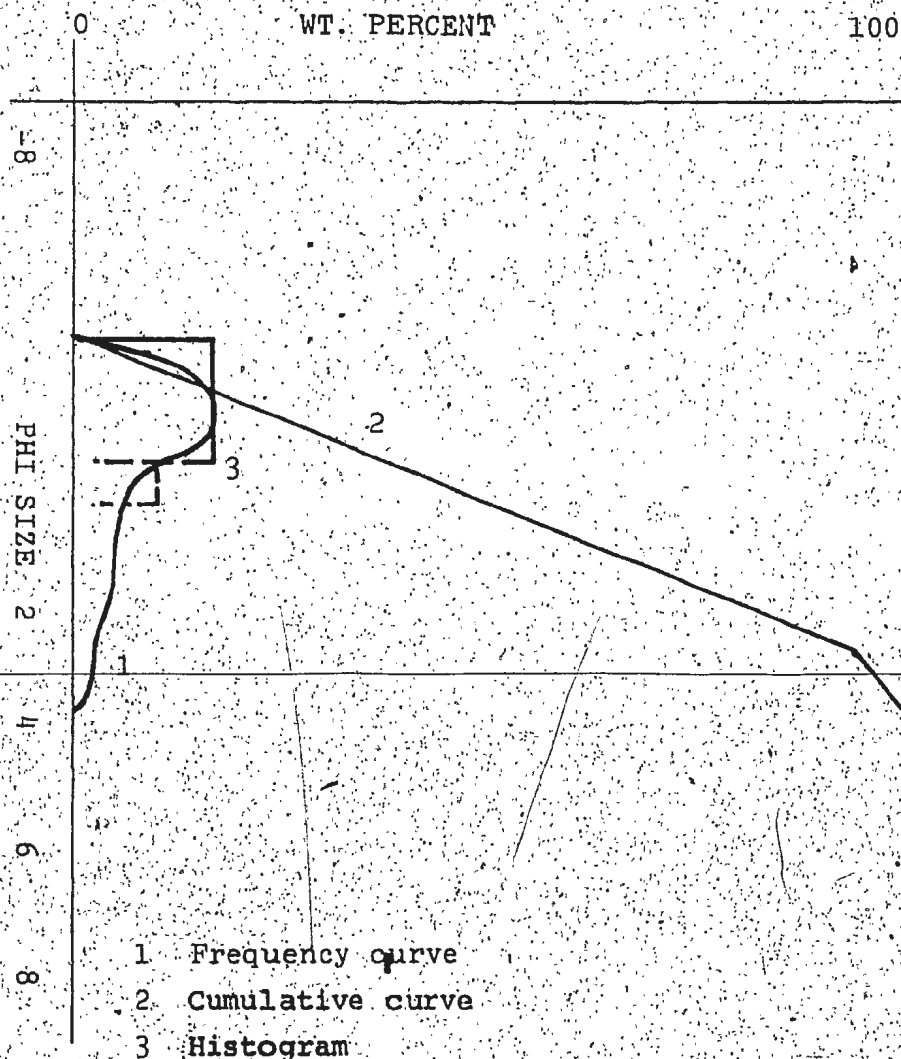
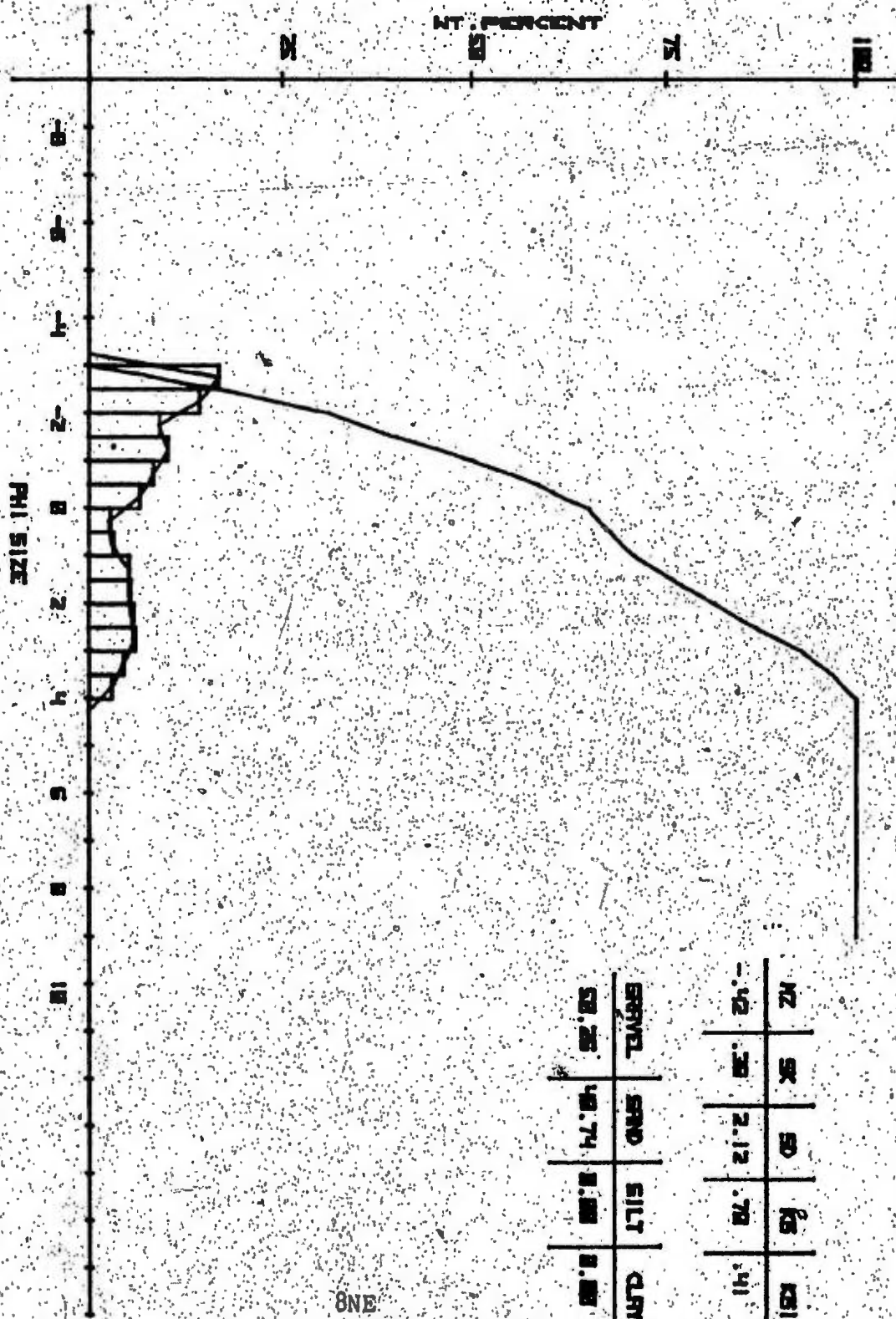
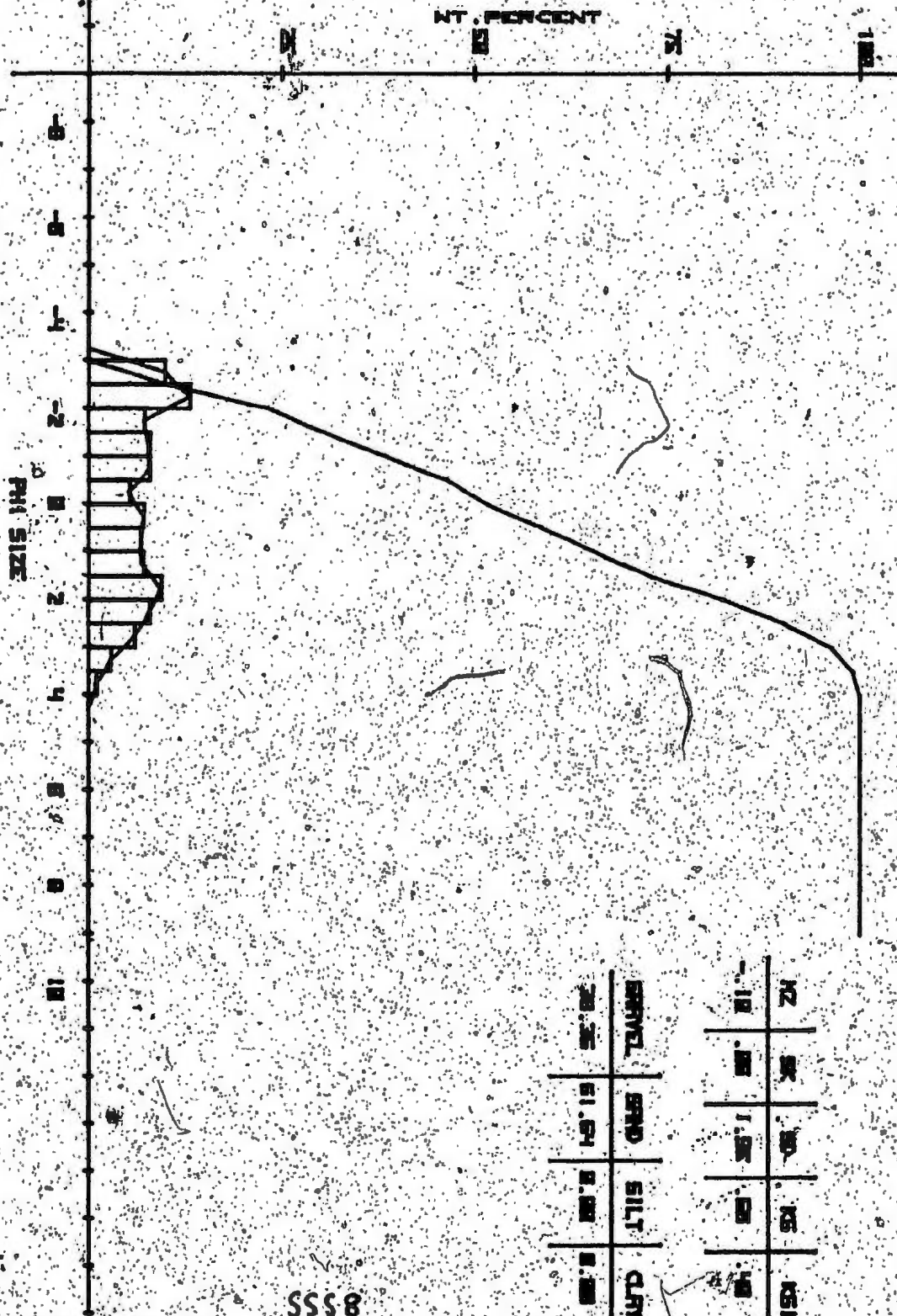


Figure 51. The following diagrams depict particle-size distributions exhibited by debris samples from Berendon and Salmon Glaciers over the size range -3 to 4 ϕ (8 to .0625mm). Values of standard deviation, mean size, skewness and kurtosis are presented in matrix fashion (see Slatt and Press, 1976). For sample descriptions refer to Appendix VI.

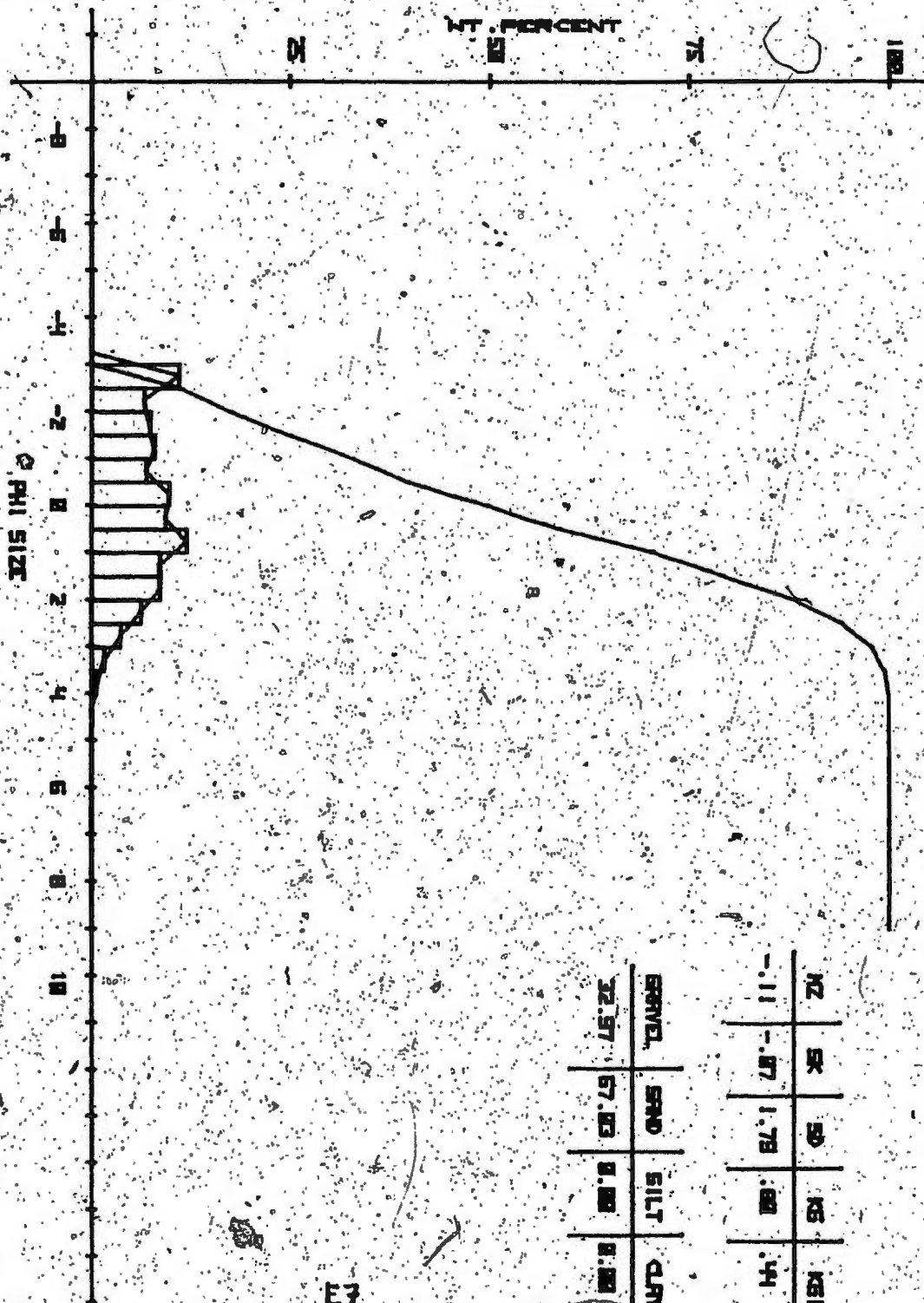


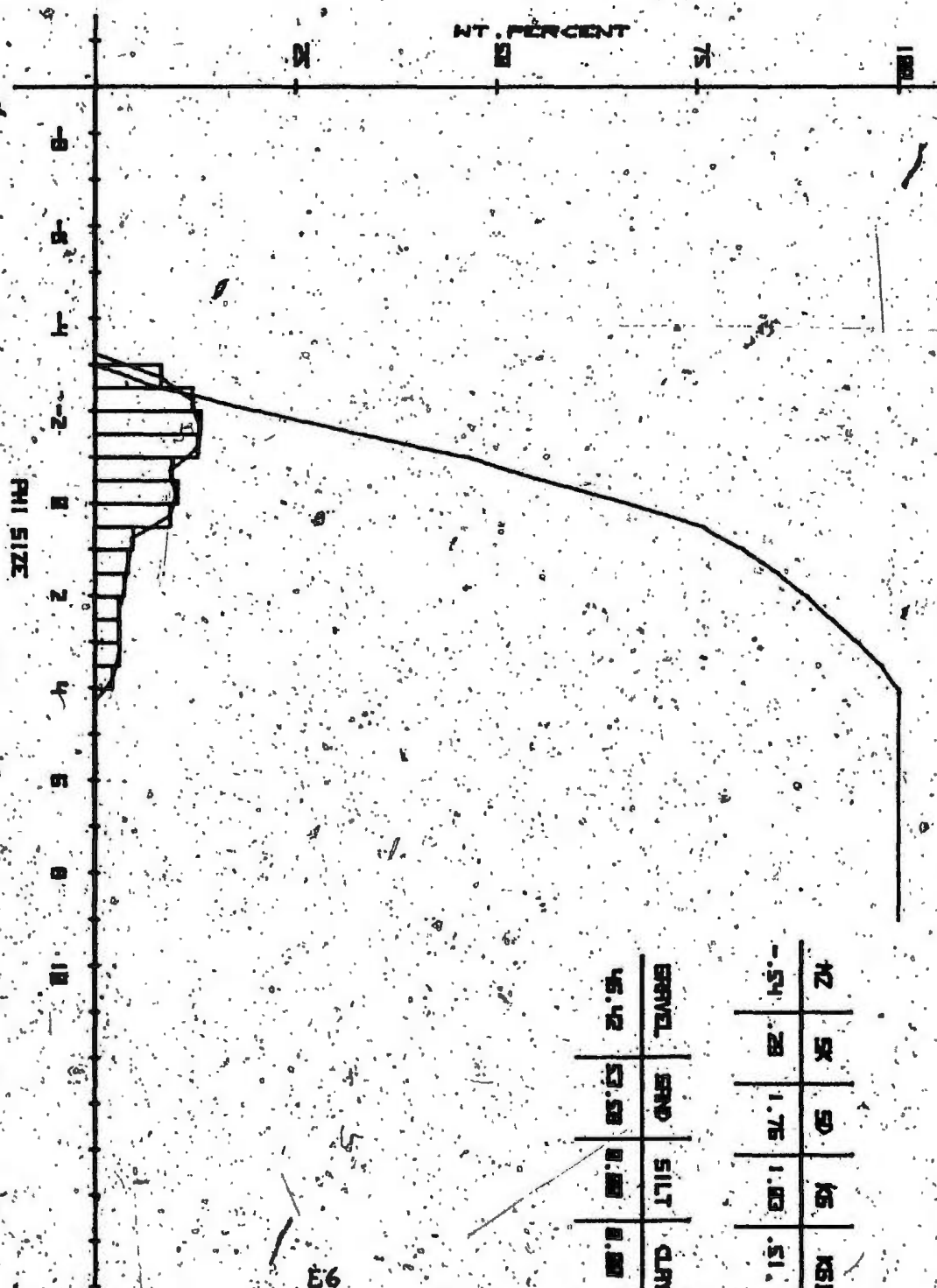
100	50	25	12.5	6.25
75	37.5	18.75	9.375	4.6875
50	25	12.5	6.25	3.125
25	12.5	6.25	3.125	1.5625
12.5	6.25	3.125	1.5625	0.78125
6.25	3.125	1.5625	0.78125	0.390625
3.125	1.5625	0.78125	0.390625	0.1953125
1.5625	0.78125	0.390625	0.1953125	0.09765625
0.78125	0.390625	0.1953125	0.09765625	0.048828125
0.390625	0.1953125	0.09765625	0.048828125	0.0244140625
0.1953125	0.09765625	0.048828125	0.0244140625	0.01220703125
0.09765625	0.048828125	0.0244140625	0.01220703125	0.006103515625
0.048828125	0.0244140625	0.01220703125	0.006103515625	0.0030517578125
0.0244140625	0.01220703125	0.006103515625	0.0030517578125	0.00152587890625
0.01220703125	0.006103515625	0.0030517578125	0.00152587890625	0.000762939453125
0.006103515625	0.0030517578125	0.00152587890625	0.000762939453125	0.0003814697265625
0.0030517578125	0.00152587890625	0.000762939453125	0.0003814697265625	0.00019073486328125
0.00152587890625	0.000762939453125	0.0003814697265625	0.00019073486328125	0.000095367431640625
0.000762939453125	0.0003814697265625	0.00019073486328125	0.000095367431640625	0.0000476837158203125
0.0003814697265625	0.00019073486328125	0.000095367431640625	0.0000476837158203125	0.00002384185791015625
0.00019073486328125	0.000095367431640625	0.0000476837158203125	0.00002384185791015625	0.000011920928955078125
0.000095367431640625	0.0000476837158203125	0.00002384185791015625	0.000011920928955078125	0.0000059604644775390625
0.0000476837158203125	0.00002384185791015625	0.000011920928955078125	0.0000059604644775390625	0.00000298023223876953125
0.00002384185791015625	0.000011920928955078125	0.0000059604644775390625	0.00000298023223876953125	0.000001490116119384765625
0.000011920928955078125	0.0000059604644775390625	0.00000298023223876953125	0.000001490116119384765625	0.0000007450580596923828125
0.0000059604644775390625	0.00000298023223876953125	0.000001490116119384765625	0.0000007450580596923828125	0.00000037252902984619140625
0.00000298023223876953125	0.000001490116119384765625	0.0000007450580596923828125	0.00000037252902984619140625	0.000000186264514923095703125
0.000001490116119384765625	0.0000007450580596923828125	0.00000037252902984619140625	0.000000186264514923095703125	0.0000000931322574615478515625
0.0000007450580596923828125	0.00000037252902984619140625	0.000000186264514923095703125	0.0000000931322574615478515625	0.00000004656612873077392578125
0.00000037252902984619140625	0.000000186264514923095703125	0.0000000931322574615478515625	0.00000004656612873077392578125	0.000000023283064365386962890625
0.000000186264514923095703125	0.0000000931322574615478515625	0.00000004656612873077392578125	0.000000023283064365386962890625	0.0000000116415321826934814453125
0.0000000931322574615478515625	0.00000004656612873077392578125	0.000000023283064365386962890625	0.0000000116415321826934814453125	0.00000000582076609134674072265625
0.00000004656612873077392578125	0.000000023283064365386962890625	0.0000000116415321826934814453125	0.00000000582076609134674072265625	0.000000002910383045673370361328125
0.000000023283064365386962890625	0.0000000116415321826934814453125	0.00000000582076609134674072265625	0.000000002910383045673370361328125	0.0000000014551915228366851806640625
0.0000000116415321826934814453125	0.00000000582076609134674072265625	0.000000002910383045673370361328125	0.0000000014551915228366851806640625	0.00000000072759576141834259033203125
0.00000000582076609134674072265625	0.000000002910383045673370361328125	0.0000000014551915228366851806640625	0.00000000072759576141834259033203125	0.000000000363797880709171295166015625
0.000000002910383045673370361328125	0.0000000014551915228366851806640625	0.00000000072759576141834259033203125	0.000000000363797880709171295166015625	0.0000000001818989403545856475830078125
0.0000000014551915228366851806640625	0.00000000072759576141834259033203125	0.000000000363797880709171295166015625	0.0000000001818989403545856475830078125	0.00000000009094947017729282379150390625
0.00000000072759576141834259033203125	0.000000000363797880709171295166015625	0.0000000001818989403545856475830078125	0.00000000009094947017729282379150390625	0.000000000045474735088646411895751953125
0.000000000363797880709171295166015625	0.0000000001818989403545856475830078125	0.00000000009094947017729282379150390625	0.000000000045474735088646411895751953125	0.0000000000227373675443232059478759765625
0.0000000001818989403545856475830078125	0.00000000009094947017729282379150390625	0.000000000045474735088646411895751953125	0.0000000000227373675443232059478759765625	0.00000000001136868377216160297393798828125
0.00000000009094947017729282379150390625	0.000000000045474735088646411895751953125	0.0000000000227373675443232059478759765625	0.00000000001136868377216160297393798828125	0.000000000005684341886080801486968994140625
0.000000000045474735088646411895751953125	0.0000000000227373675443232059478759765625	0.00000000001136868377216160297393798828125	0.000000000005684341886080801486968994140625	0.0000000000028421709430404007434844970703125
0.0000000000227373675443232059478759765625	0.00000000001136868377216160297393798828125	0.000000000005684341886080801486968994140625	0.0000000000028421709430404007434844970703125	0.00000000000142108547152020037174224853515625
0.00000000001136868377216160297393798828125	0.000000000005684341886080801486968994140625	0.0000000000028421709430404007434844970703125	0.00000000000142108547152020037174224853515625	0.000000000000710542735760100185871124267578125
0.000000000005684341886080801486968994140625	0.0000000000028421709430404007434844970703125	0.00000000000142108547152020037174224853515625	0.000000000000710542735760100185871124267578125	0.0000000000003552713678800500929355621337890625
0.0000000000028421709430404007434844970703125	0.00000000000142108547152020037174224853515625	0.000000000000710542735760100185871124267578125	0.0000000000003552713678800500929355621337890625	0.00000000000017763568394002504646778106689453125
0.00000000000142108547152020037174224853515625	0.000000000000710542735760100185871124267578125	0.0000000000003552713678800500929355621337890625	0.00000000000017763568394002504646778106689453125	0.000000000000088817841970012523233890533447265625
0.000000000000710542735760100185871124267578125	0.0000000000003552713678800500929355621337890625	0.00000000000017763568394002504646778106689453125	0.000000000000088817841970012523233890533447265625	0.0000000000000444089209850062616169452667236328125
0.0000000000003552713678800500929355621337890625	0.00000000000017763568394002504646778106689453125	0.000000000000088817841970012523233890533447265625	0.0000000000000444089209850062616169452667236328125	0.00000000000002220446049250313080847263336181640625
0.00000000000017763568394002504646778106689453125	0.000000000000088817841970012523233890533447265625	0.0000000000000444089209850062616169452667236328125	0.00000000000002220446049250313080847263336181640625	0.000000000000011102230246251565404236316680908203125
0.000000000000088817841970012523233890533447265625	0.0000000000000444089209850062616169452667236328125	0.00000000000002220446049250313080847263336181640625	0.000000000000011102230246251565404236316680908203125	0.000000000000005551115123125782702118158334044015625
0.0000000000000444089209850062616169452667236328125	0.00000000000002220446049250313080847263336181640625	0.000000000000011102230246251565404236316680908203125	0.000000000000005551115123125782702118158334044015625	0.0000000000000027755575615628913510590791670220078125
0.00000000000002220446049250313080847263336181640625	0.000000000000011102230246251565404236316680908203125	0.000000000000005551115123125782702118158334044015625	0.0000000000000027755575615628913510590791670220078125	0.00000000000000138777878078144567552953958351100390625
0.000000000000011102230246251565404236316680908203125	0.000000000000005551115123125782702118158334044015625	0.0000000000000027755575615628913510590791670220078125	0.00000000000000138777878078144567552953958351100390625	0.000000000000000693889390390722837764769791755501953125
0.000000000000005551115123125782702118158334044015625	0.0000000000000027755575615628913510590791670220078125	0.00000000000000138777878078144567552953958351100390625	0.000000000000000693889390390722837764769791755501953125	0.0000000000000003469446951953614188823848958777509765625
0.0000000000000027755575615628913510590791670220078125	0.00000000000000138777878078144567552953958351100390625	0.000000000000000693889390390722837764769791755501953125	0.0000000000000003469446951953614188823848958777509765625	0.00000000000000017347234759768070944119244793887548828125
0.00000000000000138777878078144567552953958351100390625	0.000000000000000693889390390722837764769791755501953125	0.0000000000000003469446951953614188823848958777509765625	0.00000000000000017347234759768070944119244793887548828125	0.000000000000000086736173798840354720596223969437744140625
0.000000000000000693889390390722837764769791755501953125	0.0000000000000003469446951953614188823848958777509765625	0.00000000000000017347234759768070944119244793887548828125	0.000000000000000086736173798840354720596223969437744140625	0.0000000000000000433680868994201773602981119847188720703125
0.0000000000000003469446951953614188823848958777509765625	0.00000000000000017347234759768070944119244793887548828125	0.000000000000000086736173798840354720596223969437744140625	0.0000000000000000433680868994201773602981119847188720703125	0.00000000000000002168404344971008868014905599235943603515625
0.00000000000000017347234759768070944119244793887548828125	0.000000000000000086736173798840354720596223969437744140625	0.0000000000000000433680868994201773602981119847188720703125	0.00000000000000002168404344971008868014905599235943603515625	0.000000000000000010842021724855044340074527996179718017578125
0.000000000000000086736173798840354720596223969437744140625	0.0000000000000000433680868994201773602981119847188720703125	0.00000000000000002168404344971008868014905599235943603515625	0.000000000000000010842021724855044340074527996179718017578125	0.0000000000000000054210108624275221700372639980898590087890625
0.0000000000000000433680868994201773602981119847188720703125	0.00000000000000002168404344971008868014905599235943603515625	0.000000000000000010842021724855044340074527996179718017578125	0.0000000000000000054210108624275221700372639980898590087890625	0.0000000000000000027105054312137610850186319990449295043953125
0.00000000000000002168404344971008868014905599235943603515625	0.000000000000000010842021724855044340074527996179718017578125	0.0000000000000000054210108624275221700372639980898590087890625	0.0000000000000000027105054312137610850186319990449295043953125	0.00000000000000000135525271560688054250931599952246477219765625
0.000000000000000010842021724855044340074527996179718017578125	0.00000000000000			



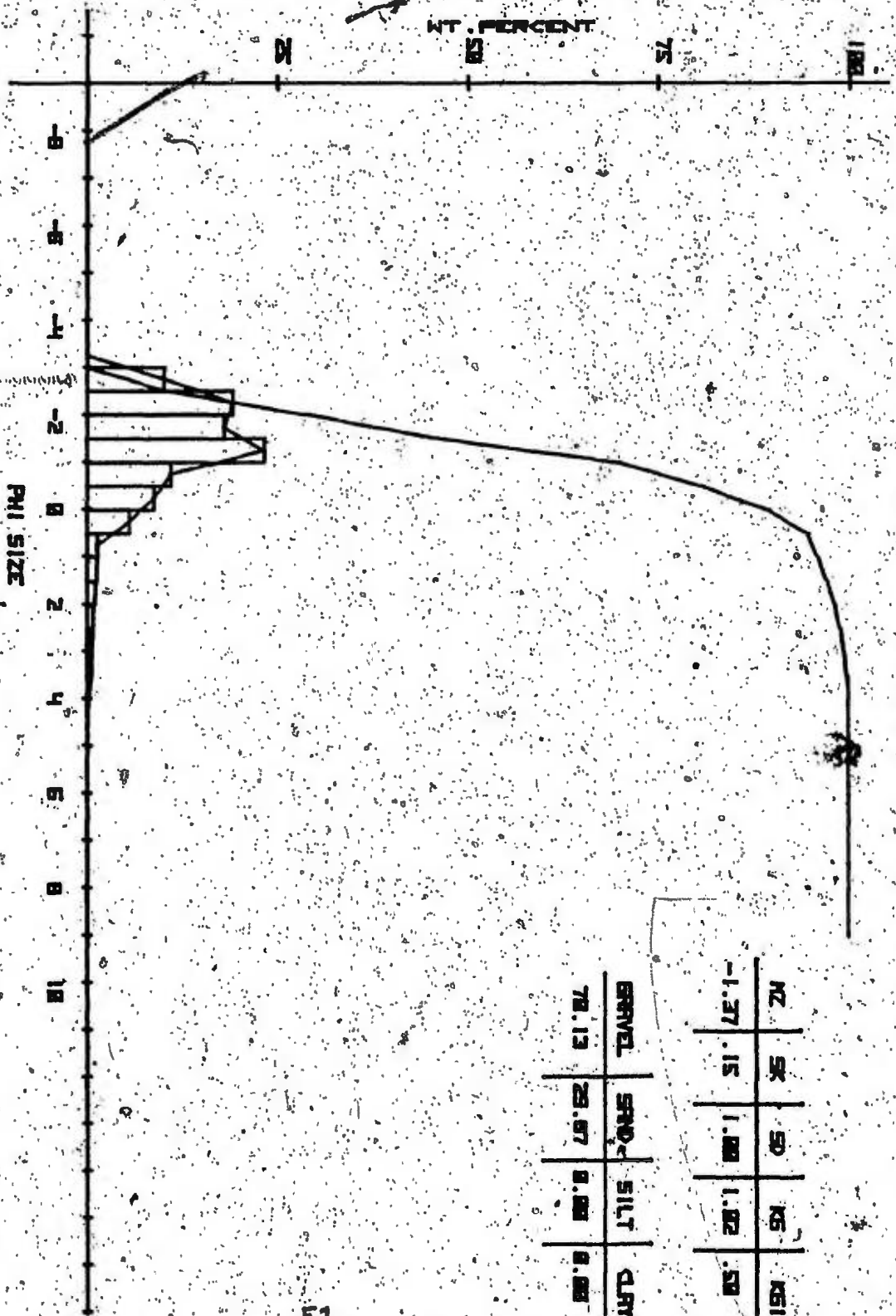
SSS8

GRAVEL	SAND	SILT	CLAY
20.35	61.64	9.00	9.00



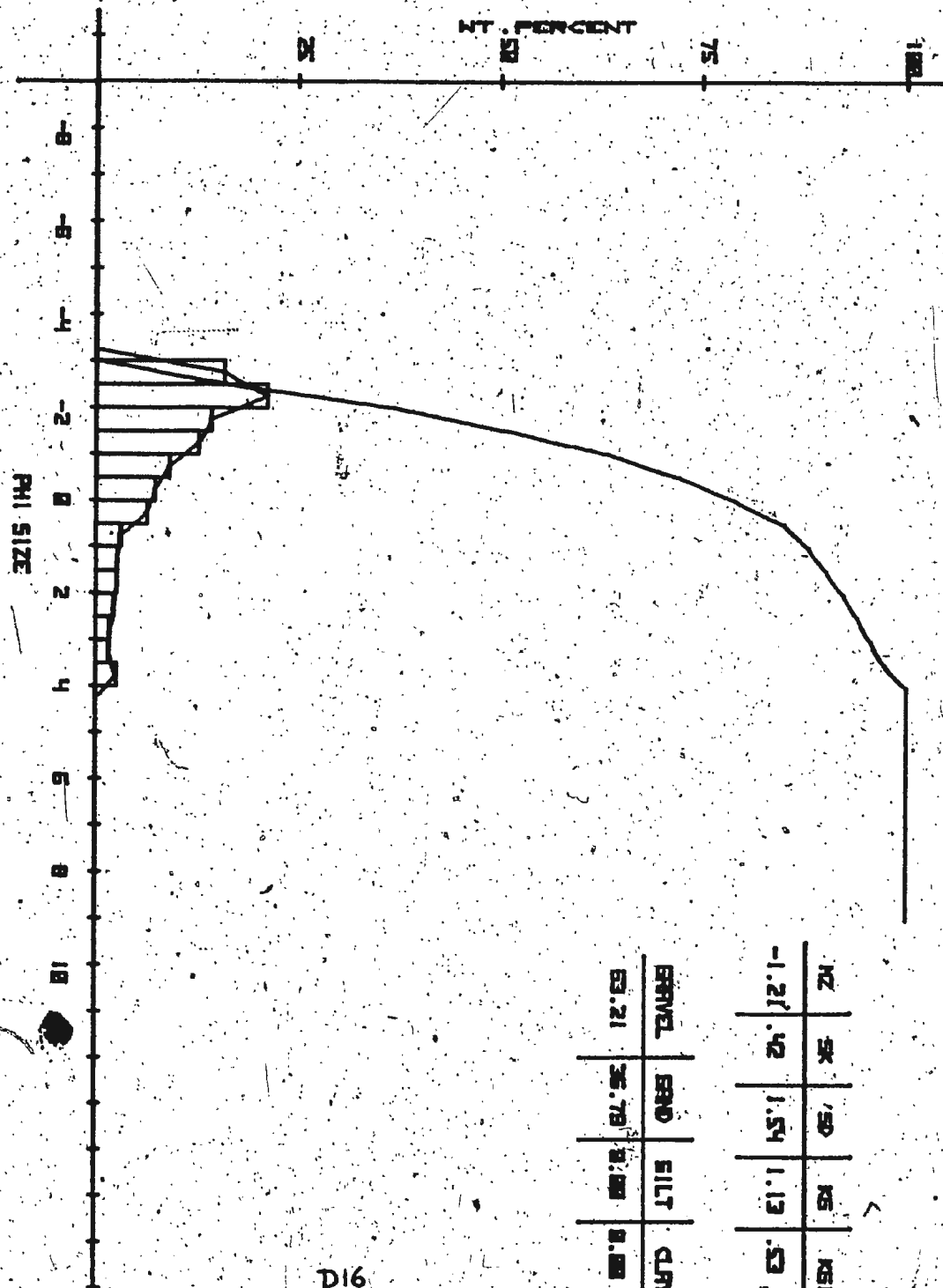


26



NZ	SK	SD	KS	KSI
-1.37	.15	1.00	1.02	.50

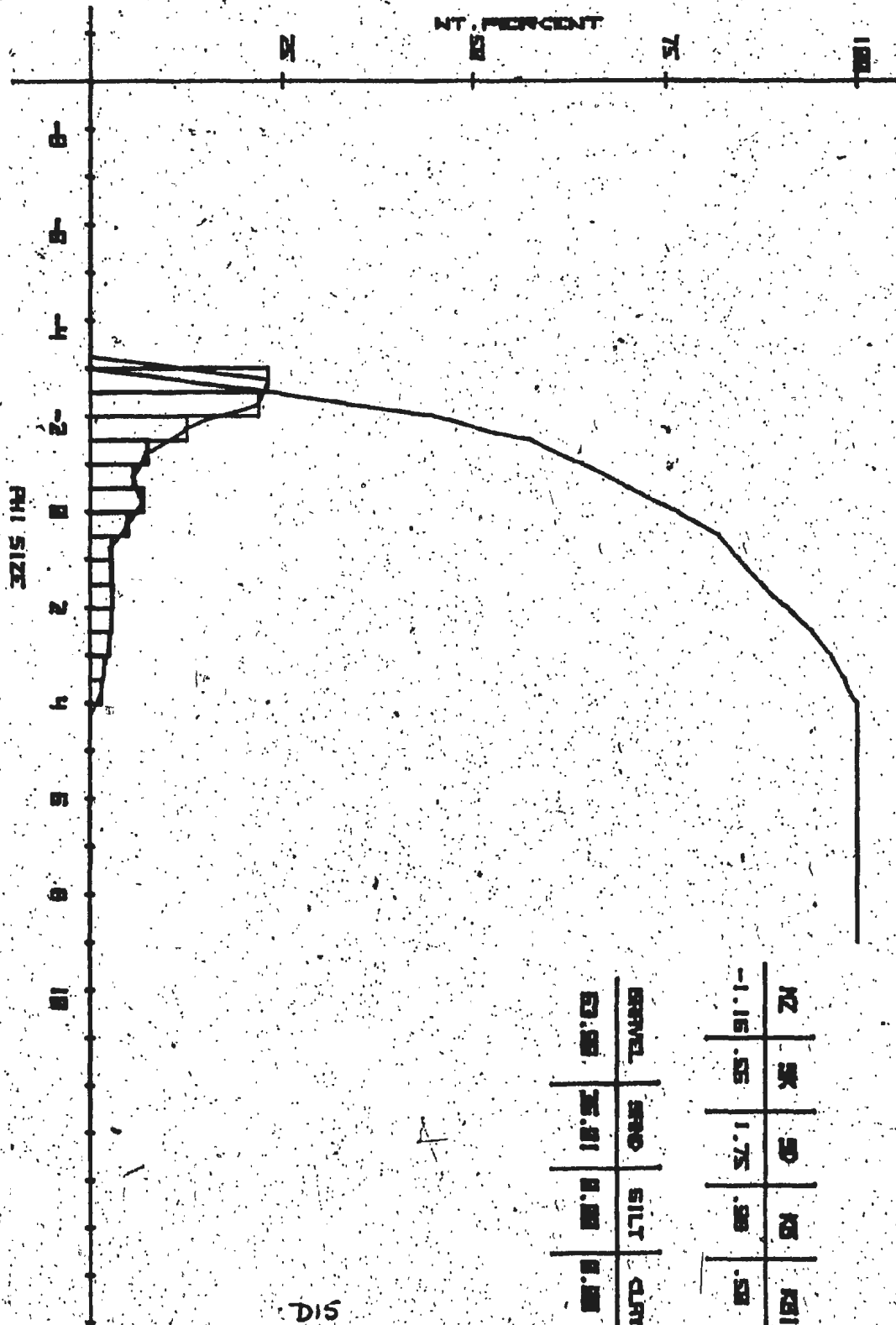
GRAVEL	SAND	SILT	CLAY
70.13	29.87	0.00	0.00

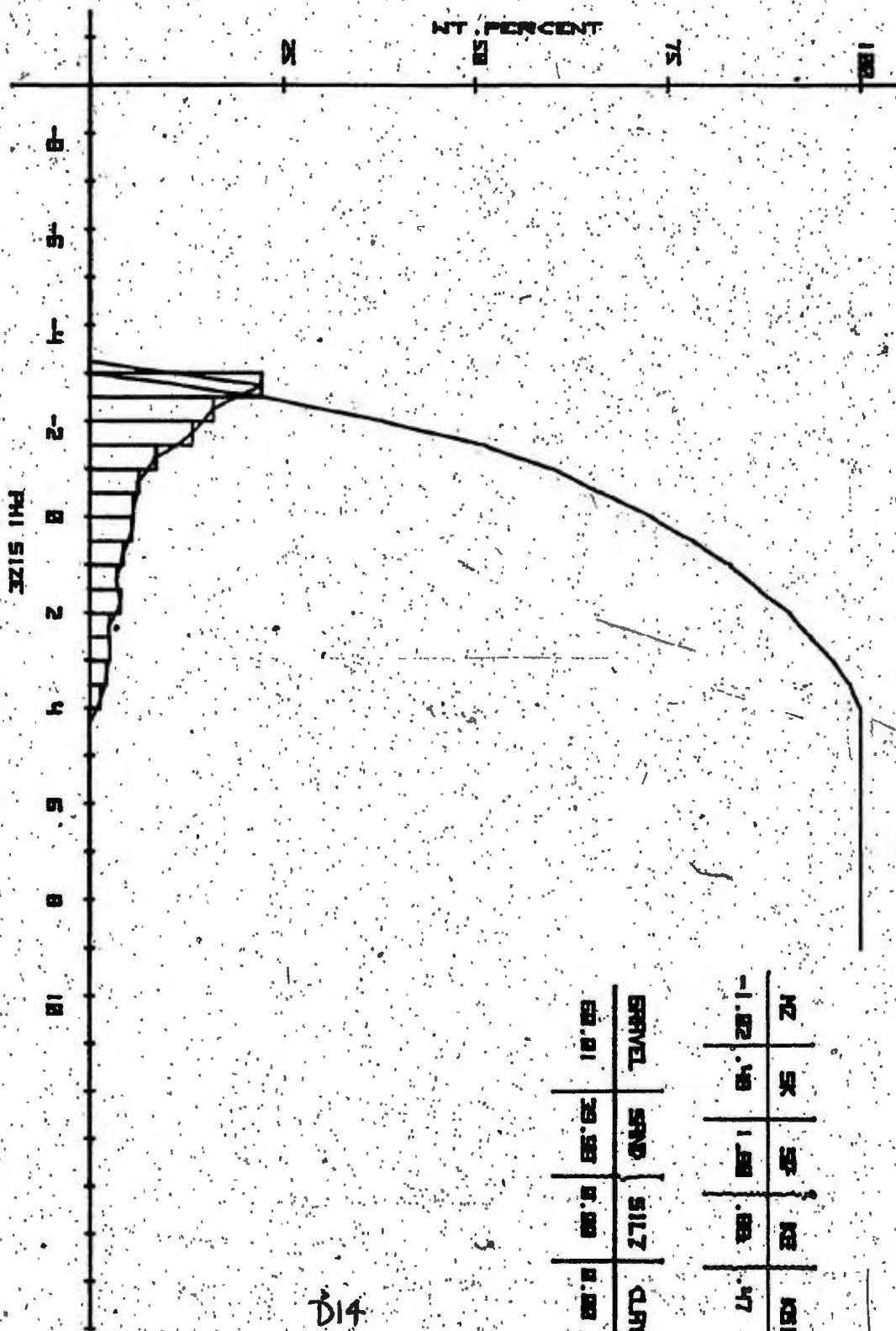


WZ	SK	SD	KS	KSI
-1.27	.42	1.54	1.13	.53

PERVEL	SENO	SILT	CLAY
63.21	36.78	0.00	0.00

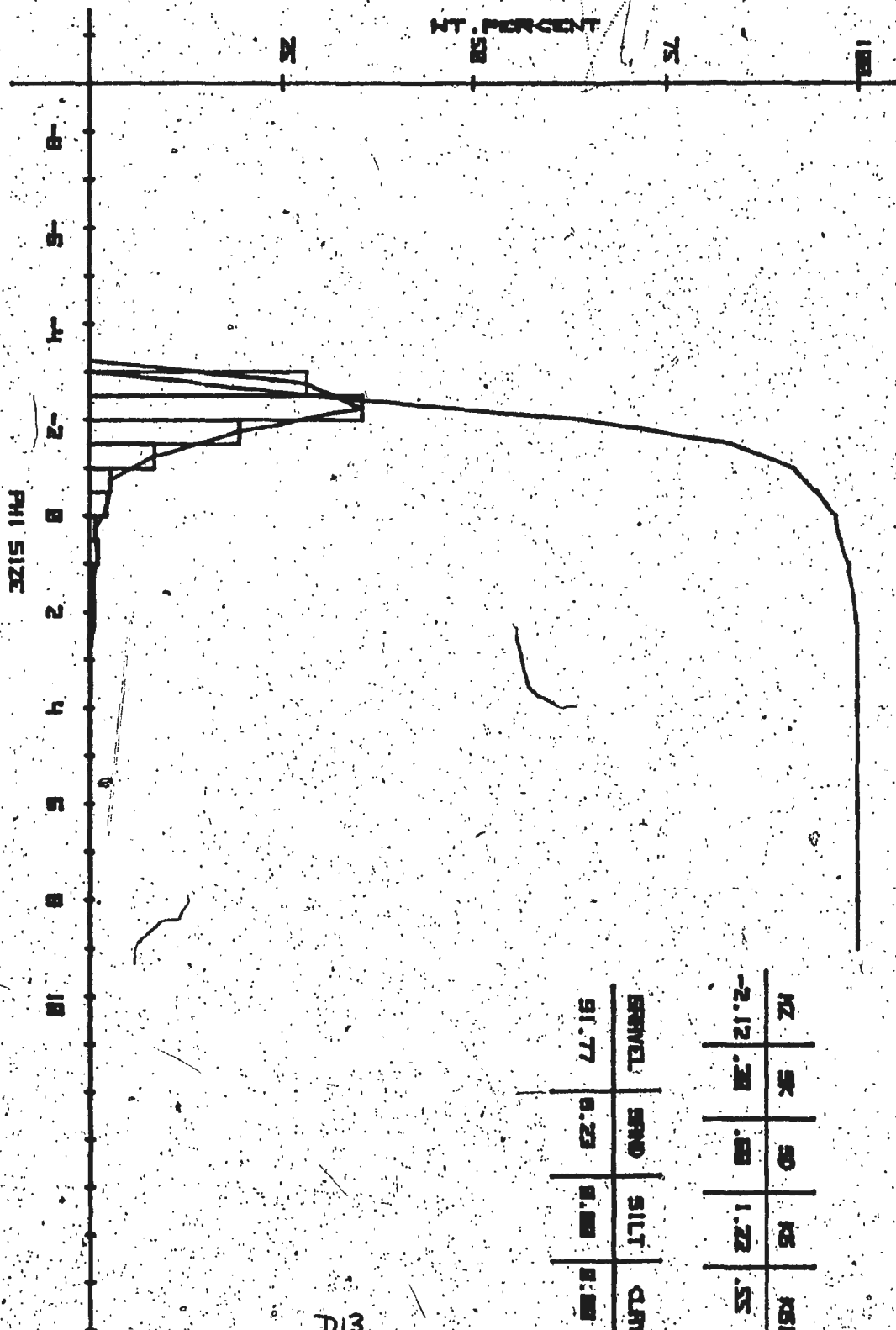
D16





20	40	60	100
100	20	10	5

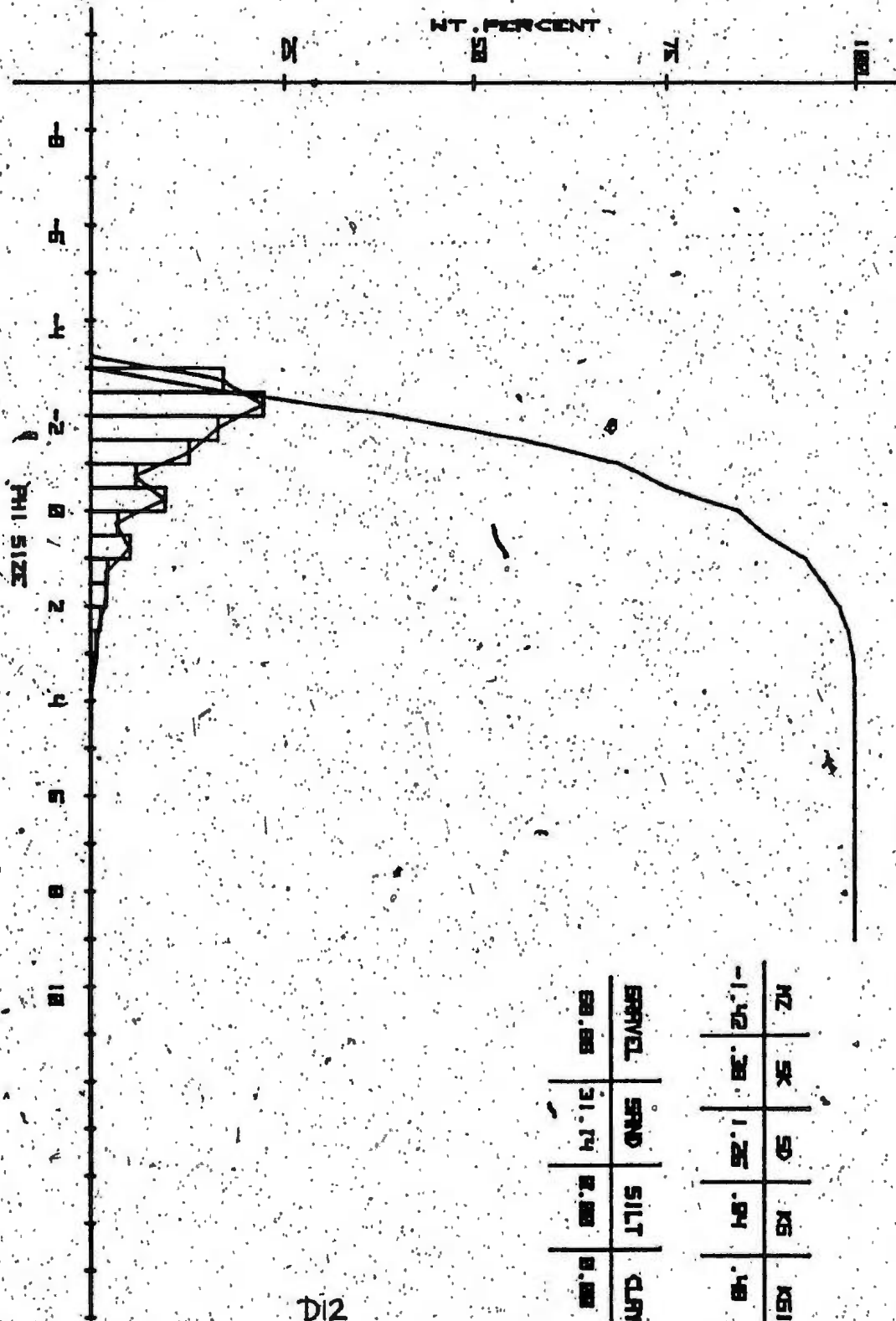
GRAVEL	SAND	SILT	CLAY
10.01	29.58	50.00	10.00



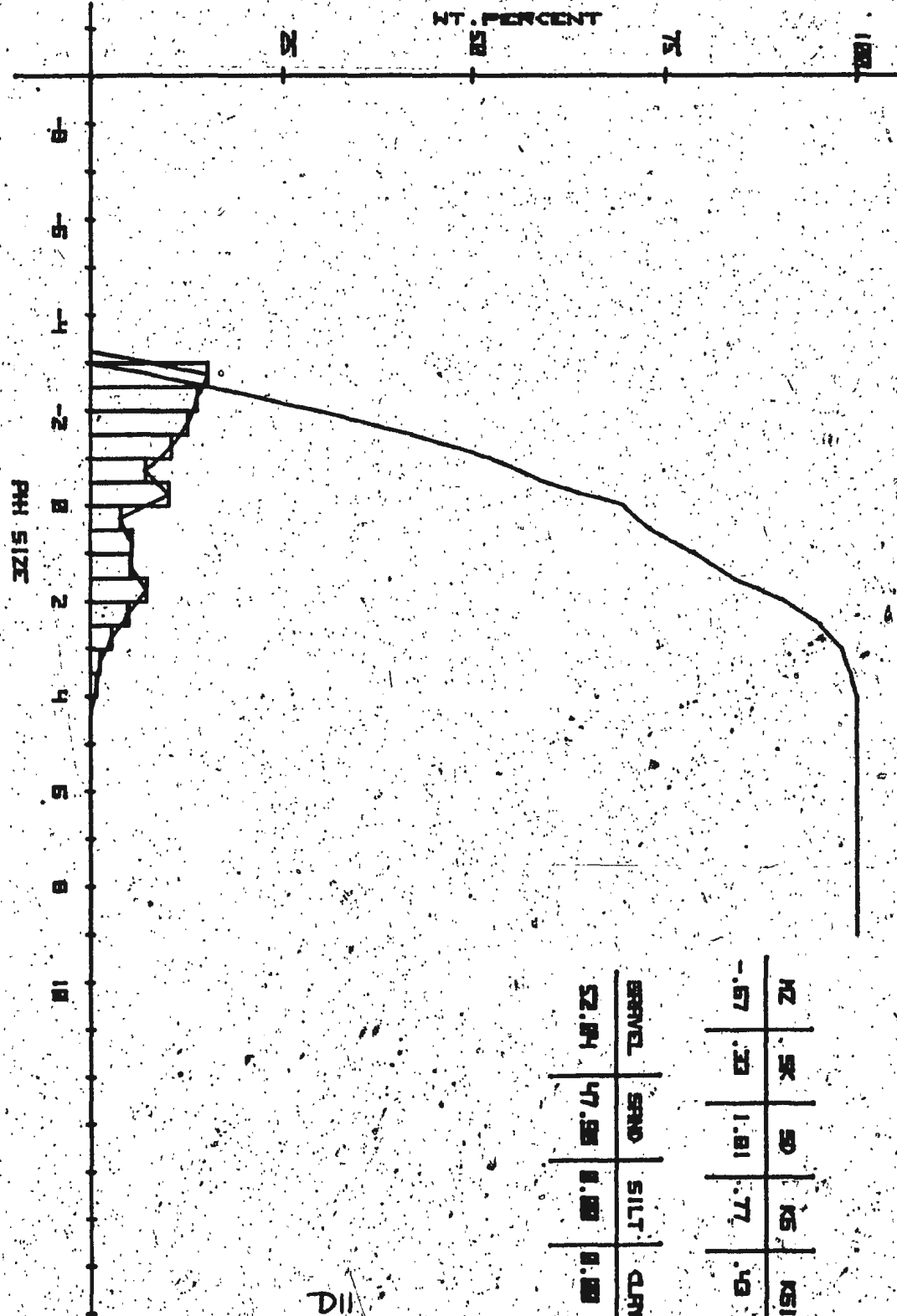
NZ	SK	SD	SS	MS
-2.12	.30	.00	1.22	.55

GRAVEL	SAND	SILT	CLAY
91.77	0.23	0.00	0.00

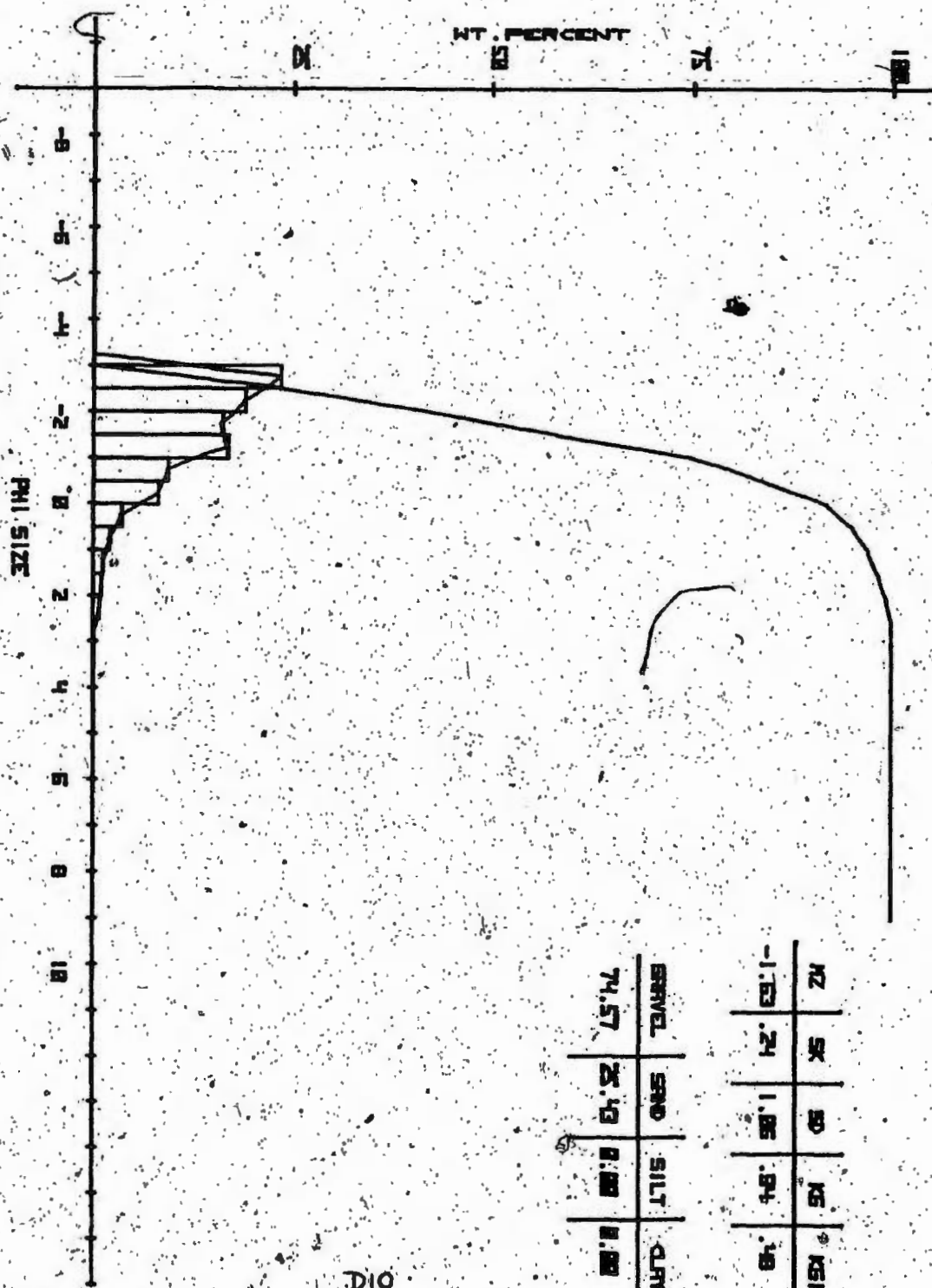
D13



D12



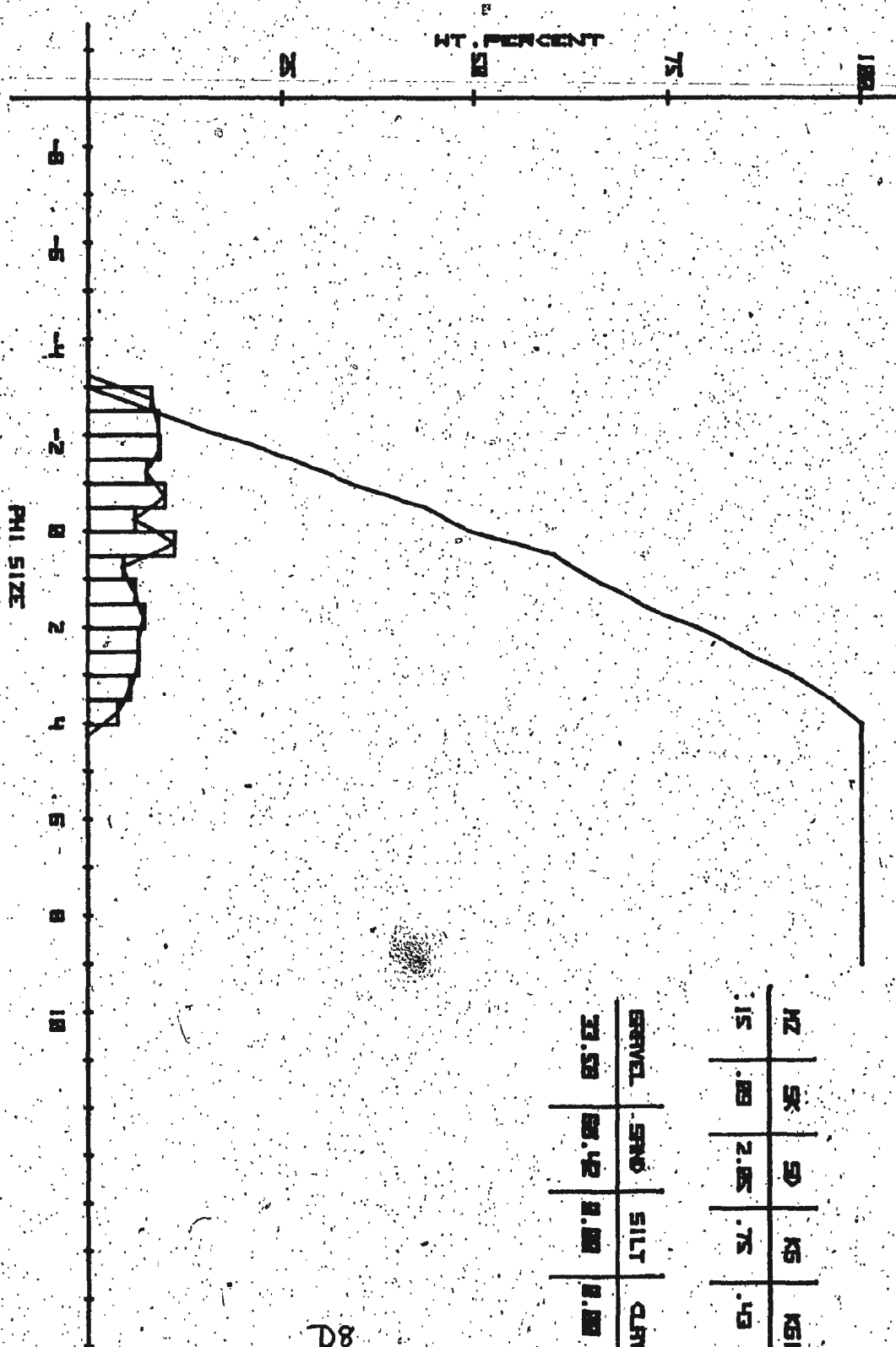
D11



74.57	25.43	0.00	0.00
GRAVEL SAND SILT CLAY			

1.63	0.25	1.06	0.04	0.00
No. 10 No. 20 No. 40 No. 60 No. 100				

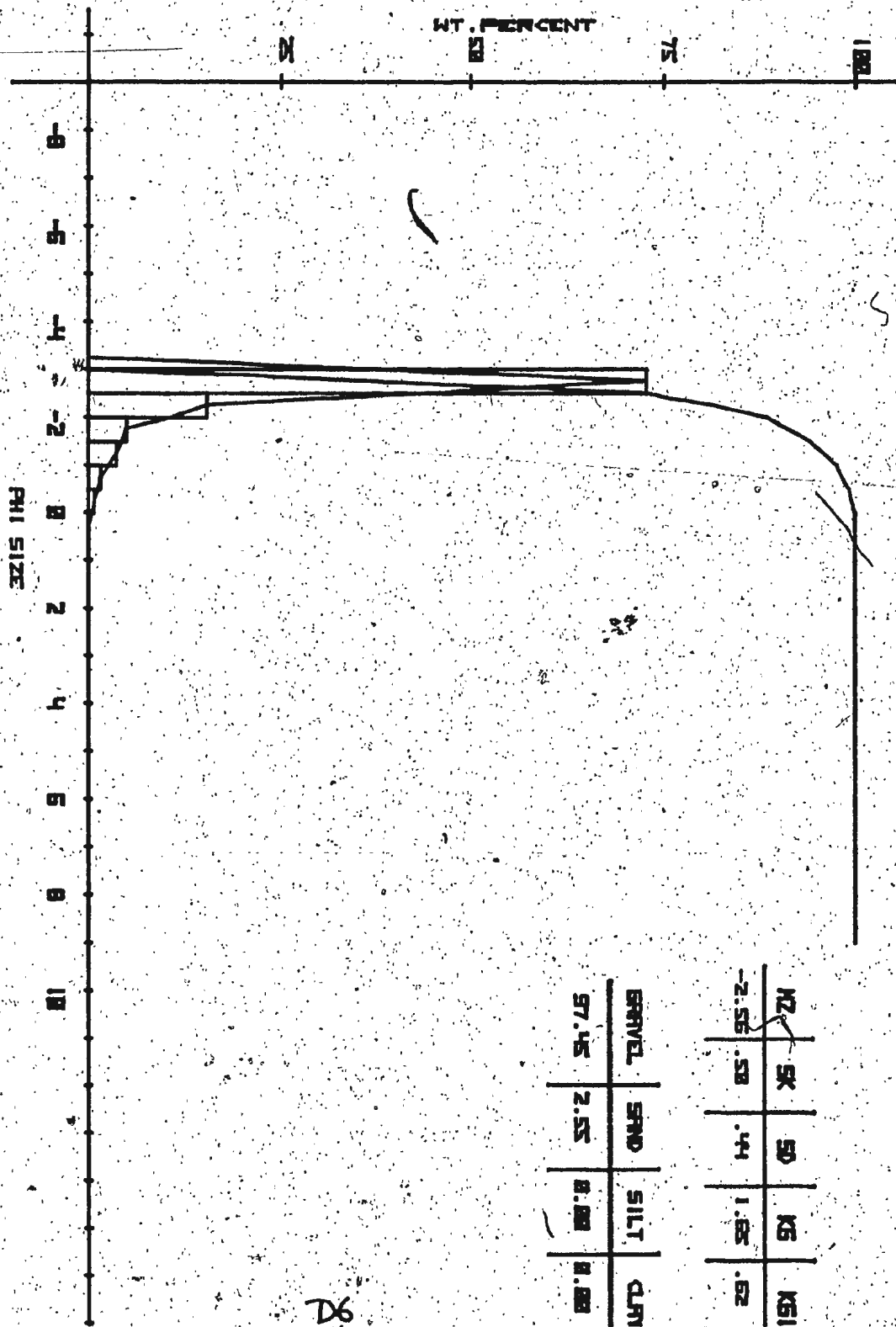
D10



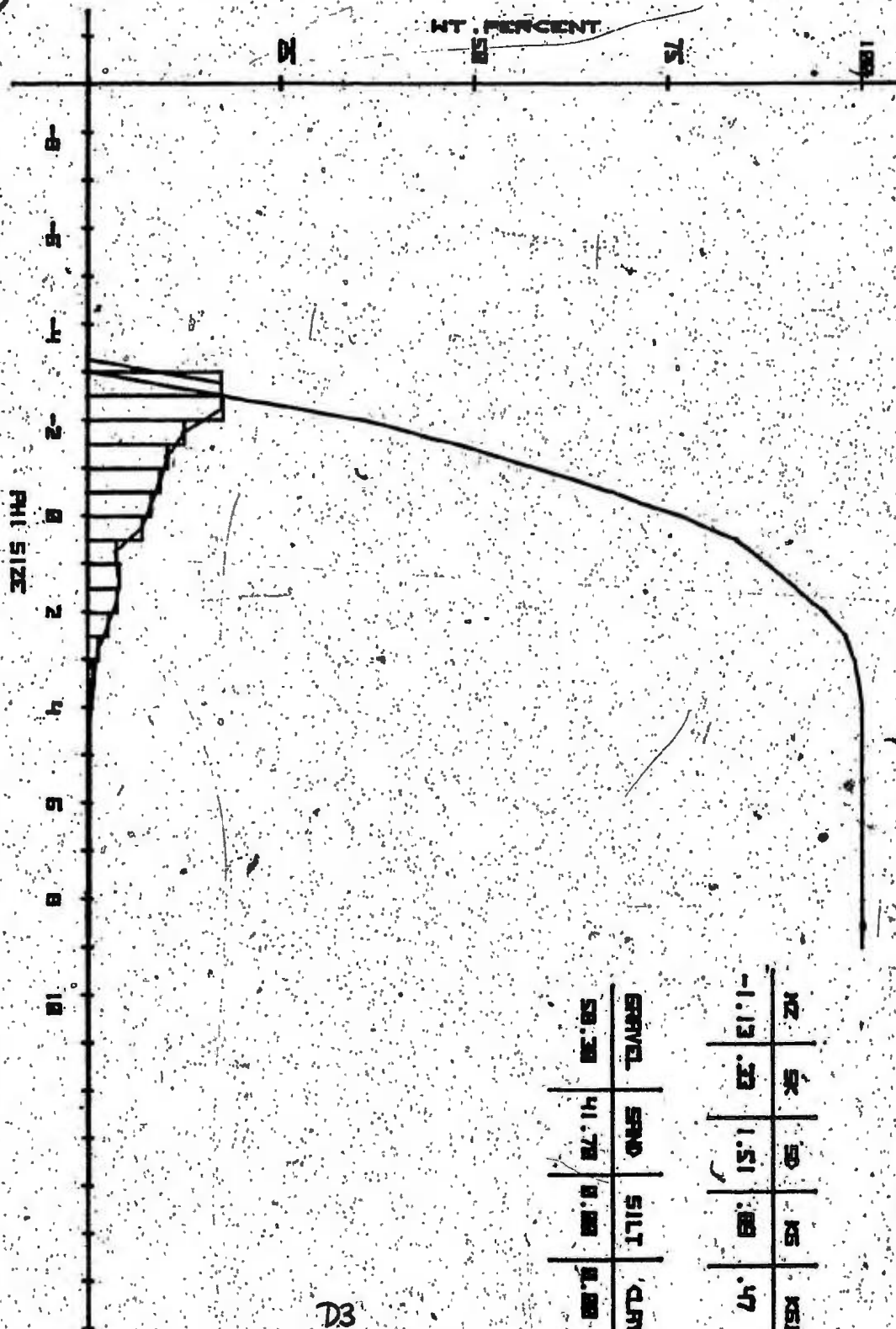
MZ	5K	9D	K5	K51
.15	.08	2.86	.75	.59

GRAVEL	SAND	SILT	CLAY
33.58	66.42	0.00	0.00

D8



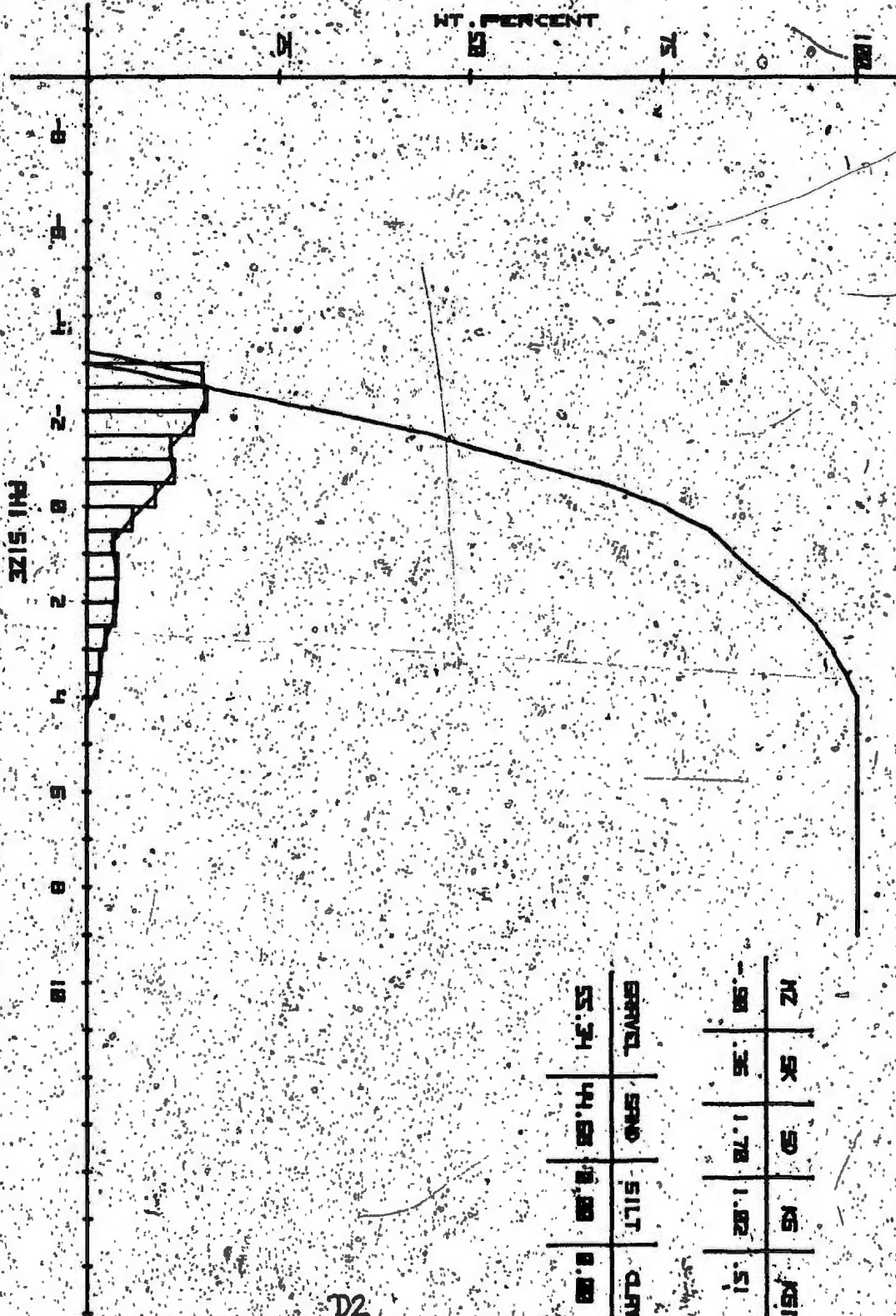
MZ	SK	SD	KS	KG1
-2.55	.58	.41	1.65	.62
<hr/>				
GRAVEL	SAND	SILT	CLAY	
97.45	2.55	0.00	0.00	



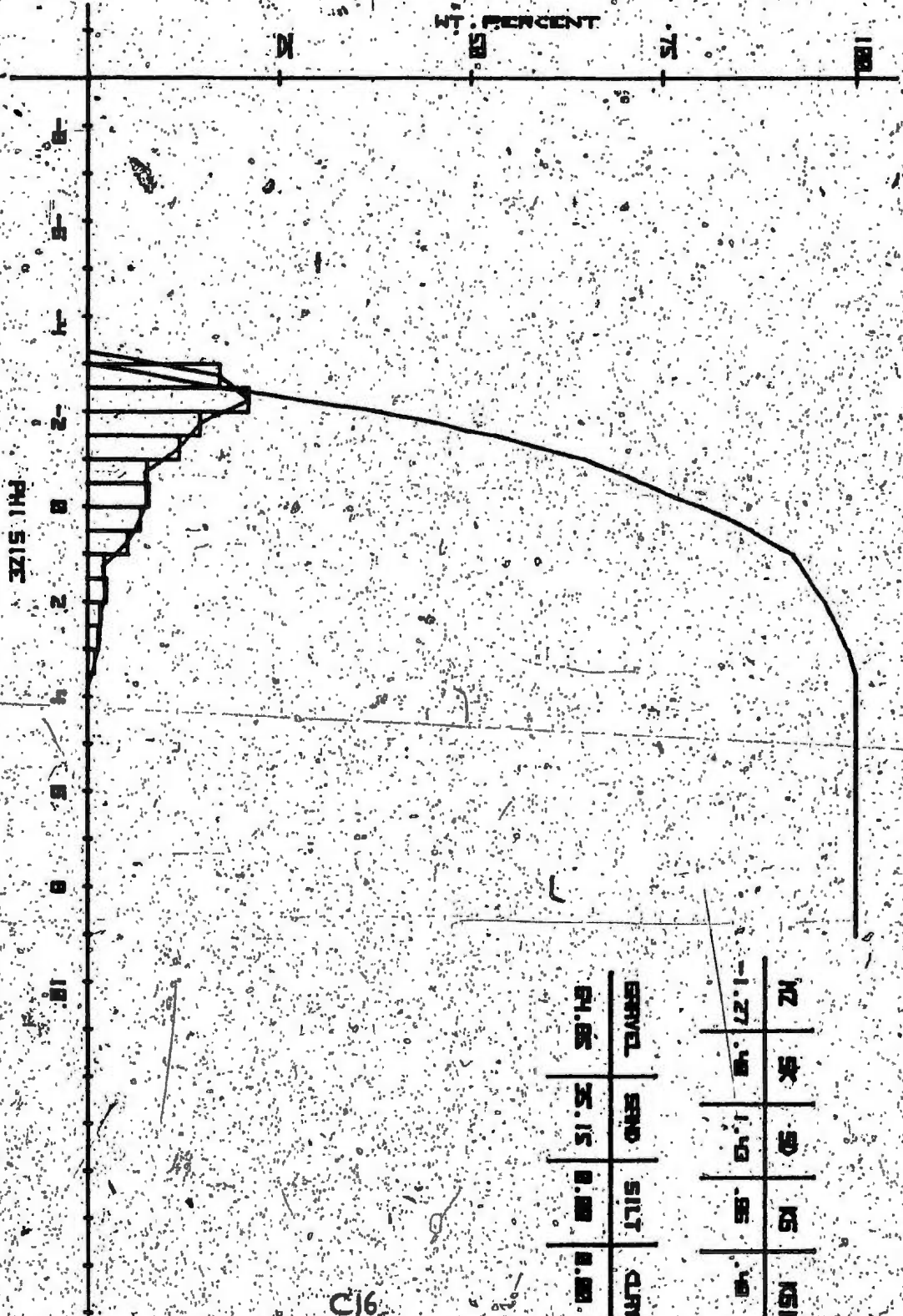
W	SR	SO	MS	ML
11.13	33	1.51	83	47

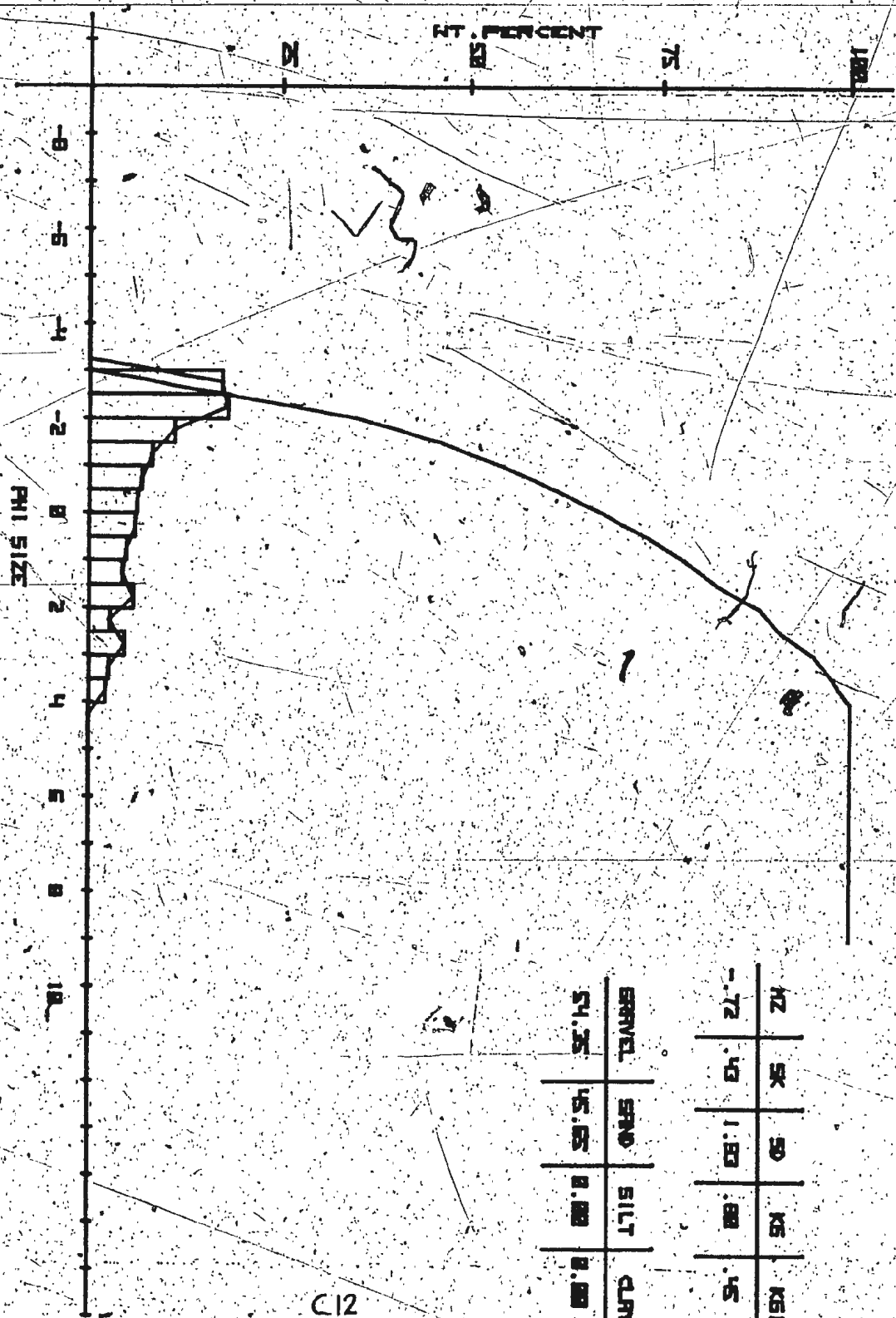
GRAVEL	SAND	SILT	CLAY
50.30	41.70	8.00	0.00

D3



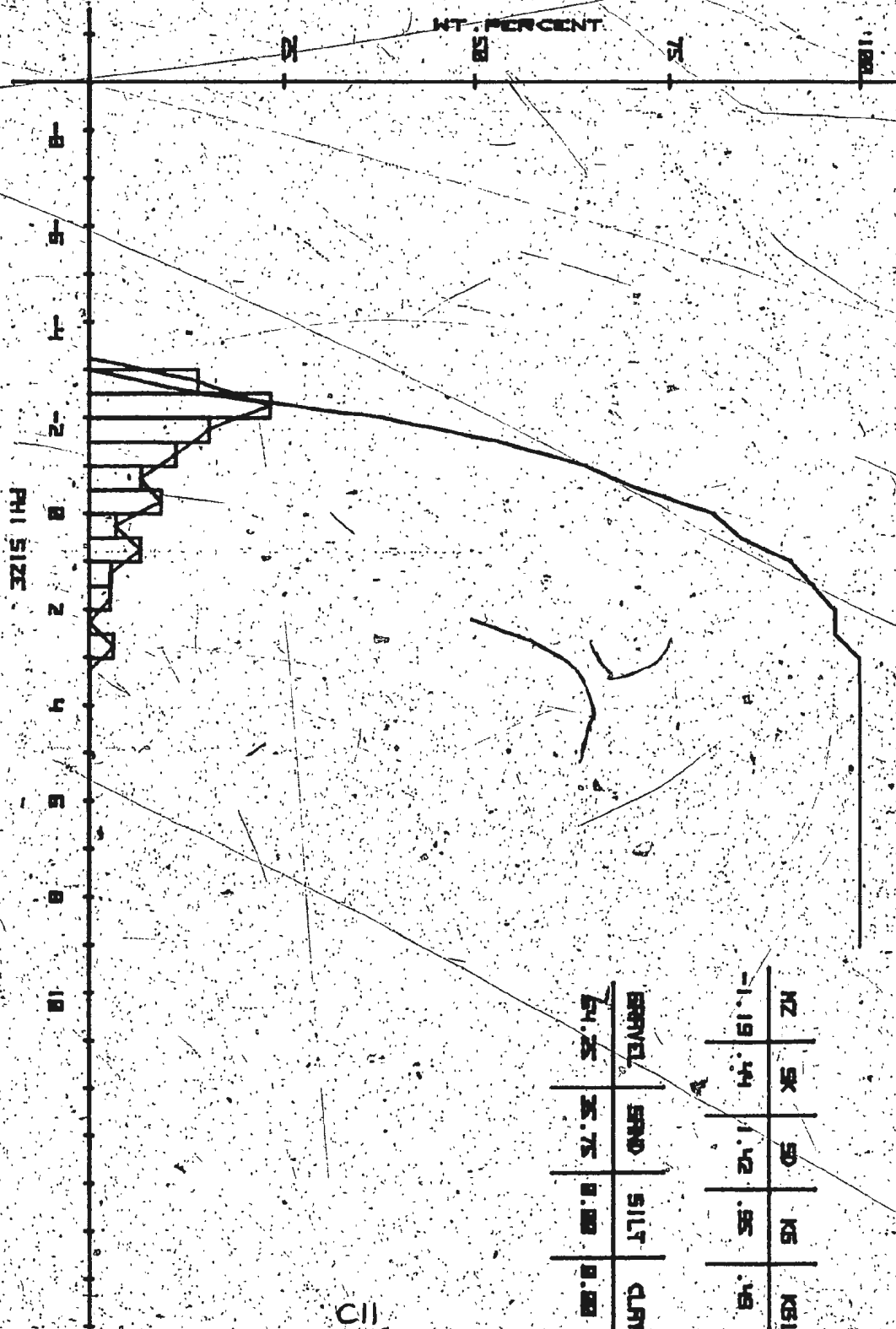
D2





2.5	5.0	7.5	10.0
GRAVEL	SAND	SILT	CLAY

C12



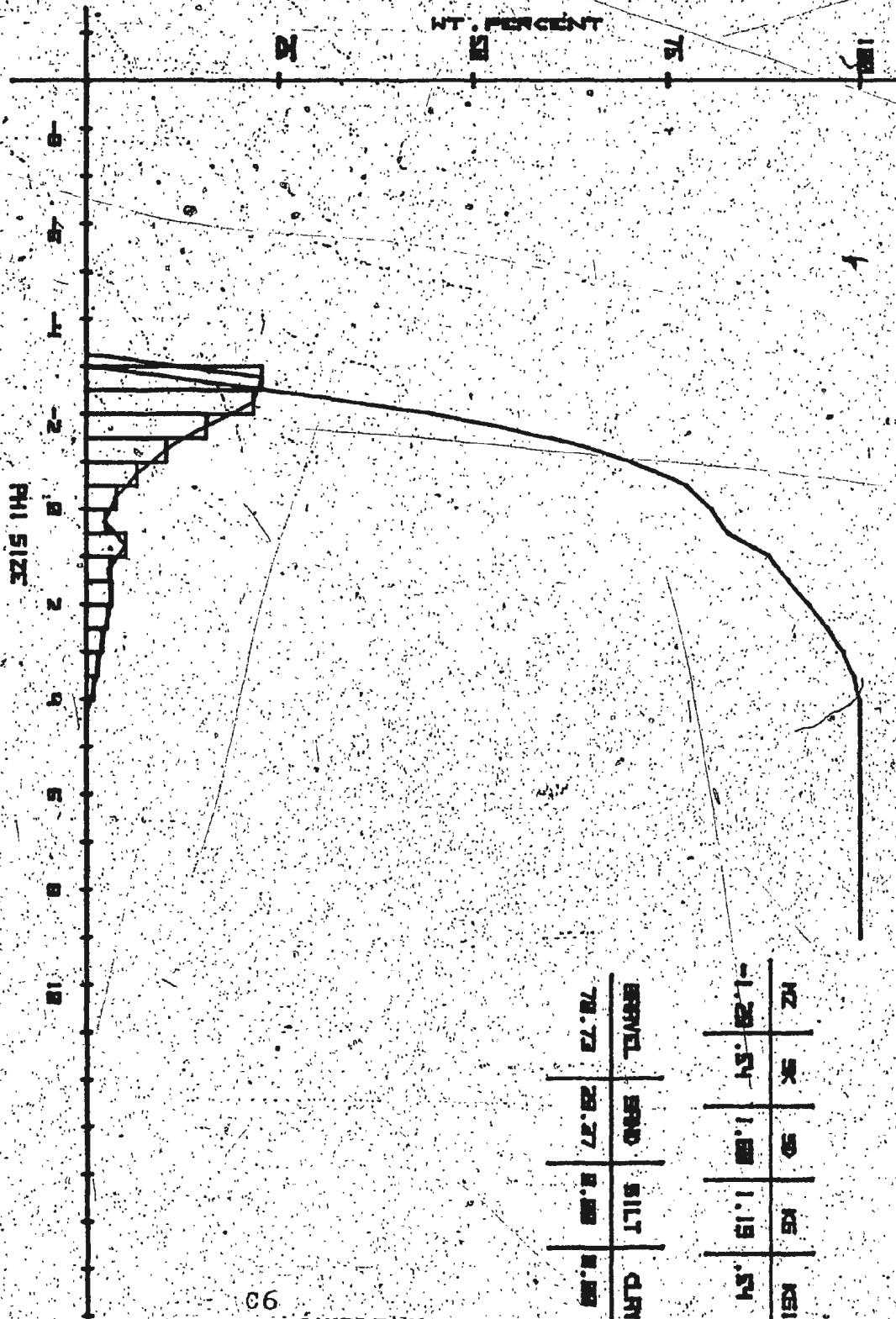
C11



SIZE	5K	10	25	60
WT. PERCENT	1.48	1.42	1.38	1.32

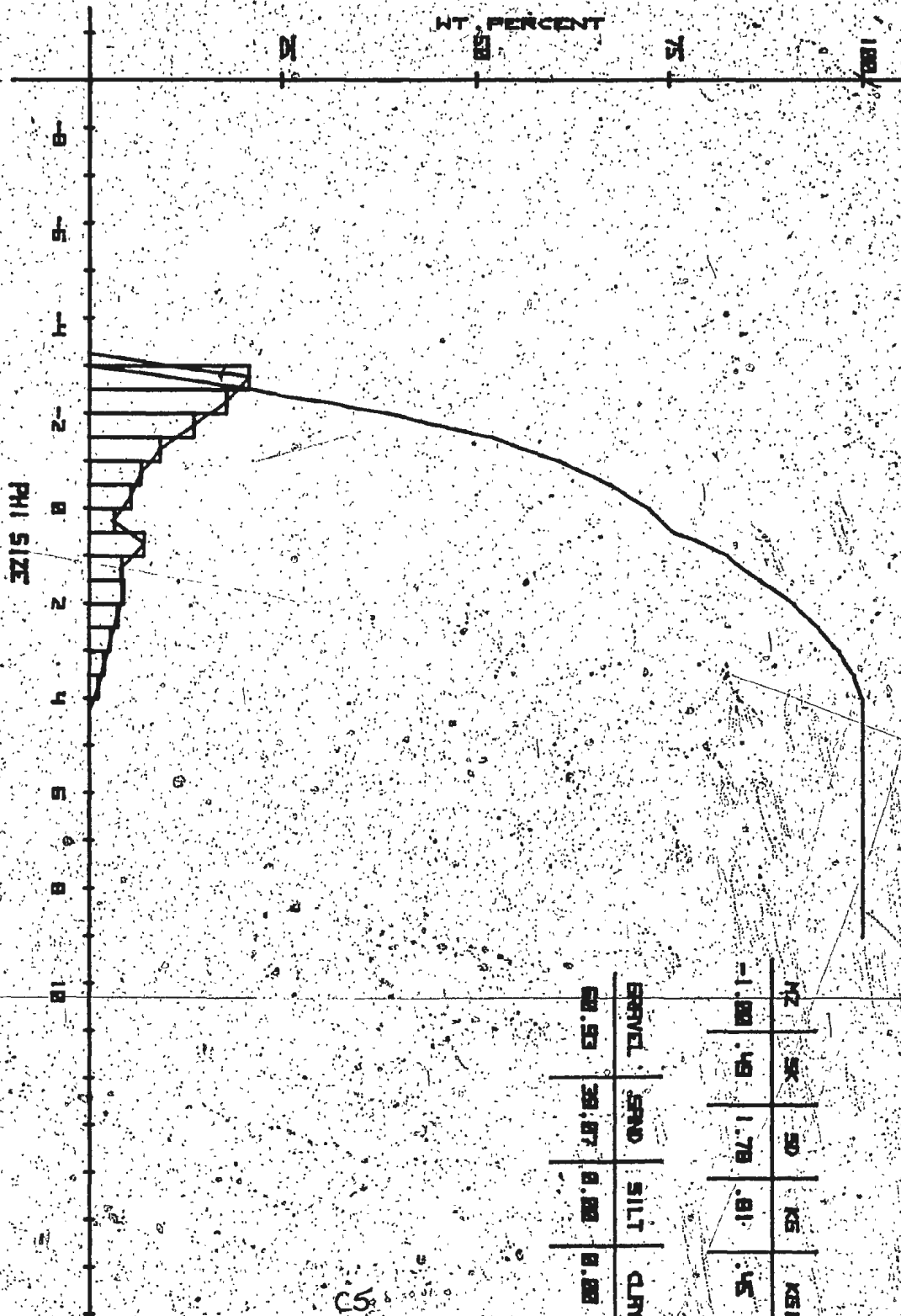
GRAVEL	SAND	SILT	CLAY
78.87	20.13	0.88	0.88

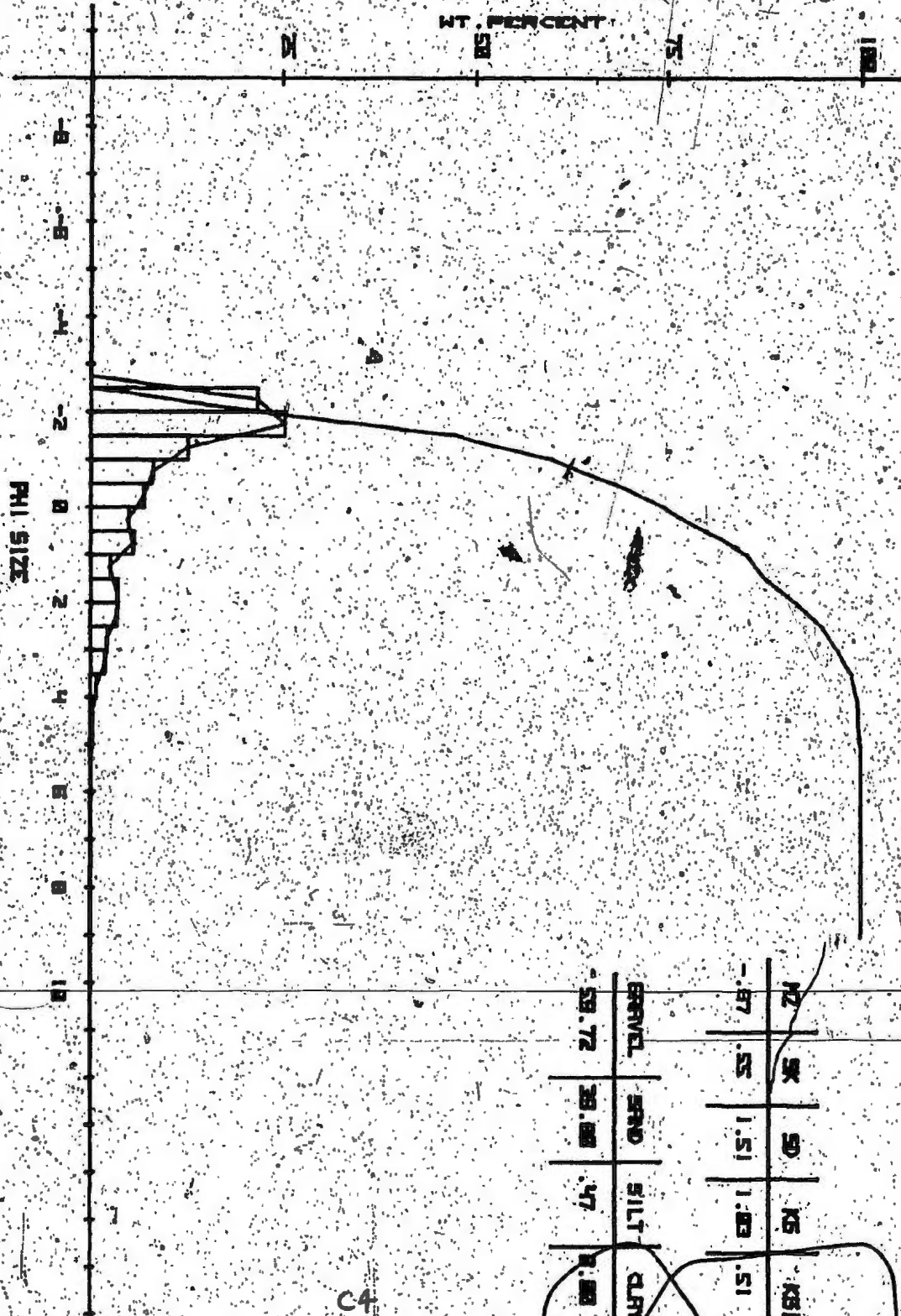
C7



C6
SAMPLE NO.

NO.	SK	SD	KS	KSI
-1.25	.54	1.00	1.19	.54
GRAVEL	SAND	SILT	CLAY	
78.73	20.27	0.00	0.00	



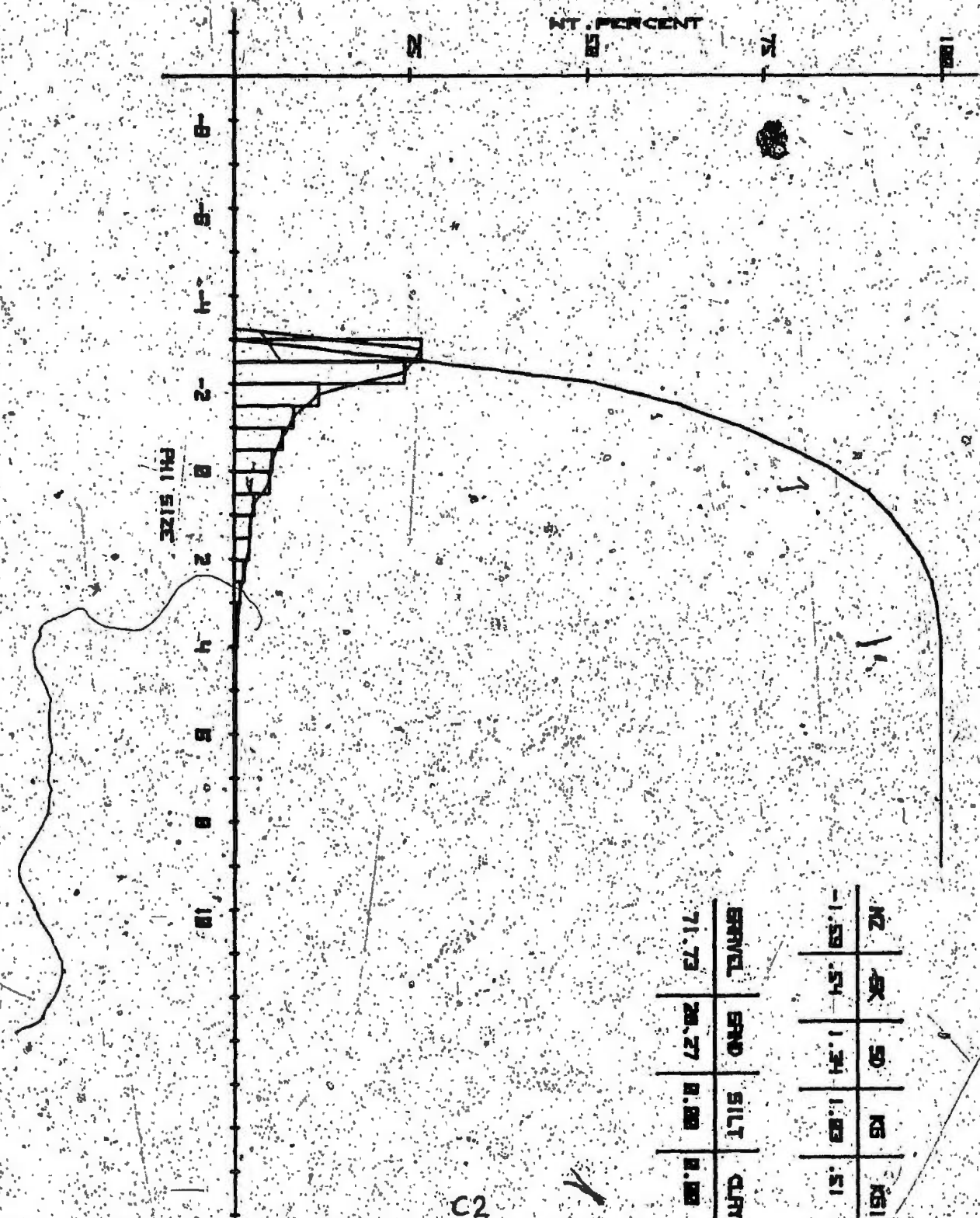


GRAVEL	SAND	SILT	CLAY
59.72	38.88	47	8.88

C4



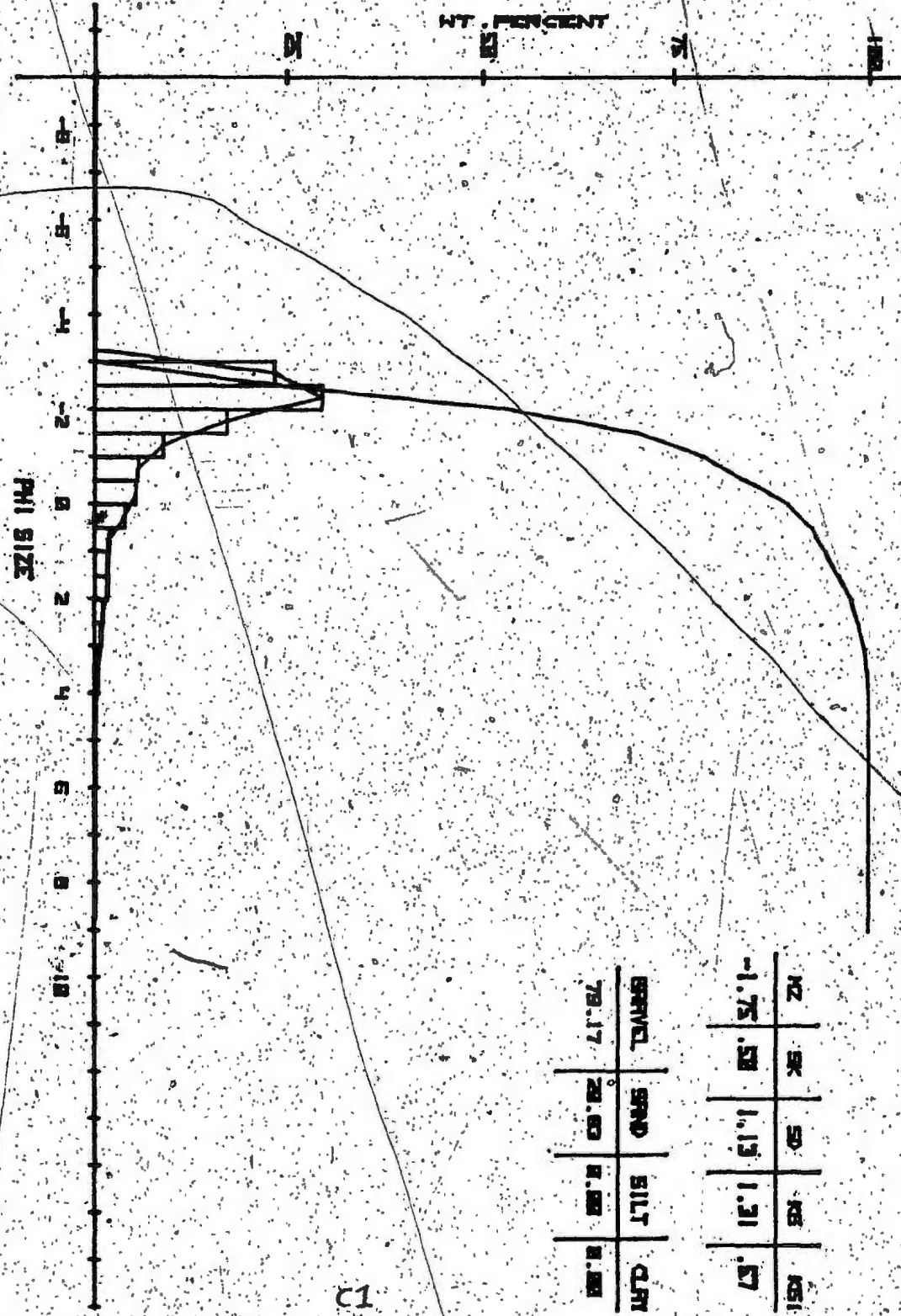
NO.	75	50	25	15
WT. PERCENT	77.49	22.52	0.00	0.00



WT	CL	SH	MS	GS
1.00	5.1	1.00	1.71	1.00

SAND	SILT	CLAY
71.73	28.27	0.00

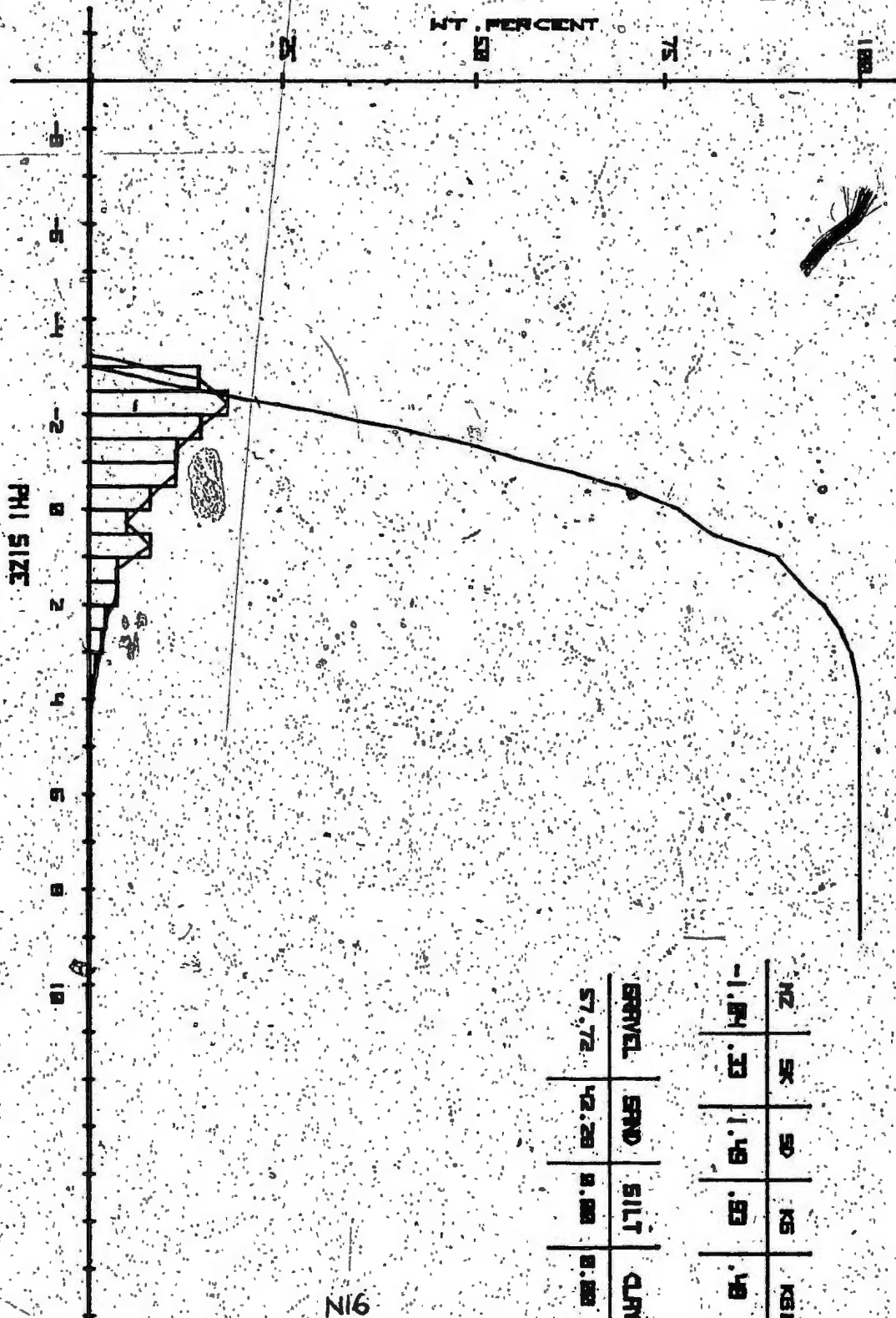
C2

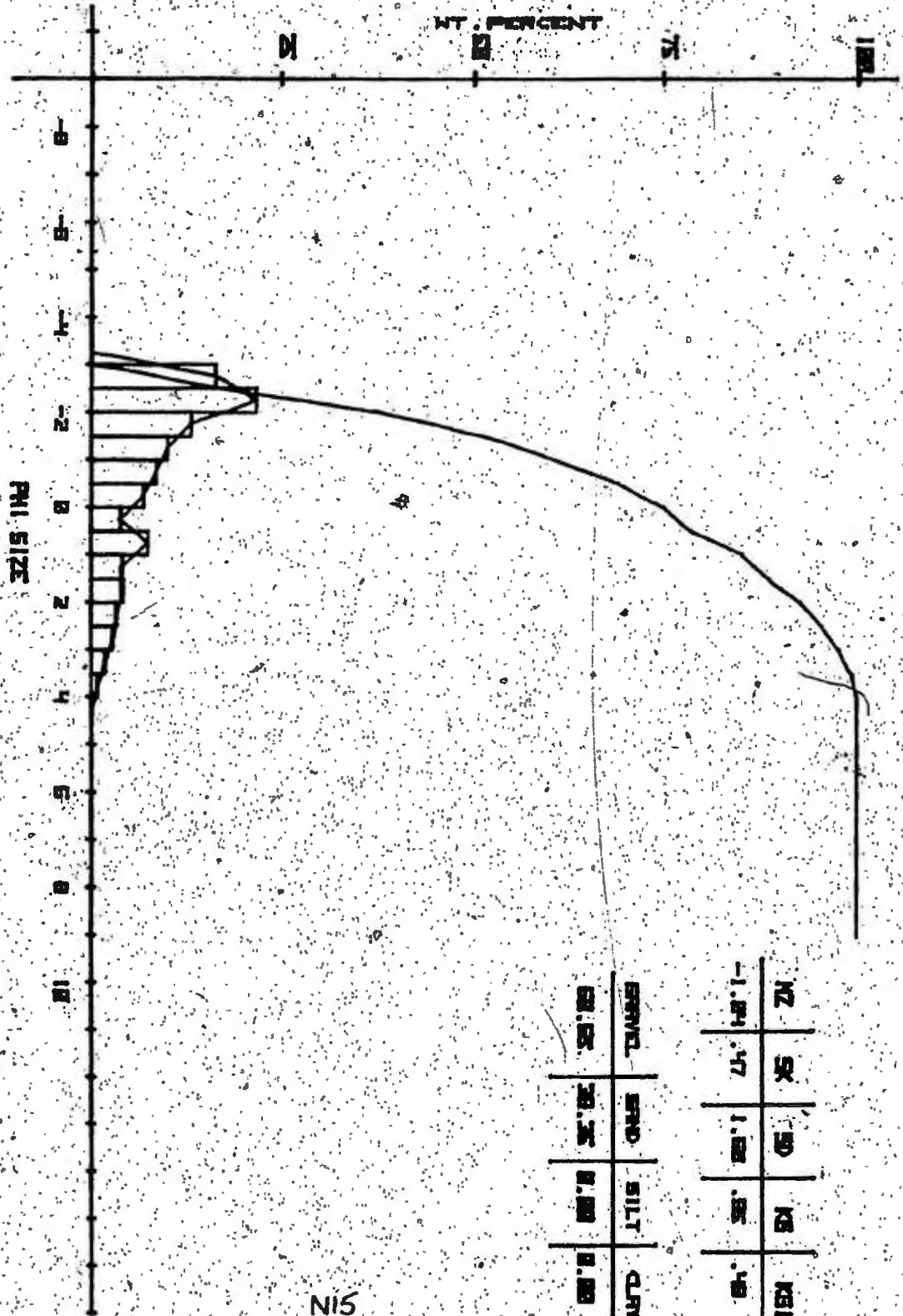


FZ	SK	SD	FS	FI
-1.75	.50	1.13	1.31	.57

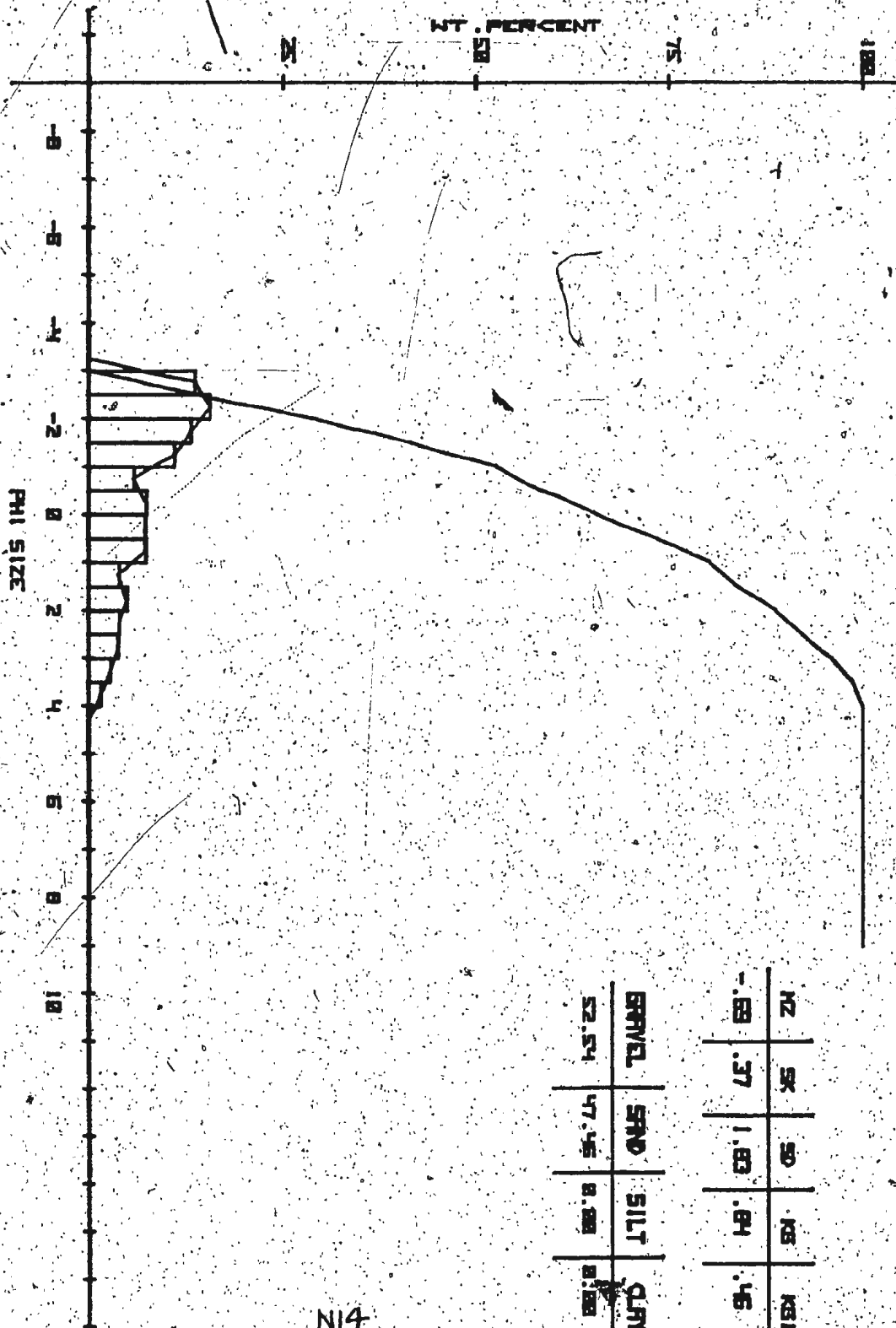
GRAVEL	SAND	SILT	CLAY
78.17	20.00	0.00	0.00

12

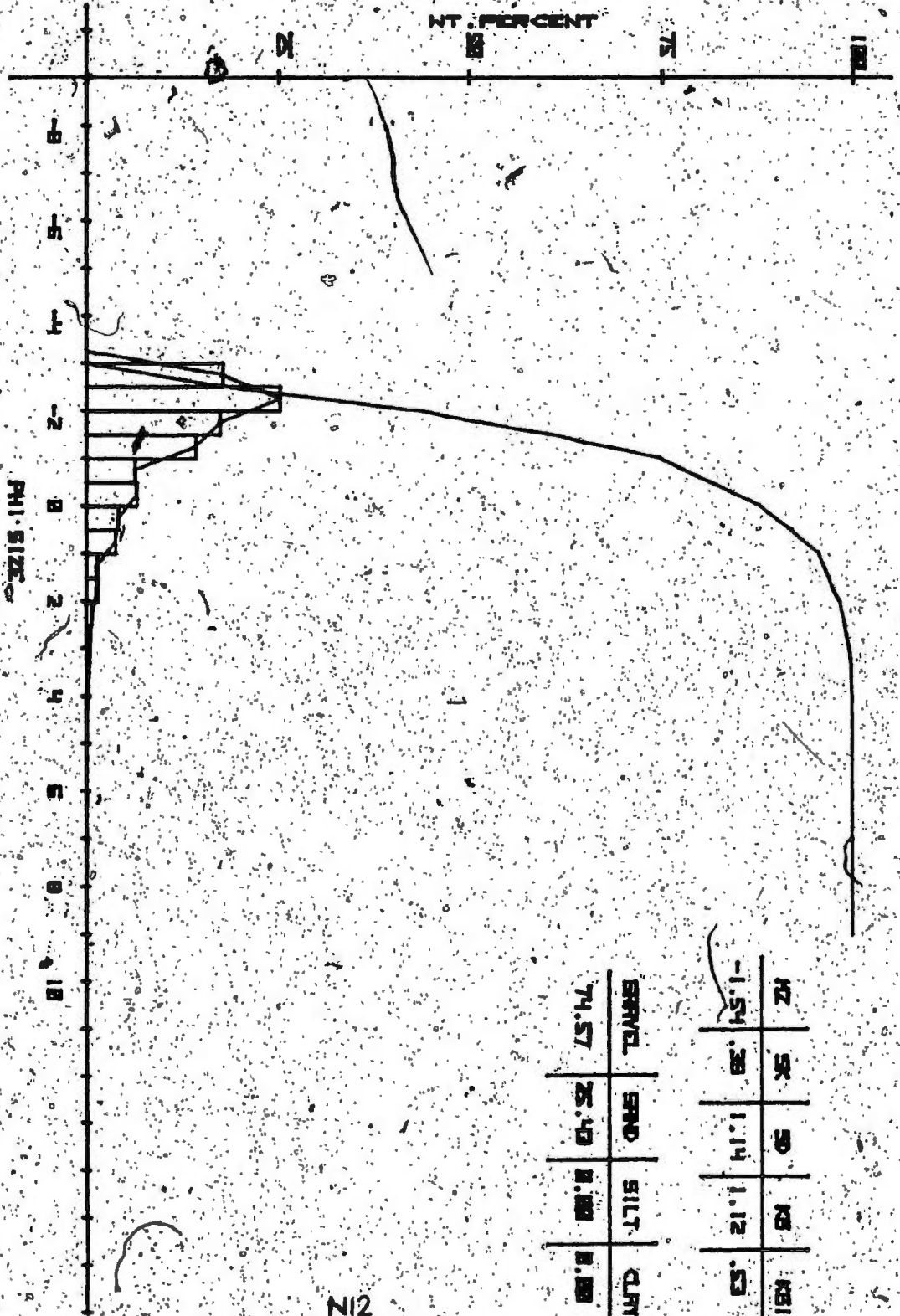




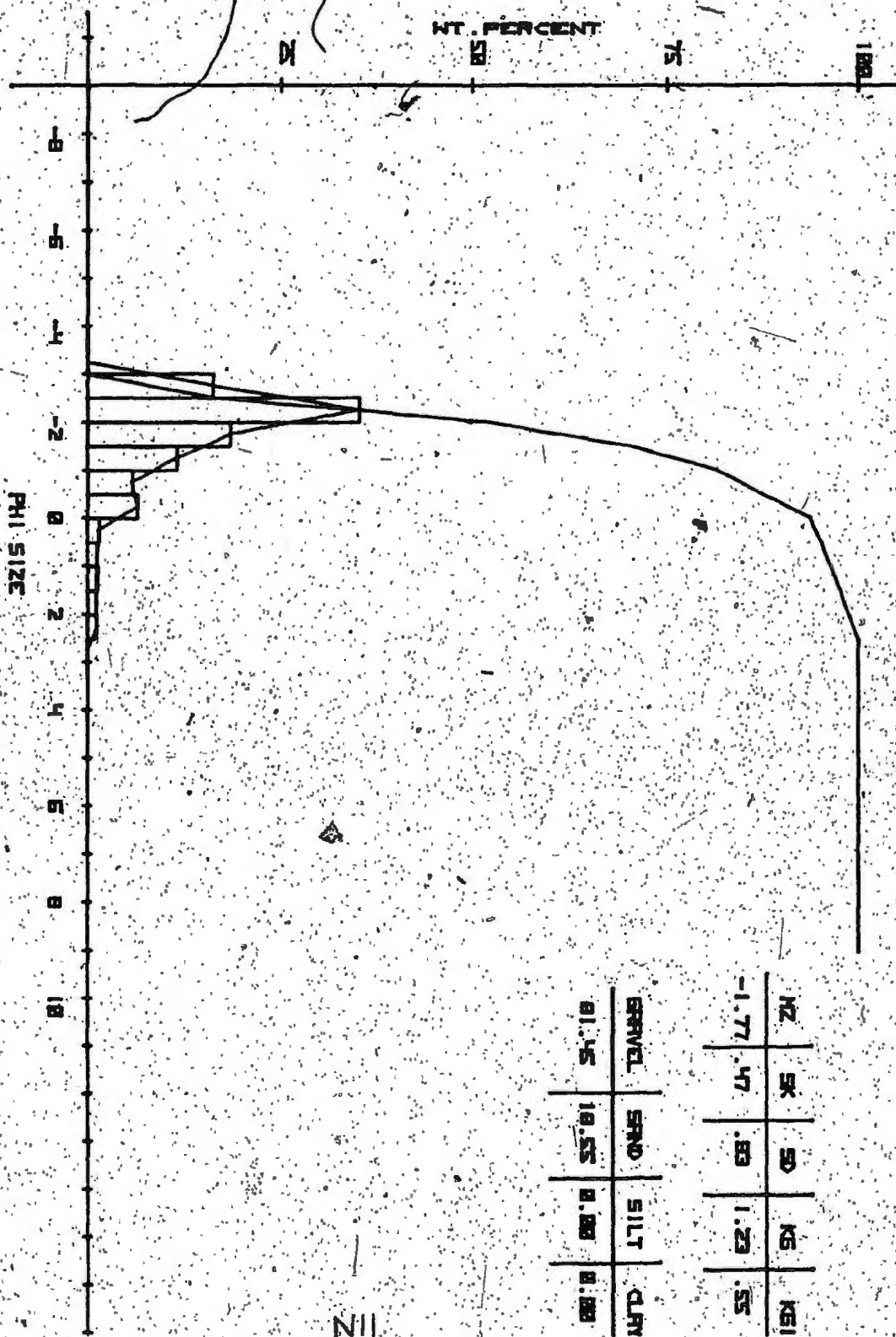
N15

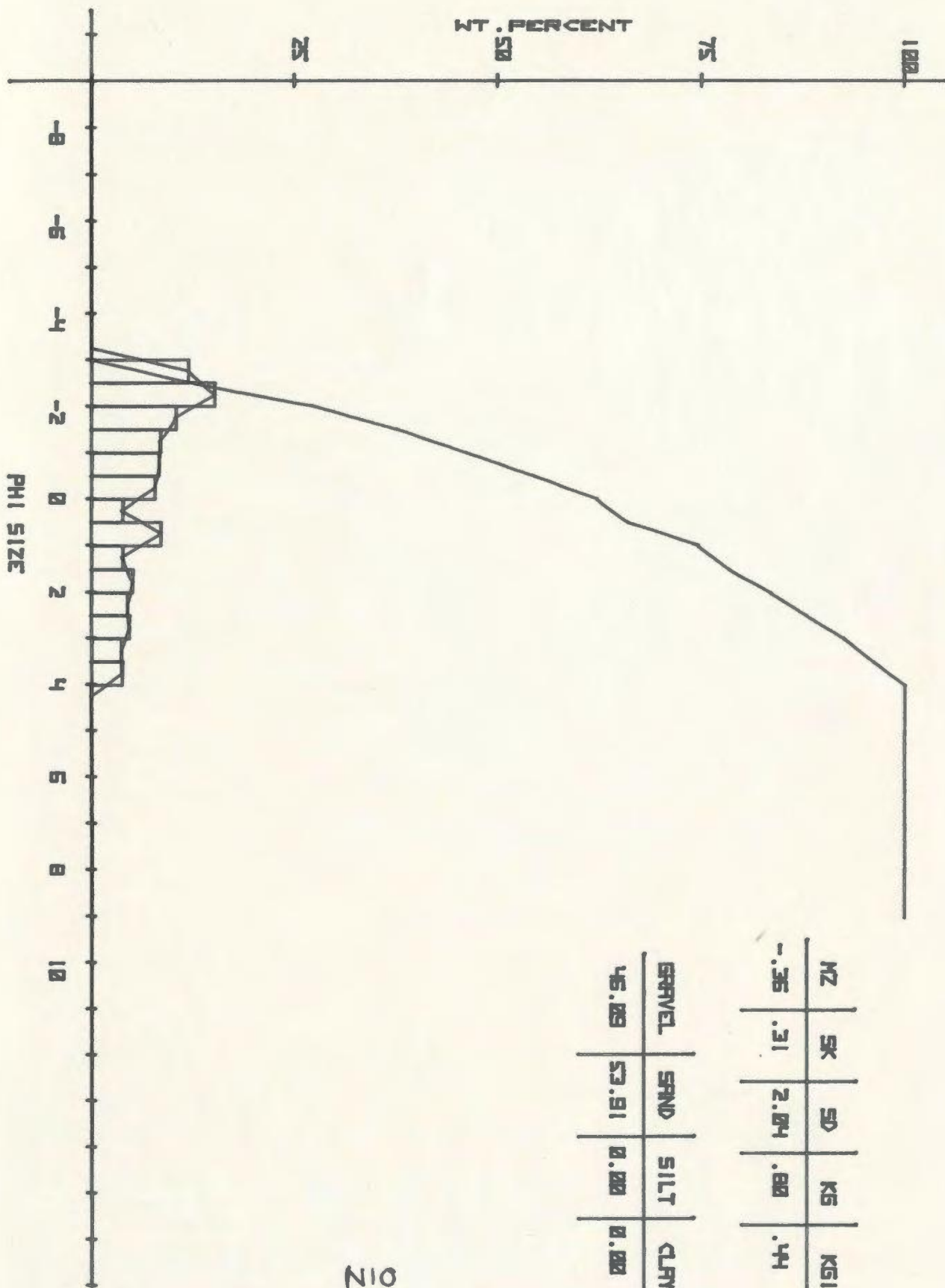


N14

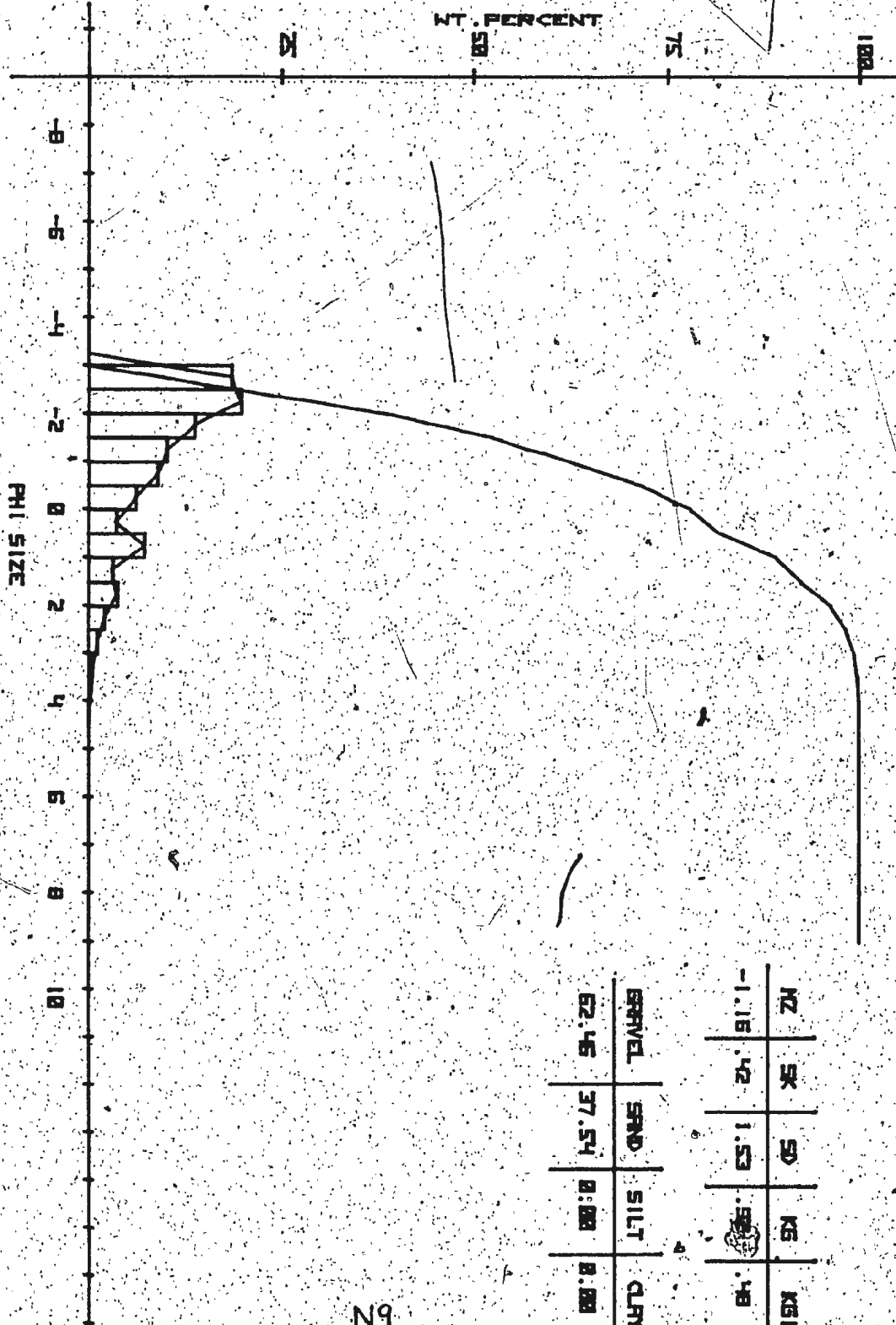


N12



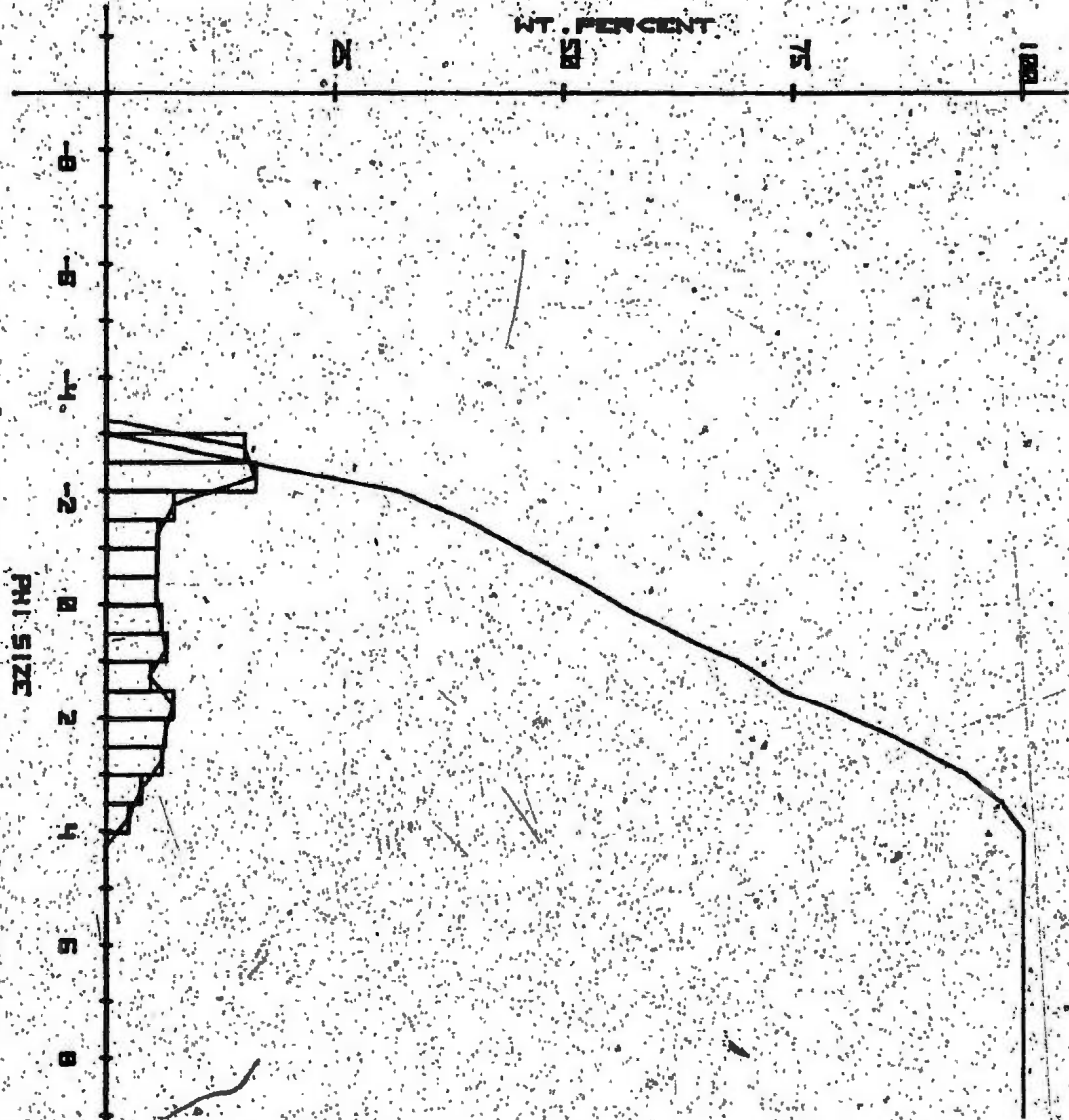


210



WZ	SK	SD	KS	KS1
-1.16	.42	1.53	0.00	.48

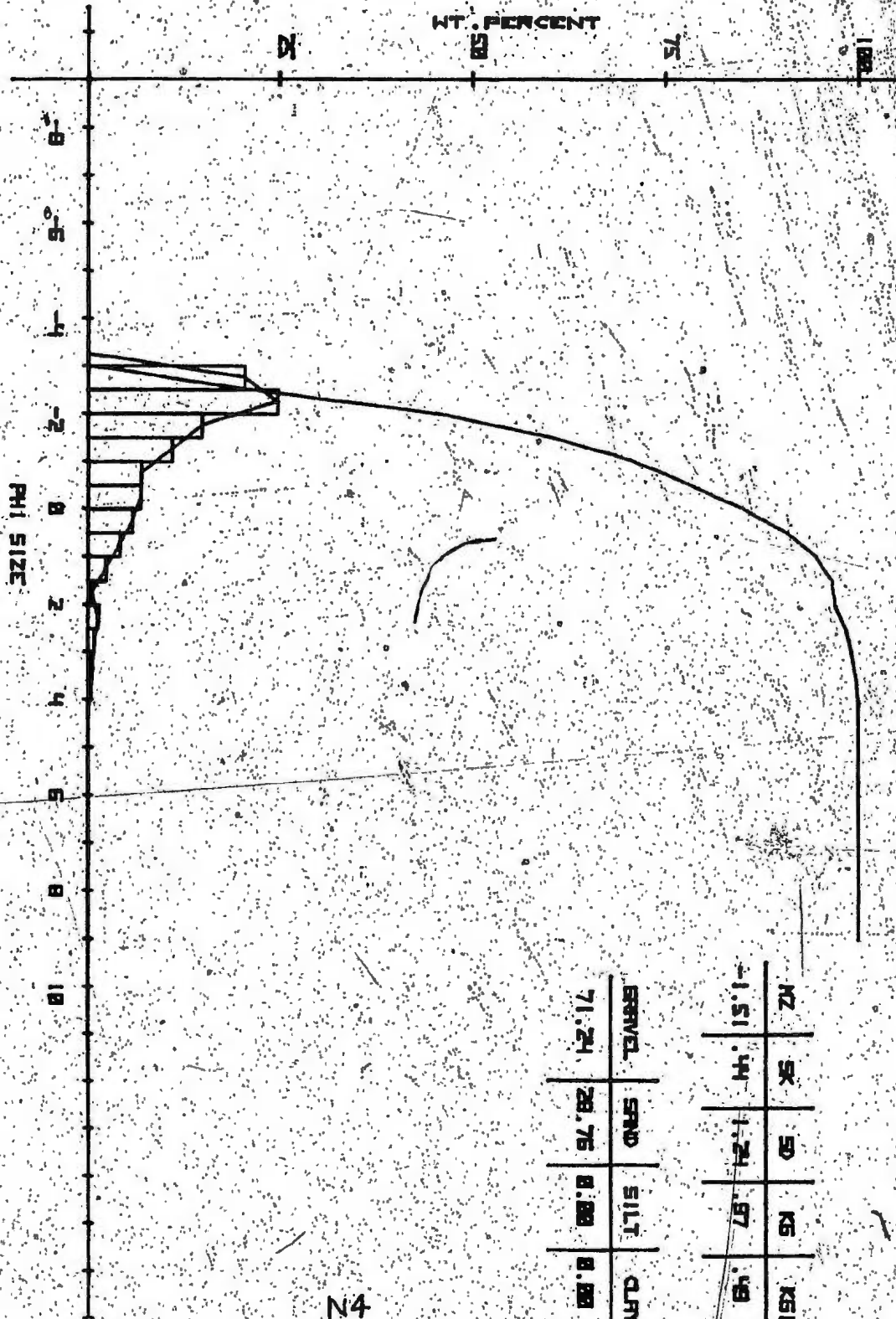
N9

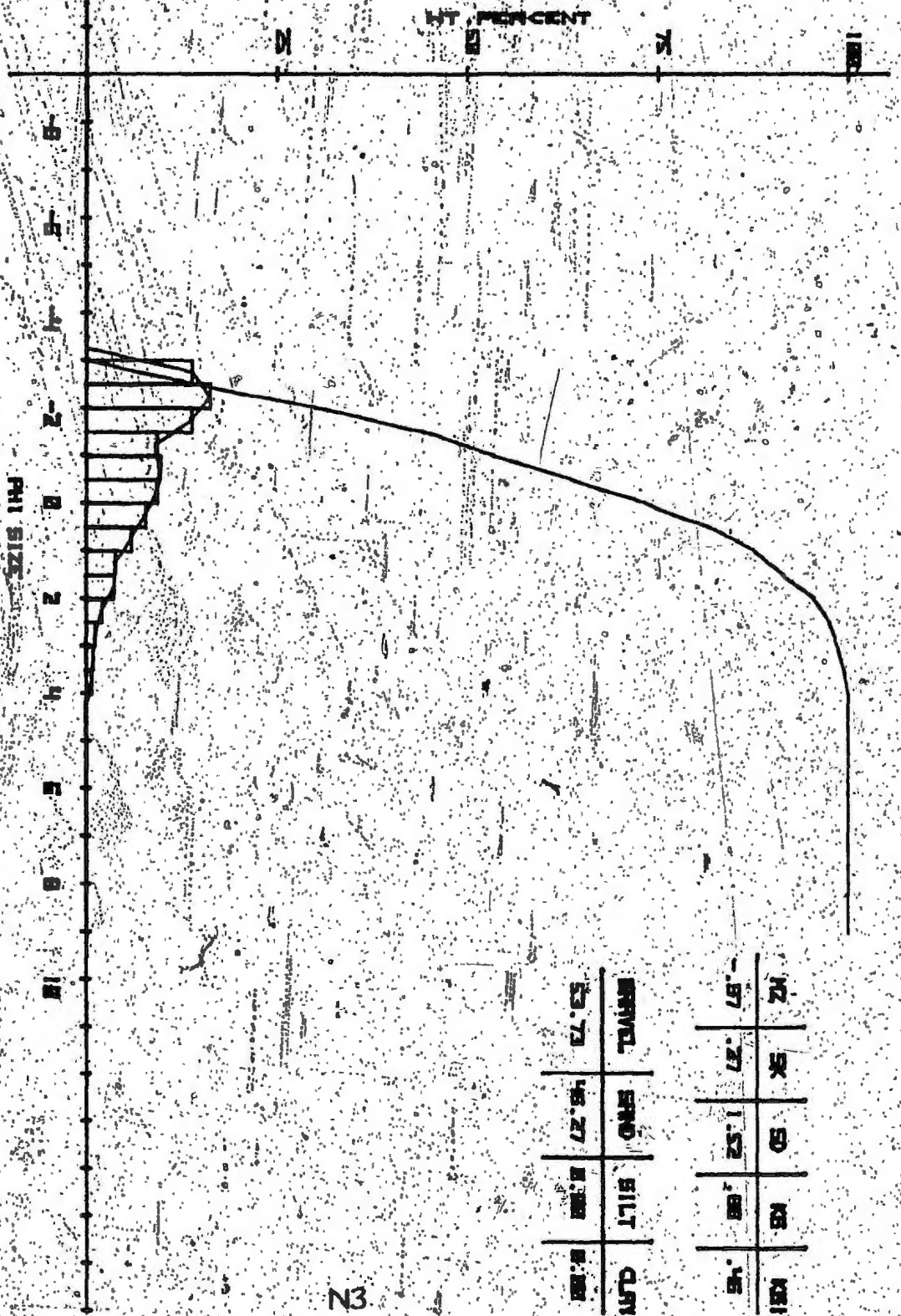


NZ	SK	SD	KS	KSI
-.27	.21	2.00	.05	.30

GRAVEL	SAND	SILT	CLAY
45.00	54.04	0.00	0.00

LN





N2	N5	D	S	KL
.57	.27	1.52	.88	.45

GRAVEL	SAND	SILT	CLAY
53.73	45.27	0.308	0.108

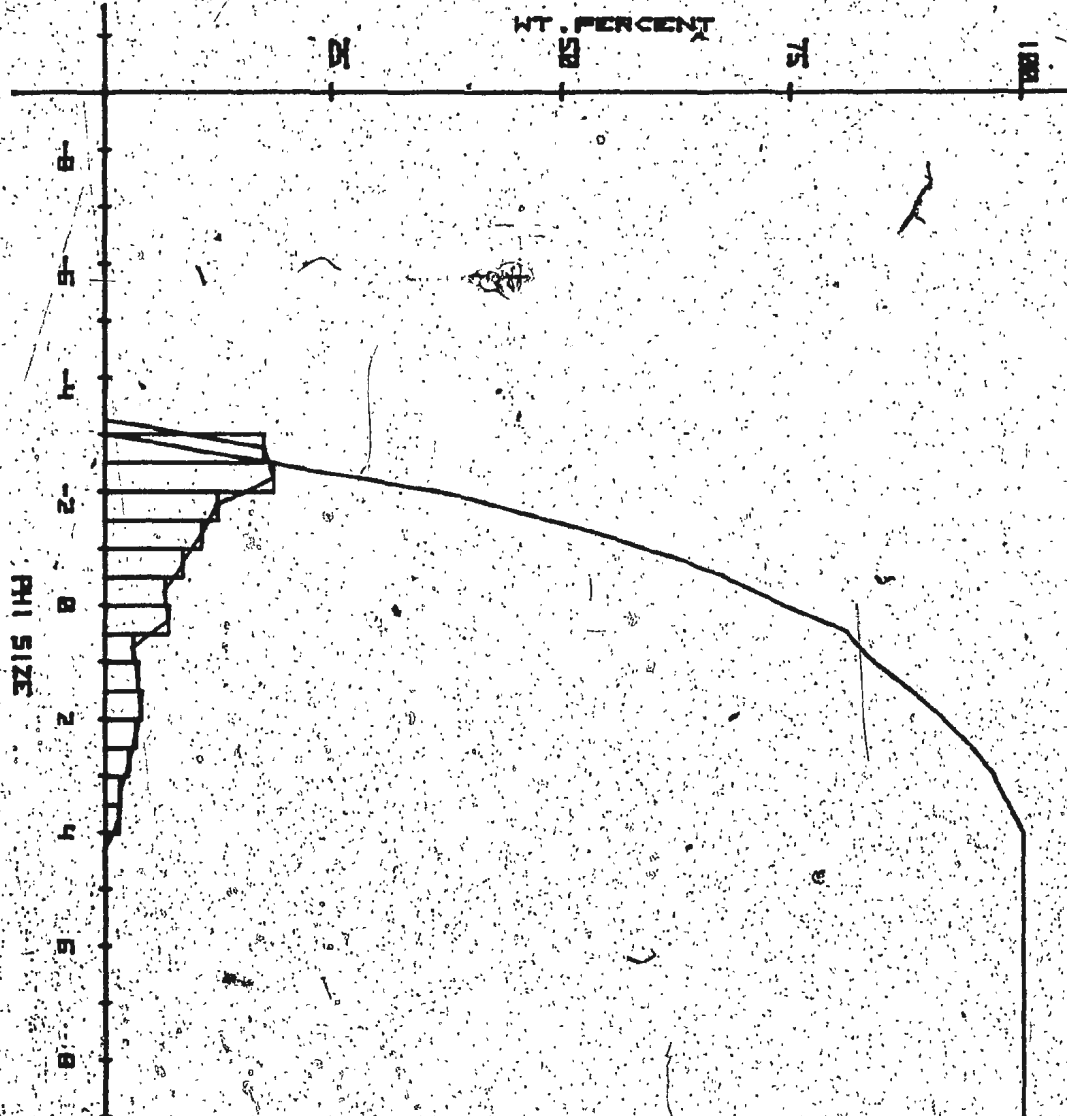
N3



N2

NZ	SK	SD	KS	KS1
1.58	.42	1.29	1.86	.51

GRAVEL	SAND	SILT	CLAY
72.33	27.67	0.00	0.00



NZ	SK	SD	KS	KSI
-.98	.42	1.71	.94	.49

SAND	SAND	SILT	CLAY
50.83	41.17	8.88	0.88

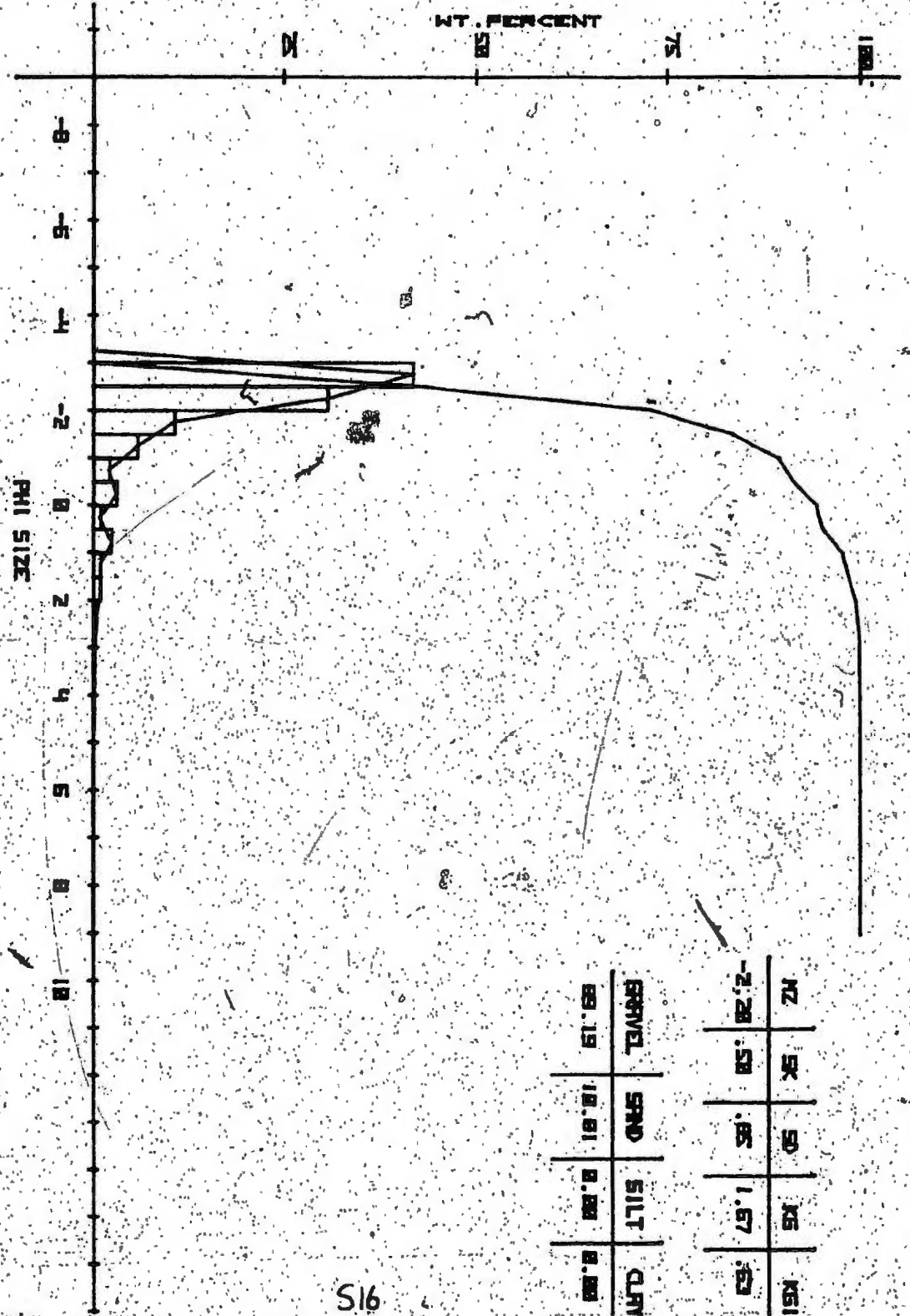
12

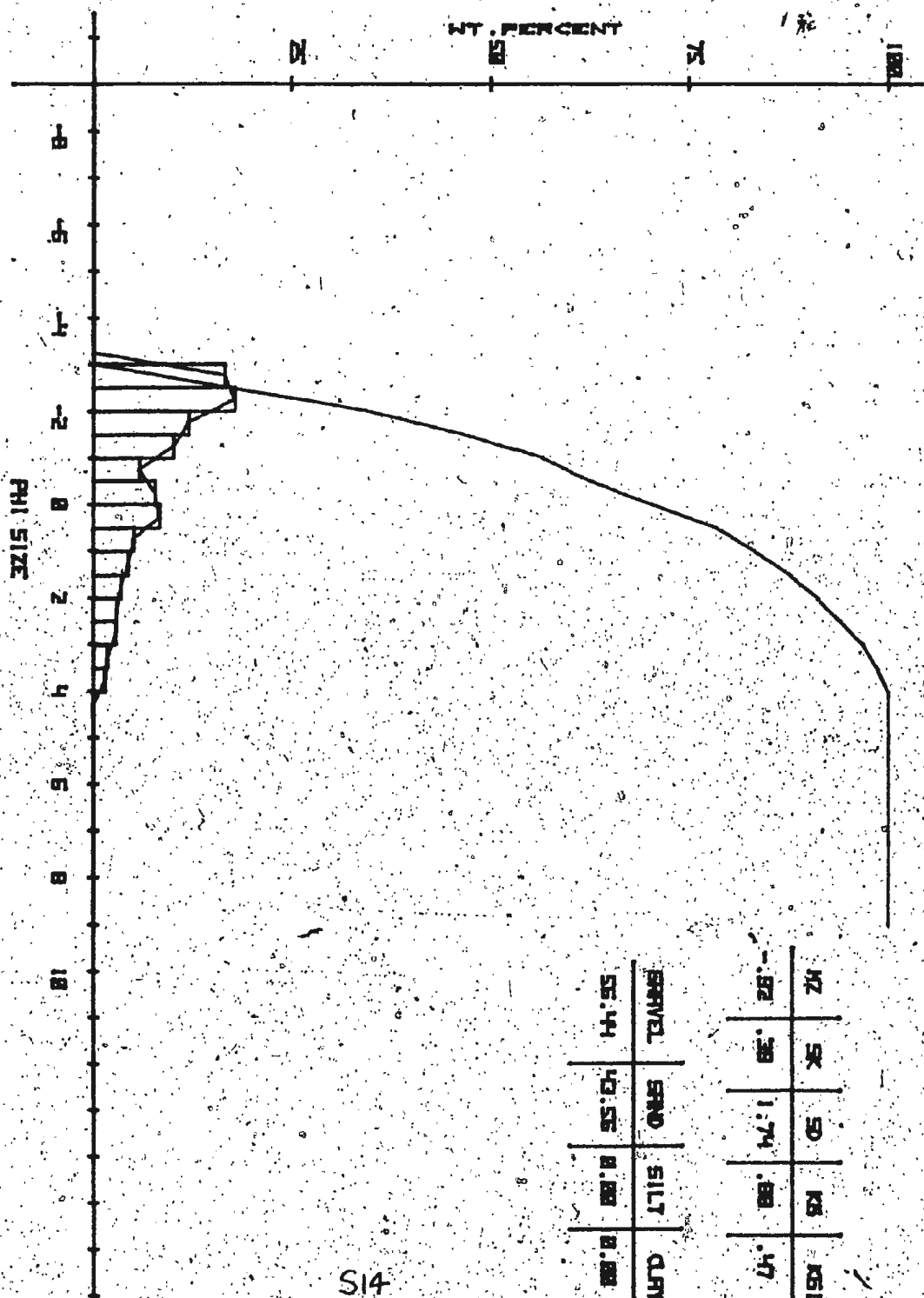
WZ	SK	SD	KG	KG1
1.46	.62	1.53	1.17	.54

GRAVEL	SAND	SILT	CLAY
72.48	27.52	0.00	0.00

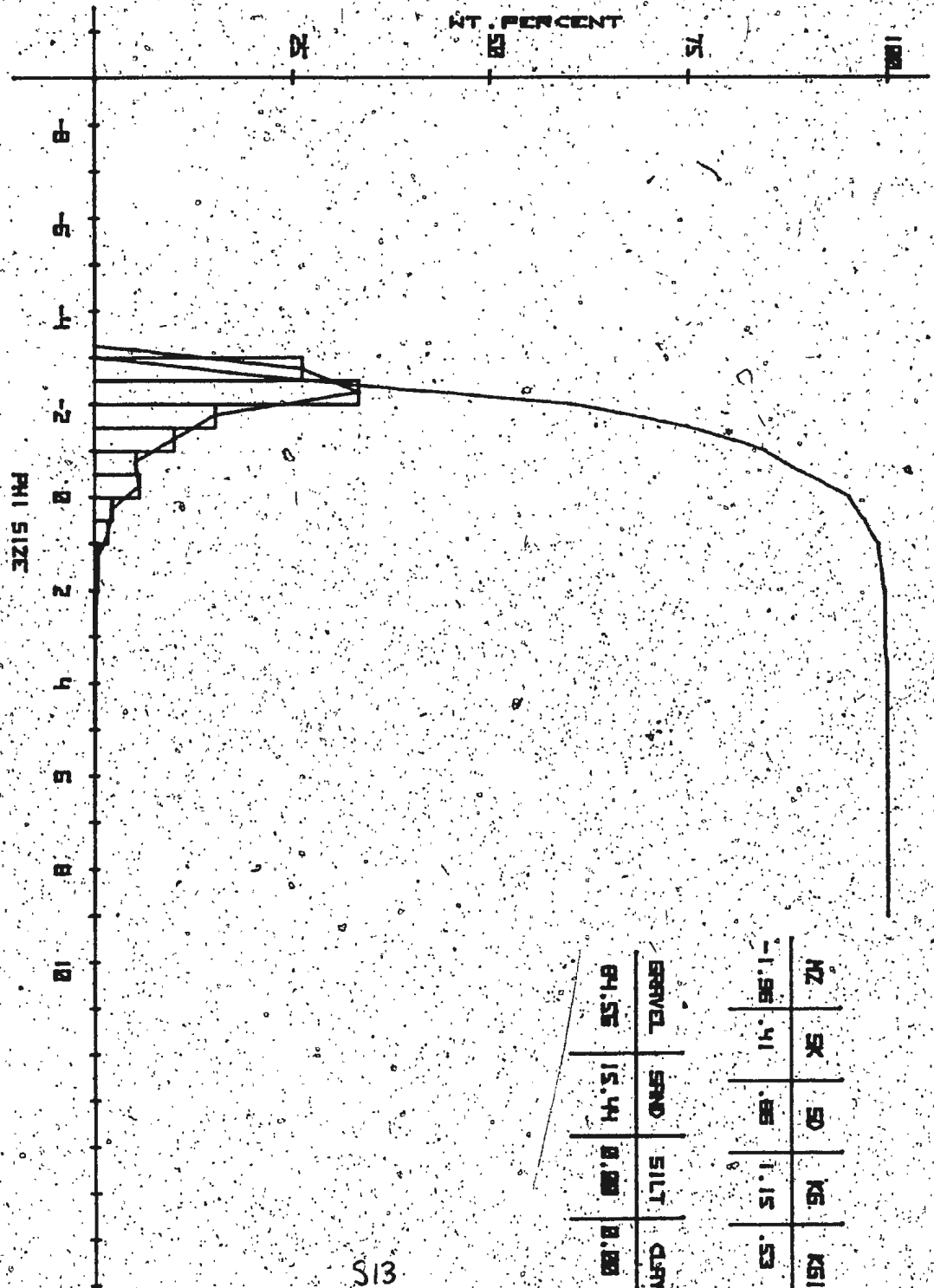
S17



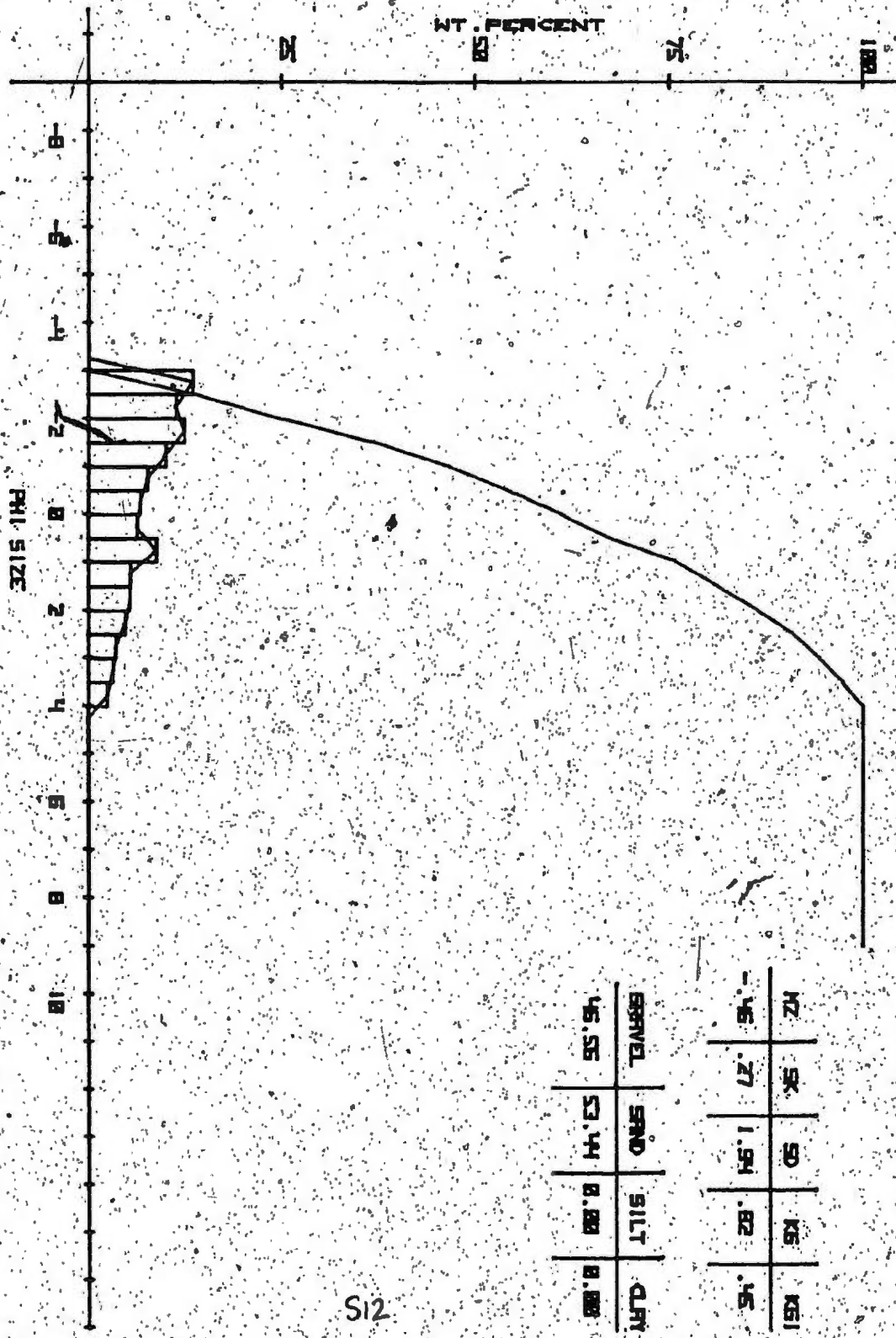




S14

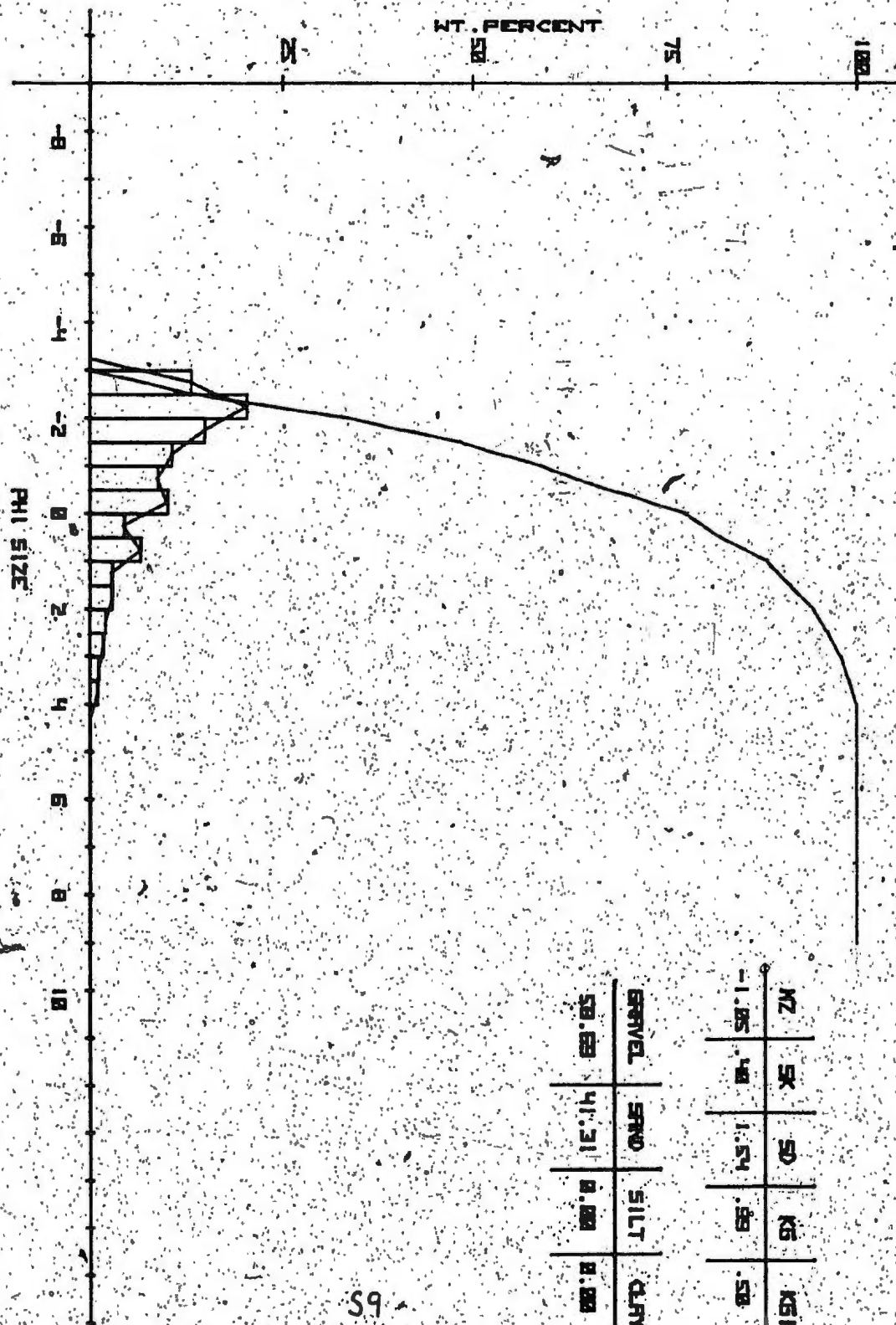


WZ	SK	SD	KS	KS1
-1.06	.41	.06	1.15	.53



NZ	SK	SD	K5	K51
15	27	1.54	.62	.15

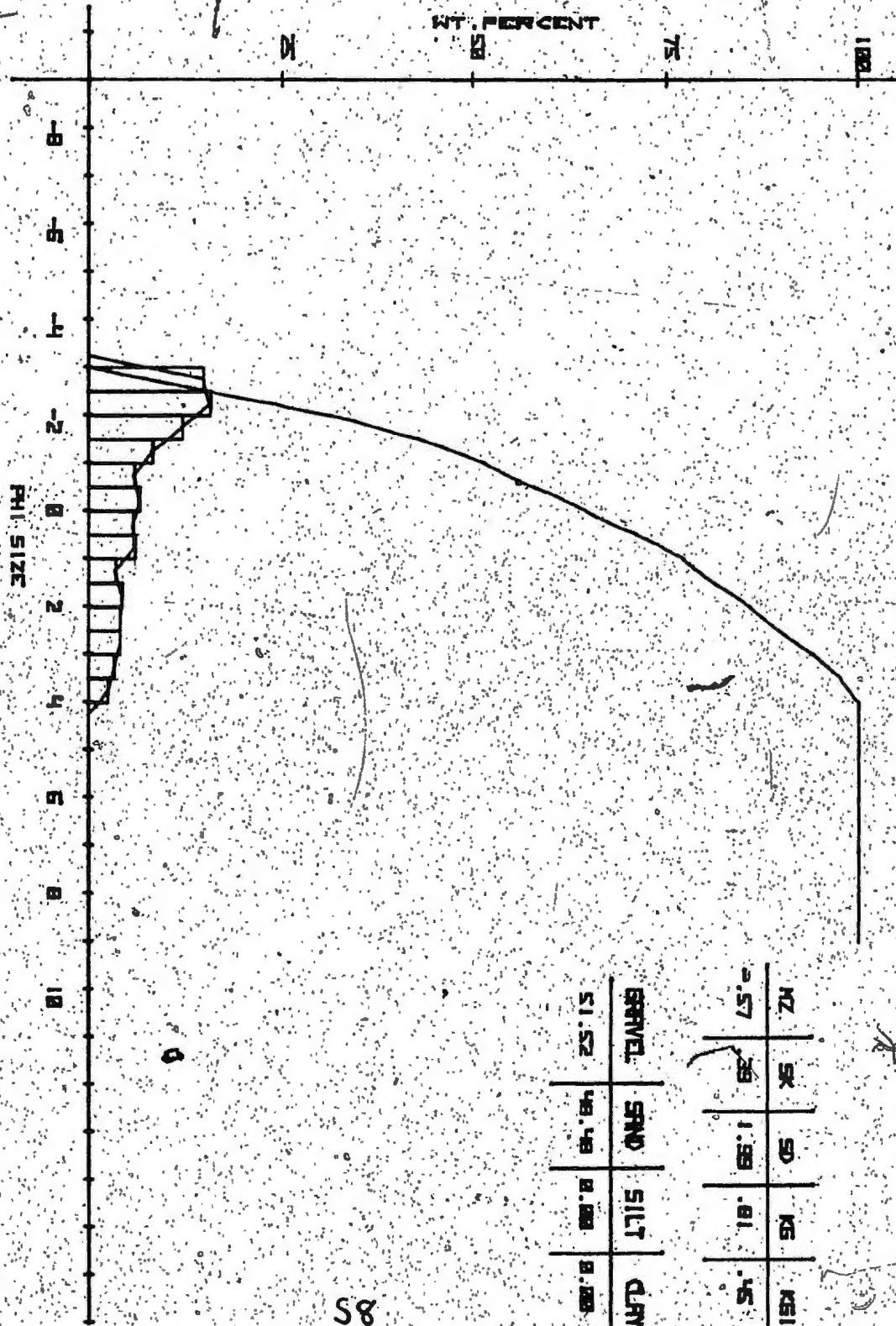
GRAVEL	SAND	SILT	CLAY
45.55	53.44	0.00	0.00



NZ	SK	SD	KB	KB1
1.05	1.0	1.54	0.59	0.58

GRAVEL	SAND	SILT	CLAY
0.03	41.31	0.00	0.00

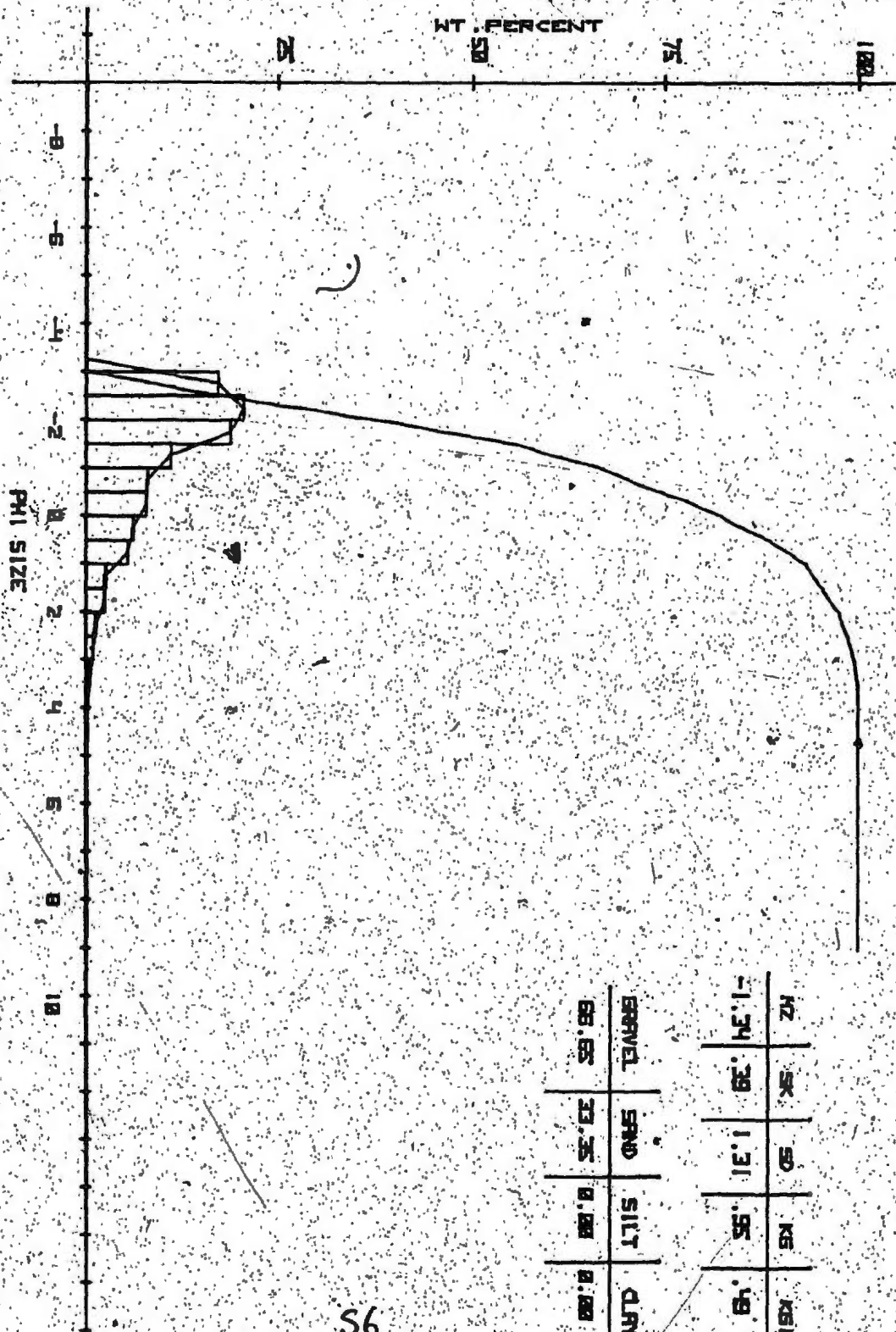
59

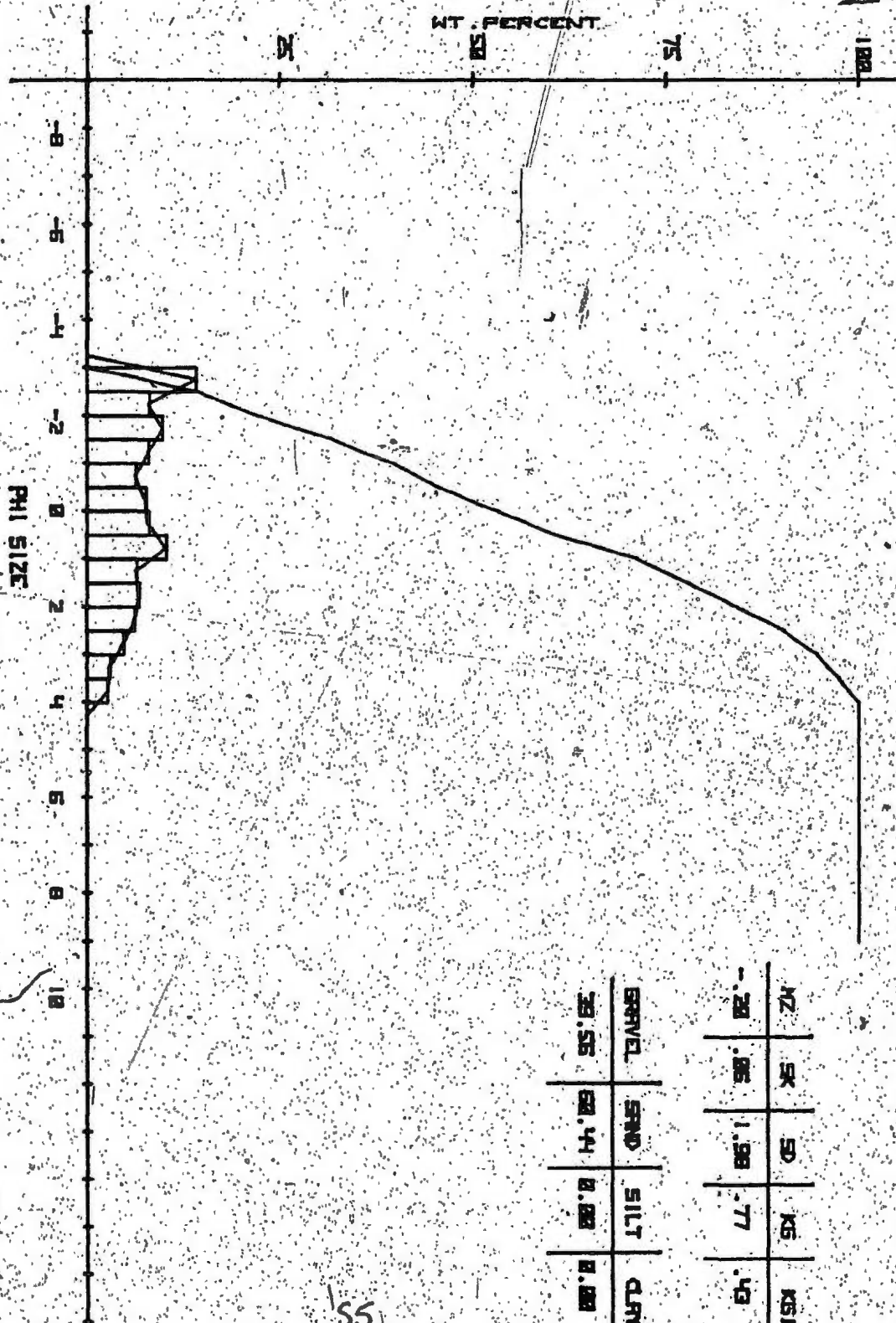


NO.	5K	5D	5G	5H
1	1.57	1.99	0.81	0.45

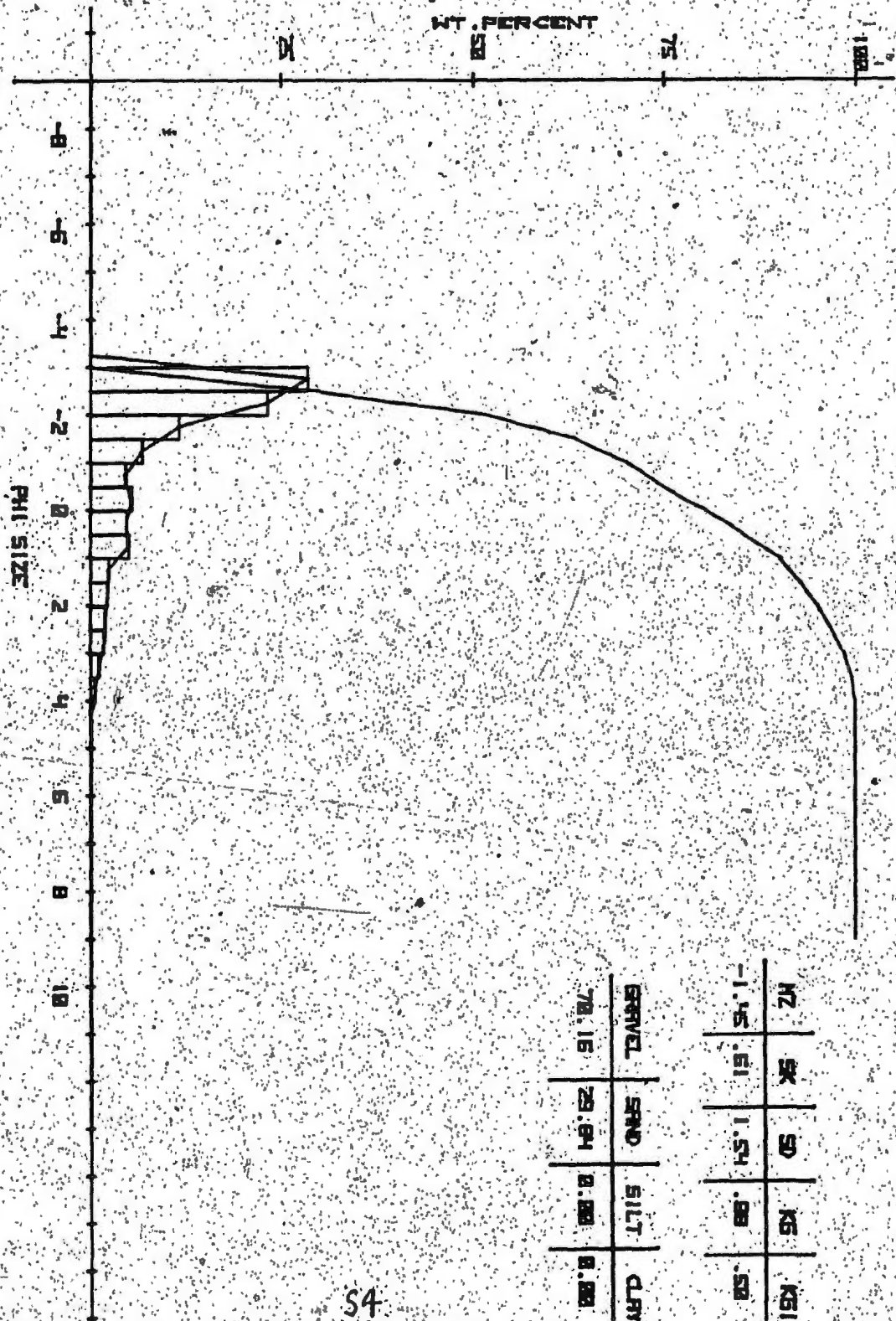
GRAVEL	SAND	SILT	CLAY
51.52	48.48	0.00	0.00

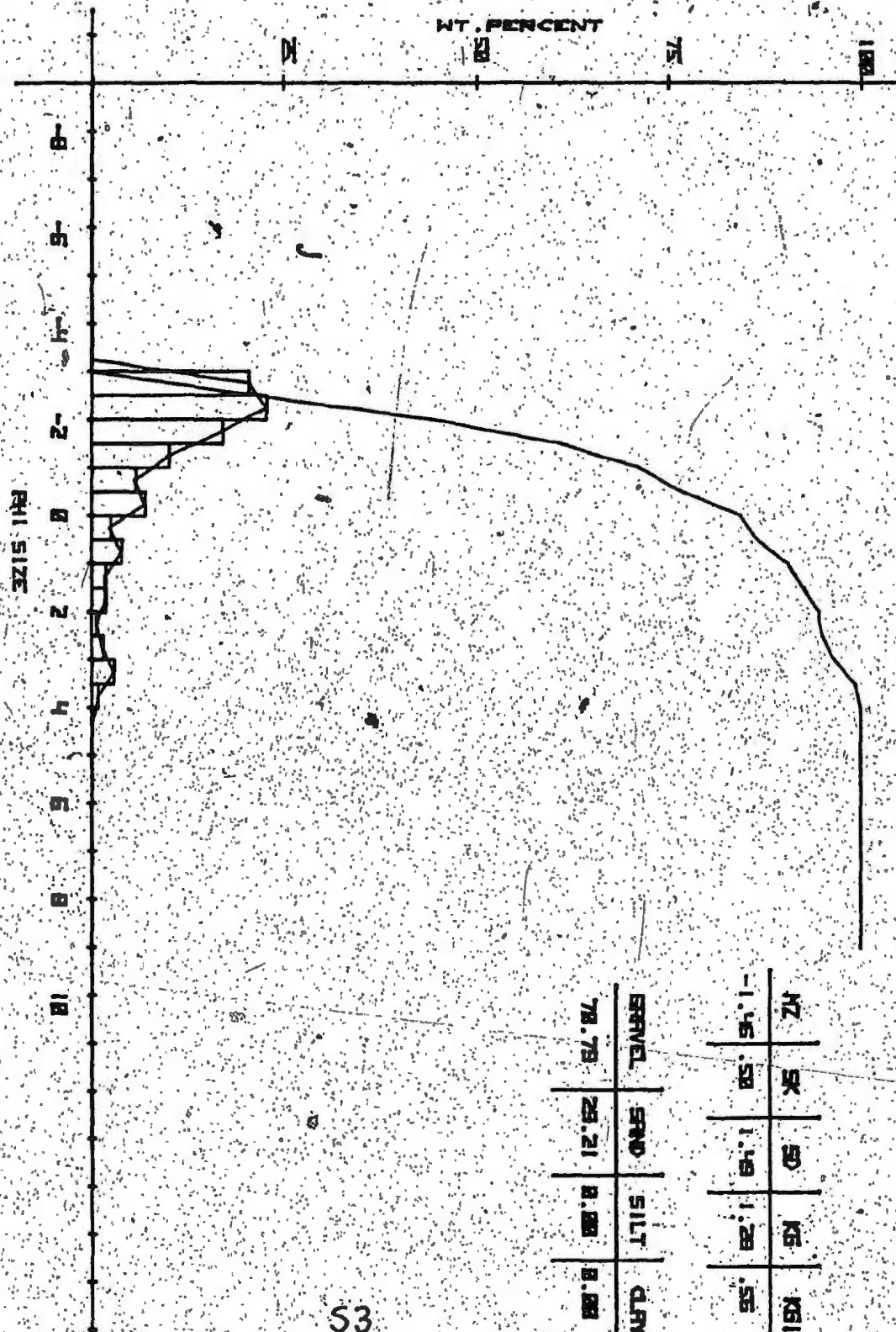
85



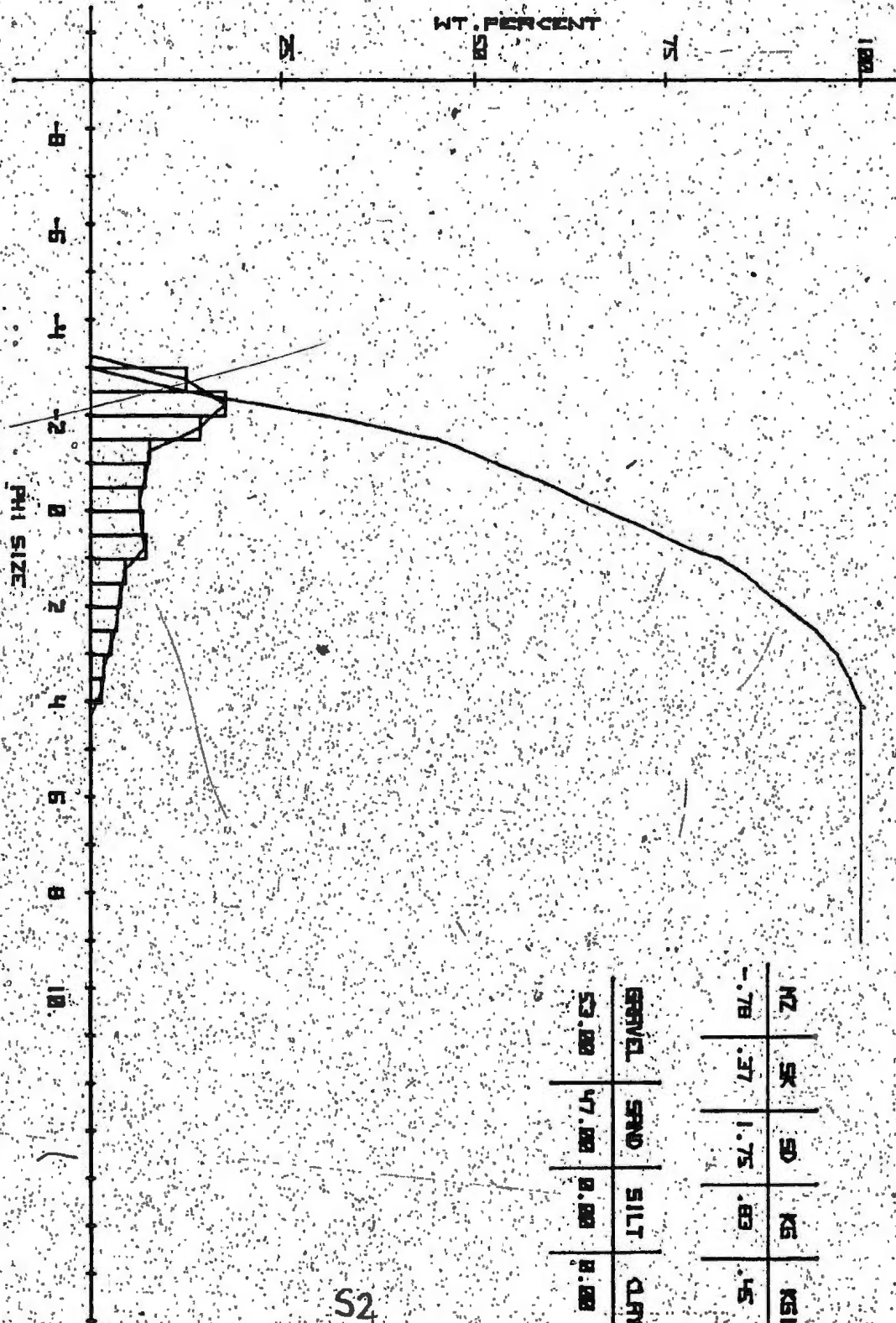


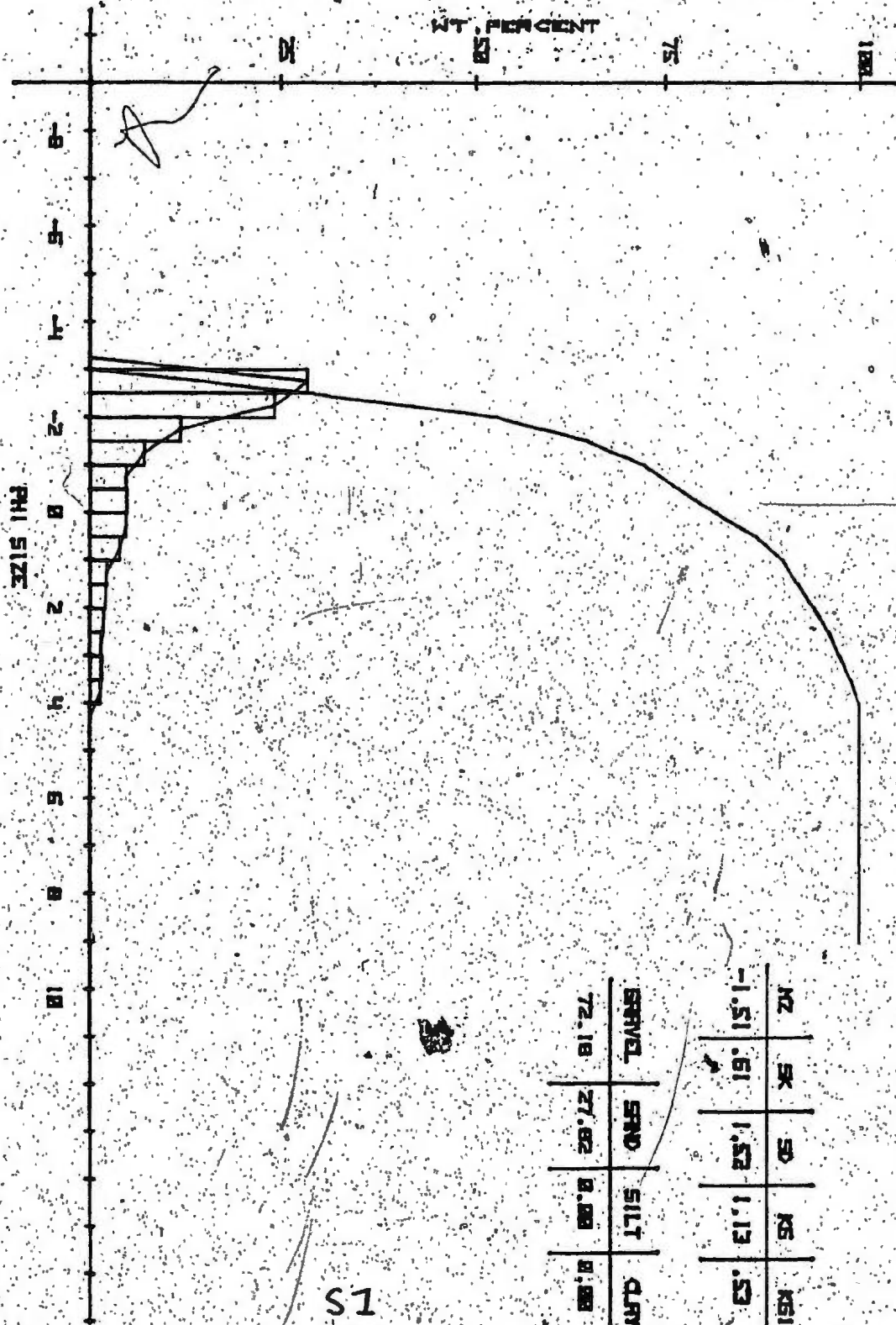
SS





42	5K	5D	KS	KS1
-1.45	.50	1.49	1.28	.55





NO.	5K	50	100	200
WT. PERCENT	1.51	1.52	1.13	0.53
GRAVEL	72.18	27.82	0.00	0.00
SAND				
SILT				
CLAY				

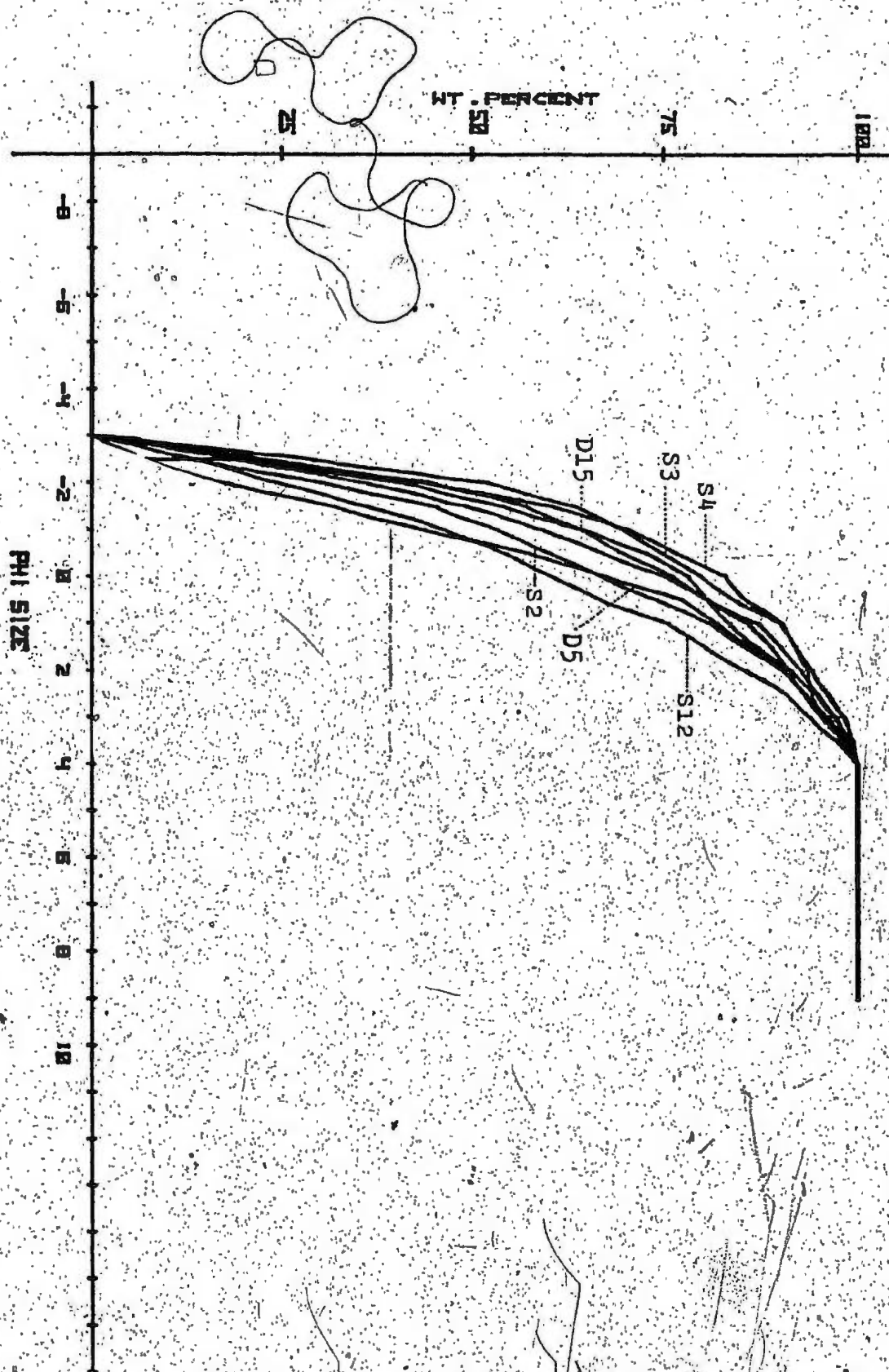


Figure 52. Berendon Glacier; debris samples collected from medial moraine SIV. Parent bedrock is volcanic conglomerate of the Hazleton assemblage.

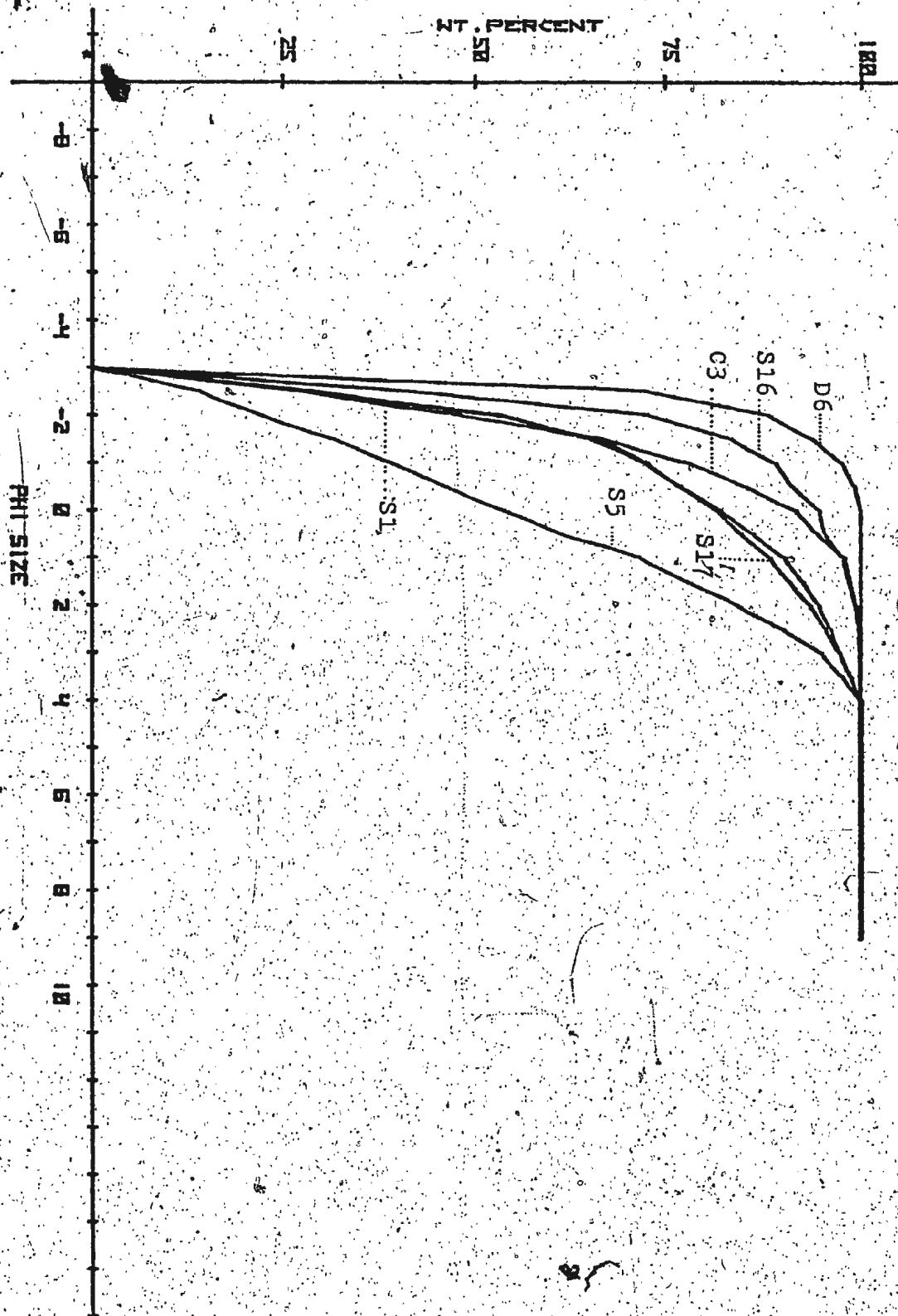


Figure 53. Berendon Glacier; debris samples collected from medial moraines SI and SII; Parent bedrock is tuff of the Hazleton assemblage.

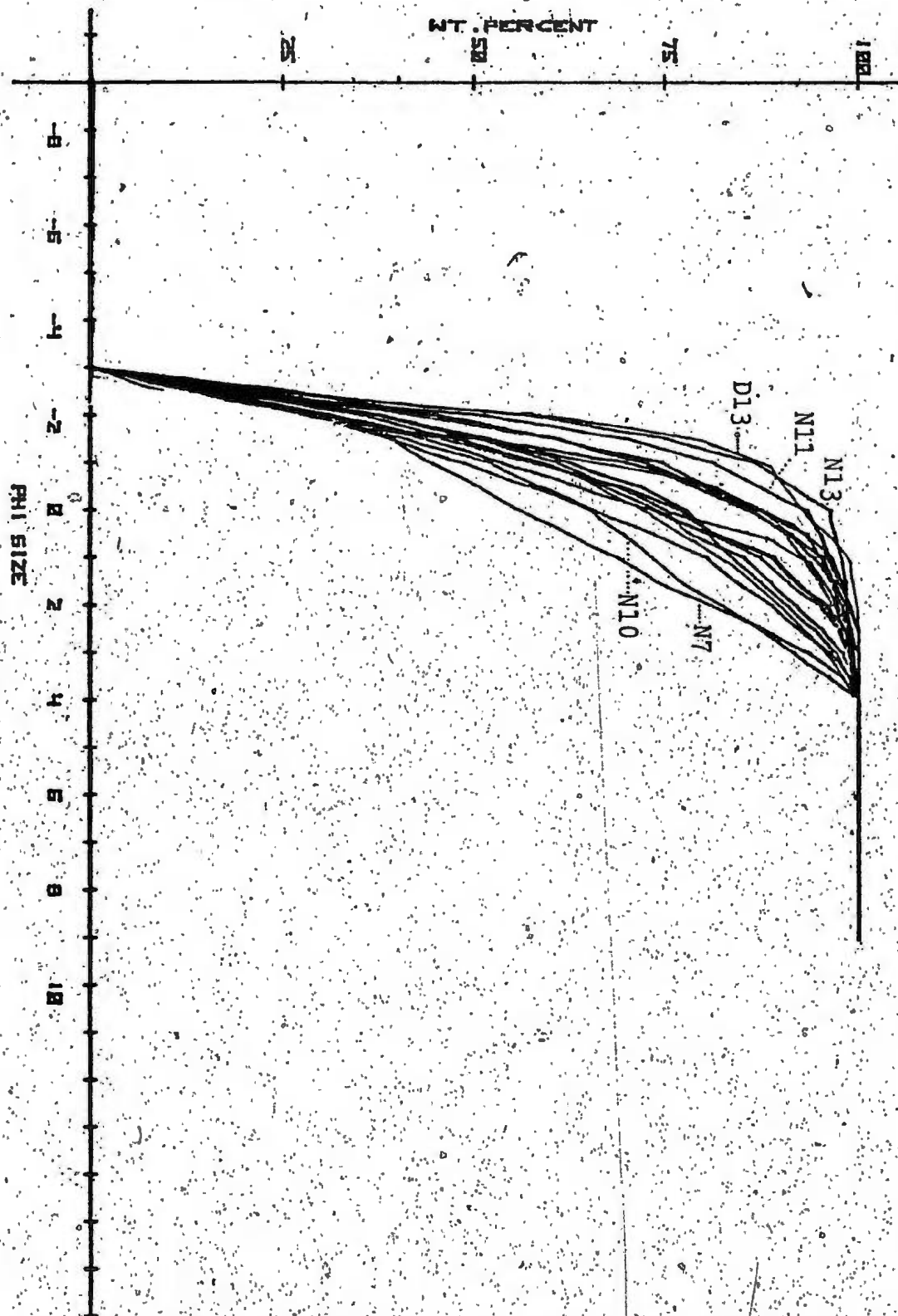


Figure 54. Berendon Glacier; medial moraine debris samples derived from argillites and siltstones of the Bowser assemblage. Medial moraines on Salmon Glacier are derived from this source and are included

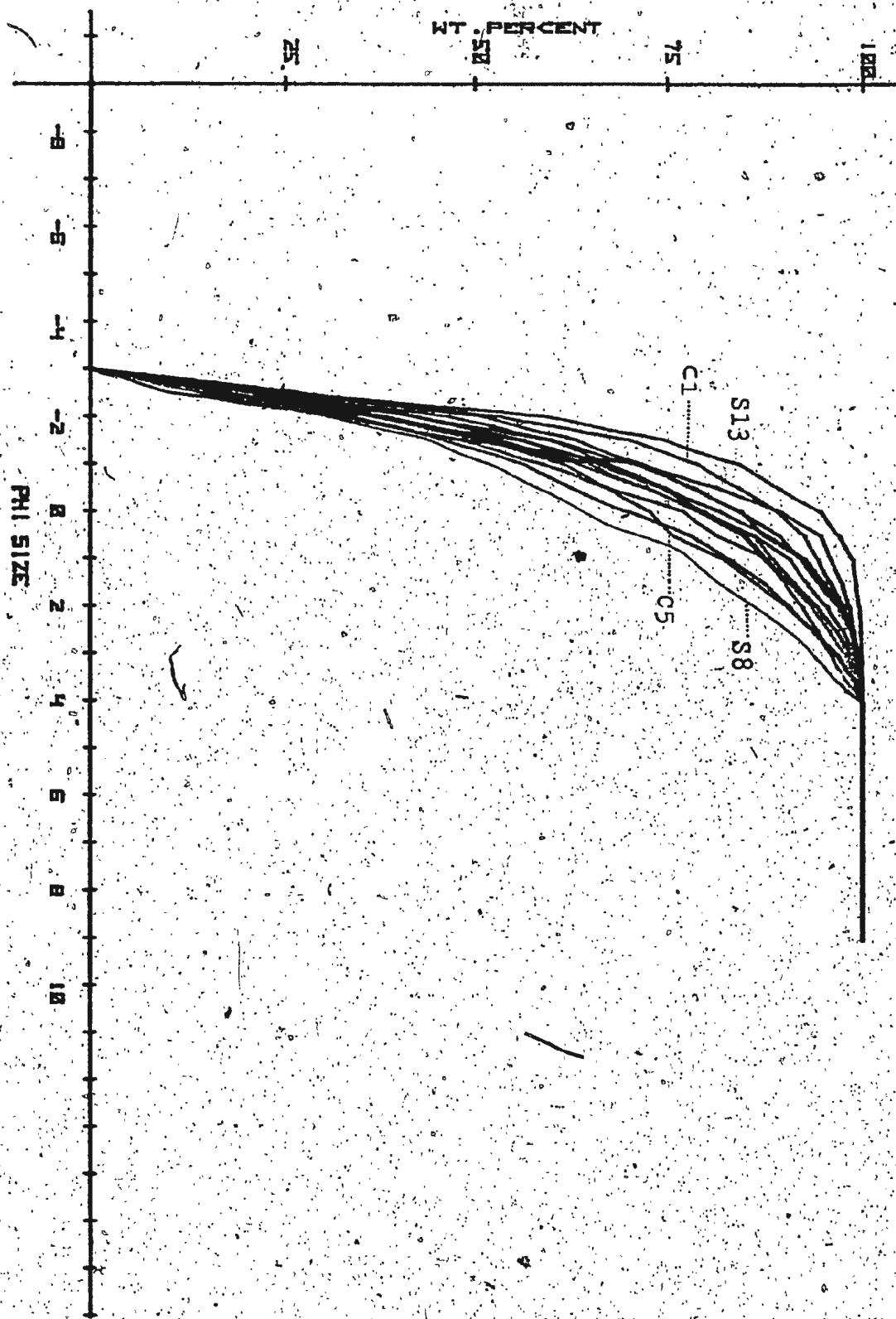


Figure 55. Berendon Glacier; debris samples collected from the Central, or confluence, medial moraine derived from volcanic conglomerate of the Hazleton assemblage.

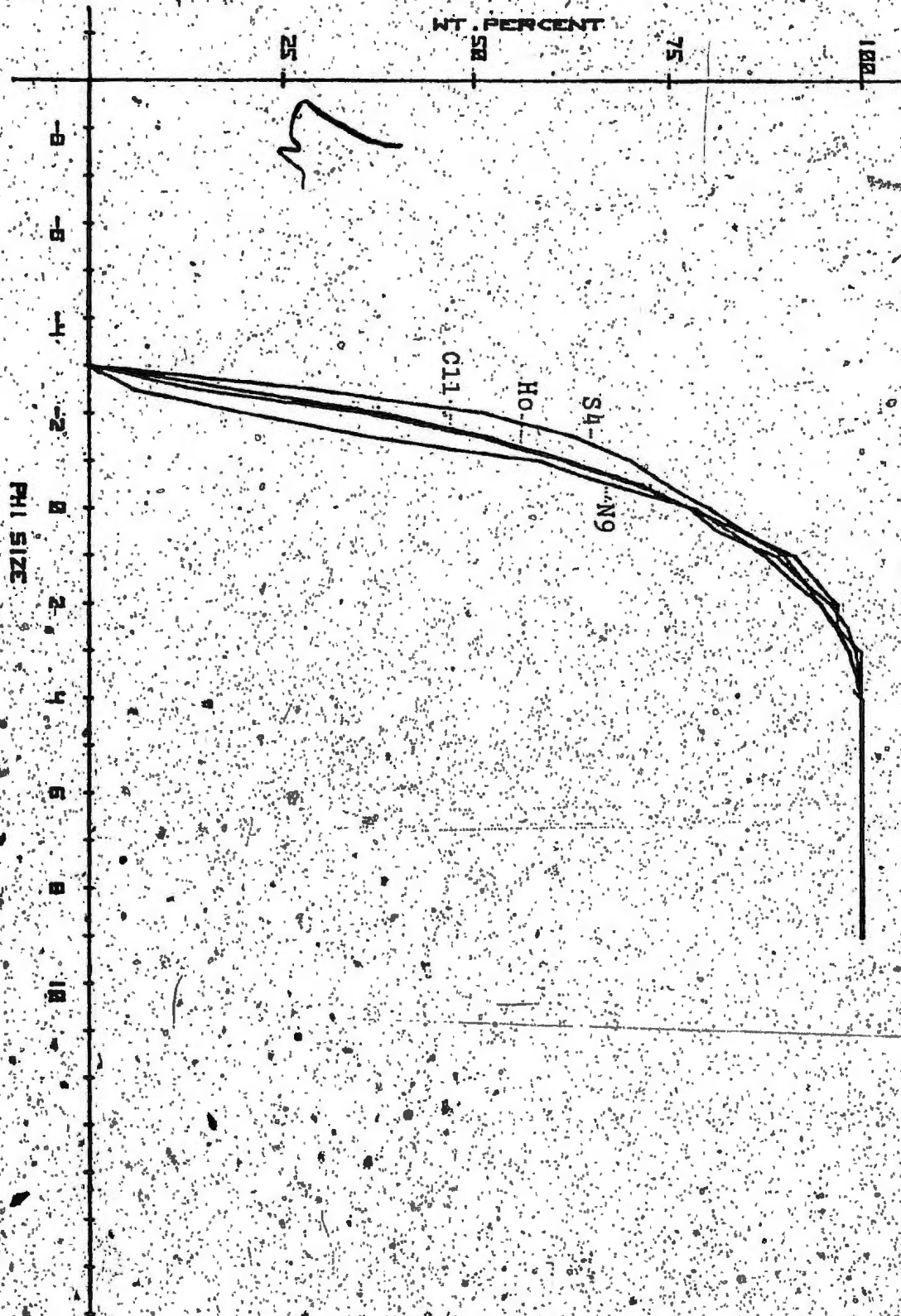


Figure 56. Berendon Glacier; samples collected from frost-shattered debris.

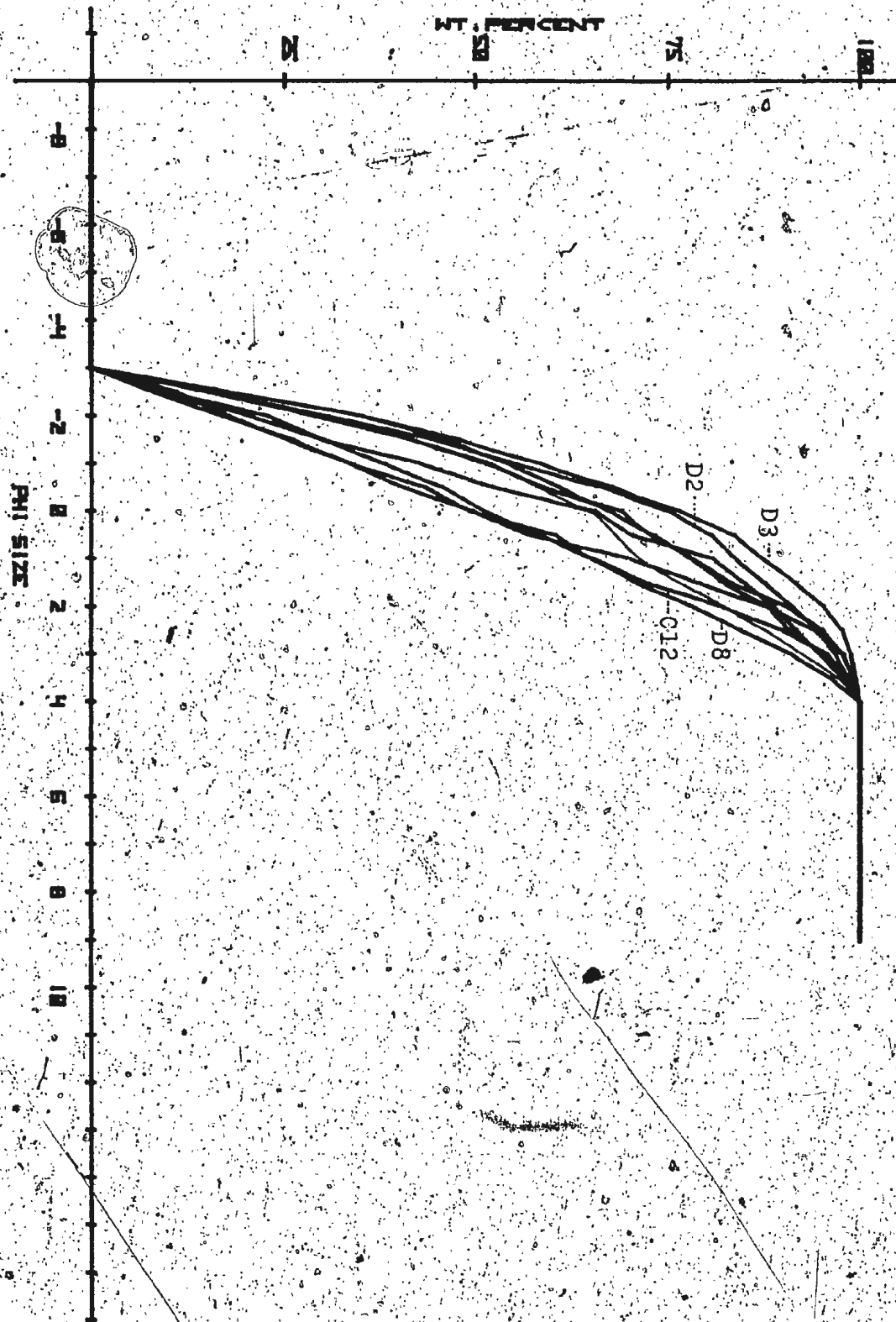


Figure 57. Herendón Glacier; subglacial debris sole and lodgement tills.

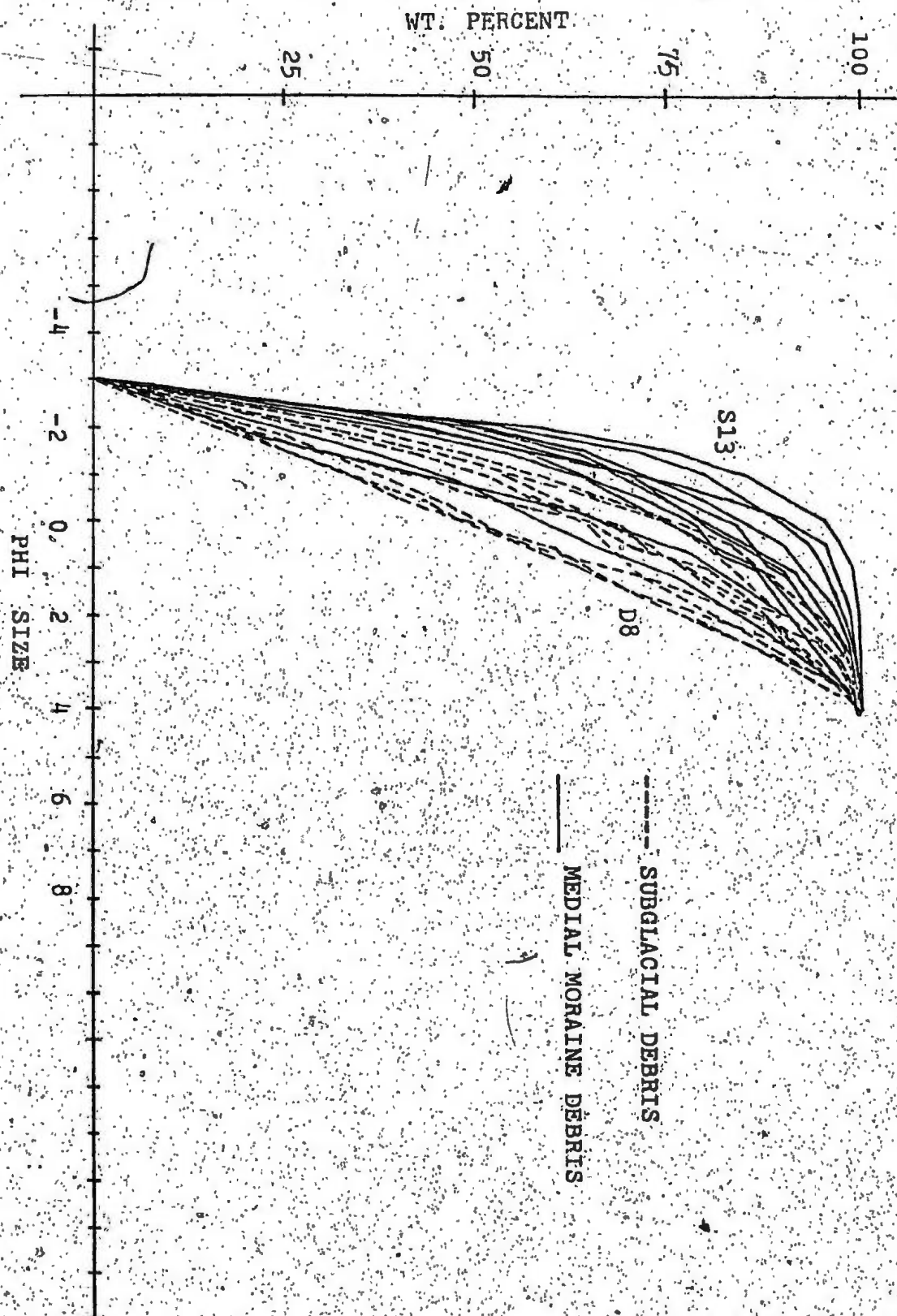


Figure 58. Berendon Glacier; subglacial (lodgement tills and basal sole debris) and medial moraine debris samples.

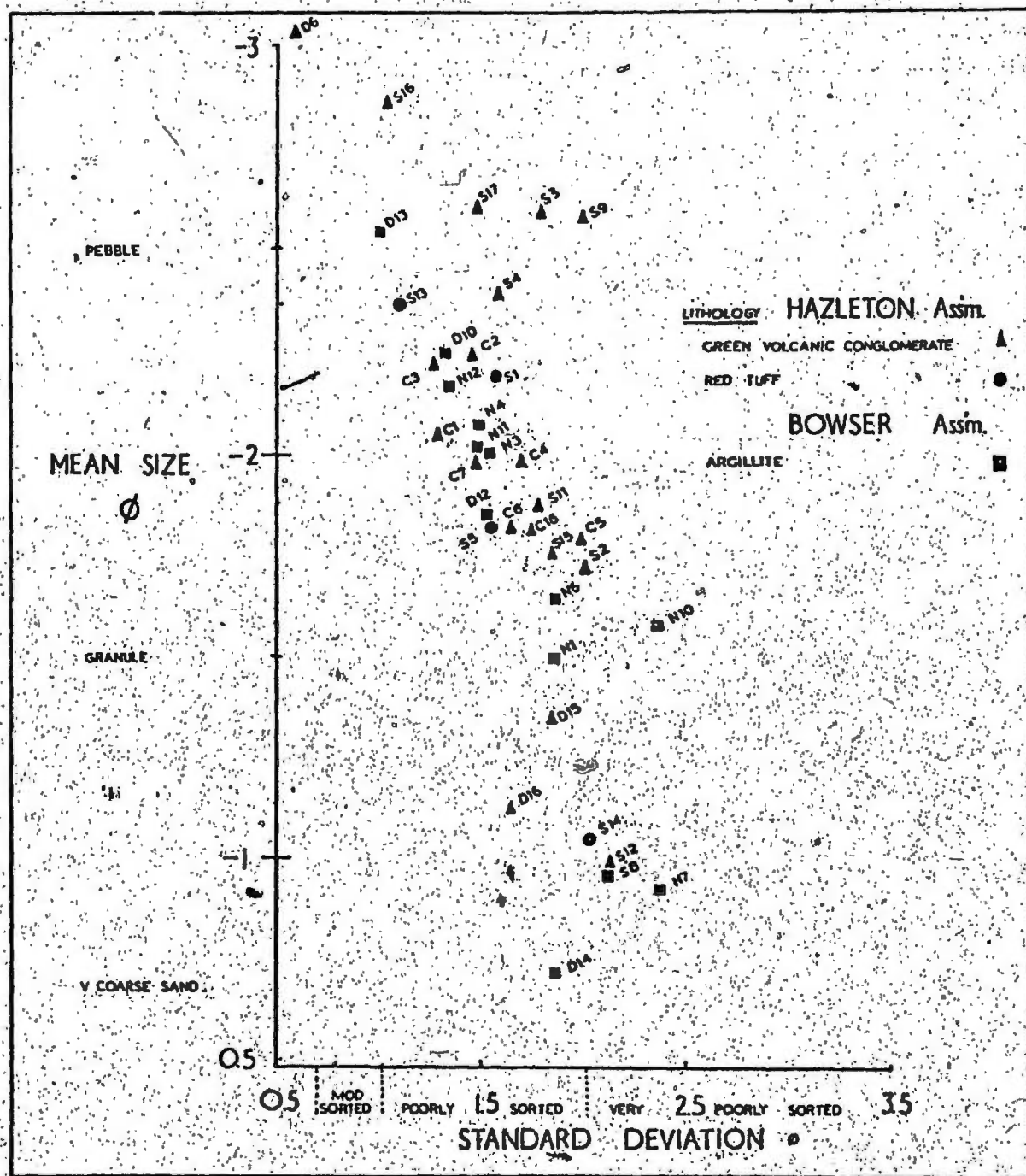


Figure 59. Berendon Glacier; medial moraine debris.
Mean size, standard deviation and parent bedrock.
(-40 to 40)

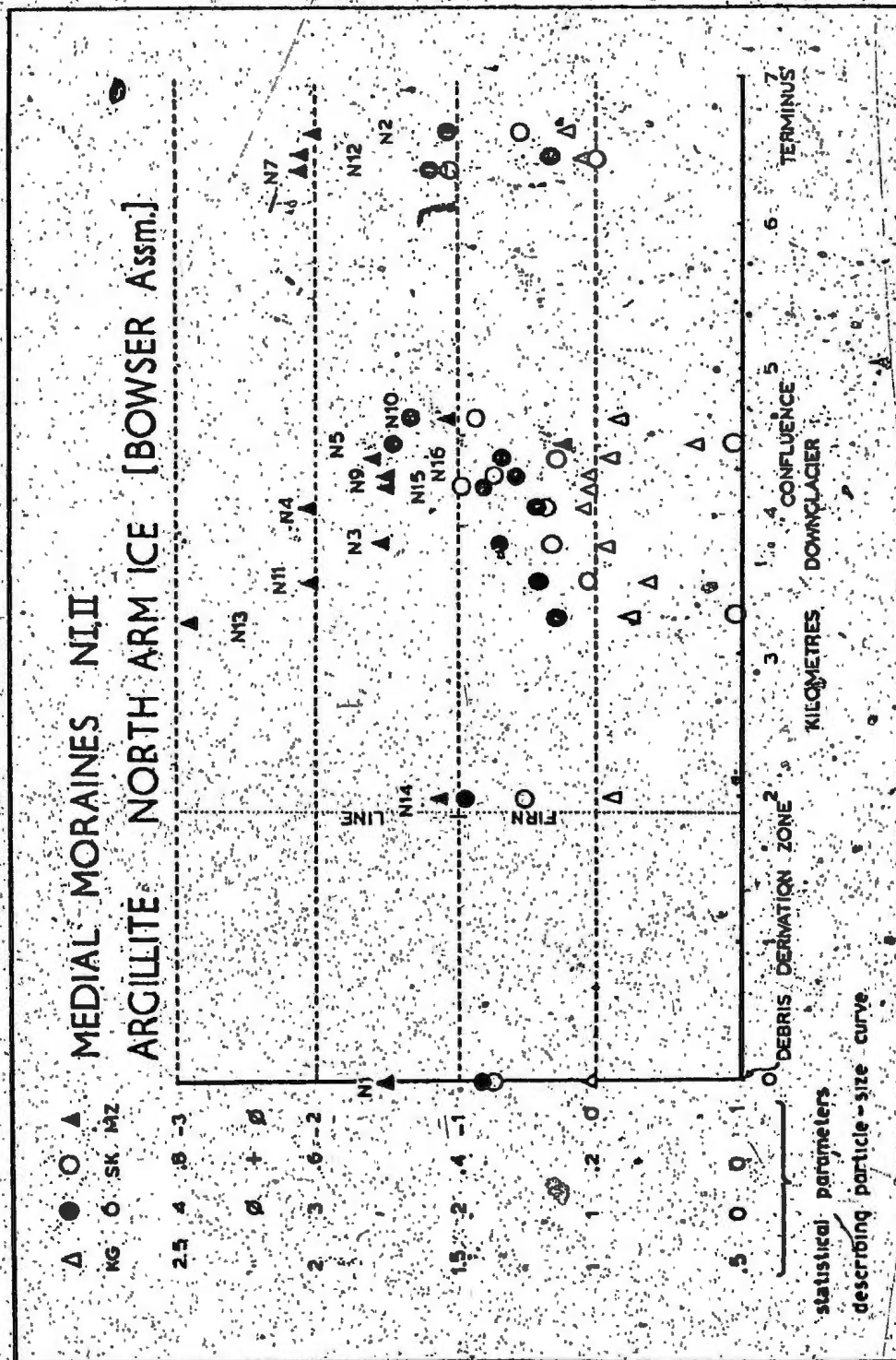


Figure 60a.

Figure 60. Berendon Glacier; medial moraine debris. Moment measure variation as a function of distance downglacier from firn basin backwalls.

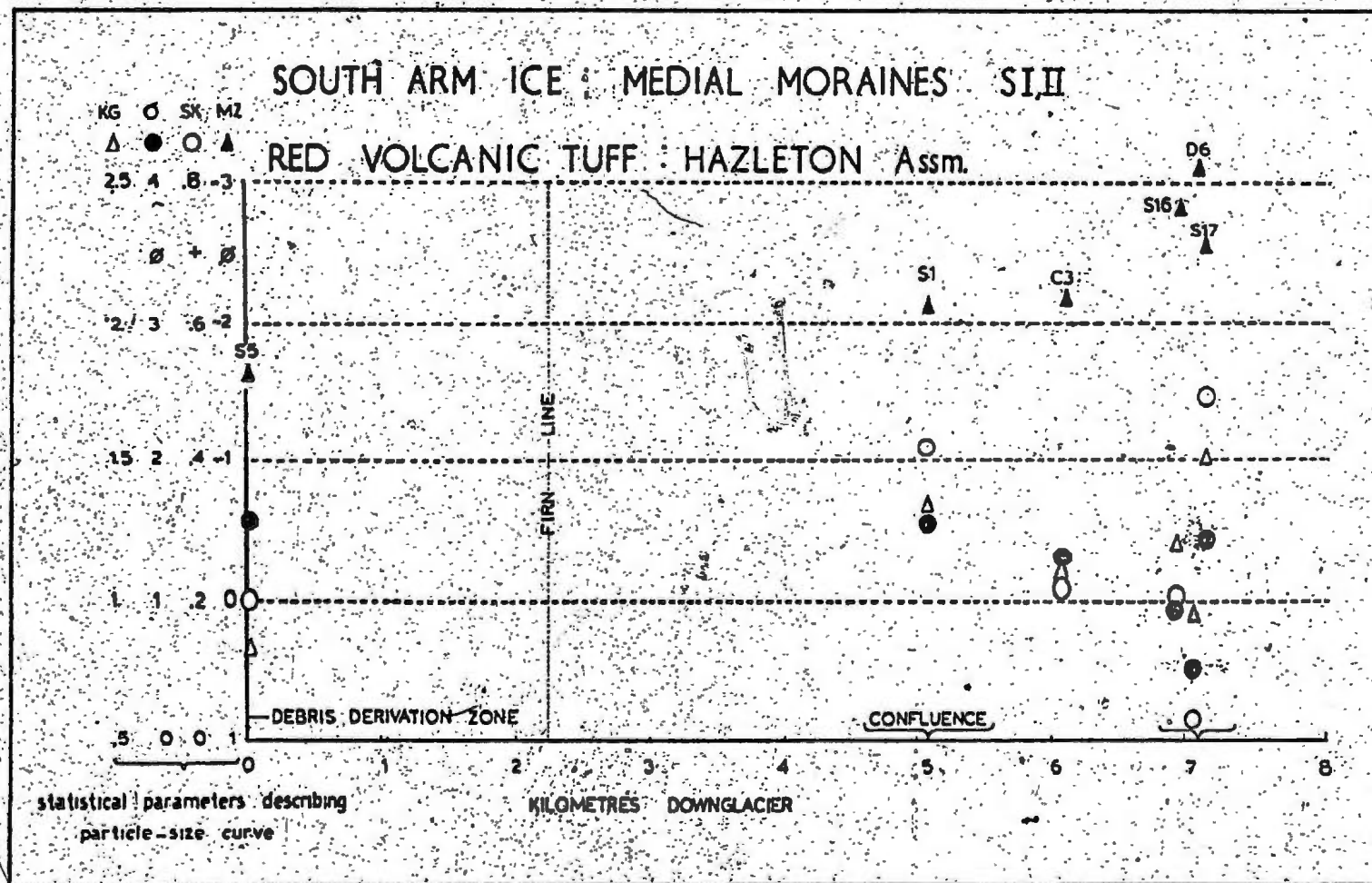
Fig. 60a ; argillite.

" 60b ; volcanic tuff.

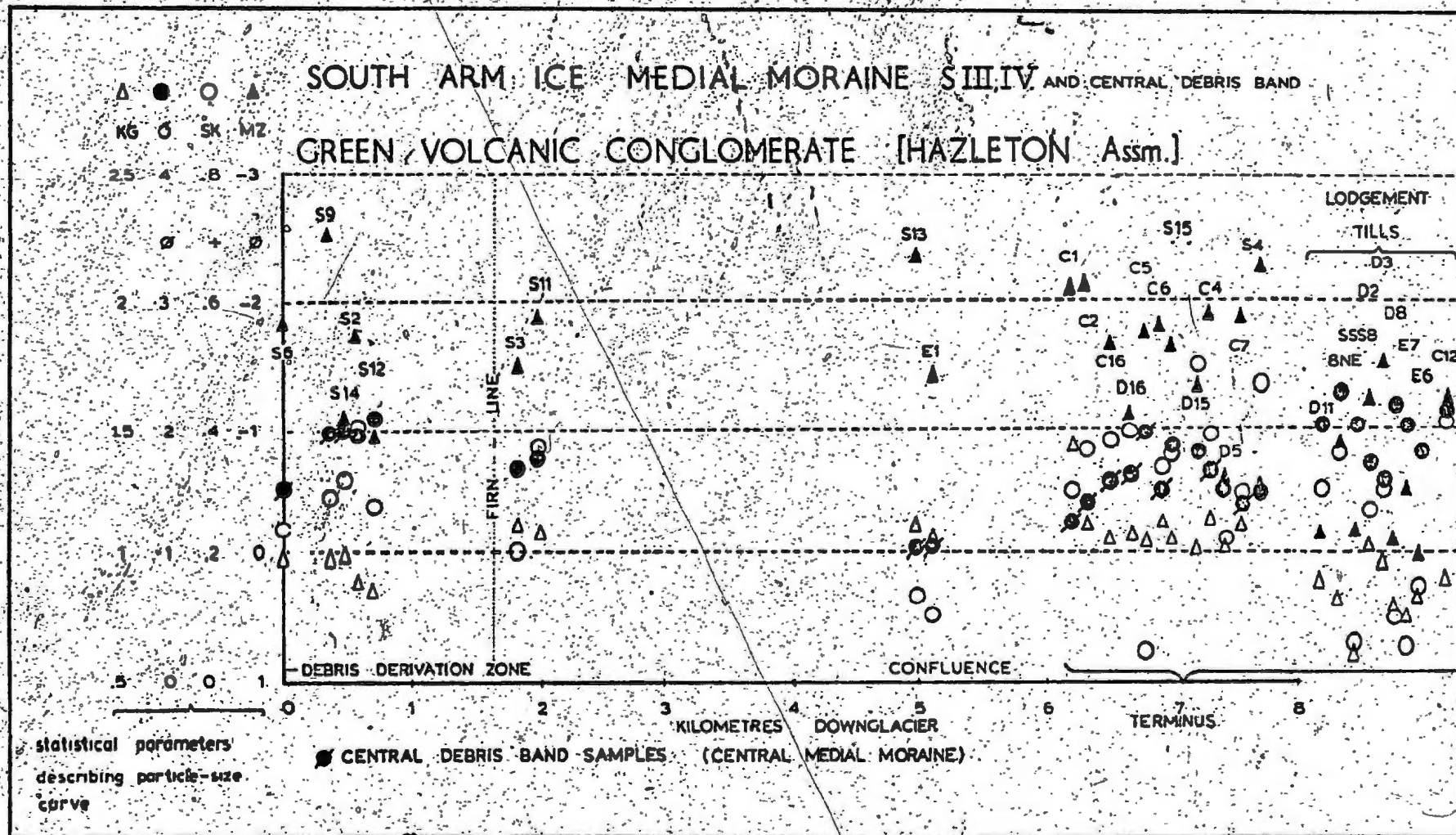
" 60c ; " conglomerate.

(-40 to 40)

Figure 60b.



PI 6ure 600c



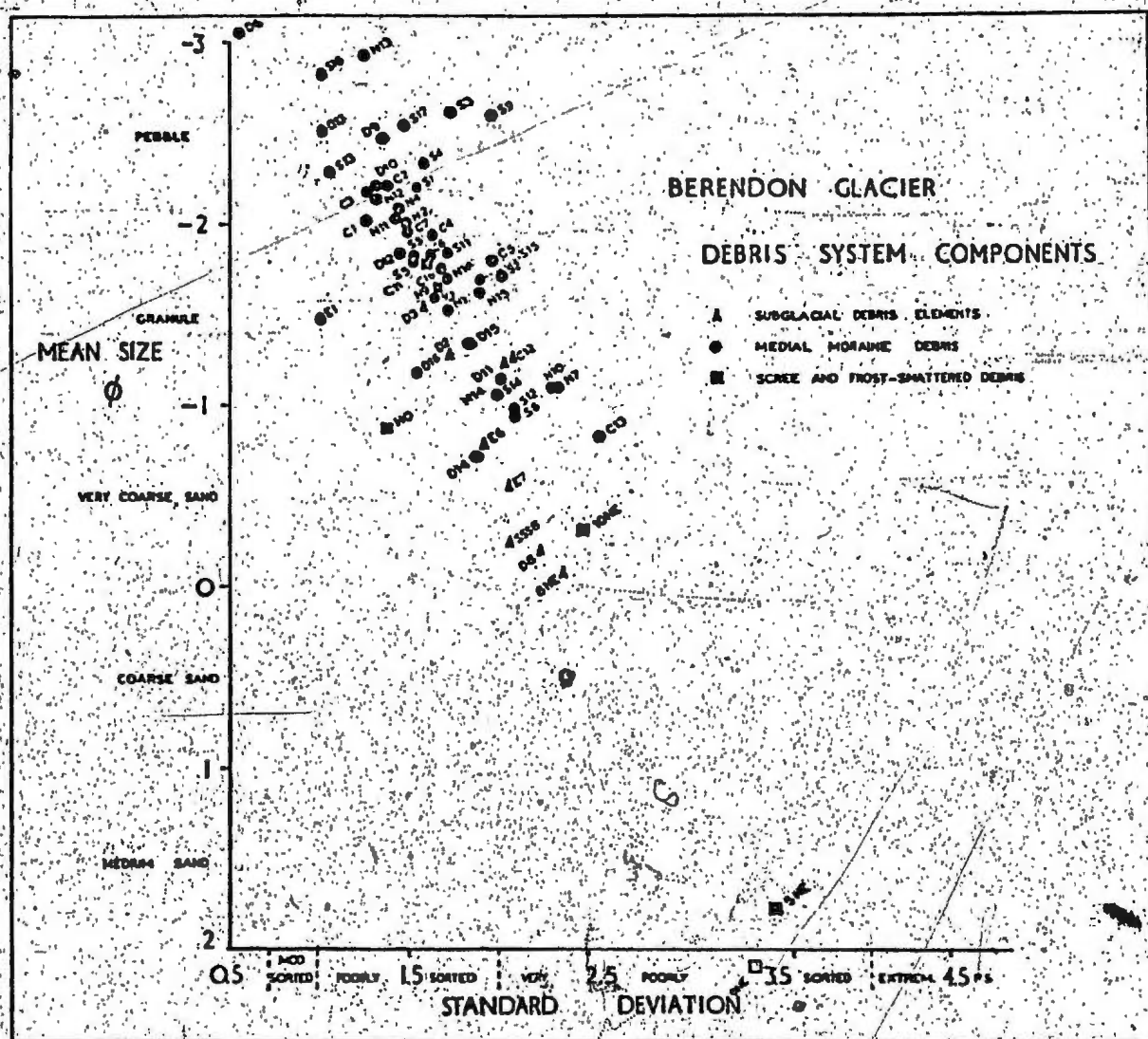


Figure 61. Berendon Glacier; elements of the debris system on the criteria of mean size and standard deviation. (-4.0 to 4.0).

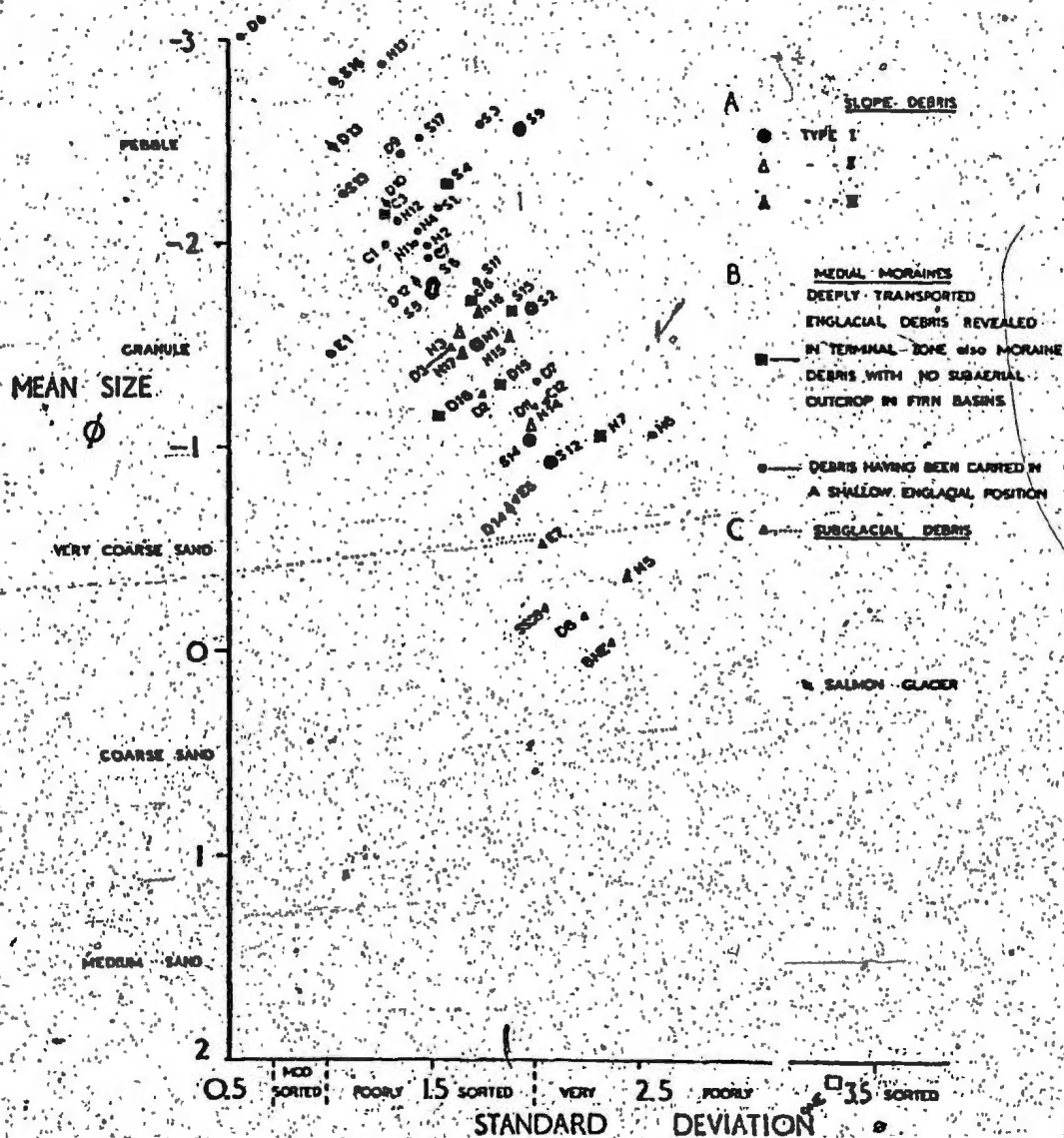


Figure 62. Berendson Glacier; elements of the debris system. Slope debris(A), medial moraine debris carried at or near the bed and at more shallow englacial positions (B) and subglacial debris. Debris samples from Salmon Glacier are included.

(-4φ to 4φ)

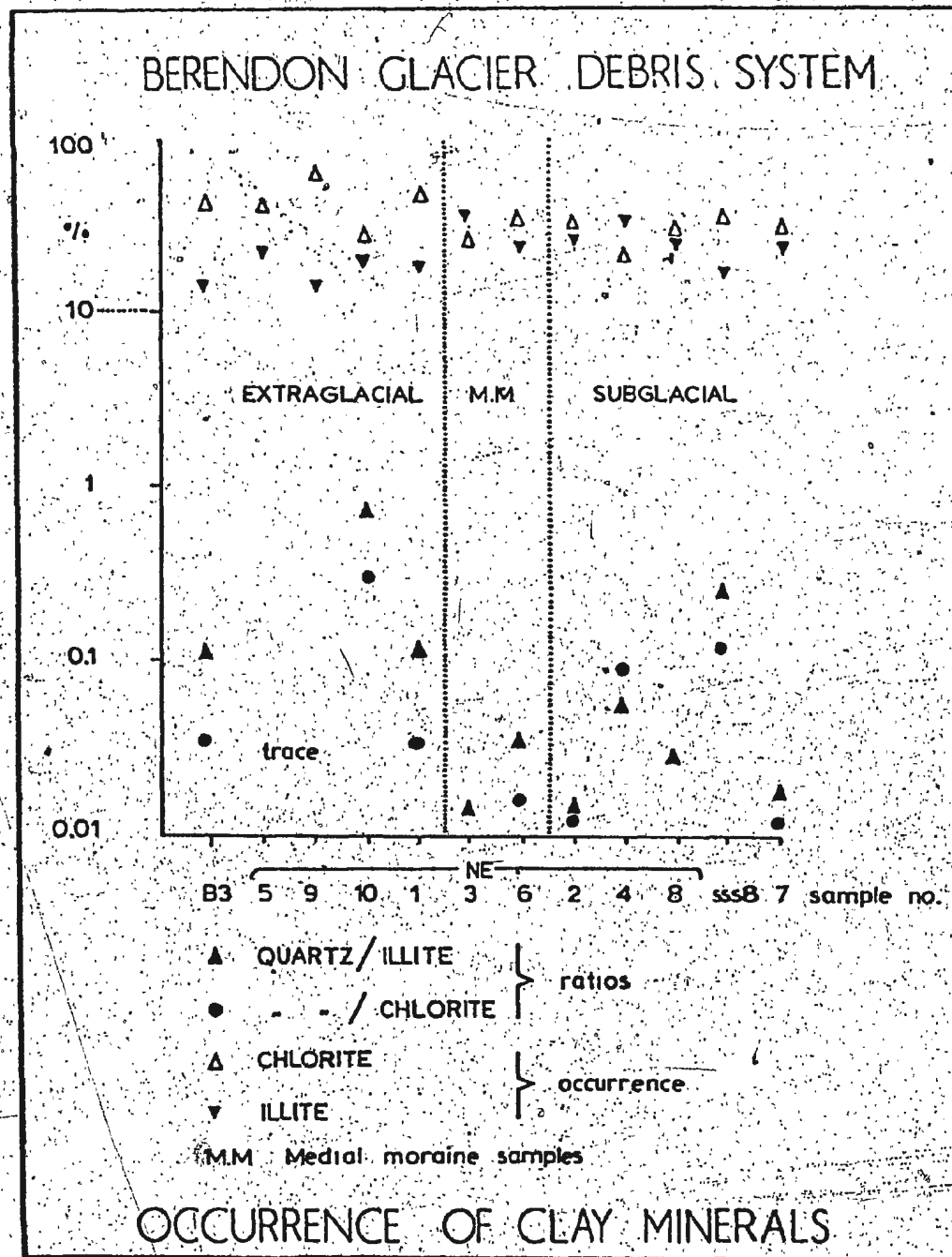


Figure 63. Berendon Glacier; clay mineralogy of the finer than 90 clay fraction (after the methods of Biscaye, 1965). Refer to Appendix VI for site and sample description.

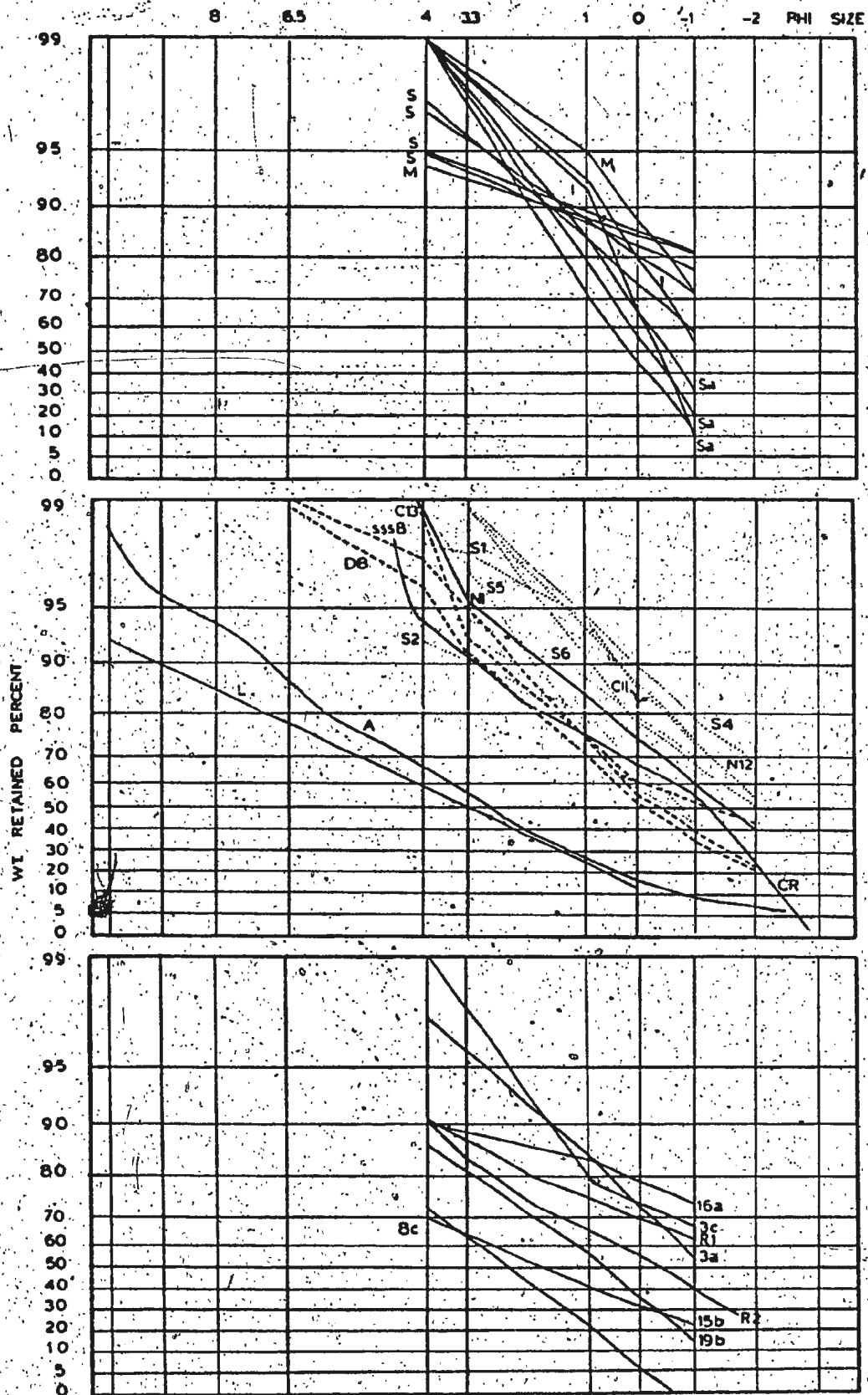


Figure 64. Grain size distributions from Berendon Glacier debris system, mid-latitude tills and frost-shattered debris plotted on "Law of Crushing" paper.
See next page for key.

FROST SHATTERED DEBRIS

WIMAN (1963) 36 cycles (-7 ___ +6c)

S1 slate
S2 mica schist
S5 quartzite
S6 gneiss

POTTS (1970) 200 cycles (-8 ___ + 8c)

I igneous
M mudstone
S shale
Sa sandstone

MARTINI (1967) 40 cycles (-7 ___ + 6c)

3a weathered porph. granite
8c mica schist
3c fresh granite
16a granite from a tor
15b vein quartz
9b fresh sandstone

RAPP (1960)

R1 talus
R2 till with rockfill

BERENDON GLACIER

S4 newly emergent debris medial moraine SIV
C11 frost shattered granodiorite
N1 North Arm backwall
C13 shear plane debris
SSS B glacier sole
DB

N12 North Arm moraine N1

▲ refer to appendix for site descriptions

ELSON (1960)

L Lodgement till from mid latitudes
A Ablation

KEY FOR ROSIN and RAMMLERS LAW OF CRUSHING PAPER



Figure 65a

Figure 65. Berendon Glacier; morphology of the
'erratic moraine' on upper South Arm .
Photograph (65a) by R.J.Rogerson, 1967.
Figure 65b ; morphology of the moraine,
August 1975.

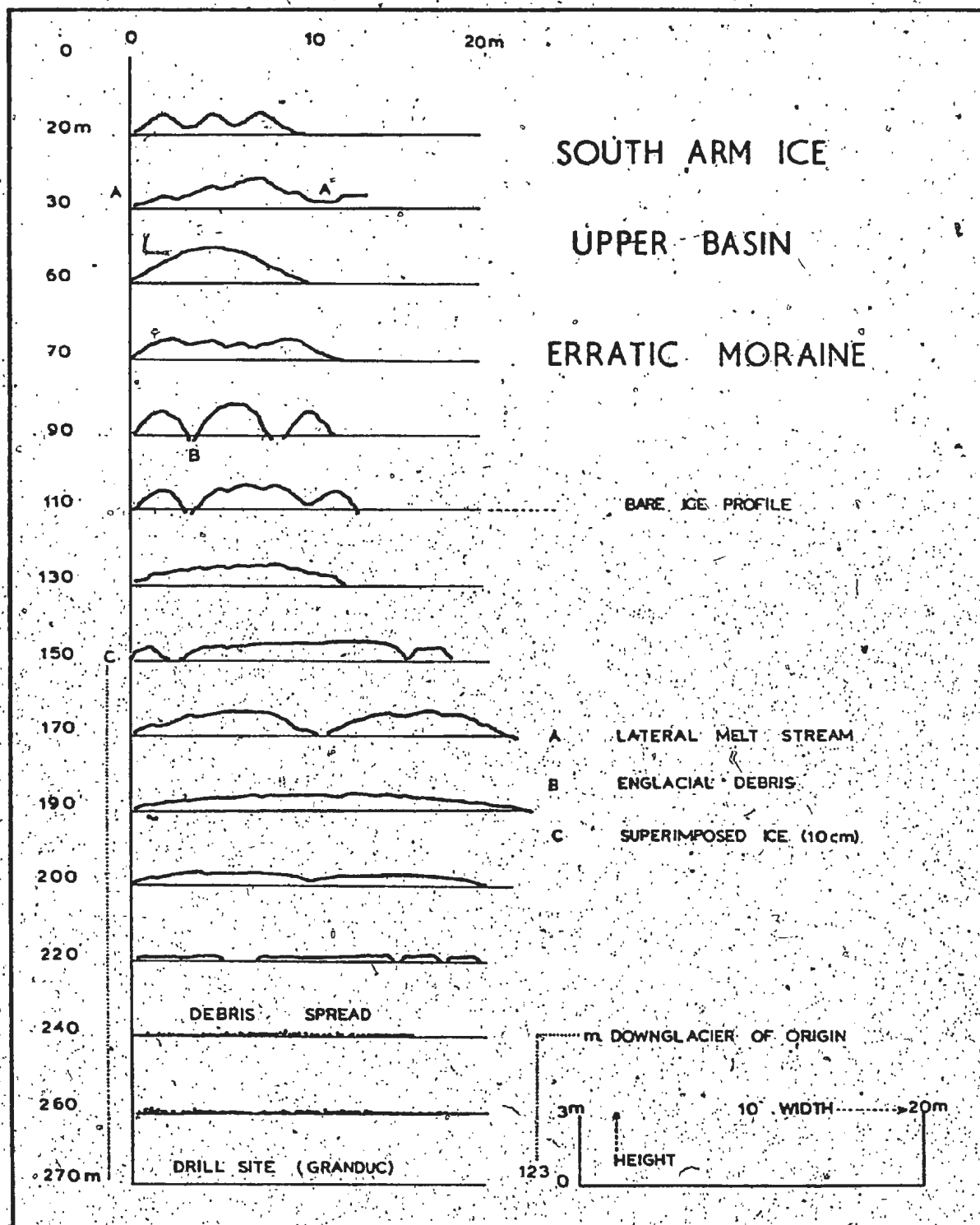


Figure 65b.

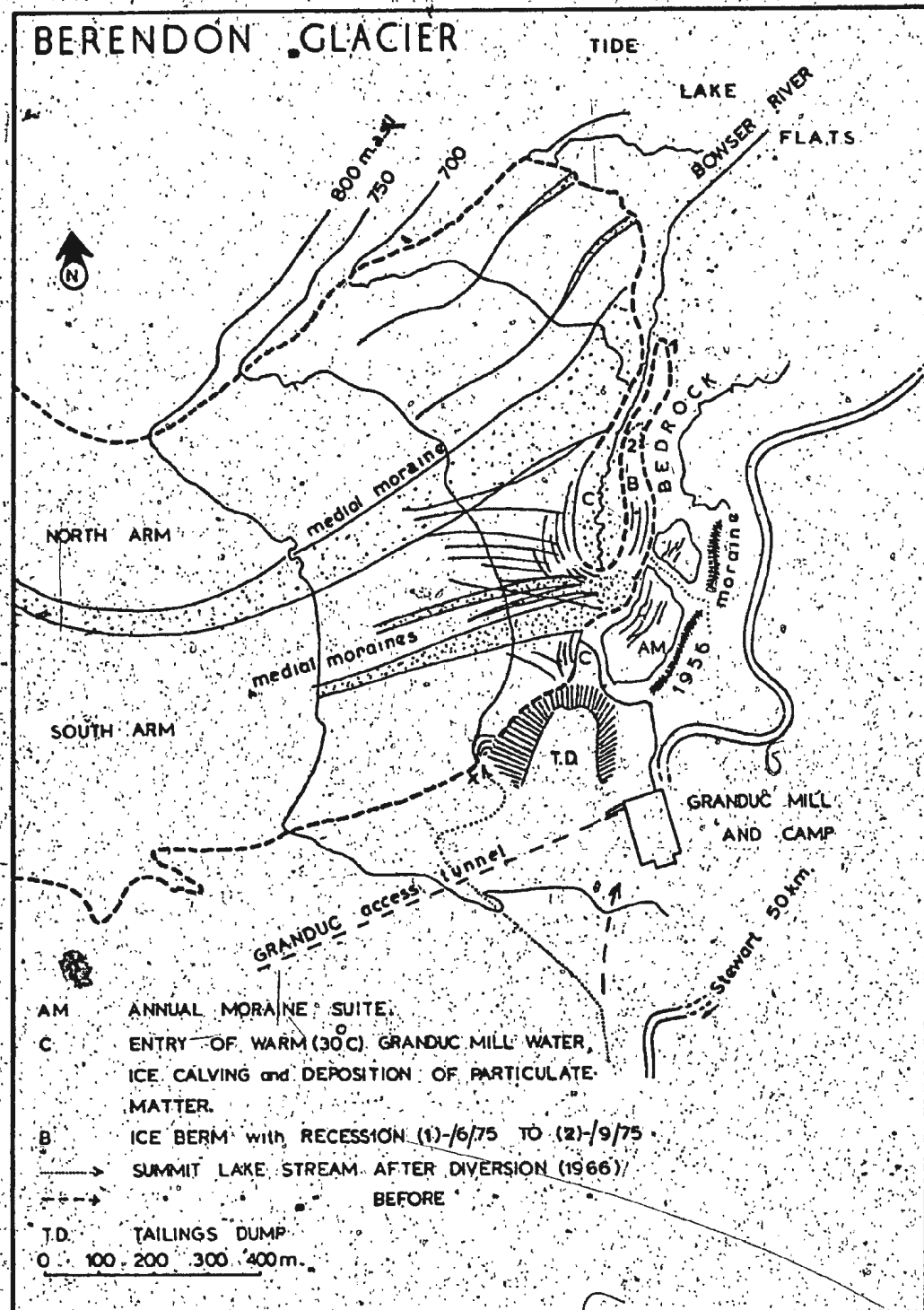


Figure 66. Berendon Glacier; the terminal area.



Figure 68. Berendon Glacier; minor moraine ridges of probable annual occurrence , South Arm terminus.

A: moraine ridge dated at 1956 A.D.

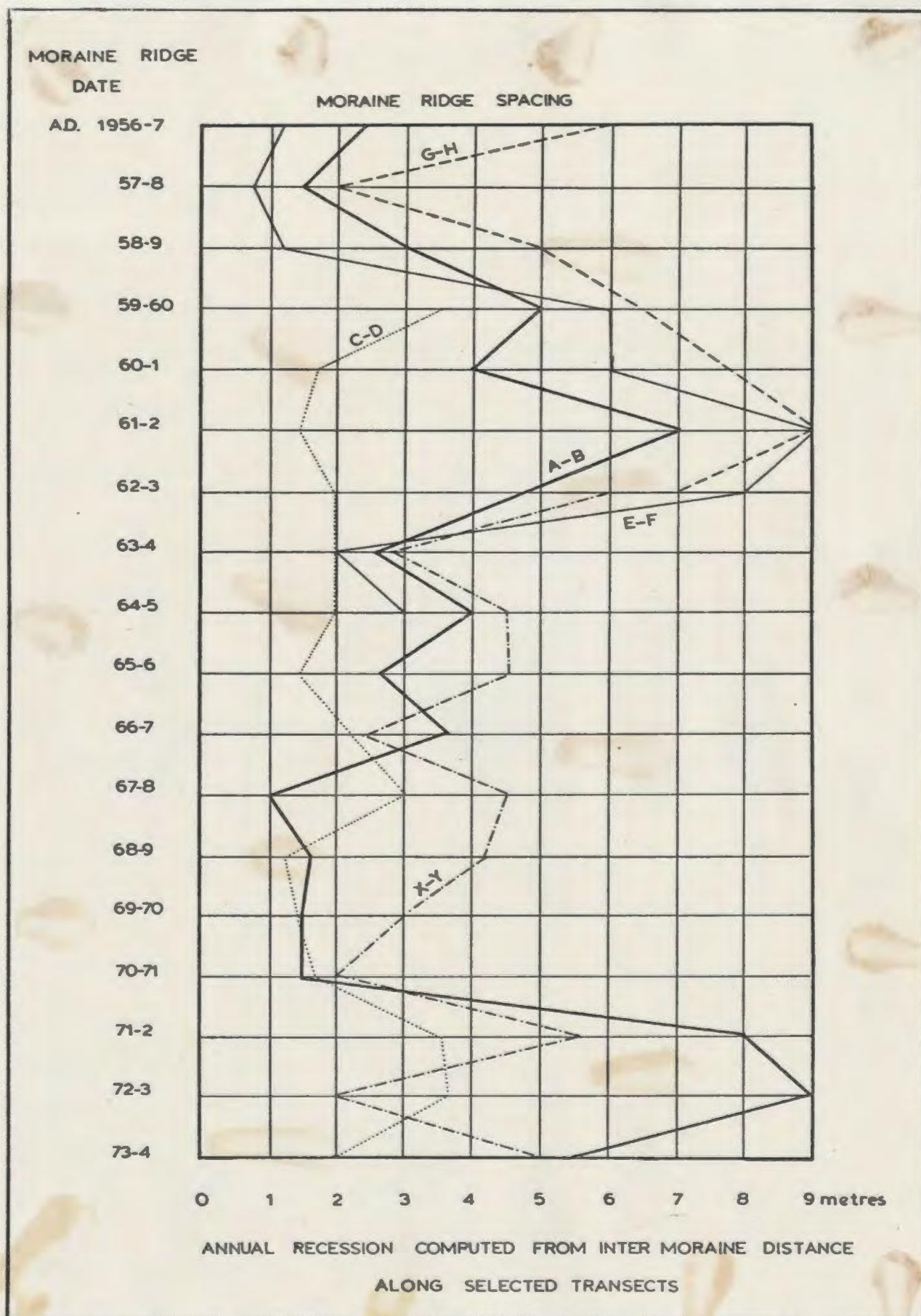


Figure 69. Berendon Glacier; minor moraine ridge spacing and indicated annual recession , South Arm ice front.



Figure 68. Berendon Glacier; minor moraine ridges of probable annual occurrence , South Arm terminus.

A: moraine ridge dated at 1956 A.D.

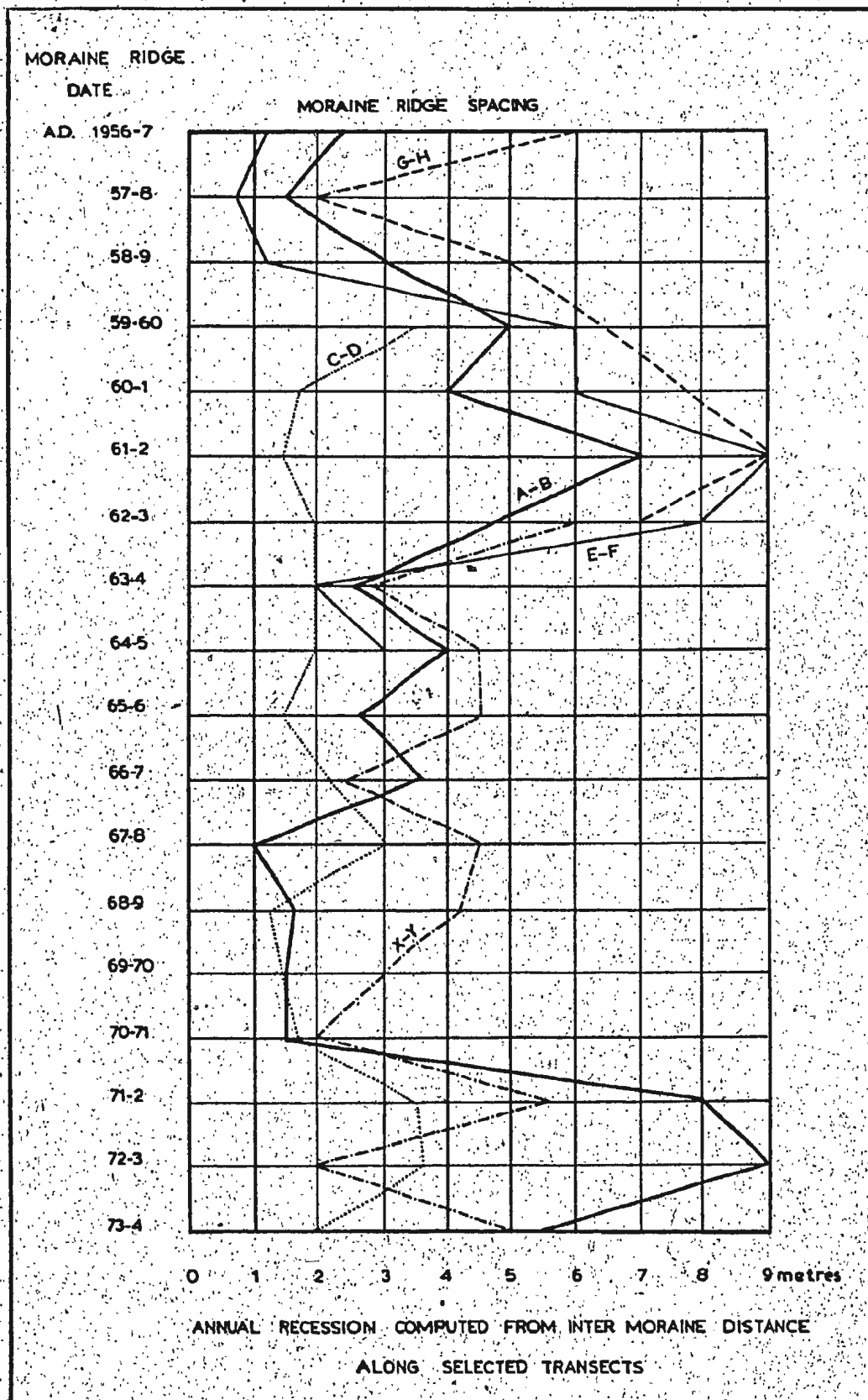


Figure 69. Berendon Glacier; minor moraine ridge spacing and indicated annual recession; South Arm ice front.



Figure 70a. July 1975



Figure 70b August 1975

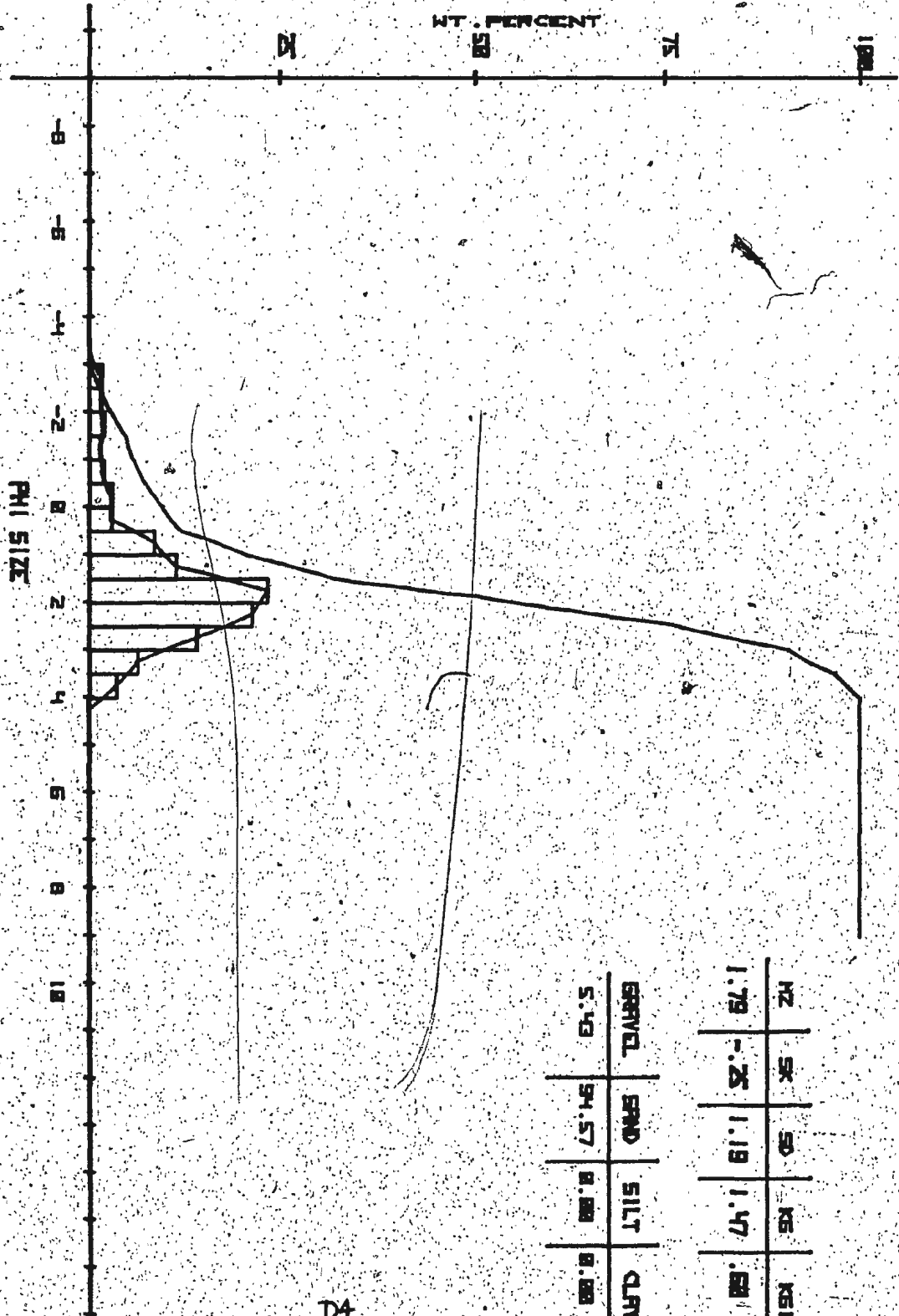
Figure 70. Berendon Glacier; emergence of a minor moraine ridge from the ice front of South Arm, 1975.

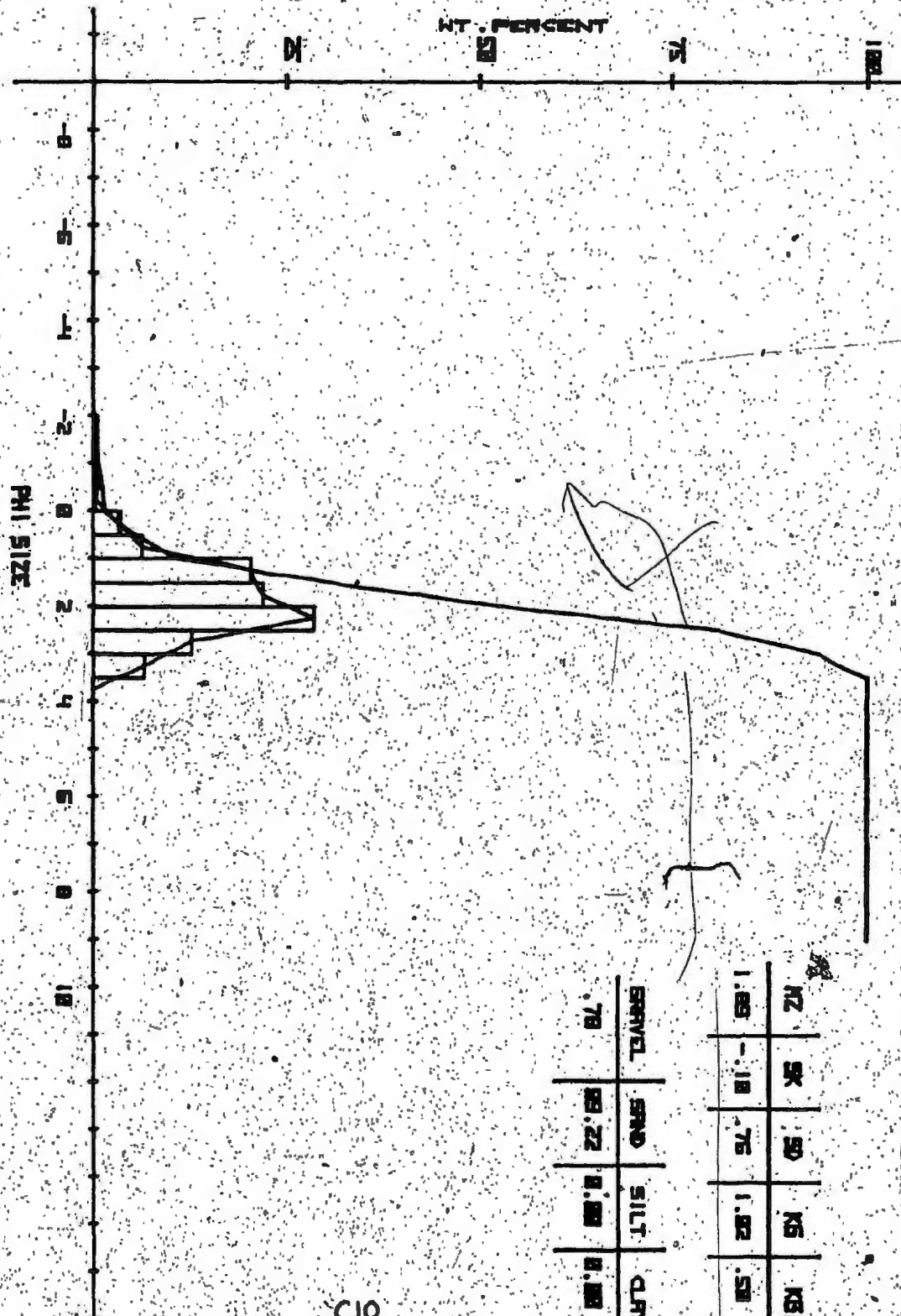


Figure 70c. September 1975

Figure 71. Berendon Glacier; particle-size distribution
of debris in the terminal area of North Arm.

Sample	Position
D4	Shear plane debris overlying ice-core.
C10	Shear plane debris.
C13	Medial moraine debris close to shear plane.
N6	Newly revealed englacial medial moraine debris close to shear plane.
C14	Granduc mill particulate outfall in mill water.

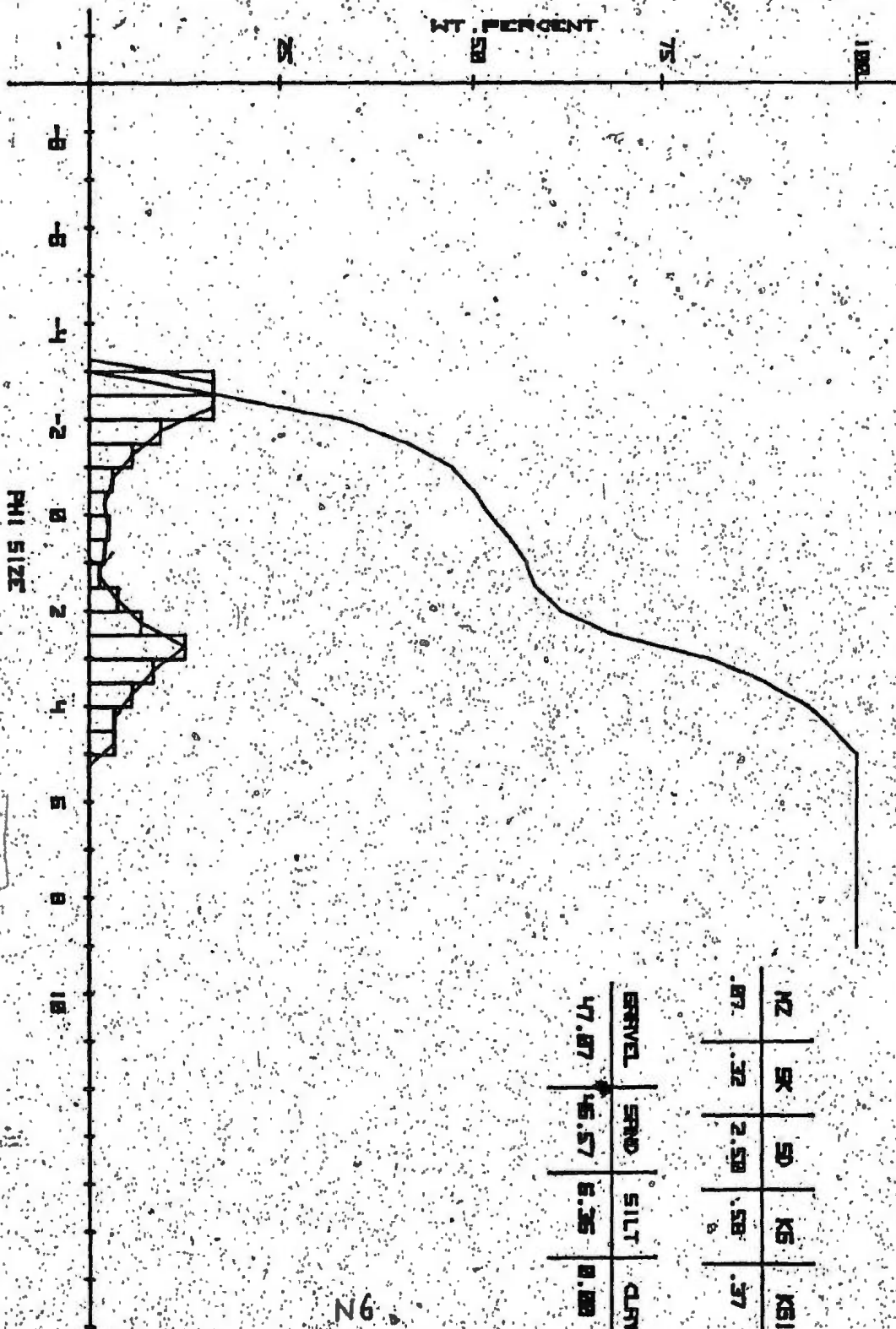




NZ	SK	SD	KS	KB
1.00	0.10	0.75	1.00	0.50

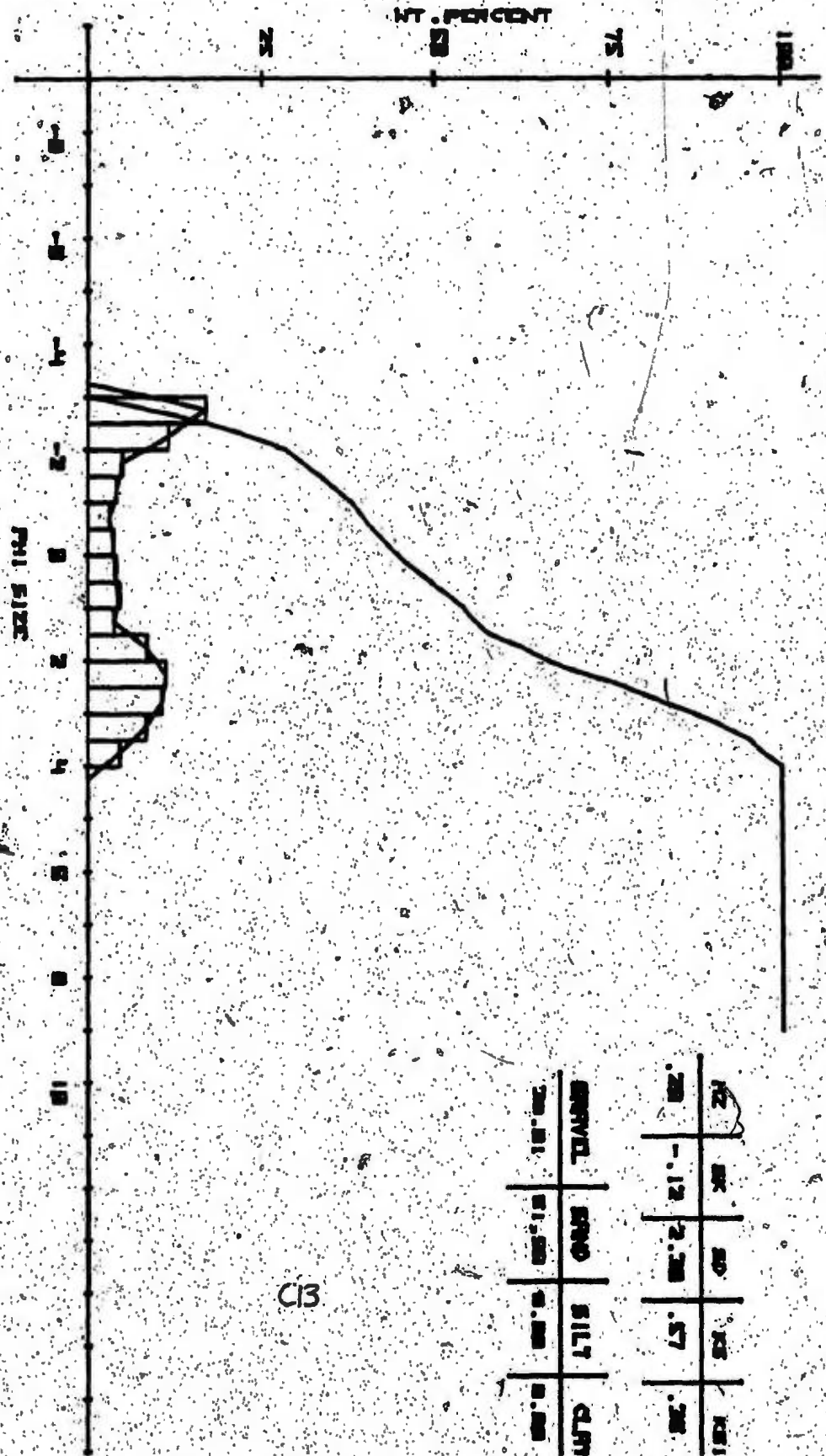
GRAVEL	SAND	SILT	CLAY
0.75	0.22	0.00	0.00

C10

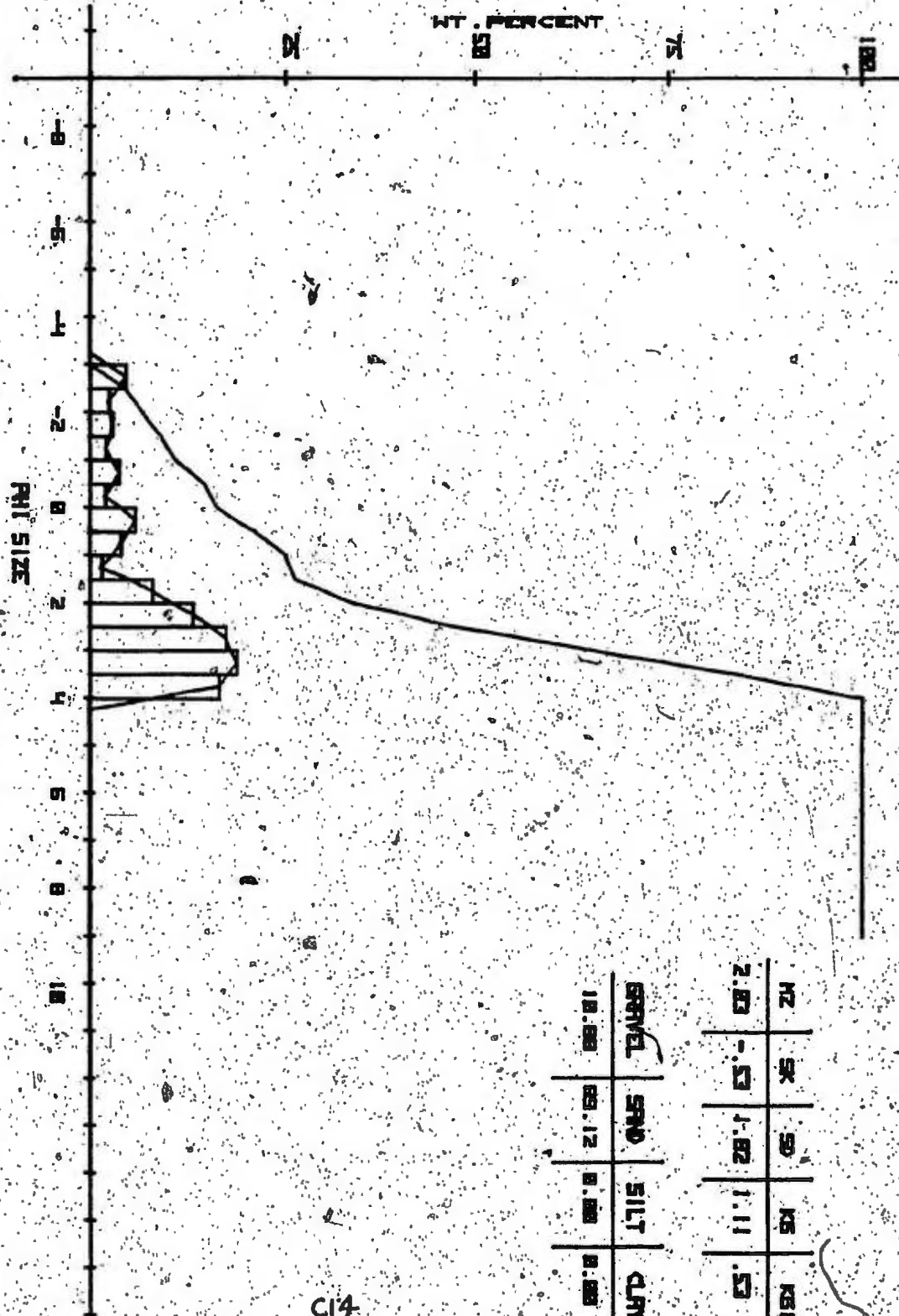


NZ	SK	SD	KS	KSI
.87	.32	2.58	.58	.37

GRAVEL	SAND	SILT	CLAY
47.87	46.57	6.35	0.18



C13



2.0	0.85	0.425	0.25
10.00	89.12	0.00	0.00

GRAVEL	SAND	SILT	CLAY
10.00	89.12	0.00	0.00

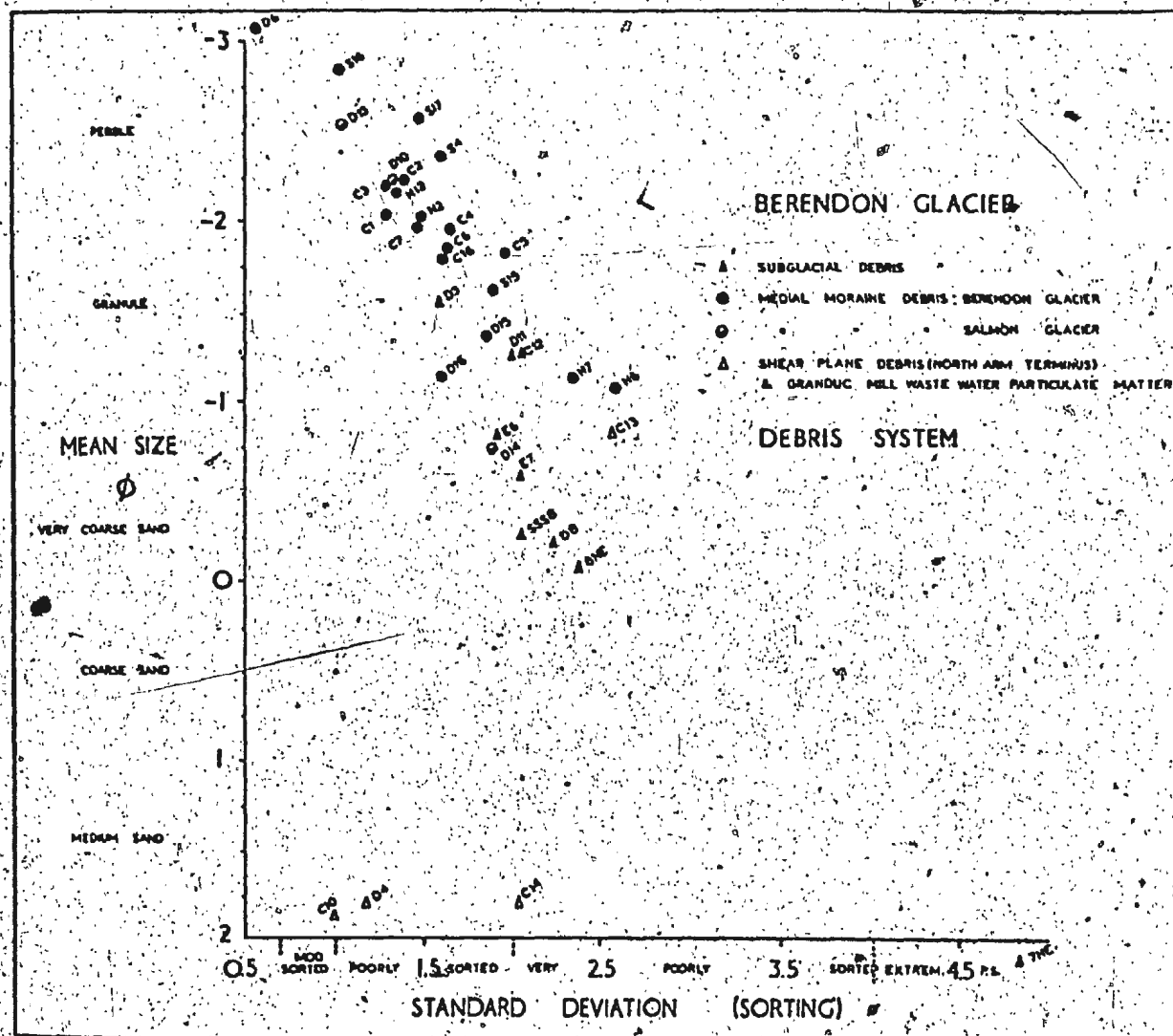


Figure 72. Berendon Glacier; elements of the debris system compared with debris found in the terminal area of North Arm. (-4.0 to 4.0)



Figure 73. Berendon Glacier; basal shear plane outcropping along South Arm ice front. The shear plane is not associated with the elevation of subglacial debris from the glacier bed. Ice revealed below the shear plane is 1.5m thick.



Figure 74. Berendon Glacier; Granduc mill stream flowing along the lower foot of a granodiorite outcrop. An isolated ice berm still retains englacial debris (A) from the Central medial moraine (B). The ice berm is moving down the bedrock slope i.e exhibits 'upglacier' movement. Note shearing (C) generated by basal, bedrock obstruction of glacier flow.



Figure 75. Berendon Glacier; open, infraglacial channel flow of Granduc mill stream, the result of the collapse of the roof of a subglacial channel. Part of the roof section is still (1975) in place (A). Granduc mill can be seen in the background.

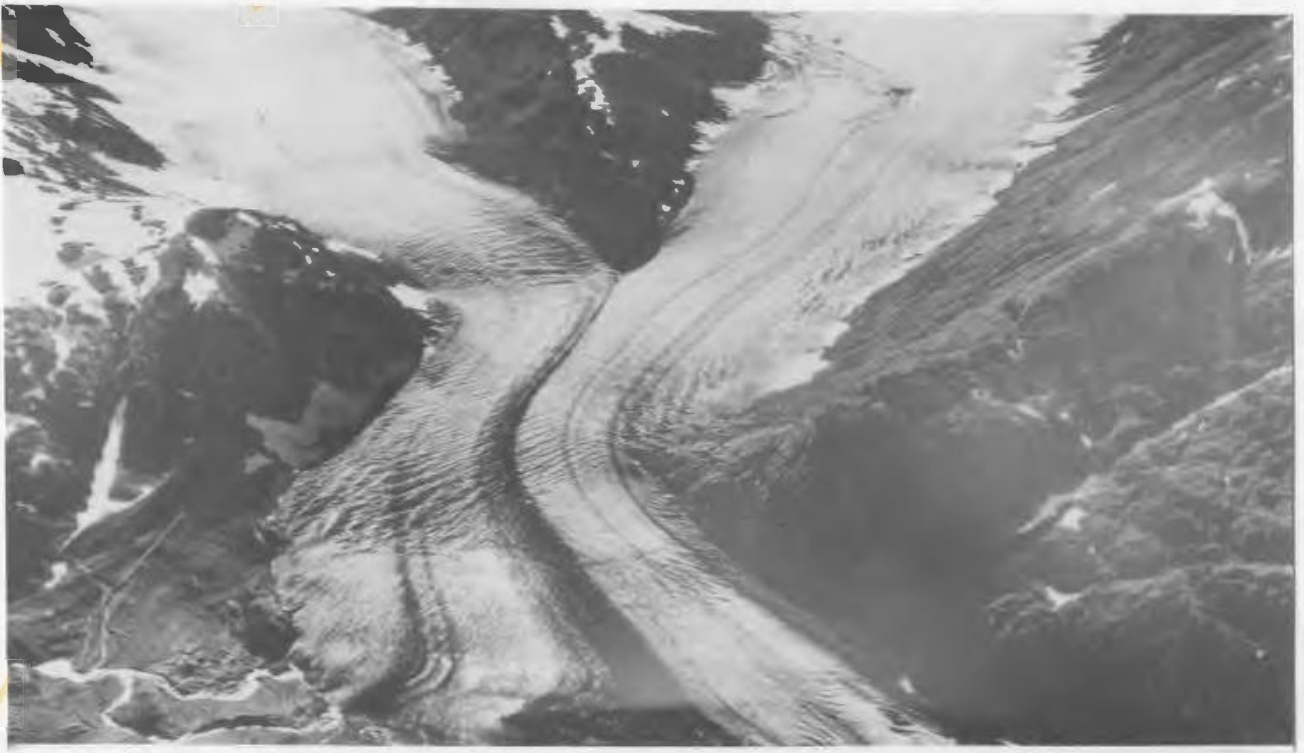


Figure 76a.



Figure 76b

Figure 76. Berendon Glacier; aerial photographs by Austin Post of the terminus in the years 1961 (a), 1969 (b), 1972 (c), and 1974 (d). Mill production and release of warm waste mill water commenced in fall 1970. Shearing activity is a marked feature of the terminus; the old Summit Lake overflow stream, diverted by Granduc construction, is sited left foreground in figure 76a.



Figure 76c.



Figure 76d.

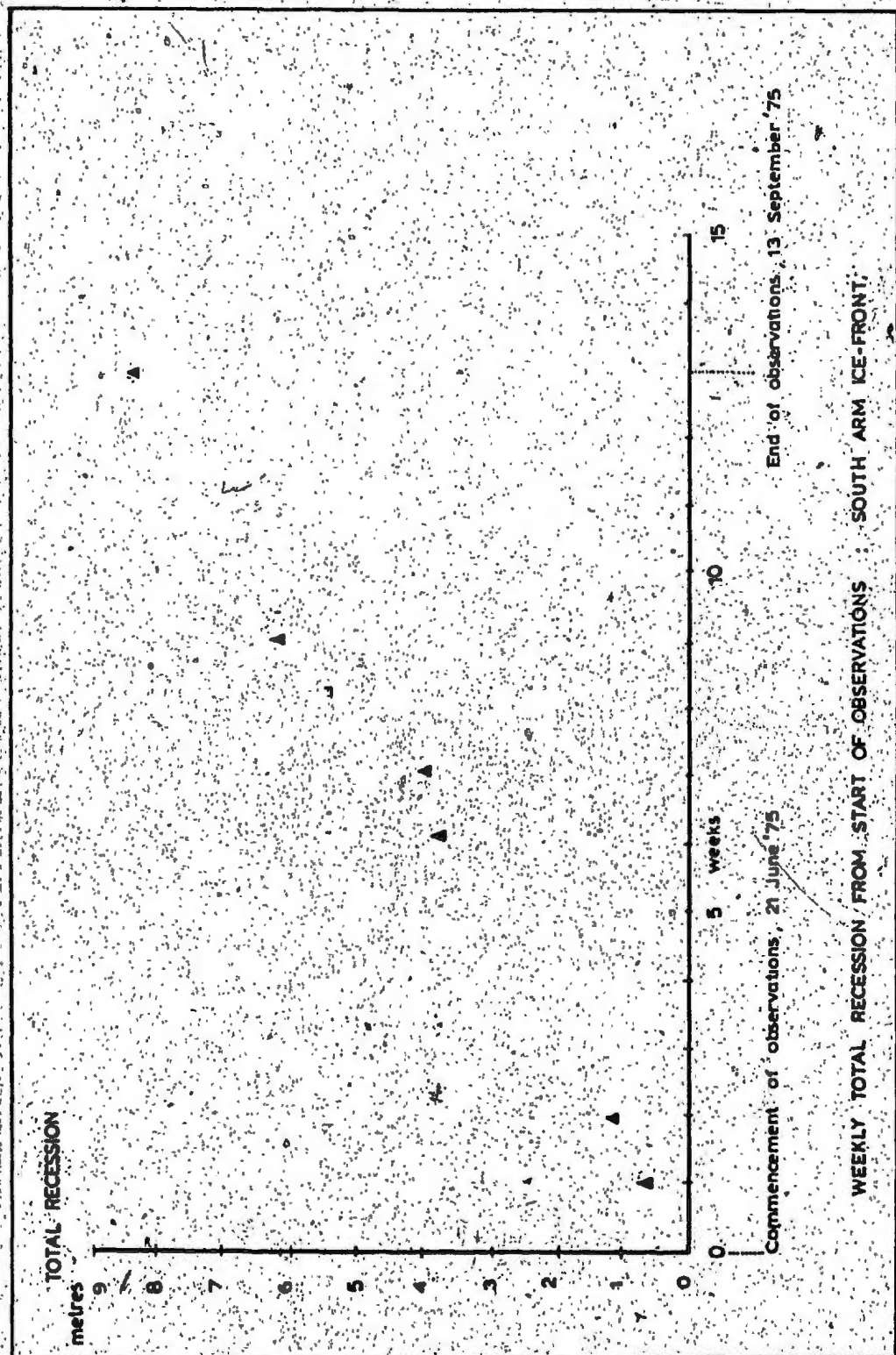
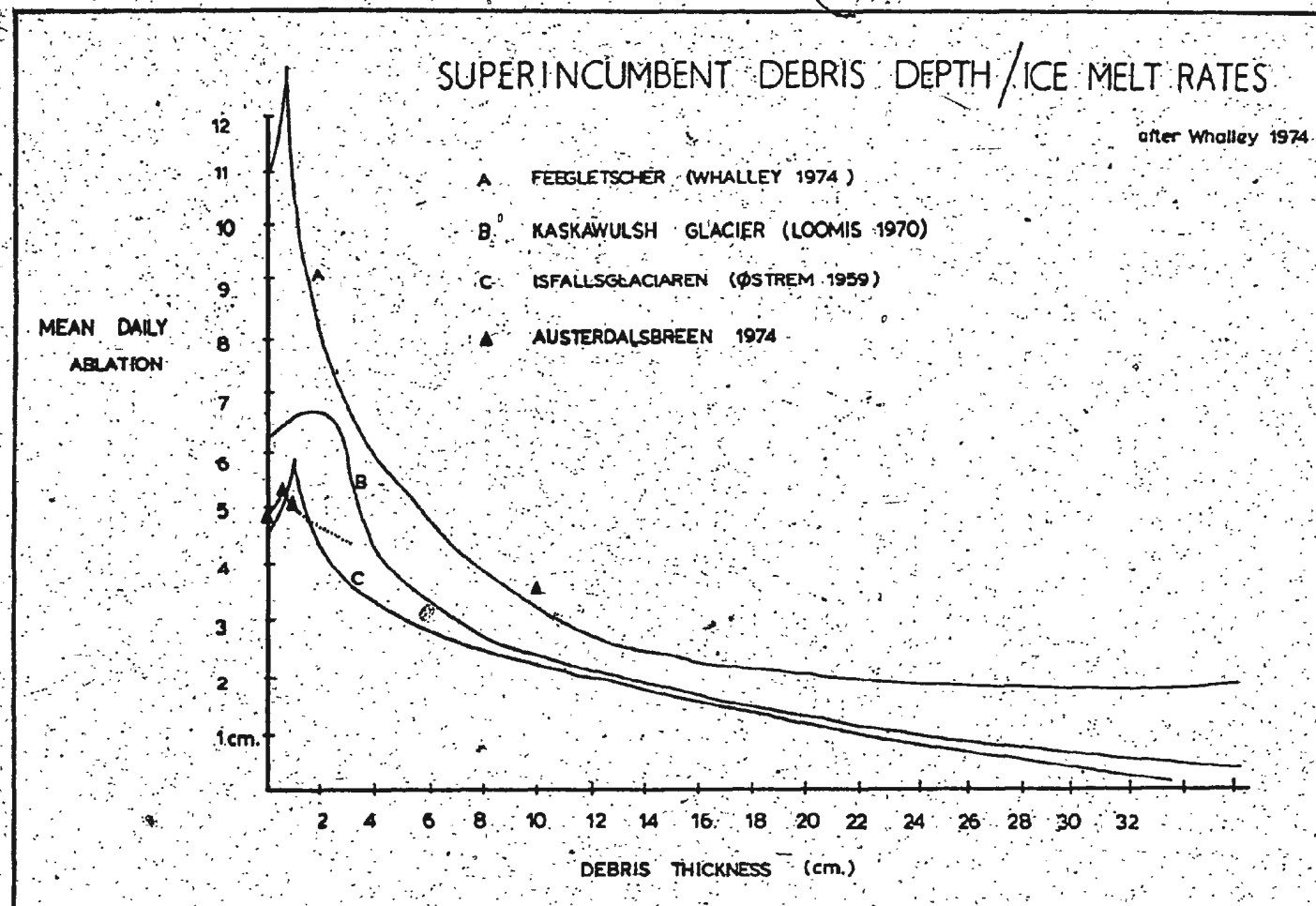
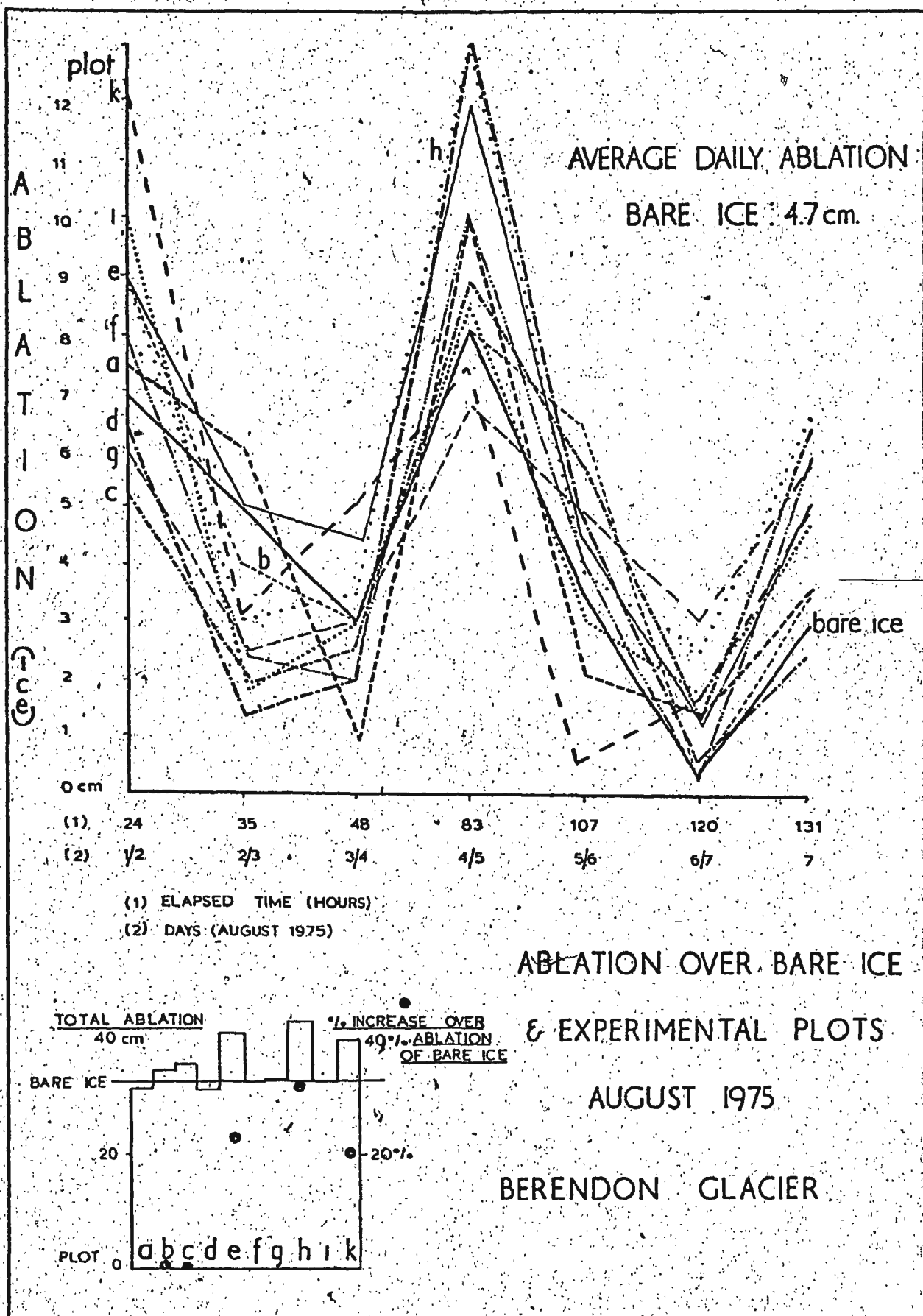


Figure 77. Berendon Glacier; weekly recession, South Arm ice-front, June to September 1975.

Figure 78. The relationship between ice melt rates and superincumbent debris depth.





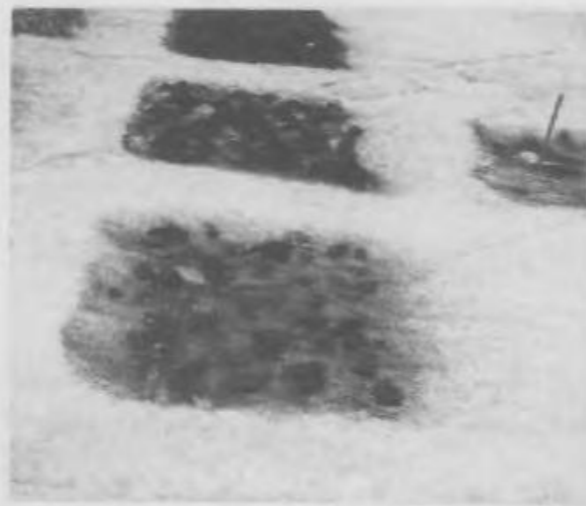
GENERAL VIEW OF DEBRIS PLOTS

South Arm ice-falls in background



PLOTS H,I,J,K

DAY 1



DAY 4

PLOTS A,B,C.

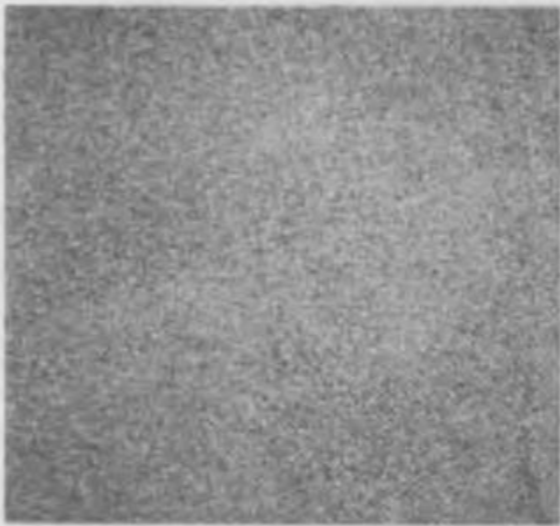
DAY 4



Figure 80. Berendon Glacier; experimental plots.

Two photographs are presented for each plot; on day 1 and day 4.

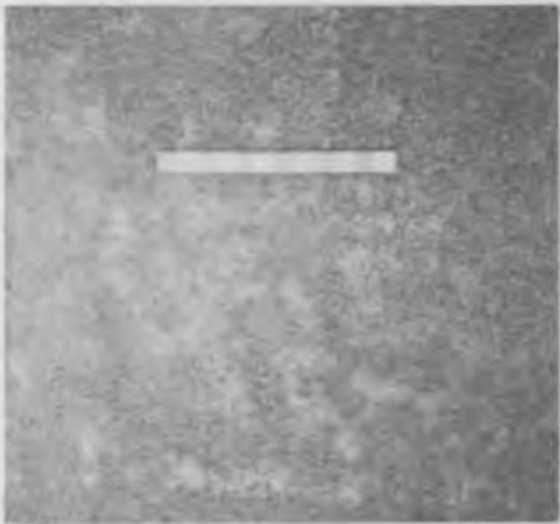
plot



A



12 in.



B



C



plot

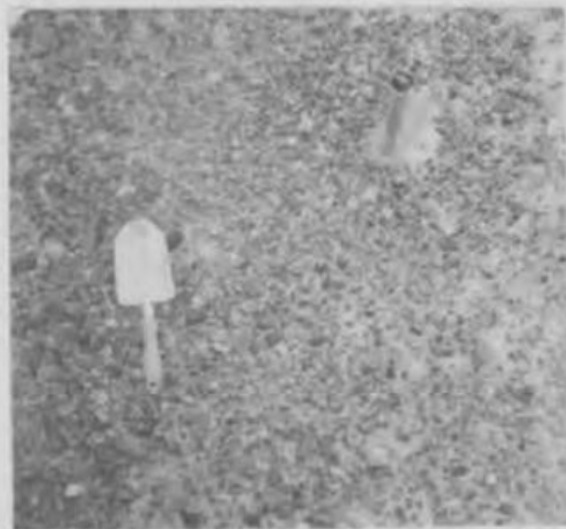
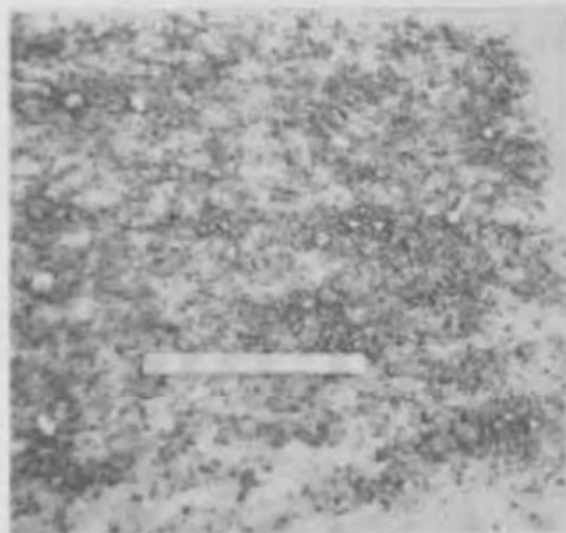
D



E



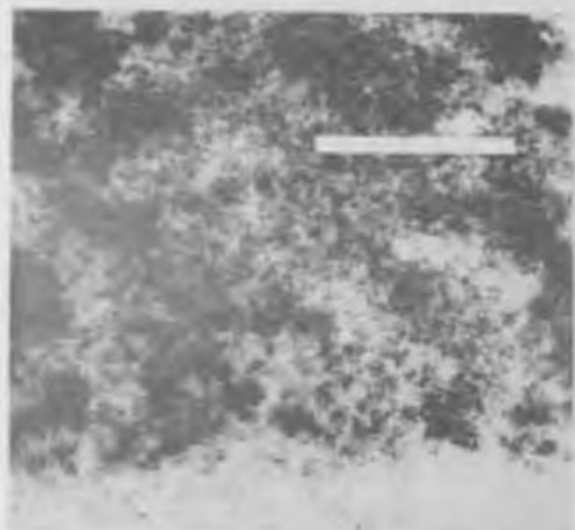
F



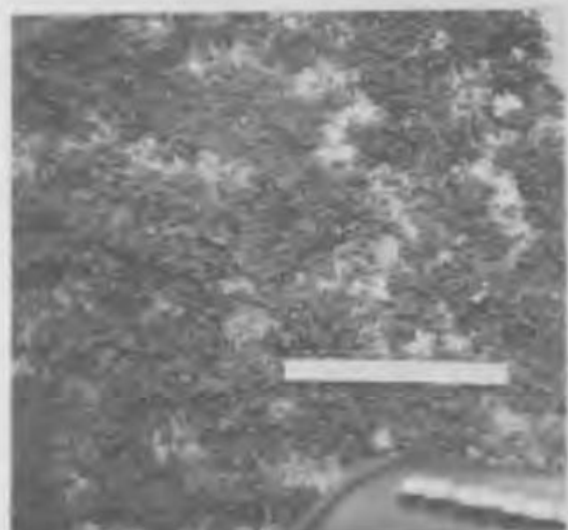
plot
G



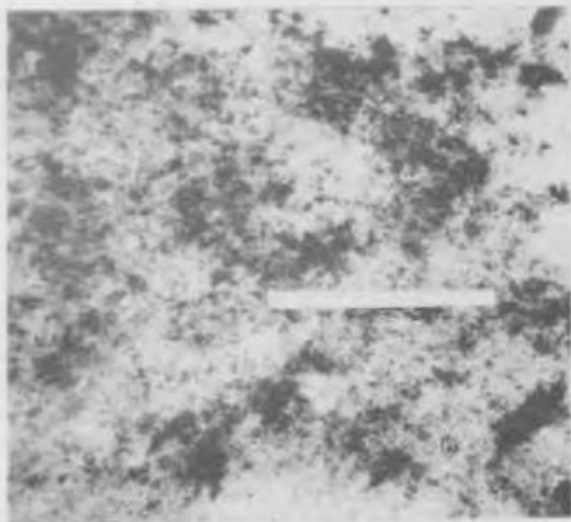
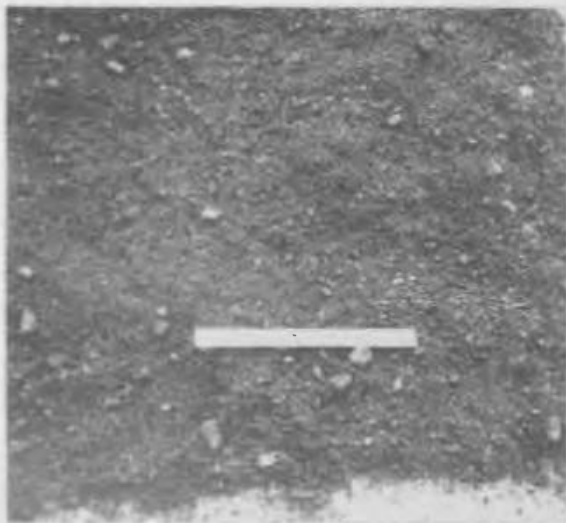
H



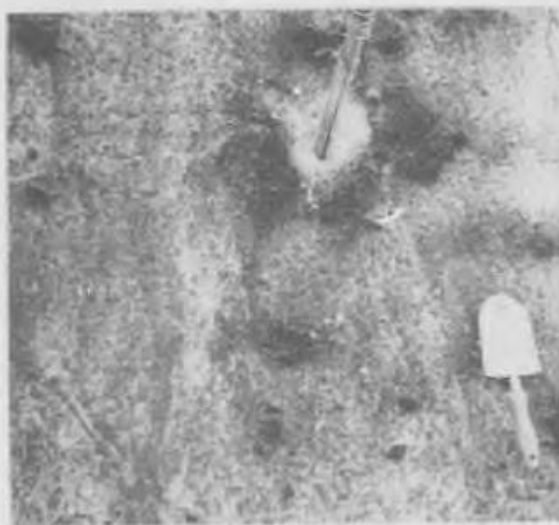
I



plot
J



K



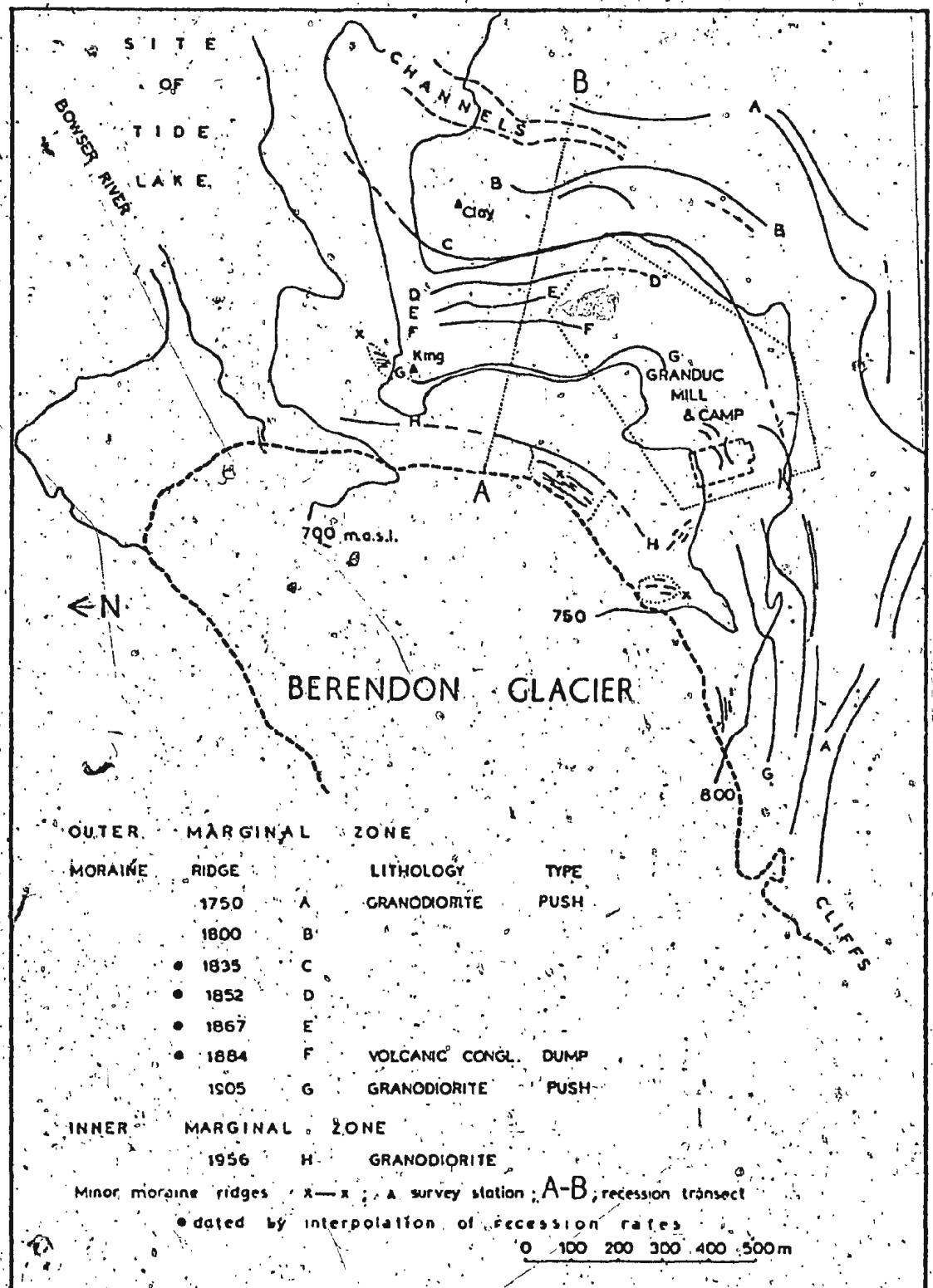


Figure 81. Berendon Glacier; recessional moraines, 1750 A.D., to the present (1975).

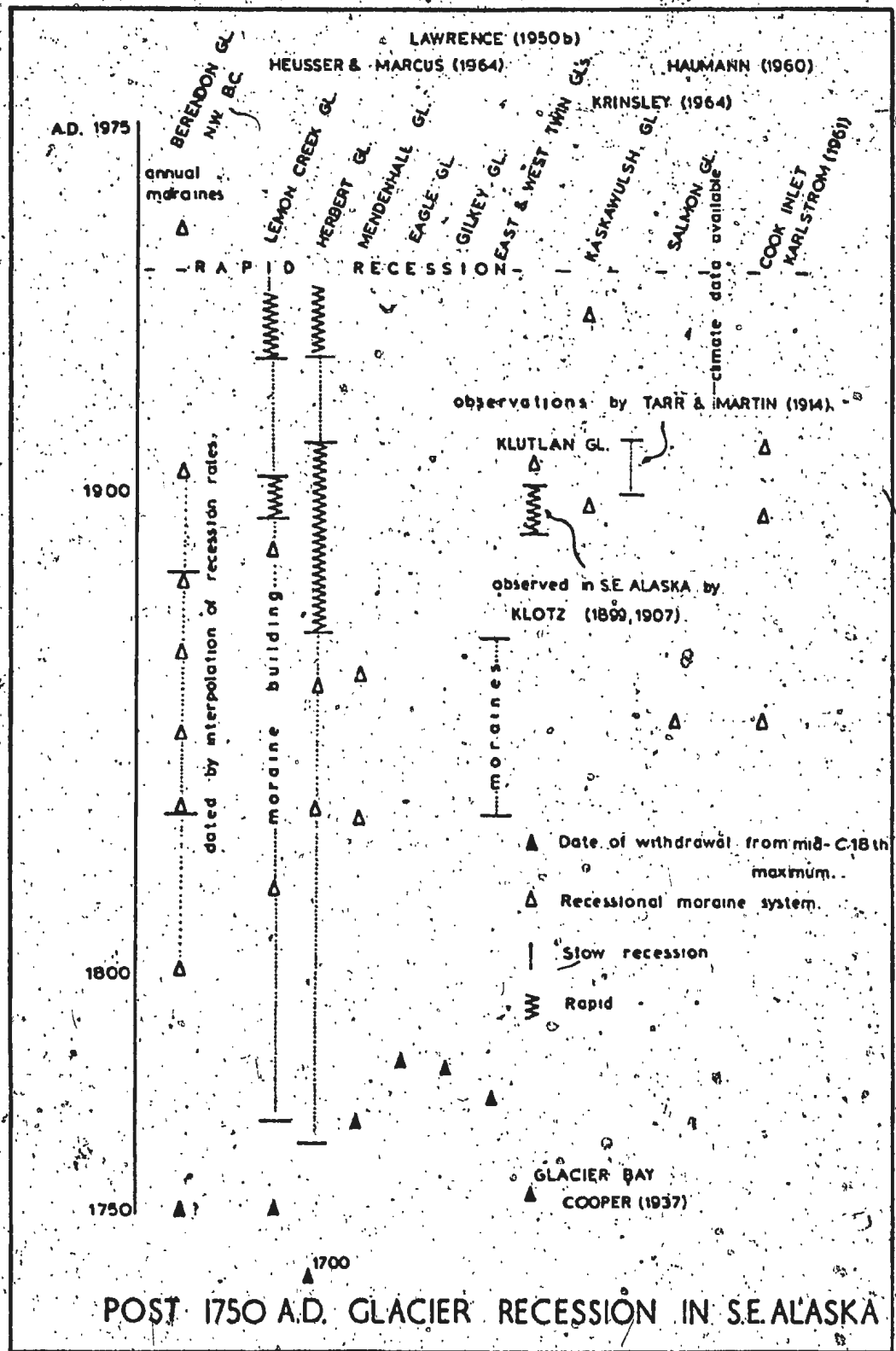
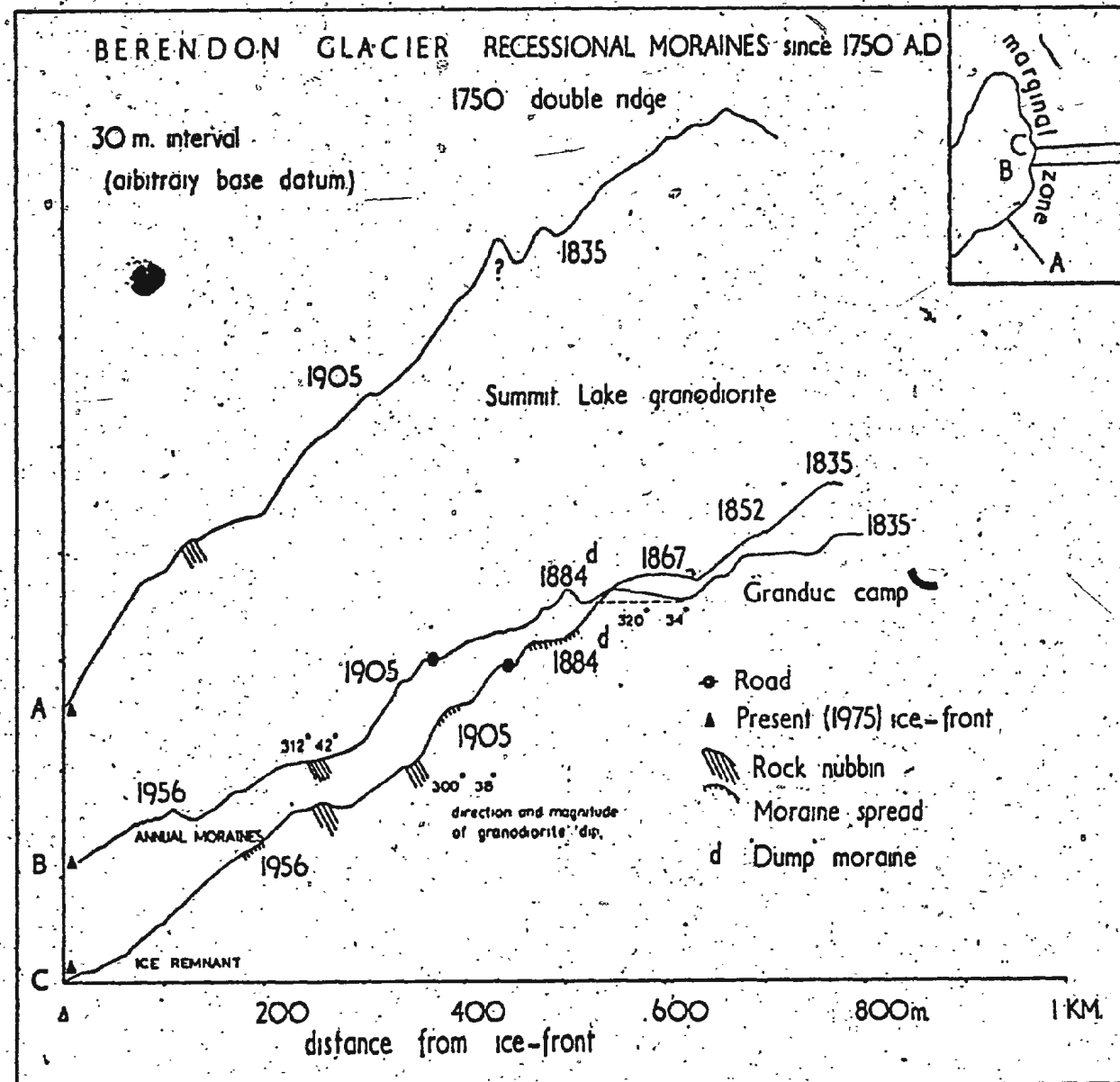


Figure 83. S.E. Alaska; glacier recession since 1750 A.D.

Figure 82. Berendon Glacier; recessional moraines, 1750 A.D., to the present, Topographic profiles.



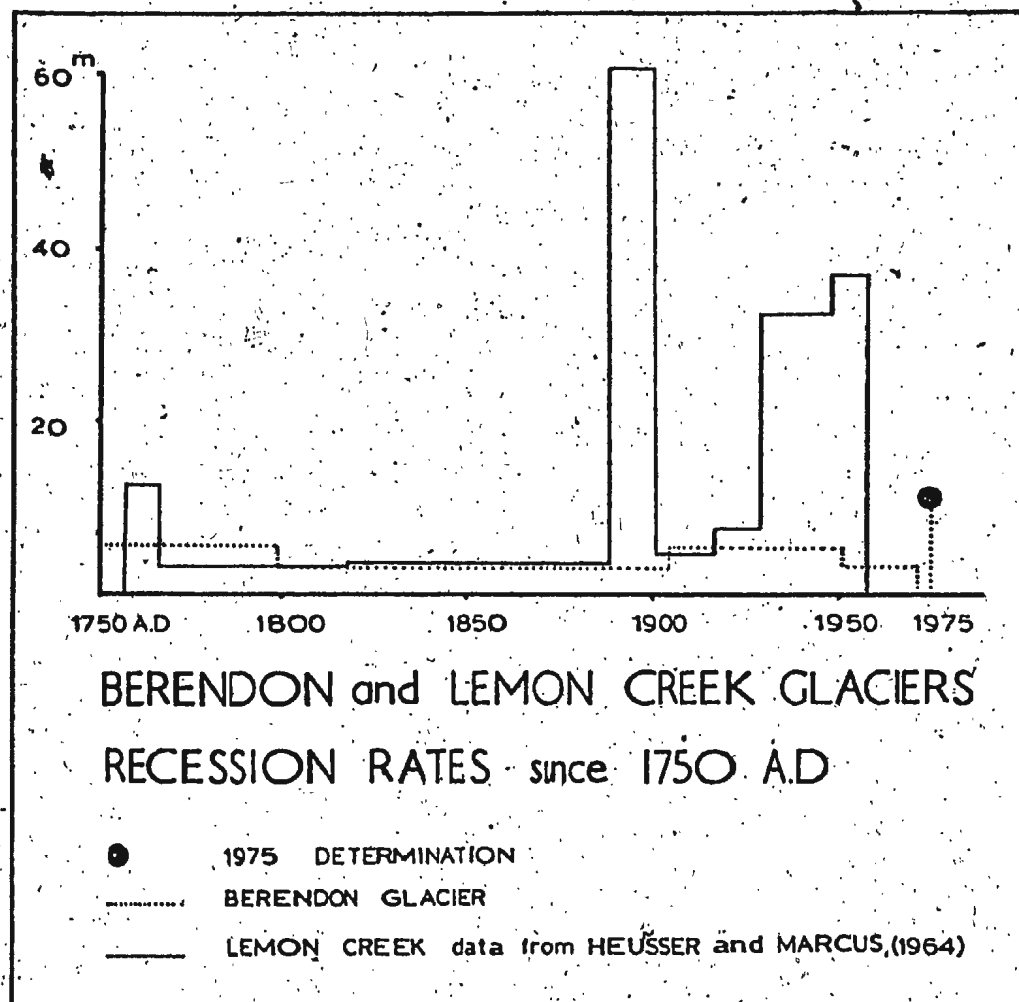
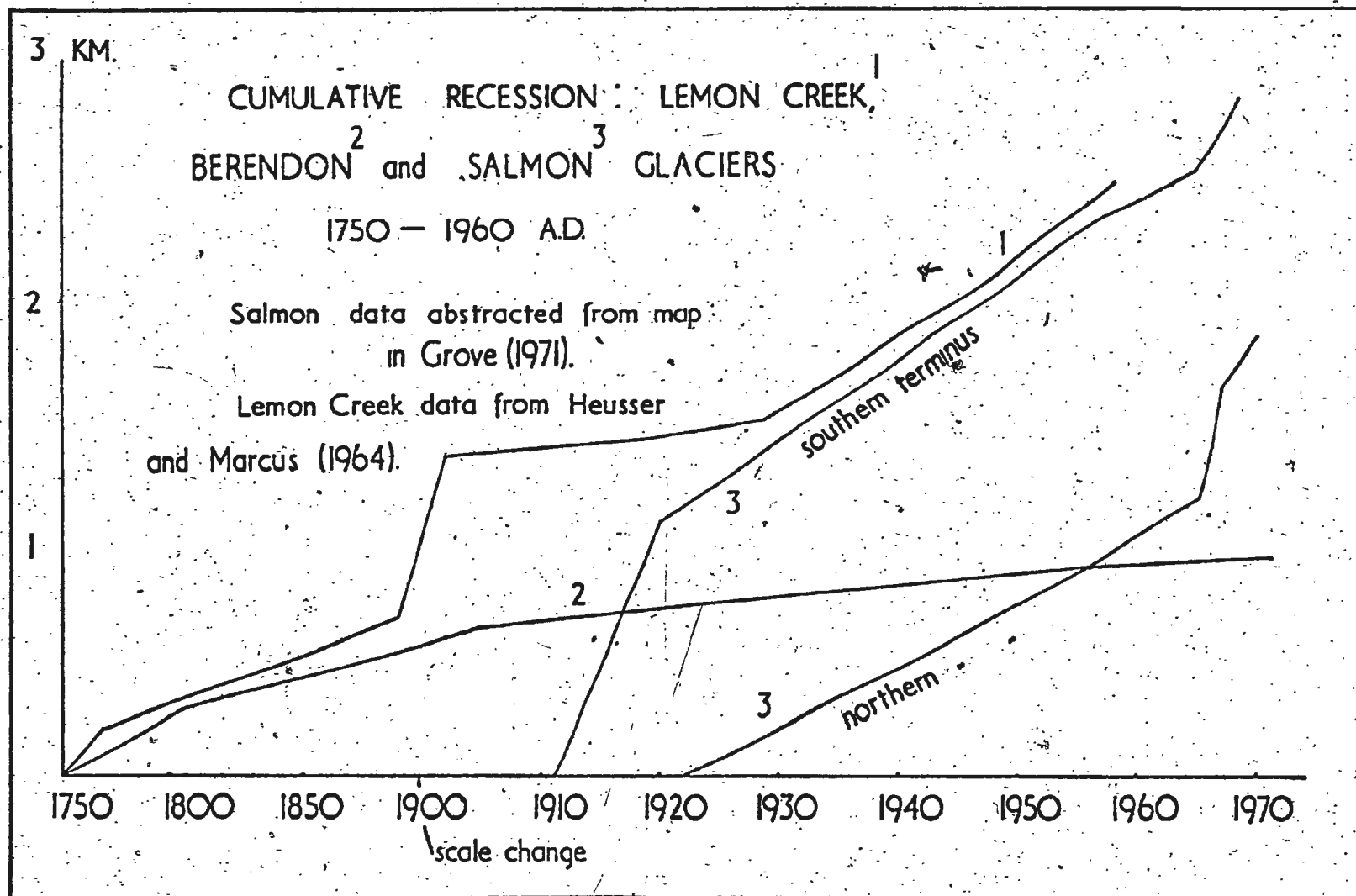
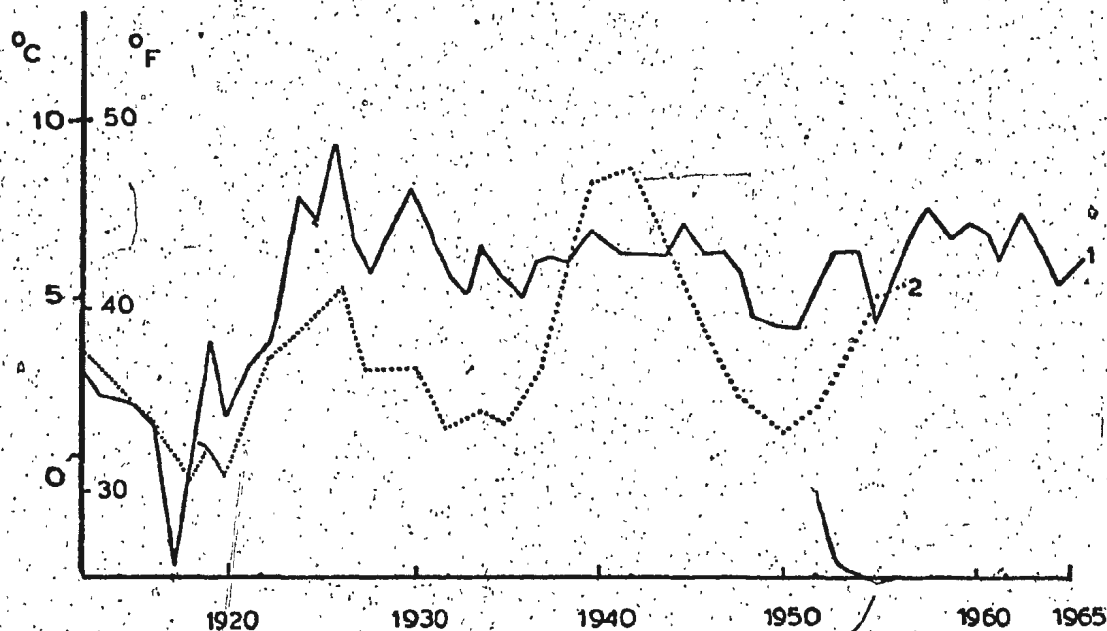


Figure 84. Comparative glacier recession rates.

Figure 85. Total cumulative recession; Berendon, Salmon and Lemon Creek Glaciers.





STEWART¹ B.C. and JUNEAU², S.E. ALASKA
Average mean temperatures since c. 1900 A.D

1 (GROVE 1971)

2 (HEUSSER and MARCUS 1964)

Figure 86. Comparative mean temperatures; Stewart, B.C., and Juneau, Alaska.

